Year : 2022

THE MONT FORT NAPPE, ITS MESOZOIC COVER AND RELATIONS TO THE UPPER PENNINICS (WESTERN SWISS ALPS)

Pantet Adrien

Pantet Adrien, 2022, THE MONT FORT NAPPE, ITS MESOZOIC COVER AND RELATIONS TO THE UPPER PENNINICS (WESTERN SWISS ALPS)

Originally published at : Thesis, University of Lausanne

Posted at the University of Lausanne Open Archive http://serval.unil.ch
Document URN : urn:nbn:ch:serval-BIB_4C8EFB4CEFFF1

UNIL | Université de Lausanne

FACULTÉ DES GÉOSCIENCES ET DE L'ENVIRONNEMENT
INSTITUT DES SCIENCES DE LA TERRE

THE MONT FORT NAPPE, ITS MESOZOIC COVER AND RELATIONS TO THE UPPER PENNINICS (WESTERN SWISS ALPS)

THÈSE DE DOCTORAT

présentée à la

Faculté des Géosciences et de l'Environnement
de l'Université de Lausanne

pour l'obtention du grade de

Docteur en Sciences de la Terre

par

Adrien Pantet

Directeur de thèse
Prof. Jean-Luc Epard

Jury

Prof. Marie-Elodie Perga
Prof. Michel Ballèvre
Dr. Yves Gouffon
Prof. Stefan Schmalholz
Prof. Lukas Baumgartner

LAUSANNE
2022

UNIL | Université de Lausanne
Faculté des géosciences et de l'environnement
bâtiment Géopolis bureau 4631

IMPRIMATUR

Vu le rapport présenté par le jury d'examen, composé de

Présidente de la séance publique :	Mme la Professeure Marie-Elodie Perga
Présidente du colloque :	Mme la Professeure Marie-Elodie Perga
Directeur de thèse :	M. le Professeur Jean-Luc Epard
Expert interne :	M. le Professeur Stefan Schmalholz
Expert interne :	M. le Professeur Lukas Baumgartner
Expert externe :	M. le Professeur Michel Ballèvre
Expert externe :	M. le Docteur Yves Gouffon

Le Doyen de la Faculté des géosciences et de l'environnement autorise l'impression de la thèse de

Monsieur Adrien PANTET

Titulaire d'un
Diplôme d'Ingénieur Géologue
de l'Université de Lausanne

intitulée

THE MONT FORT NAPPE, ITS MESOZOIC COVER AND RELATIONS TO THE UPPER PENNINICS (WESTERN SWISS ALPS)

Lausanne, le 27 octobre 2022

Pour le Doyen de la Faculté des géosciences et de l'environnement

Marie Elodie Perga

Professeure Marie-Elodie Perga

Abstract

This study focuses on the Pennine Alps, in the central part of the Alpine Arc. As this massif offers a wide section through the Alpine nappe stack, and as its geological structure and tectonometamorphic evolution have been extensively studied, it constitutes an ideal setting for the study of continental collision processes. Although the major tectonic units of the Pennine Alps were defined more than a century ago, and despite the countless studies conducted since then, fundamental questions such as the position of some major tectonic boundaries or first order geometries of some nappes, are still debated. In particular, the questions regarding the position of the boundary between the Middle Penninic Mont Fort nappe and the Upper Penninic Tsaté nappe as well as the tectonic attribution and paleogeographic origin of the Frilihorn and Cimes Blanches units have been debated for decades. These questions constitute the main topics of this study.

This work is mainly based on an important structural and stratigraphic field study over an area extending between the Bagnes and the Matter valleys. It provides new and detailed data concerning the nature of the studied contacts and allows to revise several tectonic interpretations. Both the basal contact of the Lower Triassic to Lower Cretaceous Evolène Series and the basal contact of the p.p. Upper Cretaceous non-ophiolitic Schistes Lustrés of the Série Rousse are reinterpreted as stratigraphic. These two series would therefore constitute together the autochthonous sedimentary cover of the Mont Fort nappe. Several sections of the basal contacts of these series are discordant. They are interpreted as corresponding to remnants of high-amplitude Jurassic normal paleofaults. The contact between the Série Rousse and the overlying ophiolite-bearing Schistes Lustrés is marked by the presence of the thin Triassic-Jurassic Frilihorn tectonized slices. This contact, located within the Schistes Lustrés complex of the Combin zone, is interpreted as representing the major tectonic boundary separating the Middle and Upper Penninic units. A redefinition of the Tsaté nappe is proposed, excluding the Série Rousse, and including only the ophiolite-bearing Schistes Lustrés and associated meta(ultra-)basites. In the Täschalpen area, east of Zermatt, the Permian-Jurassic Faisceau Vermiculaire series (incl. Cimes Blanches and Frilihorn Series) is in contact with the basement forming the Alphubel anticline. This contact is interpreted as stratigraphic, and the ensemble formed by the basement of the Alphubel anticline, the Faisceau Vermiculaire and the Série Rousse is interpreted as constituting the prolongation of the Mont Fort nappe, east and south of the Dent Blanche klippe, in the lower limb of the Mischabel backfold.

The proposed tectonic scheme emphasizes the significance of the Mont Fort nappe. This nappe derived from the Prepiemont distal margin constitutes a link between the Briançonnais units and the Piemont ophiolites which appears to be essential for the understanding of the structure of the Penninic nappe stack.

Résumé

Les Alpes pennines, situées dans la partie centrale de l'arc alpin, permettent d'observer une coupe de grande amplitude dans l'empilement de nappes de la partie interne de la chaîne alpine. Leur structure et leur évolution tectono-métamorphique ayant, de plus, été étudiées de manière particulièrement détaillée, elles constituent un cadre idéal pour l'étude des processus de collision continentale. Bien que les principales unités tectoniques des Alpes pennines aient été définies il y a plus d'un siècle, et malgré les nombreuses études menées depuis, des questions fondamentales concernant la structure géologique du massif restent encore débattues. Elles concernent, par exemple, la position de limites tectoniques majeures et les géométries de premier ordre de certaines nappes. En particulier, les questions concernant la position de la limite séparant les nappes du Mont Fort (Pennique moyen) et du Tsaté (Pennique supérieur), ainsi que l'attribution tectonique et l'origine paléogéographique des unités du Frilihorn et des Cimes Blanches sont débattues depuis des décennies. Ces questions constituent les sujets principaux de cette étude.

Ce travail est principalement basé sur une importante étude structurale et stratigraphique de terrain, sur un secteur s'étendant entre le Val de Bagnes et le Mattertal. Il permet d'apporter des données nouvelles et détaillées concernant la nature des contacts étudiés et de réviser plusieurs interprétations tectoniques. Le contact séparant le socle paléozoïque de la nappe du Mont Fort et la Série d'Evolène (Trias inf. - Crétacé inf.) est réinterprété comme étant de nature stratigraphique. Le contact basal des Schistes Lustrés non ophiolitiques de la Série Rousse (p.p. Crétacé sup.), sur la Série d'Evolène et le socle Mont Fort, est également réinterprété en tant que contact stratigraphique. Selon notre interprétation, la Série d'Evolène et la Série Rousse forment donc ensemble la couverture sédimentaire autochtone de la nappe du Mont Fort. Les deux contacts de base de ces séries sont caractérisés par la présence de sections discordantes. Ces sections sont interprétées comme représentant originellement des escarpements de paléofailles jurassiques. Le contact entre la Série Rousse et les Schistes Lustrés ophiolitiques sus-jacents est marqué par la présence de fines écailles, fortement déformées, de métasédiments triasiques à jurassiques de la Série du Frilihorn. Ce contact, situé à l'intérieur du complexe de Schistes Lustrés de la zone du Combin, est interprété comme représentant la limite tectonique majeure séparant les unités penniques moyennes et supérieures. Une redéfinition de la nappe du Tsaté est proposée, excluant la Série Rousse, et incorporant uniquement les Schistes Lustrés à intercalations ophiolitiques. Dans la région des Täschalpen, à l'est de Zermatt, la série permienne à jurassique du Faisceau Vermiculaire (incl. les séries des Cimes Blanches et du Frilihorn) est en contact avec le socle paléozoïque formant l'anticlinal de l'Alphubel. Ce contact est interprété comme stratigraphique. L'ensemble formé par le socle de l'anticlinal de l'Alphubel, le Faisceau Vermiculaire et la Série Rousse est interprété comme constituant le prolongement de la nappe du Mont Fort, à l'est et au sud de la klippe de la Dent Blanche, dans le flanc renversé du rétropli des Mischabel.

Le schéma tectonique proposé souligne l'importance de la nappe du Mont Fort. Cette nappe dérivée de la marge distale du domaine prépiémontais représente un lien entre les unités briançonnaises et les unités ophiolitiques piémontaises, qui apparaît comme essentiel pour la compréhension de la structure des nappes penniques.

Remerciements

Je tiens à remercier chaleureusement toutes les personnes qui m'ont aidé et soutenu au cours de ce travail, et sans qui il n'aurait pas pu être réalisé.

Mes remerciements s'adressent tout d'abord à mon directeur de thèse, Jean-Luc Epard, pour m'avoir proposé ce travail, pour tout ce qu'il m'a appris, pour sa patience et pour ses conseils toujours pertinents. Je tiens également à remercier vivement Henri Masson, qui m'a suivi tout au long de cette étude, pour le partage de ses connaissances, son enthousiasme constant, et sa bienveillance.

Je tiens également à adresser un grand merci à Claudia Baumgartner-Mora, Peter Baumgartner et Lukas Baumgartner, co-auteurs d'un chapitre de ce manuscrit, pour leur intérêt et pour ces collaborations motivantes, ainsi qu'aux membres du jury de thèse, Yves Gouffon, Michel Ballèvre, Stefan Schmalholz, Lukas Baumgartner et Marie-Elodie Perga, pour le temps investi, leurs corrections et les discussions très intéressantes au sujet de cette recherche.

J'adresse également un grand merci aux collègues géologues qui ont participé à ce travail, en particulier Christophe Jossevel, mon collègue doctorant en géologie structurale et alpine, pour les discussions motivantes, pour m'avoir accompagné de nombreuses fois sur le terrain et pour sa bonne humeur constante; Martin Robyr et Nicolas Buchs, pour m'avoir gentiment accompagné sur le terrain; Paola Manzotti, Michel Ballèvre, Gianreto Manatschal, Charlottes Ribes, Guilhem Hoareau et Nicolas Dall'Asta pour les excursions communes et les discussions intéressantes et motivantes sur le terrain; Albrecht Steck, Stefan Dall'Agnolo, Gérard Stampfli, Mario Sartori et Aymon Baud pour les discussions très intéressantes au sujet de cette étude; Alexandra Demers Roberge pour son aide précieuse pour la relecture du manuscrit; Olivier Reubi, Youness Zangui et Laurent Nicod pour leur aide au laboratoire et pour la préparation des échantillons; et tous les autres collègues et amis de l'université, qui m'ont aidé avec leurs conseils, leur soutien et leur bonne humeur pendant ces dernières années.

Mon père Didier et mon oncle Pierre Hentsch m'ont chacun accompagné quelques jours sur le terrain, notamment sur les glaciers des parties hautes du secteur étudié, je les en remercie chaleureusement.

Enfin, j'aimerais remercier de tout cœur mes amis, toute ma famille, et Maud, pour leur soutien et pour tous les bons moments partagés durant ces dernières années!

Cette thèse a été financée par l'Université de Lausanne, avec un soutien de la Société Académique Vaudoise, je les en remercie sincèrement.

Table of content

Chapter 1: Introduction

1.1. Aim of the thesis

The Pennine Alps, where this study is located, form the central part of the Alpine Arc (Fig. 1.1) and one of the highest zones of the Alps. The geological structure of the Pennine Alps, with locally strong axial plunging, offers a wide section through the Alpine nappe stack. It includes the deeply subducted parts of the European - Briançonnais s.l. continental margin (Lower and Middle Penninic nappes); the ophiolitic suture zone (Upper Penninic nappes); and the units derived from the distal Adriatic continental margin (Salassic nappes). As the Pennine Alps are also one of the most geologically studied mountain range, they constitute an ideal setting for the study of continental collision processes.

Although the description of large-scale structures and the definition of the major tectonic units of the Pennine Alps date from more than a century ago (e.g. Gerlach 1869, 1871; Argand 1908, 1911), and despite the countless studies that have been carried out in this area since the end of the 19th century, many fundamental questions still remain open. For instance, the position of certain nappe boundaries, or the first order geometries of some tectonic units are still debated topics. Such problematics are of primary importance for the understanding of orogenic processes, such as the dynamics of nappe formation and development of orogenic belts.

In particular, the positions of the boundaries between the tectonic units now called the Mont Fort, Tsaté, Frilihorn and Cimes Blanches nappes (Figs 1.1b, 1.2), which are the subject of this study, have been debated for decades. Certain contacts between these units have alternately been interpreted as original stratigraphic contacts or as Alpine tectonic contacts (Alpine thrusts), and some of these units (or part of them) have alternately been grouped together or dissociated, in different ways, according to the various tectonic interpretations of the successive authors.

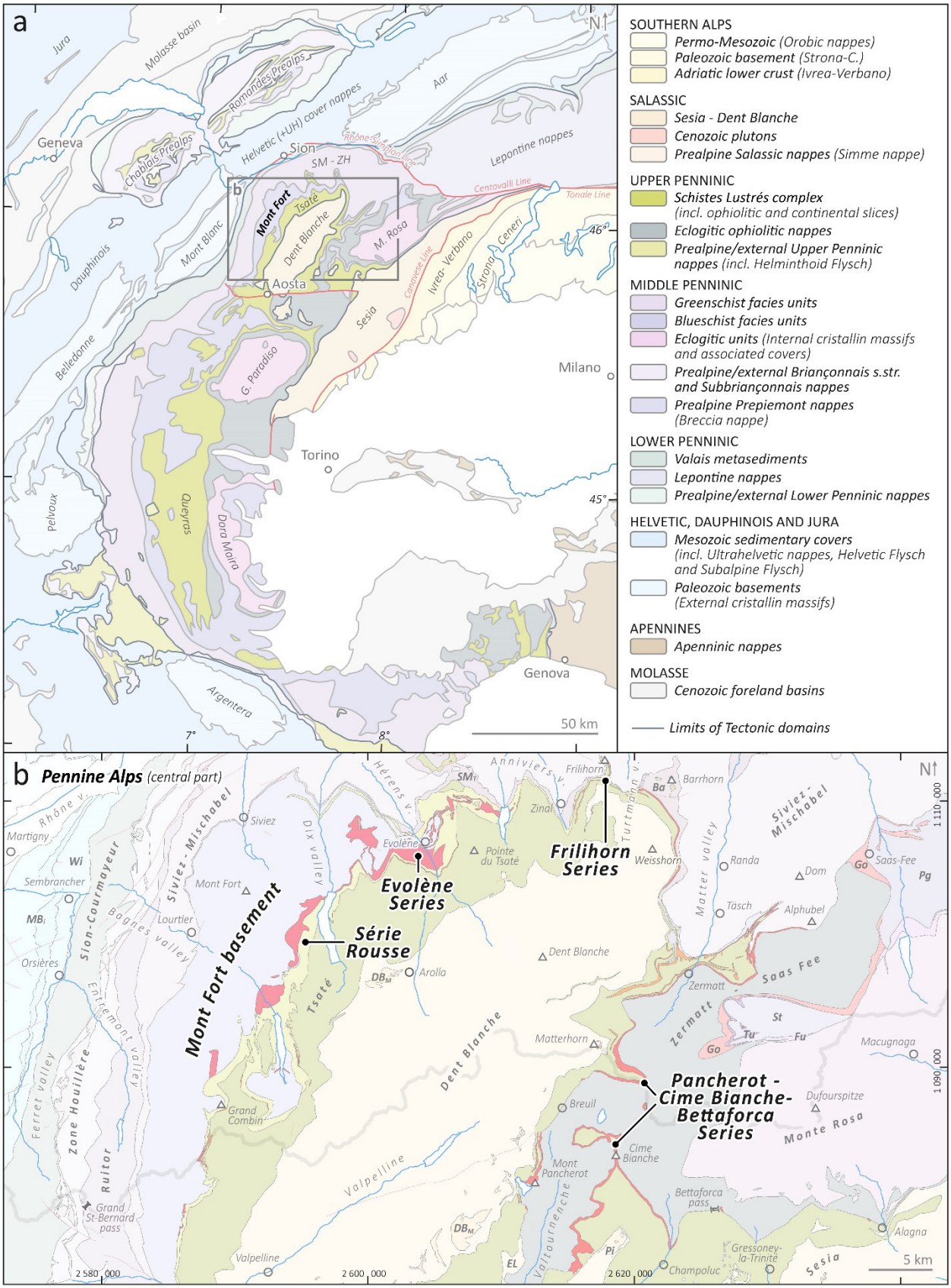

Fig. 1.1 a Tectonic map of the Western and Central Alps with location of the studied area; modified after Schmid et al. (2004, 2017), Steck et al. (1999, 2015, 2019), Ballèvre et al. (2018, 2020), Beltrando et al. (2010a, 2014), Balestro et al. (2020), Dal Piaz (1999), Bigi et al. (1992), Gouffon (1993), Deville et al. (1992) and the Tectonic map of Switzerland (2005); *SM - ZH*: Siviez-Mischabel nappe and Zone Houillère; *UH*: Ultrahelvetic nappes. **b** Tectonic scheme of the studied area after Steck et al. (1999). *Ba*: Barrhorn Series; DB_M: Dent Blanche Mesozoic; *EL*: Etirol-Levaz unit; *Fu*: Furgg zone; *Go*: Gornergrat nappe; MB_i: Internal Mont Blanc massif; *Pg*: Portjengrat nappe; *Pi*: Pillonet unit; SM_T: Siviez-Mischabel Triassic; *St*: Stockhorn basement; *Tu*: Tuftgrat Series; *Wi*: Wildhorn nappe.

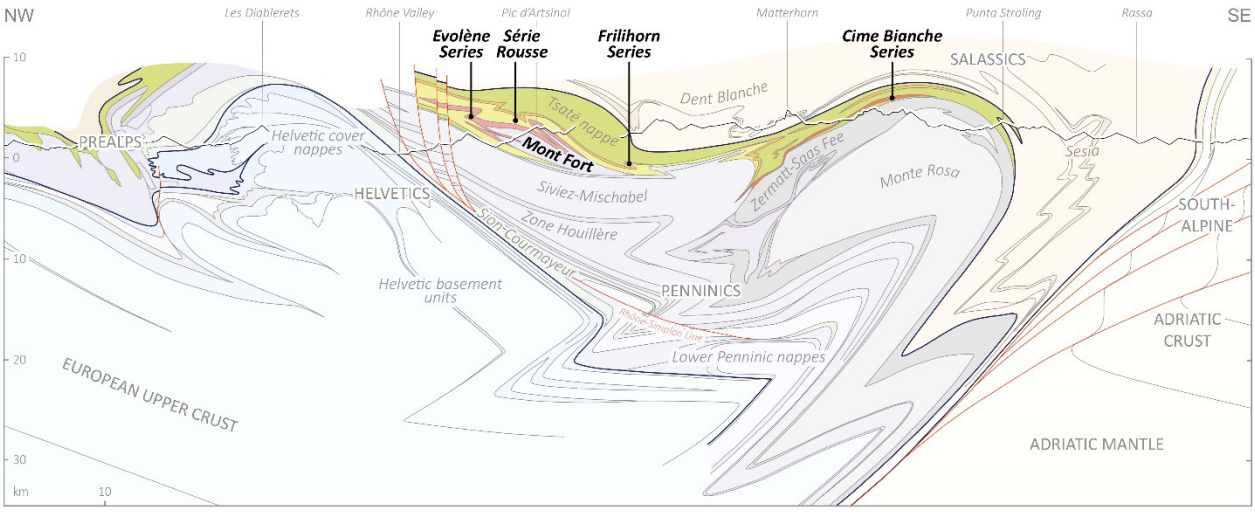

Fig. 1.2 Cross-section through the Alps of SW Switzerland and NW Italy with location of the studied units (modified after Escher et al. 1993, 1994; Steck et al. 2015).

The identification and localization of tectonic contacts in the internal sectors of the Alpine belt, where orogenic ductile deformation is extremely strong, is absolutely not obvious. Tectonic contacts could be marked by the presence of distinctive markers such as well-developed mylonitic fabrics (e.g. Trouw et al. 2010), cornieule levels (e.g. Masson 1972; Vearncombe 1982), or tectonized slices (e.g. Rabowski 1918; Lugeon 1947). In some cases, abrupt changes in the mineralogical assemblages, indicating contrasting tectono-metamorphic histories, may also help to identify tectonic contacts (e.g. Bearth 1967a; Ballèvre and Merle 1993; Angiboust et al. 2014; Manzotti et al. 2021). However, when ductile deformation is strong and when such distinctive markers are absent, the identification of the nature of a contact (tectonic or stratigraphic?) can be challenging, especially when two units of similar lithologies are tectonically juxtaposed. Moreover, the superposition, within a single tectonic unit, of two levels showing a strong rheological contrast, can lead to local shearing, which could be difficult to distinguish from a main contact separating different tectonic units.

The distinction between structures formed during the Alpine convergence and inherited structures is also often problematic. Inherited structures, such as Late Paleozoic and Mesozoic extensional faults, have been identified in numerous areas of the Alps and other orogens. In the Alps, such paleofaults have been recognized in various sectors of the Helvetic-Dauphinois domain

(e.g. Barféty et al. 1979; Dolivo 1982; Barféty and Gidon 1984; Grand et al. 1987; Epard 1990; Krayenbuhl and Steck 2009; Bellahsen et al. 2012; Boutoux et al. 2014; Cardello and Mancktelow 2014), at the transition between the Helvetic and Penninic domains (Ballèvre et al. 2018), in the Southern Alps (e.g. Bertotti et al. 1993; Real et al. 2018), in the Eastern Alps (e.g. Conti et al. 1994) and particularly in the Eastern Central Alps, where the weak Alpine deformation imprint allowed to describe and restore in detail the geometries of the pre-Alpine structures (Froitzheim and Eberli 1990; Florineth and Froitzheim 1994; Froitzheim and Manatschal 1996; Manatschal et al. 2003; Mohn et al. 2011; Beltrando et al. 2014; Ribes et al. 2019). Some Mesozoic paleofaults have also been described in the Middle Penninic domain of the Western and Central Alps (Dumont et al. 1984; Faure and Mégard-Galli 1988; Sartori 1990), but such descriptions remain relatively scarce in this domain affected by intense Alpine ductile deformation. Large Jurassic extensional paleofaults should nevertheless be widespread in the internal part of this domain corresponding to the distal hyper-extended portion of the Briançonnais-Piemont margin (e.g. Mohn et al. 2010, 2012; Beltrando et al. 2014). However, the recognition of inherited extensional structures is delicate and requires very detailed geological studies, in particular because they can easily be mistaken for orogenic compressional structures (e.g. Mohn et al. 2011, 2014; Beltrando et al. 2014; Epin et al. 2017; Lescoutre and Manatschal 2020).

This thesis aims to: (1) clarify the stratigraphic or tectonic nature of the debated contacts between the Mont Fort, Tsaté and Cimes Blanches nappes; (2) test the hypothesis of the presence of Mesozoic paleofaults within these units or at their contacts, and describe such structures if they can be identified; (3) study the tectonic and paleogeographic relations between the Mont Fort, Frilihorn and Cimes Blanches nappes; (4) highlight the stratigraphic similarities and differences between the studied units and consequences for their paleogeographic origin.

1.2. Approach

This work is essentially based on a substantial geological field study conducted over six consecutive seasons. A large-scale approach was favored, with a level of detail adapted to the interest and quality of the outcrops. The studied area extends over a region comprising the upper Bagnes, Dix, Hérens and Matter valleys; in addition, selected localities have been studied in the Anniviers, Turtmann and Valtournenche valleys (Fig. 1.1b).

In order to determine the nature of the studied contacts, a multidisciplinary approach was favored. It included: (a) the study of local stratigraphic successions along the studied units to reconstruct synthetical stratigraphic columns for each unit and describe their internal stratigraphic variations; (b) the study of lithological successions across the studied contacts, allowing, for example, to highlight large scale unconformities; (c) a structural study at various scales, from the outcrop scale, with the identification of successive deformation phases and systematic measurement of the structure orientations, to the construction of large-scale cross-sections and axial trace maps; (d) microscopic observations on selected samples for mineral determinations, study of the deformation at microscopic scale along the studied contacts and search for microfossil remnants; (e) the elaboration of detailed geological maps and large scale bedrock maps compiled after all existing maps and our own field observations. Some supplementary methods where used to study specific questions, such as: (f) 3D geometrical modeling of deformation (Shear2F software, Rey 2002), for the comparison of some specific structures observed in the field, with polyphase fragile and ductile deformation models; (g) Raman Spectroscopy on Carbonaceous Material (RSCM; Beyssac et al. 2002) performed on polished thin-sections to estimate metamorphic peak temperatures for some of the studied units and their contact zones; (h) Cathodoluminescence observations on polished thin sections, to distinguish specific patterns of trace elements and to highlight biological features remaining undetectable with classical optical microscopy.

1.3. Outline of the thesis

The three main chapters presented in this manuscript correspond to different and specific topics of the main study. They are independently published or prepared for publication within peer-reviewed journals. These include:

- *Chapter 2:* **Mimicking Alpine thrusts by passive deformation of synsedimentary normal faults: a record of the Jurassic extension of the European margin (Mont Fort nappe, Pennine Alps).** This chapter consists of an article published in the Swiss Journal of Geosciences (113:13; 09/2020; https://doi.org/10.1186/s00015-020-00366-2). Co-authors are Jean-Luc Epard and Henri Masson.

  The chapter focuses on the nature of the contact between the Mont Fort basement and the Evolène Series, as well as on the stratigraphy of the Evolène Series and the structure of the Mont Fort nappe in the Hérens and Dix valleys.

- *Chapter 3:* **Schistes Lustrés in a hyper-extended continental margin setting and reinterpretation of the limit between the Mont Fort and Tsaté nappes (Middle and Upper Penninics, Western Swiss Alps)**. This chapter consists of an article accepted for publication in the Swiss Journal of Geosciences. Co-authors are Jean-Luc Epard, Henri Masson, Claudia Baumgartner-Mora, Peter O. Baumgartner and Lukas Baumgartner.

  The chapter focuses on the Série Rousse and especially on its structure in the Bagnes and Hérens valleys, on its stratigraphy, on the nature of its basal and upper contacts, and on its relations to the Mont Fort and Tsaté nappes.

- *Chapter 4:* **Structure and stratigraphy of continent-derived metasediment units (Cimes Blanches and Frilihorn) intercalated within the ophiolites around Zermatt: Relations with the Mischabel backfold, Alphubel basement and Mont Fort nappe (Pennine Alps, SW Switzerland and NW Italy).** This chapter consists of an article in preparation.

  The chapter focuses on the Faisceau Vermiculaire Permian-Jurassic series (incl. the Frilihorn and Pancherot - Cime Bianche - Bettaforca Series) outcropping in the upper Matter valley and NE Aosta valley. Questions regarding their structure, tectonic attributions, paleogeographic origin and relations to the Mont Fort nappe are discussed.

Since this manuscript is constituted of independent chapters written, submitted and/or published at different times, some discrepancies and hypothesis divergence occur between the earlier chapters and the more recent ones, due to the evolution of the understanding of the topic. For these reasons, for example, the large-scale tectonic map provided in the first chapter, which has been elaborated in 2018-2019 and published in 2020, shows substantial differences with the one elaborated in 2022 and presented in the last chapter.

Chapter 2: Mimicking Alpine thrusts by passive deformation of synsedimentary normal faults: a record of the Jurassic extension of the European margin (Mont Fort nappe, Pennine Alps)

Adrien Pantet, Jean-Luc Epard and Henri Masson

Published in the *Swiss Journal of Geosciences, 113:13* (2020), 35–59.

Abstract

The Mont Fort nappe, former uppermost subunit of the Grand St-Bernard nappe system, is an independent tectonic unit with specific structural and stratigraphic characteristics (Middle Penninic, NW Italy and SW Switzerland). It consists in a Paleozoic basement, overlain by a thin, discontinuous cover of Triassic-Jurassic metasediments, mainly breccias, called the Evolène Series. The contact of this Series over the Mont Fort basement is debated: stratigraphic or tectonic? We present new observations that support the stratigraphic interpretation and consequently imply that the Evolène Series belongs to the Mont Fort nappe. We moreover show that the Mont Fort nappe was strongly affected by normal faulting during Jurassic. These faults went long unnoticed because Alpine orogenic deformation blurred the record. Alpine strain erased their original obliquity, causing confusion with an Alpine low-angle thrust. These Jurassic faults have been passively deformed during Alpine tectonics, without inversion or any other kind of reactivation. They behaved like passive markers of the Alpine strain.

Detailed field observations reveal the link between observed faults and specific breccia accumulations. Areas where the Evolène Series is missing correspond to sectors where the fault scarps were exposed on the bottom of the sea but were too steep to keep the syn- to post-faulting sediments. The Mont Fort nappe thus represents an example of a distal rifted margin. The succession of synsedimentary extensional movements followed by orogenic shortening generated a situation where passively deformed normal faults mimic an orogenic thrust.

2.1. Introduction

The Pennine Alps (SW Switzerland and NW Italy) show a complex tectonic architecture resulting from the Cenozoic collision of the European and Adriatic plates (e.g. Argand 1911, 1924, 1934; Escher et al. 1988, 1993, 1997; Escher and Beaumont 1997; Dal Piaz 1999; Lemoine et al. 2000; Steck et al. 2001, 2015; Schmid et al. 2004, 2017; Beltrando et al. 2010a, 2014; Mohn et al. 2014; McCarthy et al. 2018, 2020). The orogen-parallel axial plunge of the large structures, bringing all the main tectonic and paleogeographic domains of the Alps to the surface, provides one of the most complete sections through the Alpine nappe stack (Figs. 2.1 and 2.2) which consists from bottom to top of:

1.- The European continental margin, only moderately affected by the opening of the Alpine Tethys during Jurassic (Helvetic realm).

2.- More distal parts of this margin, more strongly affected by the Jurassic extension and more deeply subducted during Late Cretaceous to Cenozoic plate convergence (Lower and Middle Penninic realms).

3.- The ophiolitic suture of the Piedmont basin, main branch of the Alpine Tethys (Upper Penninic realm).

4.- Units derived from the Adriatic plate (Sesia - Dent Blanche and Simme units).

Hence, the Pennine Alps are one of the most carefully studied sectors of the Alps, which provides an ideal object for understanding ocean opening as well as continental collision processes.

The Mont Fort nappe which is the subject of the present work is of particular interest in this regard. This nappe (first defined by Escher 1988) belongs to the Middle Penninic realm and occupies a central position in the nappe stack of the Pennine Alps (Fig. 2.2).

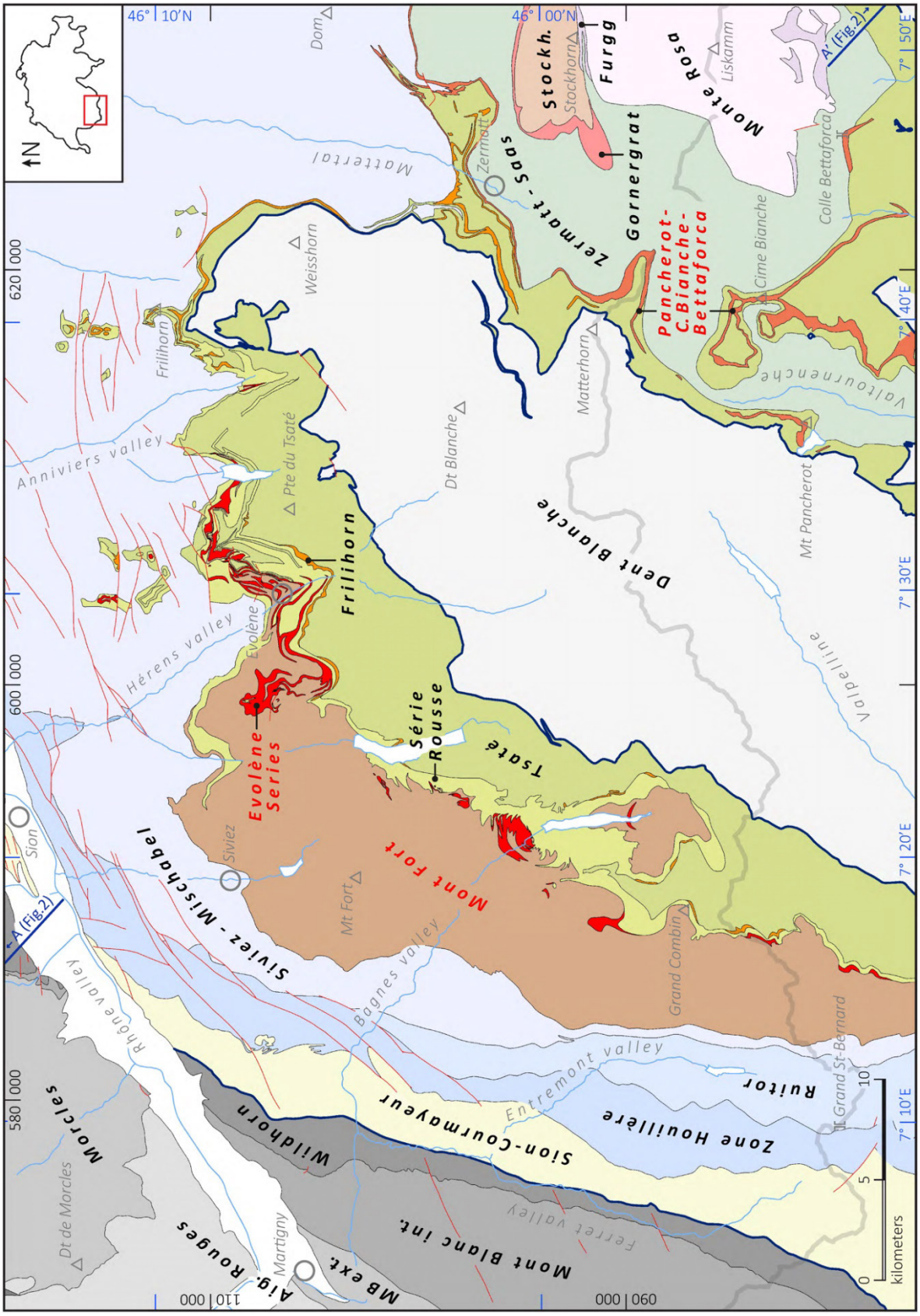

Fig. 2.1 Tectonic map of the Alps of SW Switzerland and NW Aosta Valley (IT). Modified after Allimann (1990), Steck et al. (1999), Sartori and Epard (2011), Scheiber et al. (2013), Dal Piaz et al. (2015b) and Steck et al. (2015). Blue lines indicate the limits of the Penninic units.

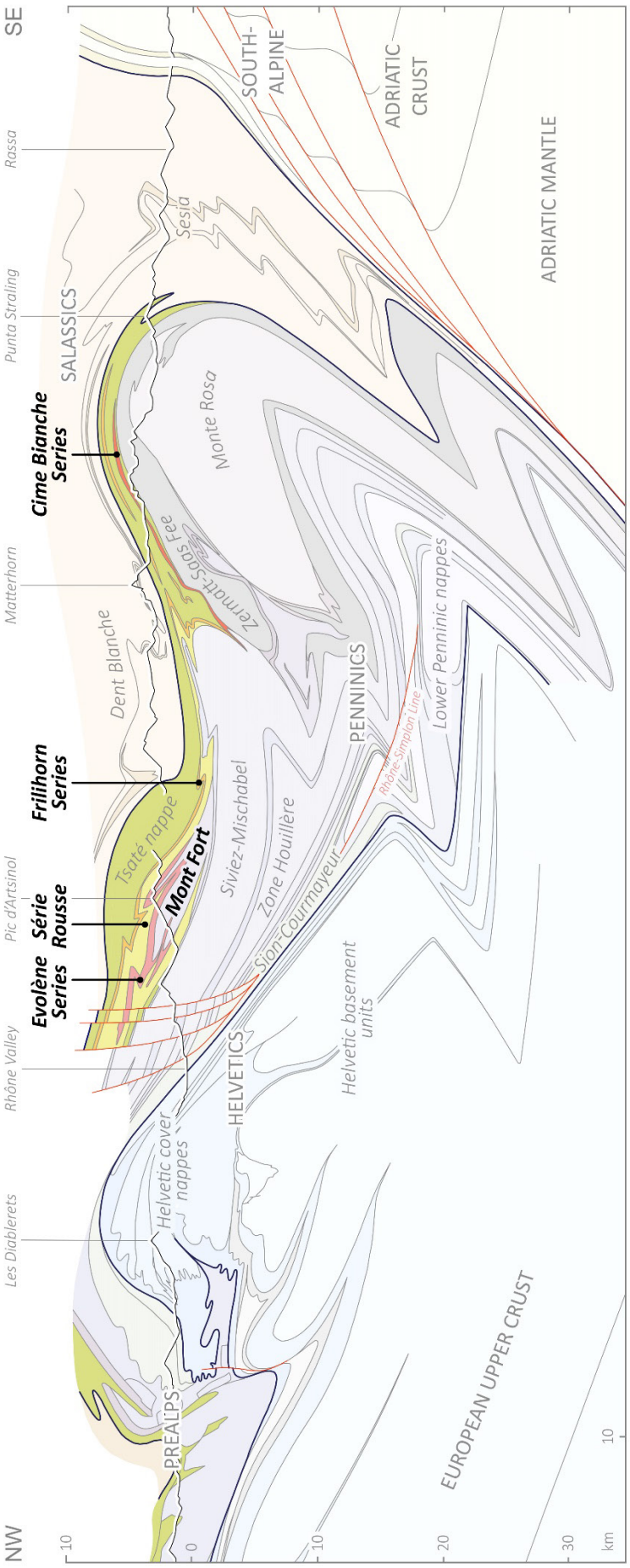

Fig. 2.2 Cross-section through the Penninic nappes of South-Western Switzerland (modified after Escher et al. 1993, 1994; Steck et al. 2015).

This study leads to a new appraisal of the importance of extensional faulting of Jurassic age on the European margin of the embryonic Alpine Tethys. The recognition of such paleofaults mistaken for Alpine thrusts by some authors has direct consequences regarding its relationships with Upper Penninic units.

2.2. Geological setting: the Prepiedmont domain and the Mont Fort nappe

The Lower and Middle Penninic realms are particularly complex. They include a very important paleogeographic element: the *Briançonnais* domain. The central part of this element, as for example exposed around Briançon and in the Prealps, is characterized by Mid-Jurassic uplift and emergence (e.g. Debelmas 1955; Ellenberger 1958; Baud and Septfontaine 1980; Jaillard 1988; Sartori 1990; Hürlimann et al. 1996; Lemoine et al. 2000; Decarlis et al. 2017a; Chenin et al. 2019) that defines the domain referred to as *Briançonnais s.str.* below. In a broader sense the term Briançonnais is also used for designating a much larger area that we will refer to as *Briançonnais s.l.* (Fig. 2.3). It includes distinct subdomains such as the more external Subbriançonnais and the more internal Prepiedmont (see below regarding the definition of these subdomains), which were submitted to various uplift and subsidence pulses during the Jurassic.

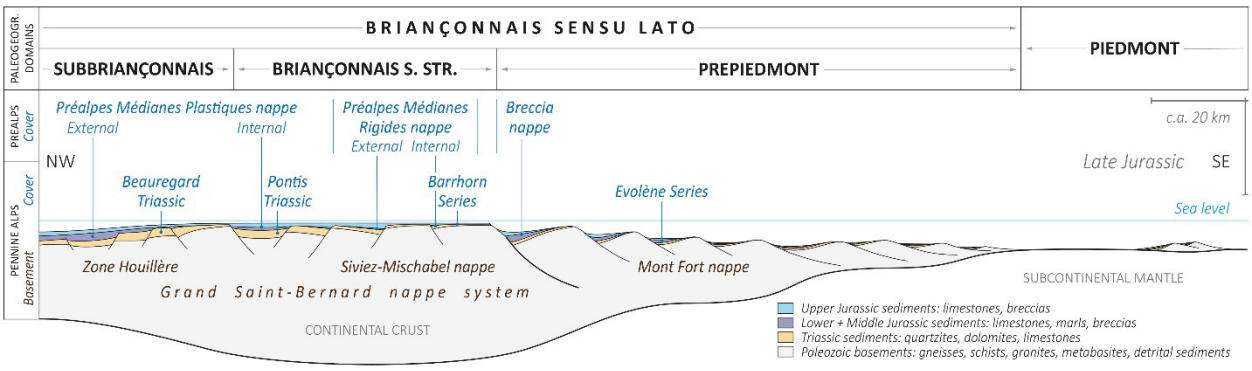

Fig. 2.3 Late Jurassic transect of the Briançonnais s.l. paleogeographic domain in SW Switzerland (after i.a. Trümpy 1960; Baud and Septfontaine 1980; Sartori 1990; Septfontaine 1995; Plancherel et al. 1998; Mohn et al. 2010, 2012; Decarlis et al. 2017a). The distance between the Préalpes Médianes Rigides and the Breccia nappe basins is uncertain and represents a minimal estimate (the domain separating these 2 basins is often referred to as *Ultrabriançonnais).*

The Triassic stratigraphy of the various subdomains of the Briançonnais s.l. is more uniform and shows an up to 1000 m thick sequence of Middle to Late Triassic carbonates characterized by very specific facies (e.g. Trümpy 1960, 1980; Mégard-Galli and Baud 1977; Escher et al. 1997; Baud et al. 2016). These carbonates were deposited on a subsiding but always-shallow platform and constitute one of the best guidelines for large-scale Mesozoic Alpine reconstitutions. Another feature that seems to be shared all along the Briançonnais s.l. domain is the presence of Early Permian calc-alkaline magmatism (Ballèvre et al. 2020), whose age contrasts with the Carboniferous age of the late-Variscan magmatism in the Helvetic domain (e.g. Bussy and von Raumer 1994; von Raumer et al. 2013; Ballèvre et al. 2018). It is important to carefully distinguish the Briançonnais s.str. and s.l. domains. These two concepts are different and both necessary. The margins of the Triassic outside the Briançonnais s.str. platform, where the carbonates get thinner, are still poorly known and ill-defined but they extend largely beyond those of the Mid-Jurassic uplifted zone that defines the Briançonnais s.str.. On its external (northern) border, the gradual thinning of the typical Triassic Briançonnais s.l. facies until complete disappearance has been emphasized in the Central Alps by Galster et al. (2012). On the internal (southern) border, we fall across the problem of the Prepiedmont domain, to which the Mont Fort nappe is attributed.

There is a considerable confusion in the paleogeographic nomenclature of the domain located between the Briançonnais s.str. rise and the Piedmont oceanic basin (also referred to as Piedmont-Liguria basin by many authors). This historical confusion reflects the difficulty of the subject. Even if reputed authors used the words Briançonnais or Piedmont (sometimes tempered by various adjectives) for designating this intermediate domain, we think it to be preferable to avoid these words because in this context their use carries a great risk of increasing the nomenclatorial disorder. Here we will use the term *Prepiedmont* that was precisely defined in the seminal paper of Lemoine (1961) as a transition from the Briançonnais s.str. Jurassic rise towards the

Piedmont trough. Since then this word has proved useful for describing the paleotectonic evolution of the northern margin of the Piedmont oceanic domain all along the Western Alpine arc (e.g. Caron 1977; Dumont et al. 1984; Marthaler 1984; Dall'Agnolo 1997; Plancherel et al. 1998; Decarlis and Lualdi 2011; Haupert et al. 2016), until the most recent works of Decarlis et al. (2017a, 2017b) and Ribes et al. (2019). Our stratigraphic observations (see further) show that the Prepiedmont domain can be conveniently included as a second order subdivision into the Briançonnais s.l., beside the Subbriançonnais and the Briançonnais s.str. (Fig. 2.3; in agreement with the geodynamic reconstitution of Decarlis et al. 2017a, 2017b): this is a way to reconcile different nomenclatorial propositions.

Type areas for the definition of the Prepiedmont stratigraphy are the Roche-des-Clots series in the French Alps east of Briançon (formerly the Gondran series; Lemoine et al. 1978; Dumont 1983) and the Breccia nappe in the Prealps (Lemoine 1961). This second area is particularly important for our work because of the great similarity between the Breccia and Mont Fort nappes (see further). The Middle Jurassic evolution of the Prepiedmont domain is exactly opposite to that of the Briançonnais s.str.: the Prepiedmont is collapsing and deepening at the very moment when the Briançonnais s.str. is uprising and emerging (cf. Chenin et al. 2019). This is also the time when the Piedmont ocean starts to open (e.g. Bill et al. 1997). A characteristic of the Prepiedmont Jurassic sediments is the abundance of breccias and other coarse-grained detrital sediments generated by this extension at the passive margin.

The *Mont Fort* nappe shows typical features indicating that its paleogeographic origin has to be looked for in the Prepiedmont domain. It was defined by Escher (1988; Escher et al. 1988) as the upper tectonic subdivision of the former Grand St-Bernard (GSB) nappe system, which is the largest tectonic unit in the classical synthesis of the Pennine Alps by Argand (1911). Its name appears more or less simultaneously in the publications of several colleagues, students or visitors

of Escher (e.g. Escher and Masson 1984; Allimann 1987, 1989; Sartori 1987; Woodtli et al. 1987). More recent works emphasize its tectonic independence from the former GSB nappe, from which it differs notably by:

- the absence of a structural connection: following these units towards SW in Italy, they always remain clearly separated (Gouffon 1993; Gouffon and Burri 1997);

- slightly higher pressure during Alpine metamorphism, denoted by the abundance of glaucophane in the metabasites (Wegmann 1922; Vallet 1950; Schürmann 1953; Wust and Baehni 1986; Escher 1988; Thélin et al. 1994; Steck et al. 2001, fig. 1; Bousquet et al. 2004); however a modern mineralogical study is still lacking;

- a Mesozoic sedimentary cover rich in breccias of Jurassic age, characteristic of the Prepiedmont domain (Marthaler 1984; Escher 1988), and definitely distinct from the Briançonnais s.str. and the Subbriançonnais series that characterize the Jurassic of the rest of the former GSB nappe (Ellenberger 1952, 1958; Trümpy 1960; Escher 1988; Sartori 1990).

For all these reasons the Mont Fort nappe is considered a totally independent tectonic unit, distinct from the rest of the GSB nappe system and its subdivisions.

The Mont Fort nappe consists of a thick Paleozoic basement, overlain by a discontinuous and generally thin cover of Triassic-Jurassic sediments called the *Evolène* Series (Escher 1988). This series has been originally considered to represent the sedimentary cover of the Mont Fort nappe, stratigraphically overlying the Mont Fort basement. All our observations support this interpretation. However this view has been strongly debated during the last 25 years and confronted with a different tectonic interpretation according to which the Evolène Series is considered to represent an allochthonous slice with respect to the Mont Fort basement. According to this second model, the basal contact of the Evolène Series would be an Alpine thrust, and this

series would be linked to a different tectonic unit, the Cimes Blanches nappe (e.g. Sartori and Marthaler 1994; Escher et al. 1997; Steck et al. 1999; Tektonische Karte der Schweiz 2005; Sartori et al. 2006). The choice between these two models has major implications for the tectonic reconstitution of the NW Pennine Alps in general. One of the aims of this study is to present the facts that support the stratigraphic interpretation of this contact and to develop its consequences.

The Evolène Series is in turn overlain by a set of calcschists and fine-grained detrital limestones called the *Série Rousse* that is paleontologically dated from the base of the Late Cretaceous (Marthaler 1984). In the working region the Série Rousse forms the lower part of a thick complex of calcschists traditionally called Schistes Lustrés in the Western Alps. The contact of the Série Rousse over the Evolène Series is unconformable and its nature is the subject of current research. We will not treat here the problems posed by the Série Rousse (work in progress). Instead this paper focusses on the Evolène Series and its relations with the Mont Fort basement. Below is a short description of the local units.

2.3. The Mont Fort basement

The Mont Fort basement consists of the following lithostratigraphic units:

1.- The older Mont Fallère unit (Gouffon 1993; Gouffon and Burri 1997) is made of rusty brown, often graphitic micaschists. This unit is poorly represented in the study area.

2.- The Métailler Formation, mainly made of albitic paragneisses, is a thick detrital sequence (greywackes to arkoses and micaschists) with abundant intercalations of metabasites (including pillow basalts and sill-like bodies of gabbros). It forms the core of the nappe (Oulianoff 1954; Schaer 1960; Bearth 1963; Burri 1983; Thélin and Ayrton 1983; Gouffon 1993; Chessex 1995; Gouffon and Burri 1997; Sartori et al. 2006). Its age has long been debated, but recent

LA-ICPMS U-Pb dating of magmatic zircons from two gabbros, at least partially cleared up this debate in yielding ages around 456 to 462 Ma (Ordovician) (Gauthiez et al. 2011).

3.- The Greppon Blanc Fm. is an up to more than 1000 m thick sequence of continental detrital sediments, mainly quartzschists and phyllitic quartzites. It is classically ascribed to the Permian (Schaer 1960). More recently Sartori et al. (2006) defined a Col de Chassoure Fm. which is essentially identical with the Greppon Blanc Fm., but for the fact that its upper limit is placed slightly lower. For our purpose it is more convenient to keep the traditional designation Greppon Blanc with its traditional limits.

A particular feature of the Mont Fort basement is the absence of granitic intrusions, in contrast with the rest of the former GSB nappe and other Penninic nappe basements where Paleozoic granites are always present (e.g. Bearth 1964a; Bussy et al. 1996a; Genier et al. 2008; Scheiber et al. 2014; Bergomi et al. 2017; Ballèvre et al. 2018, 2020). However a few intercalations of rhyolitic flows and ignimbrites, of Early to Middle Permian age, occur above the base of the Greppon Blanc Fm. (Bussy et al. 1996b; Derron et al. 2006; Sartori et al. 2006).

2.4. The Evolène Series: stratigraphic synthesis and new data

2.4.1. Introduction

The Evolène Series directly overlies the Mont Fort basement. Along the normal limb of the Mont Fort nappe, the Evolène Series is discontinuous and often incomplete or absent (Fig. 2.1). We will argue that such absences are due to Jurassic erosion and/or to paleofaults. The Evolène Series is best developed around the frontal folds of the Mont Fort nappe. It is lacking in the overturned limb of the nappe (Fig. 2.1).

Figure 2.4a presents a synthetic theoretical column based on combining and crosschecking all local observations.

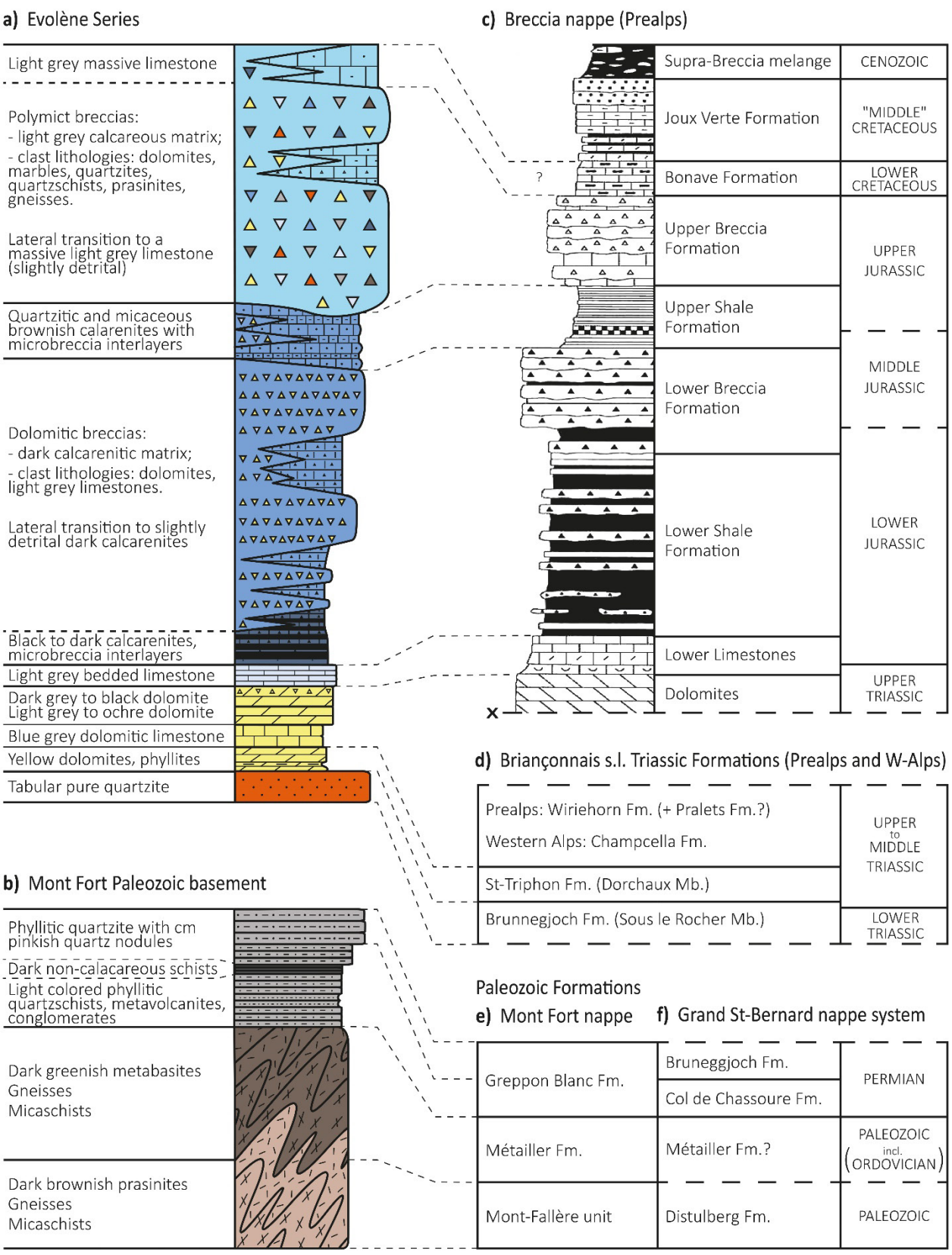

Fig. 2.4 Stratigraphy of the Evolène Series and Mont Fort basement compared to the Prealps and the rest of the former GSB nappe. **a** Synthetic stratigraphic column of the Evolène Series. **b** Synthetic stratigraphic column of the Mont Fort Paleozoic basement. **c** Synthetic stratigraphic column of the Breccia nappe in the Prealps (modified after Dall'Agnolo 1997, 2000). **d** Triassic Formations of the Briançonnais s.l. domain (Prealps and Western Alps). Only the Briançonnais Triassic Formations having an observed equivalent in the Mont Fort nappe are listed. **e** Geological Formations defined in the Mont Fort Paleozoic basement. **f** Geological Formations defined in the GSB Paleozoic basements. Scales in a to e are different and arbitrary.

Thickness of the layers is extremely variable, both because of irregular sedimentation on a tectonically active, very mobile basin floor, and because of subsequent Alpine deformation. Relative thicknesses given in Fig. 2.4a are very approximate and often arbitrary because of the high amount of strain during Alpine deformation.

Robust stratigraphy is a prerequisite for unravelling tectonic structures and paleogeography. Like in many other parts of the Penninics, the stratigraphy of the Evolène Series was for long a mystery because of poverty in biostragraphically significant and well preserved fossils and because of the blurring of the sedimentary record by strong Alpine deformation. However, fortunately enough several portions of the Penninic Mesozoic sedimentary covers were "décollées", transported and piled up in the foreland of the belt, particularly in the Prealps (Fig. 2.2). There they escaped most of the metamorphism and deformation. In these external zones, their study can provide useful clues on the stratigraphy of the sediments that originally bordered them but remained attached to their Penninic basement. In the case of the Triassic-Jurassic Evolène Series, two nappes of the Prealps provide crucial details for comparison: (1) regarding the Triassic, the Préalpes Médianes Rigides nappe appears to be relevant for comparison as it displays one of the most complete and typical Triassic stratigraphic sequences of the Briançonnais-derived units of the Prealps (e.g. Ellenberger 1952; Trümpy 1954; Botteron 1961; Mégard-Galli and Baud 1977; Baud and Septfontaine 1980; Hürlimann et al. 1996); (2) regarding the Jurassic, a comparison with the Breccia nappe derived from the Prepiedmont domain (Lemoine 1961; Weidmann 1972; Plancherel et al. 1998) provides a solid base for stratigraphic analysis.

2.4.2. Triassic of the Evolène Series: affinities with the Briançonnais s.l.

The Triassic of the Evolène Series starts with a level of pure white tabular quartzite, similar to the basal quartzite that is classical in many other Penninic cover series and traditionally ascribed to the Lower Triassic. In the Prealps Sartori et al. (2006) named this level the Sous le Rocher

Member. At Evolène, if not thickened by folding, its thickness varies from 0 to 20 m, much thinner than in the typical Briançonnais s.str. series. Original thickness variations (down to local absence) can be appropriately explained by the gradual transgression of the sea upon the weak paleorelief of the Triassic peneplain.

The base of the Triassic tabular quartzite always lies with a concordant contact on top of the uppermost layers of the Greppon Blanc Fm. represented by phyllitic quartzites. A progressive transition between the two lithologies can be observed by a gradual decrease of the phyllitic component on a few dm (Allimann 1987, 1990). A similar transition is commonly observed at the Mesozoic/Paleozoic contact in the rest of the GSB nappe system (e.g. Sartori 1990; Sartori et al. 2006; Genier et al. 2008).

The tabular quartzite of the Evolène Series is followed by a carbonate sequence, mainly dolomite, whose thickness never exceeds a few tens of meters, again much thinner than in the Briançonnais s.str.. At its base it may contain very thin quartzo-micaceous bands suggestive of pelitic intercalations, a fact often observed at the base of the Briançonnais carbonate sequence (Dorchaux Member; Baud 1987). This dolomite can be accompanied by cornieule (rauhwacke), at one point by gypsum (pinched in the synclinal core of a frontal fold above Evolène; Allimann 1990) and by limestones that provide more precise stratigraphic indications. The best outcrops are observed in the cliffs of the torrent NE of Evolène (Allimann 1990). There we note the occurrence of a several meters thick layer of grey-bluish, finely laminated limestone similar to the “calcaire rubané” of the Champcella (or Wiriehorn) Fm. of the Briançonnais Triassic in the French Alps and the Prealps. This formation has been recently assigned to the Late Anisian (early Middle Triassic; Baud et al. 2016). Another noteworthy feature is the occasional presence of blocks of typical Briançonnais Triassic limestones reworked in the Jurassic breccias of the Evolène Series, in particular fossiliferous and vermiculated limestones (Allimann 1987, 1990; A. Baud,

A. Escher and P. Viredaz, pers. comm.; a sample containing well preserved *Physoporella* is deposited at the Sion Museum, courtesy of N. Kramar). Some of these rocks are very characteristic of the Saint-Triphon Fm. defined in the Prealps (Early to Middle Anisian; e.g. Mégard-Galli and Baud 1977; Baud 1987).

To conclude, the Triassic of the Mont Fort nappe displays a facies identical to that of typical Briançonnais s.str. occurrences, but with a much reduced thickness. This fits well with its position at the border of a platform, progressively flooded by the transgression of the sea near the southern limit of the Briançonnais s.l. Triassic domain. In the Mont Fort nappe these formations have been largely attacked by erosion during the Early to Middle Jurassic.

2.4.3. Jurassic of the Evolène Series: signification of the Jurassic breccias

The Jurassic of the Evolène Series is characterized by thick layers of breccia deposited over much thinner series of limestones and marls. The latter start with a m-thick level of light grey, bedded, sometimes oolitic limestone. In the Prealps a similar level is attributed to the earliest Jurassic (Hettangian; Chessex 1959). This level is overlain by fine-grained, generally dark, (dolo)calcarenites and marls of variable thickness, coarsening upwards and gradually passing to the breccias. Older authors already mentioned the presence of breccias in this position, e.g. in the Pic d'Artsinol, Sasseneire and Mauvoisin areas (Joukowsky 1907; Wegmann 1922; de Szepessy Schaurek 1949; Hagen 1951). The great analogy of the breccias of the Evolène Series with those of the Breccia nappe in the Prealps has been pointed out several times (Joukowsky 1907; Escher 1988; Escher et al. 1997; Sartori et al. 2006; Marthaler et al. 2008b). Our study enhances the similarity of the Evolène breccia layers with the Jurassic of the Breccia nappe in the Prealps.

In the Prealps it is modern practice to still use the old stratigraphic nomenclature of Lugeon (1896; e.g. Chessex 1959; Weidmann 1972; Dall'Agnolo 1997; Plancherel et al. 1998). The Jurassic

columns of the Mont Fort and Breccia nappes are so similar that this practice has been successfully extended to the Evolène Series (Fig. 2.4). This figure 2.4 will exempt us from a detailed description. Below we only add the following remarks:

1.- A commonly accepted mechanism for the origin of these submarine, often massive breccias has been proposed in the classical works of Trümpy (1960), Lemoine (1967) and Weidmann (1972): their genesis would result from very active extensional faulting followed by the collapse of fault scarps and the transport of the debris on the bottom of the sea by various kinds of gravity-driven down-slope currents. Certainly, this mechanism is very plausible, but in the areas discussed here (Mont Fort and Breccia nappes) the existence of important faults of Jurassic age has rarely been confirmed by direct field observations. Our work will show that these faults are indeed well developed, but, because of intense Alpine deformation, they remained unrecognized until nowadays.

2.- The Lower Breccia (late Early to Middle Jurassic) and the Upper Breccia (latest Jurassic) represent distinct events, always separated by a time interval (estimated at ca. 10 Ma in the case of the Breccia nappe) that is dominated by pelitic to fine-grained detrital sedimentation. The formation of the oldest Piedmont ophiolites (166 Ma, on the OCT in the Gets nappe; Bill et al. 1997) is approximately synchronous with the last episodes of deposition of the Lower Breccia. These deposits thus mark the final break-up of the continental crust. The youngest preserved Piedmont ophiolites (155 Ma, in the Tsaté nappe; Decrausaz et al. 2021) fall into the period of relative quiescence between the two Breccia Formations. This means that at that time the continental margin was stabilized and that extension was localized in the exhumed mantle. However, the geodynamic interpretation of the movements that generated the Upper Breccia remains enigmatic.

3.- The nature of the components of the breccias reflects the progressive erosion of the source areas. Thus the breccias display a kind of "inverse stratigraphic column" of the source areas. The first layers of breccia are often made only of dolomitic Triassic clasts, tightly packed in a rare, very fine-grained matrix (Fig. 2.5a). These monomict breccias can be very easily confused with a genuine Triassic dolomite ("reconstituted" or "regenerated Triassic" in the sense of Lemoine 1967), and this confusion has sometimes been an important cause of mistakes even in the non-metamorphic and little deformed Breccia nappe in the Prealps. This is still more the case in the strongly deformed Mont Fort nappe, where the distinction of the Jurassic Breccia from the Triassic dolomite can become extremely difficult and the resulting confusions may lead to a gross overestimation of the amount of Triassic formations. The clasts of Lower Triassic quartzites and Paleozoic basement rocks (Figs. 2.5b and 2.5c) only become frequent higher up, particularly in the Upper Breccia.

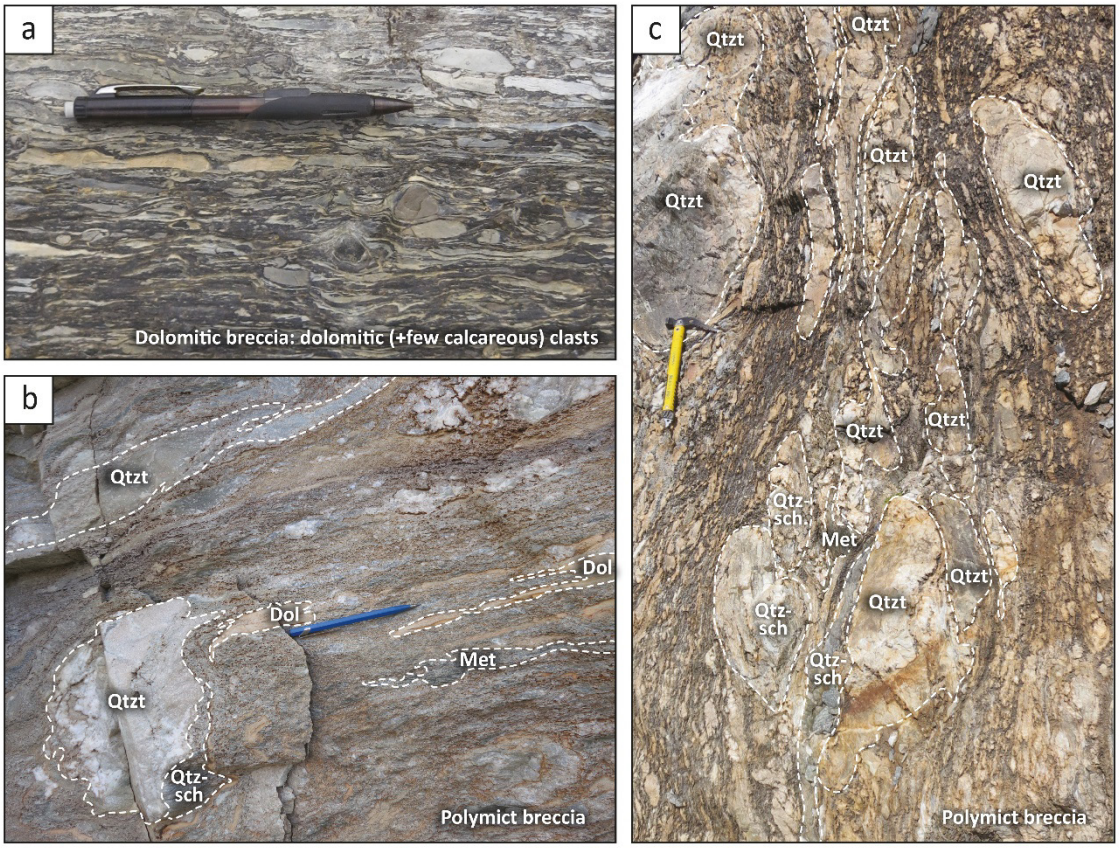

Fig. 2.5 Typical facies of the Evolène Series breccias. **a** Matrix-supported dolomitic breccia: clasts are mainly dolomitic; matrix is dark and calcarenitic [599'460/107'270]. **b** Clast-supported polymict breccia [595'370/101'930]. Main clasts lithologies: pure quartzite (Qtzt), quartzschists (Qtz-sch), metabasites (Met) identical to those of the Métailler Fm. (Mont Fort basement), dolomites (Dol). **c** Clast-supported coarse polymict breccia. Block fallen from the Pointe du Vasevay southern face [593'810/097'240].

2.5. Alpine thrust or deformed normal faults?

2.5.1. The cover/basement contact: stratigraphic or tectonic?

As mentioned above, the contact of the Evolène Series upon the Mont Fort Paleozoic basement was initially considered as stratigraphic (e.g. Wegmann 1922; Allimann 1987; Escher 1988). However several authors soon proposed that it would be a tectonic contact, namely an Alpine thrust (e.g. Sartori and Marthaler 1994; Steck et al. 1999; Sartori et al. 2006; Marthaler et al. 2008b). This second interpretation rapidly became dominant in the literature and official documents (e.g. Tektonische Karte der Schweiz 2005).

It is based on the fact that the contact is often discordant at the map scale, with a small angular obliquity on both sides of the discontinuity: (1) on one side the Mesozoic Evolène Series can overly various levels of the Paleozoic basement; and (2) on the other side various levels of the Mesozoic series can form its base and rest over the basement (Figs. 2.6-10). The angular obliquity between basement and cover is usually small, not exceeding a few degrees. It is understandable that, at first sight, this situation might give the impression of a tectonic contact representing a low-angle thrust fault.

In the framework of the tectonic interpretation of this contact, the Evolène Series was considered as allochthonous with respect to the Mont Fort basement and would belong to a distinct tectonic unit, namely the so-called Cimes Blanches nappe (e.g. Sartori and Marthaler 1994; Escher et al. 1997; Steck et al. 1999; Sartori et al. 2006). However some of these authors left small basal portions of the Evolène Triassic in the Mont Fort nappe. The type locality of the Cimes Blanches nappe is found elsewhere, namely in the Cime Bianche summits located southeast of the Dent Blanche nappe (Fig. 2.1). These summits exhibit one of the largest outcrops of a slice of metasediments well exposed around and south of Zermatt, the Pancherot - Cime Bianche - Bettaforca Unit (Dal Piaz 1988, 1999; Vannay and Allemann 1990). Stratigraphy, internal

structure and origin of this unit are still poorly known and problematic (Dal Piaz et al. 2015a; Steck et al. 2015; Passeri et al. 2018; work in progress). In any case it is important to note that the Pancherot – Cime Bianche – Bettaforca occurrences of the Cimes Blanches nappe are totally disconnected from the Evolène Series in map and profile view (Figs. 2.1 and 2.2).

We are thus confronted with a conflict between two opposite interpretations of the contact between Mont Fort Paleozoic basement and overlying cover of Mesozoic sediments: stratigraphic or tectonic? We will present new field observations that support the stratigraphic interpretation. In other words we will show that the Evolène Series is the original autochthonous cover of the Mont Fort basement. But we will also show that the geometry of the contact has been deeply influenced, first by the activity of synsedimentary normal faults, then by the subsequent deformation of these faults during the Alpine orogeny. The key factor for our interpretation is the demonstration that the angular discordance of these normal faults with bedding was erased by Alpine tectonic strain.

Fig. 2.6 The Mont Fort nappe and surrounding tectonic units in SW Switzerland. Own data completed with a synthesis of the existing maps (Allimann 1990; Burri et al. 1998; Gabus et al. 2008; Sartori and Epard 2011; Sartori et al. 2011; Swisstopo Geocover mapping; and the unpublished diploma theses of the University of Lausanne from: Moix and Stampfli 1980, Rey 1992, Kramar 1997, Baillifard 1998, Favre 2000 and Glassey 2013). The location of the outcrops of Fig. 2.12 are indicated by **Fig. 2.12a**, **Fig. 2.12b**, etc. The location of the logs of Fig. 2.15 is indicated by **L1-L14**. The position of the cross-sections of Figs. 2.8 and 2.10 is labeled **B-B'**, **C-C'** and **D-D'.** ►

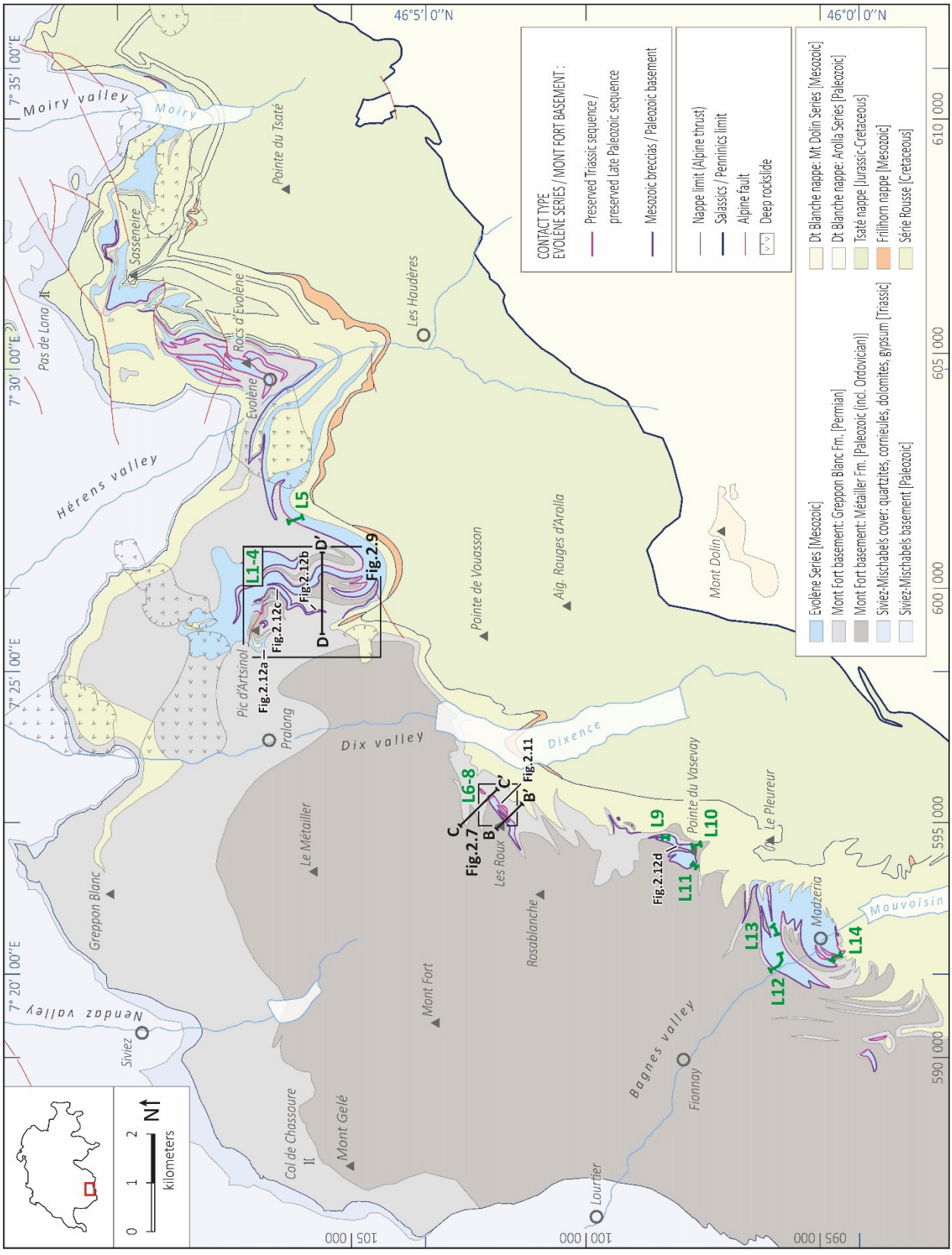
46°5' 0"N
46°0' 0"N
7° 35' 00"E
7° 30' 00"E
7° 25' 00"E
7° 20' 00"E
610 000
605 000
600 000
595 000
590 000
095 000
100 000
105 000
Moiry valley
Moiry
Pointe du Tsaté
Sasseneire
Pas de Lona
Rocs d'Evolène
Evolène
Les Haudères
Hérens valley
L5
L1-4
Fig.2.12b
Fig.2.12c
Fig.2.12a
Fig.2.9
D
D'
Pic d'Artsinol
Pralong
Pointe de Vouasson
Aig. Rouges d'Arolla
Mont Dolin
Dix valley
Dixence
L6-8
Fig.2.7
Fig.2.11
B
B'
C
C'
Le Métailler
Les Roux
Pointe du Vasevay
L9
L10
L11
Fig.2.12d
Le Pleureur
Greppon Blanc
Rosablanche
Madzeria
Mauvoisin
L13
L14
L12
Nendaz valley
Siviez
Mont Fort
Bagnes valley
Fionnay
Col de Chassoure
Mont Gelé
Lourtier
CONTACT TYPE
EVOLÈNE SERIES / MONT FORT BASEMENT :
Preserved Triassic sequence / preserved Late Paleozoic sequence
Mesozoic breccias / Paleozoic basement
Nappe limit (Alpine thrust)
Salassics / Penninics limit
Alpine fault
Deep rockslide
Dt Blanche nappe: Mt Dolin Series [Mesozoic]
Dt Blanche nappe: Arolla Series [Paleozoic]
Tsaté nappe [Jurassic-Cretaceous]
Frilihorn nappe [Mesozoic]
Série Rousse [Cretaceous]
Evolène Series [Mesozoic]
Mont Fort basement: Greppon Blanc Fm. [Permian]
Mont Fort basement: Métailler Fm. [Paleozoic (incl. Ordovician)]
Siviez-Mischabels cover: quartzites, cornieules, dolomites, gypsum [Triassic]
Siviez-Mischabels basement [Paleozoic]
0
1
2
kilometers
N

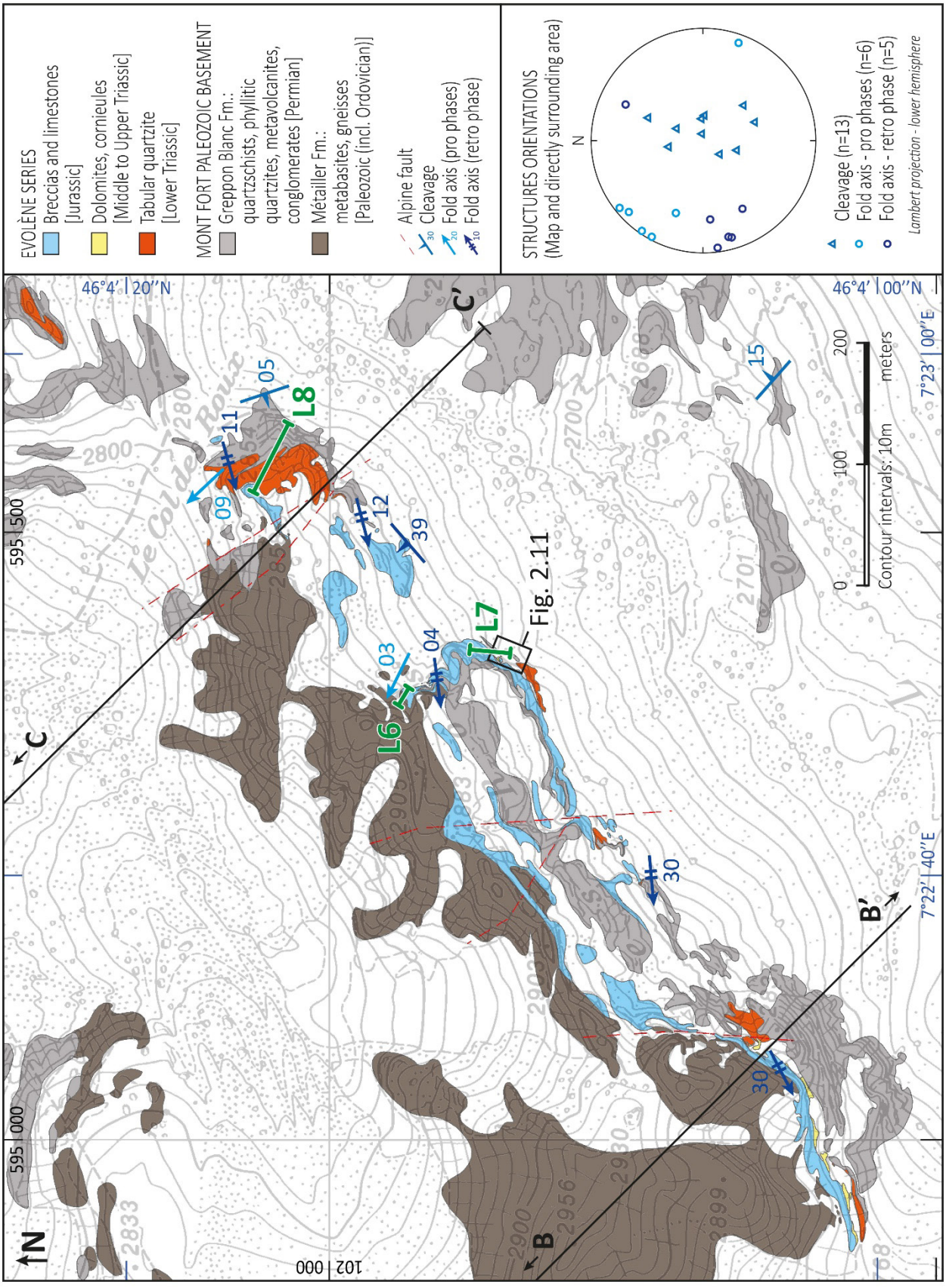

Fig. 2.7 Detailed geological map of the Roux area (Dix valley); for location see Fig. 2.6. Own data completed with a synthesis of the existing maps (Swisstopo Geocover mapping; Rey 1992, unpublished diploma thesis, University of Lausanne). B-B' and C-C' refer to the cross-sections of Fig. 2.7. **L6-L8** refer to the logs of Fig. 2.15. Topographic base ©1990 Cadastre VS.

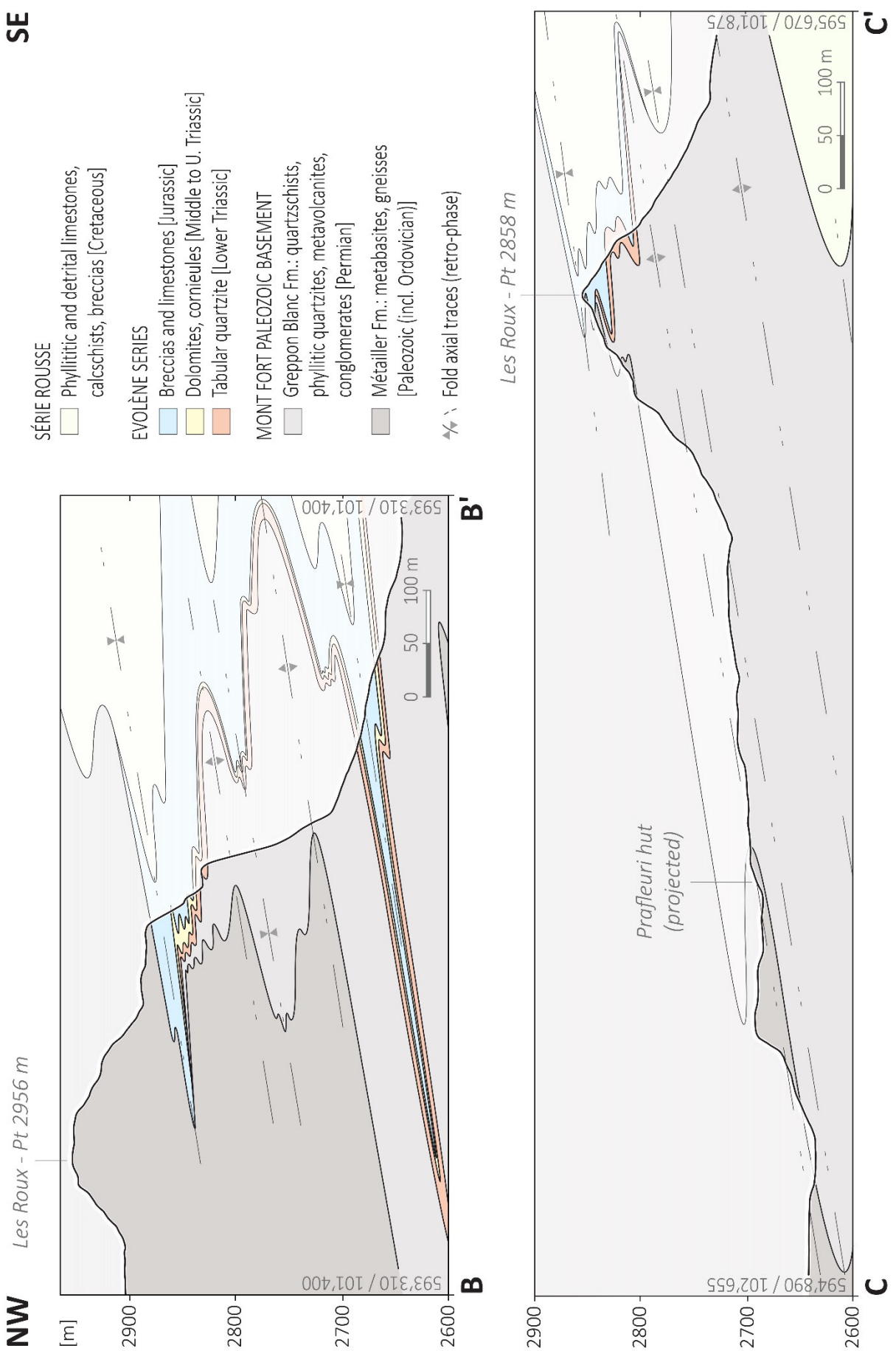

Fig. 2.8 Cross-sections through the Roux area (Dix valley); for location see Figs. 2.6 and 2.7.

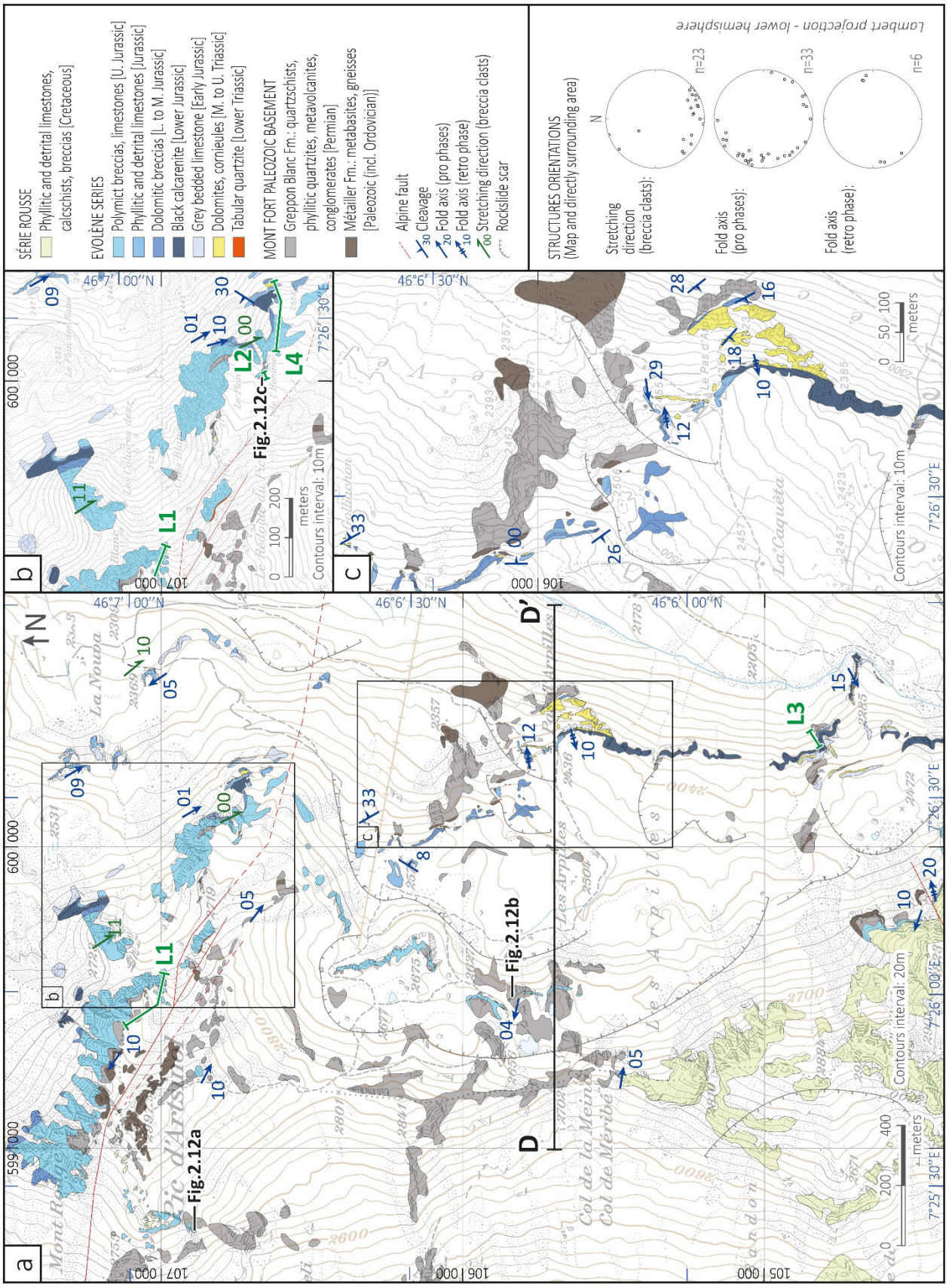

Fig. 2.9 Detailed geological maps of the Artsinol area (Hérens and Dix valleys). Own data completed with a synthesis of the existing maps (Allimann 1990; Swisstopo Geocover mapping; and the unpublished diploma theses of the University of Lausanne from Moix and Stampfli 1980 and Kramar 1997). **Fig. 2.12a**, **Fig. 2.12b**, etc. refer to the locations of the outcrops of Fig. 2.12. **D-D'** refer to the cross-section of Fig. 2.10. **L1-L4** refer to the logs of Fig. 2.15. **a** General map. Topographic base ©swisstopo (BA20045). **b** Detailed map of the Plan de l'Homme area. Topographic base ©1990 Cadastre VS. **c** Detailed map of the Pas d'Arpilles area. Topographic base ©1990 Cadastre VS.

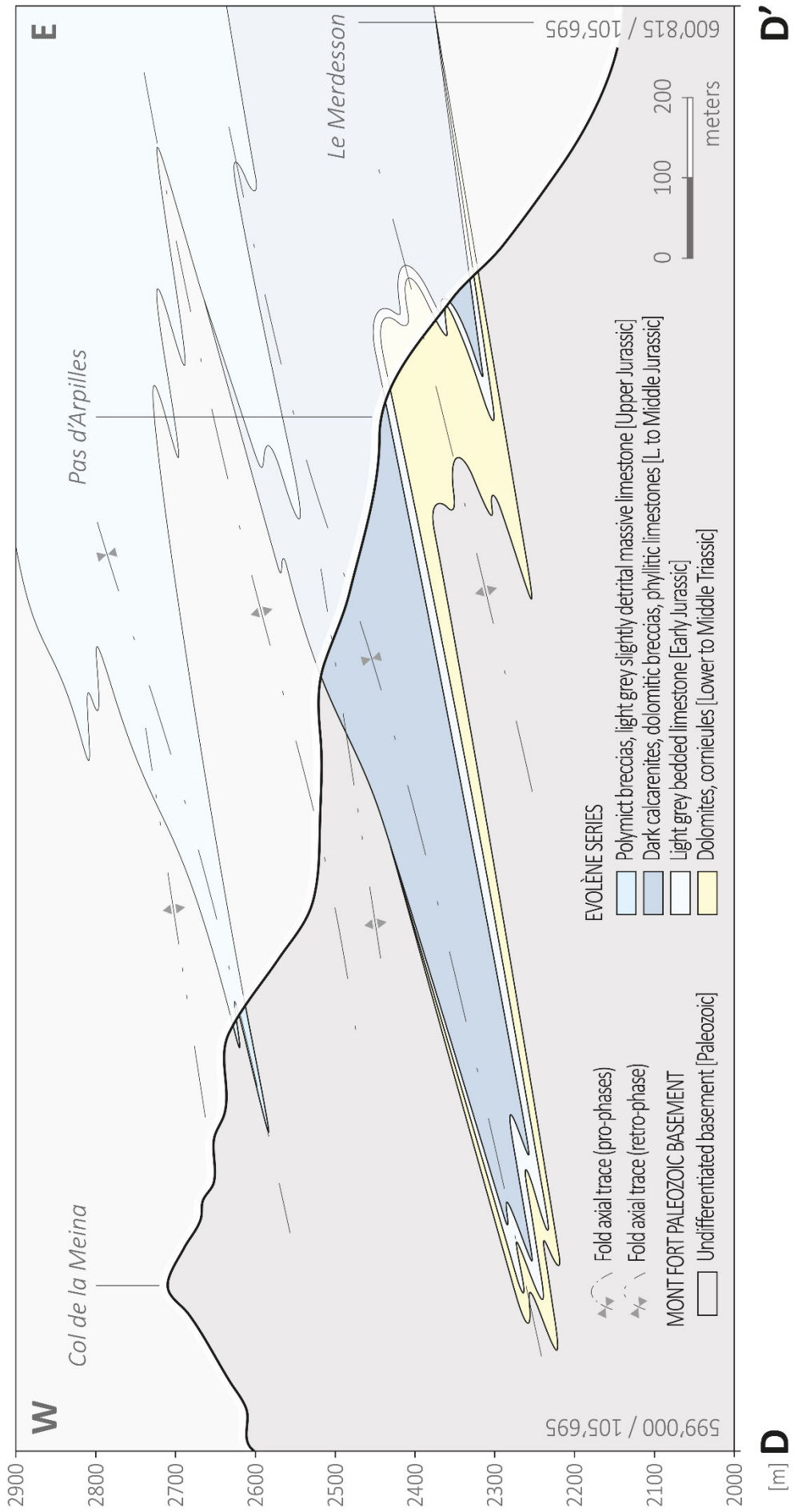

Fig. 2.10 Cross-section through Les Arpilles and Col de la Meina, in the Artsinol area (Hérens valley) based on the cross-section from Kramar 1997 (unpublished diploma thesis, University of Lausanne); for location see Fig. 2.9.

2.5.2. The case of a concordant contact

The basal contact of the Evolène Series is not always discordant on top of the underlying basement. Locally it can also be concordant and reveal a complete stratigraphic sequence on both sides, without any important gap with respect to the reference column of Fig. 2.4. Here we present an example that is observable in the Roux area (Fig. 2.11).

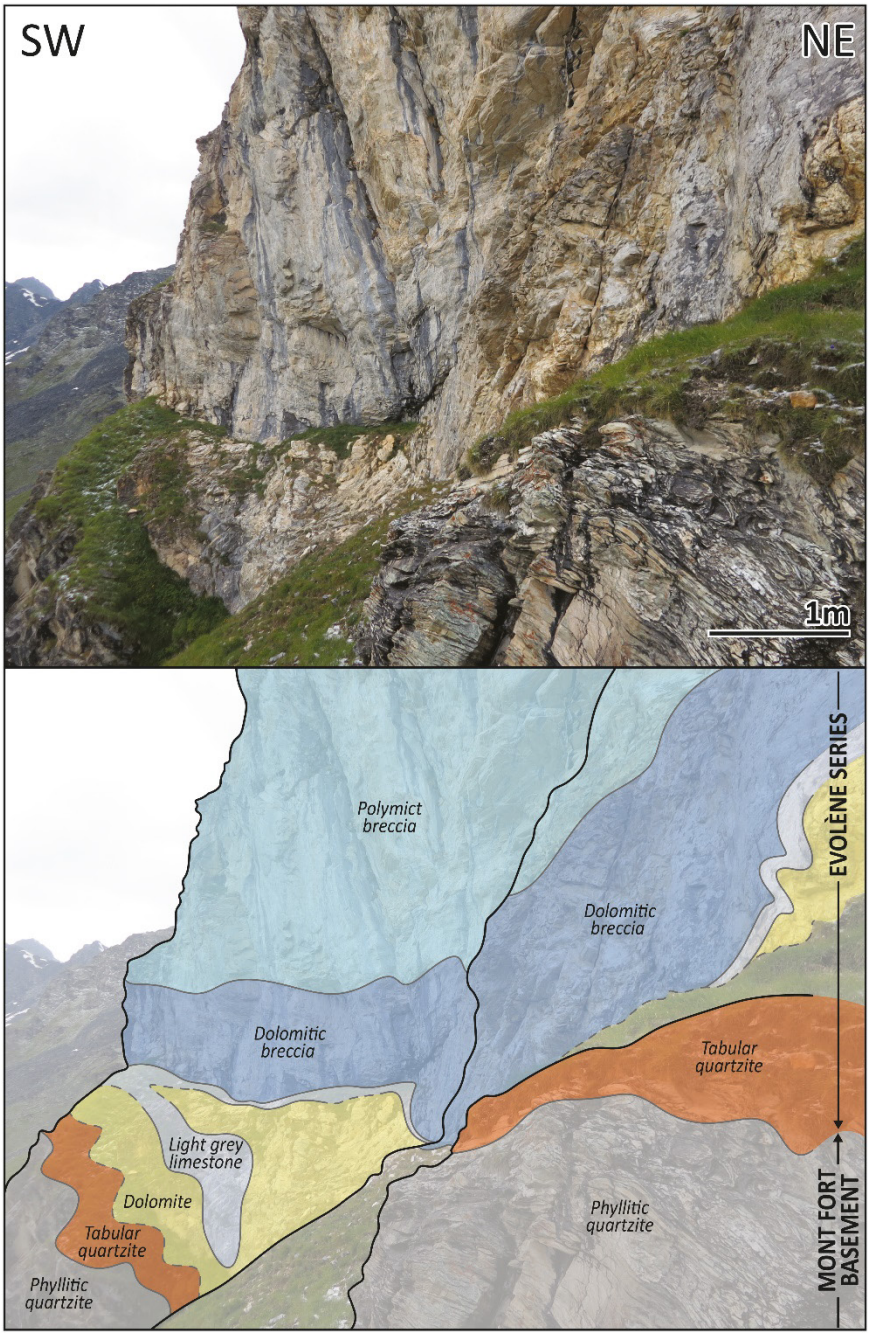

Fig. 2.11 Contact of the Mesozoic Evolène Series over the Mont Fort Paleozoic basement in the Roux area at locality [595'420/101'870] (cf. Figs. 2.6-8). The basement is formed by a phyllitic quartzite that belongs to the uppermost levels of the Permian Greppon Blanc Fm.. The cover exposes the normal succession of the L. Triassic pure quartzite, M. to U. Triassic dolomite, Early Jurassic bedded limestone and the thick L. to U. Jurassic breccias. The contacts between the formations are concordant although affected by a strong Alpine deformation.

This outcrop exposes the normal superposition of all the stratigraphic formations from the Permian Greppon Blanc Fm. in the basement, up to the Jurassic breccia in the cover. Although these rocks are all affected by a rather strong Alpine deformation, no formation is missing. We note that the base of the Mesozoic sequence is essentially complete and relatively well preserved. The type and the intensity of deformation along, or in the vicinity of the contact, are similar to those in the rest of the outcrop. There is no hint of any important translation of the Evolène Series with respect to the basement. We can repeat the same observations at several places along the contact (sections of the contact outlined in pink on Fig. 2.6).

2.5.3. The case of a basal gap

As mentioned above, the superposition of the Mesozoic Evolène Series over the Mont Fort Paleozoic basement is frequently discordant, with an angular obliquity of a few degrees, often only noticeable at the map scale (Figs. 2.6-10). This obliquity causes a gap of variable importance along the cover/basement contact, such that any layer of the Evolène Series, Triassic or Jurassic, may rest upon the Mont Fort Paleozoic. This discordance has been at the origin of the proposition that this contact is a thrust and corresponds to a nappe boundary. However, like in the concordant case, we do not observe abnormally high deformation along this discontinuity of the sort we could expect if it would separate two tectonic units. There is no particular increase in strain intensity, no hint of more intense shearing of the rocks. At the microscopic scale, the contact is sharp and shows no particular mark of movement (Fig. 2.12 a and b). We did not observe any structure that would suggest that this contact is an Alpine thrust.

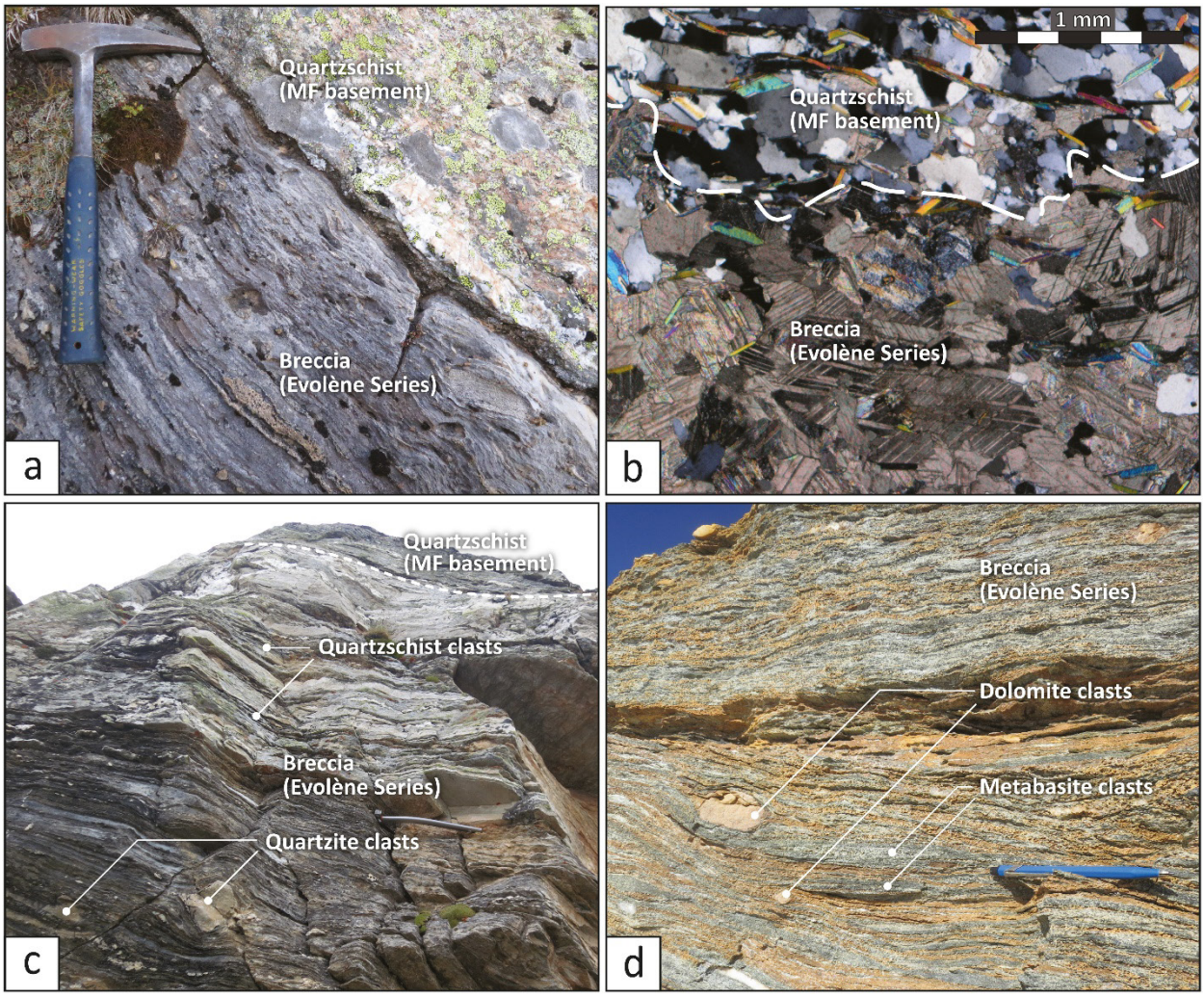

Fig. 2.12 Contacts between the Evolène Series Jurassic breccias and the Mont Fort Paleozoic basement. **a** Overturned contact between the Evolène U. Jurassic polymict breccia and the Mont Fort Permian quartzschists [598'730/106'890]. Note the absence of mylonitic levels or abnormal rock deformation at contact. Location on Fig. 2.9a. **b** Same type of contact, observed in thin-section (cross-polarized light), [599'440/105'890]. No abnormal deformation is observed even at the grain scale. Location on Fig. 2.9a. **c** Overturned contact between the Evolène U. Jurassic polymict breccia and the Mont Fort Permian quartzschists [600'010/106'750]. Within the first 3 m from the contact, the breccia is very rich in quartzschist clasts (reconstituted basement). Location on Fig. 2.9b. **d** Evolène U. Jurassic polymict breccia showing an abundance of metabasite clasts [594'470/098'040]. The clast lithology is identical to that of the Mont Fort metabasites (Métailler Fm.), which are outcropping less than 10m away. Location on Fig. 2.6.

2.5.4. Local source of the clasts

We already noted that the clasts of the Evolène breccias reproduce an "inverse stratigraphy" of the source areas. It is customary that the Jurassic erosion first destroyed the Mesozoic carbonates before attacking the basement, an evolution that eventually gave birth to the polymict rocks that are much more abundant higher in the column. This applies particularly to those breccias whose basal contact is concordant and whose sequence respects the stratigraphic order. However, when discordances and gaps put the polymict breccias in direct contact with the Paleozoic basement,

it is interesting to note that the composition of this local basement exerts a control over the nature of the clasts, as already noted by Allimann (1987). For instance, when in contact with quartzschists of the Mont Fort Greppon Blanc Fm., the breccia is often rich in quartzschist clasts (Fig. 2.12c). When in contact with the Mont Fort Métailler Fm., the polymict breccia generally contains metabasite elements (Fig. 2.12d). In the same order of ideas, it is striking that the Evolène breccias, that surmount a basement exceptionally poor in Paleozoic granites, never contain clasts of granite, contrary to other Penninic detrital series that often contain material of granitic origin. A similar correlation between the clasts of the breccias and the rocks exposed in the neighboring basement has been noted in the Prepiedmont domain of the French Alps by Lemoine (1967).

2.6. Discussion: passive ductile orogenic deformation of synsedimentary faults

The concordant contacts are clearly stratigraphic. Not only are they the base of essentially complete sequences (with respect to the reference stratigraphic column Fig. 2.4), but also they never display any hint of translation or unusual shear movement. This type of contact, although it can only be observed in good conditions at a few places, is crucial for the regional interpretation. These places are like pins that fix the Evolène Series to the underlying basement. It would be extremely difficult to imagine a mechanism that would fix the cover at some places and authorize large displacements at others. This constitutes a very strong argument for the autochthony of the Evolène Series as a whole, over the Mont Fort basement.

This interpretation is confirmed by the local provenance of the detrital material. This observation strongly suggests that the Evolène breccias formed in close vicinity of the parts of the Mont Fort basement with which they are today in contact. In other words, this proofs that this contact is original and stratigraphic.

The above-mentioned observations support the stratigraphic interpretation of the concordant as well as discordant contacts. However, an explanation of the frequent gaps and discordances is needed. The absence of any particular deformation along most surfaces marking a lithological discontinuity suggests that these surfaces existed before the deposition of the sediments that surmount them. On the other hand, the fact that the same discontinuities cut large parts of the stratigraphic column implies that they must be younger. This apparent contradiction is interpreted to mean that these discontinuities are semi-contemporaneous in respect to the deposition of the breccias. The formation of the Evolène breccias can thus be considered as a consequence of the movement along these discontinuities, by coupled erosion and deposition.

A straightforward explanation of such gaps and discordances would be stretching by normal faulting of the area forming the future Mont Fort nappe predating Alpine folding and thrusting. An episode of brittle faulting during Jurassic times would be in agreement with commonly accepted views on the paleotectonic evolution of the Alpine Tethys and its margins. In the case of our working area the interpretation of such discontinuity surfaces in terms of normal faults is not obvious because the observed obliquity to the layering is usually very small. This is probably the reason why they have not been recognized as such previously.

The strain related to Alpine shortening in all these rocks is so strong that the original angular relationships are only rarely preserved. Alpine deformation is indeed spectacular, both at the hm to km scale, as is revealed by the tight folding of the whole stratigraphic sequence (Figs. 2.8 and 10), and, at the cm to dm scale, by the shapes of the clasts (Figs. 2.5 and 2.12).

The theory of the deformation of oblique surfaces by tectonic strain has been developed by Ramsay (1967 chap. 9). This author demonstrated that, in general, increasing strain results in a progressive obliteration of angular discordances (in special cases the obliquity can increase, but in practice this is rare). This theory has been extensively applied, most notably to the deformation of

discordant dykes in high-grade rocks. These dykes are gradually parallelized to older structures such as bedding and foliation (Escher et al. 1975; Escher and Watt 1976). Faults are planar markers that respond to later strains the same way: their obliquity is gradually erased by increasing strain until they become subparallel to the stratigraphic layering (Figs. 2.13 and 2.14). If applied to normal faults, this evolution will generate a situation where these faults will be, at first sight, easy to confuse with thrusts, all the more since the trace of the fracture in the basement can be very difficult to detect. This geometric transformation can be modeled by software that treats this problem in a rigorous quantitative way, as discussed in the next chapter.

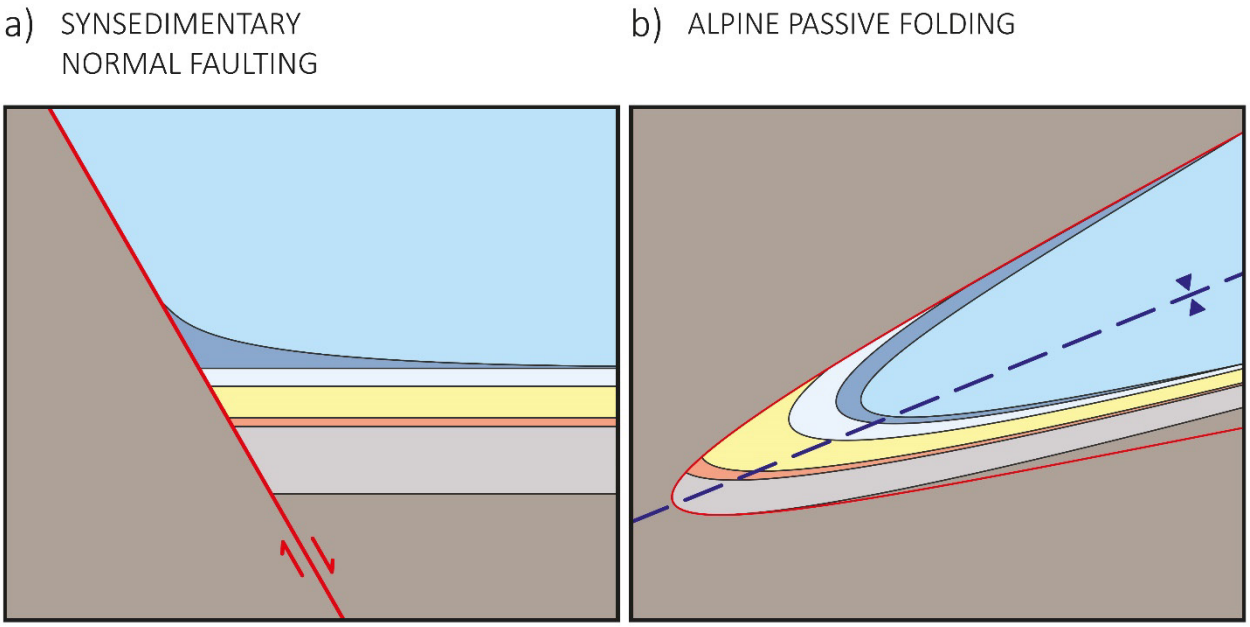

Fig. 2.13 Conceptual model of passive deformation of a pre-existing discordance. Conceptual model of passive deformation of a pre-existing discordance. **a** Initial geometry resulting from the movement of a high-angle synsedimentary normal fault. **b** Transformation of the initial geometry by heterogeneous simple shear (sinusoidal function). Modeling was performed using the Shear2F software (Rey 2002).

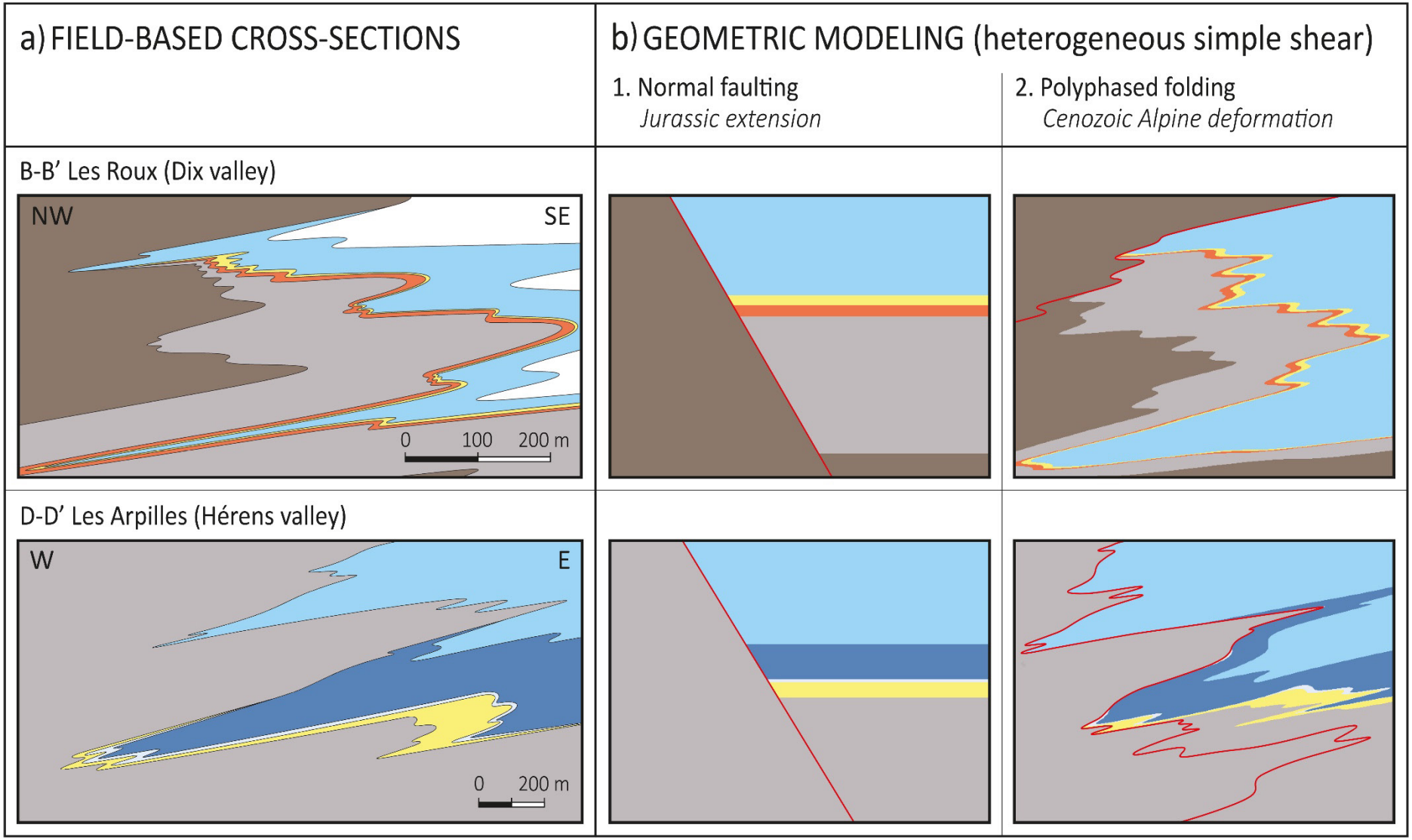

Fig. 2.14 Pre-folding restoration of the cross-sections of Figs. 2.8 and 2.10 by geometrical modeling. Pre-folding restoration of the cross-sections of Figs. 2.8 and 2.10 by geometrical modeling. **a** Simplified cross-sections B-B' and D-D' (Figs. 2.8 and 2.10). **b** Geometric models obtained by heterogeneous simple shear superimposed on an initial normal fault. Modeling performed with Shear2F software (Rey 2002). Model outputs are vertical cross-sections through the 3D models. Detailed parameters of the applied deformations are given in the Additional files. This demonstrates that the observed present-day geometry can be obtained by folding on an initial normal-fault.

An important vertical component of movement along these faults is revealed by the paleobathymetric evolution of the Prepiemont domain during Jurassic (from shallow to deep-water sediments) and by the evolution of the source of the clasts (from younger to older). A horizontal, transcurrent component is also possible, but we have no way to reckon it.

During Alpine shortening our synsedimentary normal faults behaved like *passive markers* of strain. This merits to be underlined, because it is in contrast with numerous cases described in the literature where pre-existing faults are remobilized, often with a different sense of movement, e.g. normal faults inversed as thrusts (cf. Bonini et al. 2012 and references therein). Indeed such cases of remobilization of an older fault are by far the most frequently described ones and have become classical. This is, however not the case in the Mont Fort nappe, where older faults are deformed without being reactivated. We do not doubt that remobilization of pre-existing discontinuities may frequently occur elsewhere. However, we also think that the occurrence of ductile, passive deformation of faults has been underestimated. This mechanism might play an important role when the deformation takes place at depth in a thick-skin type tectonic context (cf. Epard and Escher 1996; Lafosse et al. 2016; Spitz et al. 2020). In all the examples presented here, Alpine deformation of the Jurassic synsedimentary faults is passive. This is not completely new: other examples of passive ductile deformation of paleo-normal faults have been described in the Alps, e.g. in the Helvetic realm by Krayenbuhl and Steck (2009) who showed how ductile folding of normal fault blocks, without reactivation, can generate structures that at first sight simulate thrusted slices.

The areas located in the normal limb of the Mont Fort nappe where the Evolène Series is missing (Fig. 2.6) correspond to the sectors where the fault scarps were exposed on the bottom of the sea, but were too steep to keep the syn- to post-faulting sediments (Fig. 2.15). In these sectors the Mont Fort basement is today covered either by post-Jurassic sediments or by a higher tectonic unit.

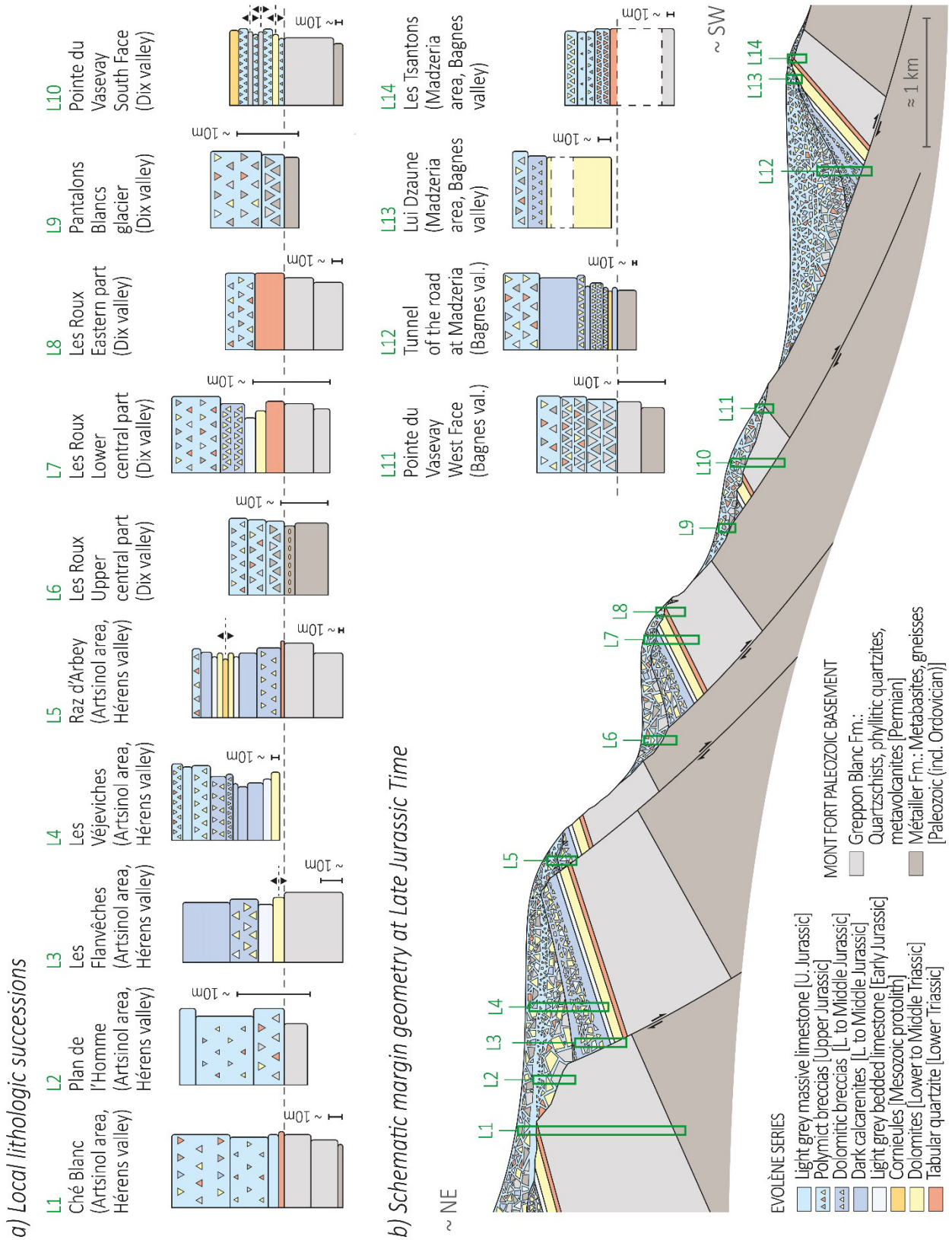
a) Local lithologic successions
L1 Ché Blanc (Artsinol area, Hérens valley)
L2 Plan de l'Homme (Artsinol area, Hérens valley)
L3 Les Flanvêches (Artsinol area, Hérens valley)
L4 Les Véjeviches (Artsinol area, Hérens valley)
L5 Raz d'Arbey (Artsinol area, Hérens valley)
L6 Les Roux Upper central part (Dix valley)
L7 Les Roux Lower central part (Dix valley)
L8 Les Roux Eastern part (Dix valley)
L9 Pantalons Blancs glacier (Dix valley)
L10 Pointe du Vasevay South Face (Dix valley)
L11 Pointe du Vasevay West Face (Bagnes val.)
L12 Tunnel of the road at Madzeria (Bagnes val.)
L13 Lui Dzaune (Madzeria area, Bagnes valley)
L14 Les Tsantons (Madzeria area, Bagnes valley)
~ 10m
b) Schematic margin geometry at Late Jurassic Time
~ NE
~ SW
≈ 1 km
EVOLÈNE SERIES
Light grey massive limestone [U. Jurassic]
Polymict breccias [Upper Jurassic]
Dolomitic breccias [L. to Middle Jurassic]
Dark calcarenites [L. to Middle Jurassic]
Light grey bedded limestone [Early Jurassic]
Cornieules [Mesozoic protolith]
Dolomites [Lower to Middle Triassic]
Tabular quartzite [Lower Triassic]
MONT FORT PALEOZOIC BASEMENT
Greppon Blanc Fm.: Quartzschists, phyllitic quartzites, metavolcanites [Permian]
Métailler Fm.: Metabasites, gneisses [Paleozoic (incl. Ordovician)]

◄ **Fig. 2.15** Local lithological successions observed in the Mont Fort nappe and hypothetical Late Jurassic margin reconstruction. **a** Local lithological successions observed in the Evolène Series and in the Mont Fort basement along their contact. The locations of the logs are given on Figs. 2.6, 2.7 and 2.9. The coordinates of their topographic bases and tops respectively are indicated below: L1 (tectonically overturned) [599'410/107'106] to [599'577/106'990]; L2 (tectonically overturned) [600'005/106'755] to [600'023/106'752], the picture of Fig. 2.12c is from the topographic upper part of the log; L3 [600'400/104'840] to [600'340/104'810]; L4 [600'250/106'720] to [600'070/106'700]; L5 [601'590/106'620] to [601'655/106'270]; L6 [595'355/101'940] to [595'370/101'930], the picture of Fig. 2.5b is from the middle part of the log; L7 [595'400/101'850] to [595'405/101'880], the picture of Fig. 2.11 corresponds to the main part of the log; L8 [595'600/102'040] to [595'535/102'065]; L9 [594'673/098'370] to [594'687/098'357], the base of the breccia is extremely rich in Métailler clasts (similar to the picture of Fig. 2.12d); L10 [594'520/097'630] to [594'460/097'760], modified after Gouffon and Burri (1997); L11 [594'112/097'742] to [594'122/097'745]; L12 [591'870/096'090] to [592'260/095'840]; L13 [592'905/095'960] to [593'005/096'035]; L14 [591'995/094'615] to [591'910/094'690]. **b** Reconstruction of the structure of the Mont Fort basement and Evolène Series at Late Jurassic Time. All the lithological successions described in a) can fit in this reconstruction, with a position in accordance with their current structural location. Relative thickness of the formations differs in a and b, due to highly heterogeneous Alpine deformation.

According to our reconstitution the Mont Fort nappe appears as a typical example of a distal rifted margin. The modern concept of distal margins has been particularly well developed on the Adriatic margin of the Alpine belt (e.g. Froitzheim and Eberli 1990; Florineth and Froitzheim 1994; Froitzheim and Manatschal 1996; Manatschal et al. 2003; Mohn et al. 2011, 2012; Epin et al. 2017; Ribes et al. 2019), less on the European side. This is probably due, in part, to the fact that on the NW border of the Tethys the corresponding series in this paleogeographic position have often been affected during orogeny by much more intense ductile deformation, creating supplementary difficulties and traps that are exemplified in the Mont Fort nappe.

2.7. Geometric modeling

Geometric modeling has been performed using the Shear2F software (Rey 2002), in order to apply passive folding deformation on initial geometries corresponding to normal faults (Figs. 2.13 and 2.14). The aim of this modeling is to argue that the mechanism of passive folding of an initial normal fault geometry is suitable to explain the origin of the complex structures observed along the basal contact of the Evolène Series. The objective here is not to reproduce all details and complexity of the Alpine tectonic history of the Mont Fort nappe, but only to show that the structures observed at the basal contact of the Evolène Series can be reproduced by deformation of discordances originally formed by normal faults.

The Shear2F software allows applying multiphase passive superimposed deformation on initial 3D pixel-sets. These initial pixel-sets are composed of different horizontal layers, whose number, individual thickness and colors can be parameterized. For 3D simple-shear deformations, the following parameters can be set: 1) the orientation of the shear plane; 2) the orientation of the flow direction of the material in the shear plane (vector “a”, shear displacement, in Ramsay 1967); 3) the variation of the amplitude of the vector "a", which is determined by a function, as e.g. a composite sine-function in which the amplitudes and the wavelengths can be parameterized (other types of function are also available such as a step function to model fault, or freely drawn function to model more complex structures).

For the two models presented in Fig. 2.14b, the parameters of the multiphase deformations were adjusted in such a way that the final geometries of the models approximate the ones of the field cross-sections (Figs. 2.8, 2.10 and 2.14a). Three successive phases of deformation were applied on initial 3D horizontal-layered pixel-sets:

- one step-function allowing introducing a high-angle normal fault in the pixel-set, in order to model the effect of the Jurassic extension;
- two superimposed composite phases of heterogeneous simple-shear, in order to model the Cenozoic Alpine deformation.

Detailed parameters of the applied deformation functions are given as Additional files (Add. files 2.1 and 2.2). The model outputs presented in Fig. 2.14b are 2D cross-sections through the 3D models.

Since the presented modeling is able to reproduce the main characteristics of the observed structures, it confirms the view that that passive folding of an initial normal fault geometry can explain the complex structures observed along the basal contact of the Evolène Series.

2.8. Conclusions

The main results of this study are the following:

1.- The Evolène Triassic-Jurassic Series represents the Mesozoic cover of the Mont Fort nappe. It stratigraphically overlies the Mont Fort Paleozoic basement.

2.- Discordant contacts, accompanied by a gap of variable importance, frequently observed along the cover/basement boundary, represent paleo-normal faults of Jurassic age.

3.- The usually very small angular discordances result from the erasing of the original obliquity of the faults by Alpine strain (Fig. 2.14). This geometric transformation is responsible for the misleading appearance of these normal faults as representing a thrust.

4.- Collapse and syntectonic erosion of the active faults provided the material that forms the Jurassic breccias. This study reveals the link between observed faults and specific breccia accumulations (Fig. 2.15).

5.- Our model explains the discontinuous localization of the Evolène Series upon the Mont Fort basement. Its absence corresponds to places where the denuded faults were exposed at the bottom of the sea (Fig. 2.15).

6.- According to our reconstitution the Mont Fort nappe appears as a typical example of a distal rifted margin (Fig. 2.3).

7.- Contrary to examples frequently described in other regions, the Jurassic faults of the Mont Fort nappe were not reactivated during Alpine tectonics. They responded passively to ductile Alpine deformation such as to mimic a thrust.

Abbreviations

GSB: Grand St-Bernard

OCT: Ocean-Continent transition

Geographic coordinates refer to the Swiss grid (CH1903)

Supplementary information (see Appendix)

Additional file 2.1: Shear2F models parameters

Additional file 2.2: Schear2F freely drawn profile function for the Roux model 1st order retro folds.

Acknowledgments

The authors would like to thank the following people, who were of great support in carrying out this study: Michel Ballèvre and Paola Manzotti for guiding us in the Mont Pancherot; Gianreto Manatschal, Yves Gouffon and Mario Sartori for the highly interesting discussions regarding the results and interpretations; Charlotte Ribes for her advices and for accompanying us on the field in the Artsinol and Pointe de Chalune areas; Albrecht Steck for the discussion about the regional geological structure; Aymon Baud for his advices concerning the Triassic stratigraphic interpretations. We are grateful to M. Ballèvre and an anonymous reviewer for the constructive reviews that improved the manuscript and to S. Schmid for handling of the paper and constructive comments.

The many unpublished diploma/master theses of the University of Lausanne focusing on various parts of the study area constituted a fundamental basis for its geological description and understanding. They were carried out by Jean-Rodolphe Moix and Etienne Stampfli (1980), Jean Savary (1982), Olivier Besson (1986), Jean-Marc Rey (1992), Nicolas Kramar (1997), François-Joseph Baillifard (1998), Olivier Favre (2000), Pierre-Alain Wülser (2002), Laure Gauthiez (2011) and Jérémie Glassey (2013).

Chapter 3: Schistes Lustrés in a hyper-extended continental margin setting and reinterpretation of the limit between the Mont Fort and Tsaté nappes (Middle and Upper Penninics, Western Swiss Alps)

Adrien Pantet, Jean-Luc Epard, Henri Masson, Claudia Baumgartner-Mora, Peter O. Baumgartner and Lukas Baumgartner

Article accepted for publication in the *Swiss Journal of Geosciences*

Abstract

The Schistes Lustrés form a large and complex unit at the top of the Penninic nappe stack of the Alpine belt. Calcschists, partly of Late Cretaceous age, constitute the dominant lithology. They are closely associated both with blueschist facies Piemont-Ligurian ophiolites and continent-derived Mesozoic metasediments. The question of whether the Schistes Lustrés originated on continental or oceanic crust has been extensively debated among Alpine geologists and is locally still controversial. We present here new structural and stratigraphic observations, as well as Raman graphite thermometry (RSCM) data, for the Schistes Lustrés complex of the Combin zone in the Hérens, Dix and Bagnes valleys. Our observations indicate that the basal part of this Schistes Lustrés complex (defined as the Série Rousse) is systematically devoid of ophiolitic material, and rests in stratigraphic contact on the underlying Triassic - Lower Cretaceous metasediments and Paleozoic basement of the Mont Fort nappe (Prepiemont paleogeographic domain). The unconformity at the base of the Schistes Lustrés complex is interpreted as resulting from the sedimentation of the Série Rousse on a paleorelief formed by remnants of Jurassic normal fault scarps, and not as an Alpine tectonic contact, as previously proposed. The lithostratigraphic comparison with the Breccia nappe in the Prealps, as well as a foraminifer discovery, allows us to better constrain the age of the Série Rousse. It extends from the middle of the Early Cretaceous (Aptian?) to the Late Cretaceous (Campanian to earliest Maastrichtian?).

In contrast, the upper contact of the Série Rousse with the ophiolite-bearing Schistes Lustrés clearly corresponds to an Alpine thrust. The thrust zone is underlined by thin, discontinuous slices of highly strained continental-margin derived Mesozoic metasediments (Frilihorn slices). RSCM data show that the recrystallization of the organic matter progressively increases on both sides towards this contact. This contact, internal to the Schistes Lustrés complex, is reinterpreted as the major tectonic contact separating the Middle Penninic Mont Fort nappe from the Upper Penninic Tsaté nappe (defined here as including only the ophiolite-bearing Schistes Lustrés and associated meta(ultra-)basites. This study clearly documents that the Schistes Lustrés consist of sediments either deposited on oceanic crust, showing locally preserved stratigraphic contacts with ophiolitic or serpentinized sub-continental mantle slivers, or sediments still resting stratigraphically on a former hyper-extended continental margin.

3.1. Introduction

The Schistes Lustrés form one of the largest lithological groups in the Western Alps and the Western Central Alps (Fig. 3.1). They crop out in the upper part of the Penninic nappe stack in an intermediate tectonic position between the units derived from the Briançonnais (s.l.) continental margin, the eclogitic Piemont-Liguria ophiolites and the units derived from the Adriatic continental margin (Fig. 3.1). They constitute a set dominated by calcschists showing ophiolitic intercalations, up to several hundred meters thick. The name Schistes Lustrés refers to the glossy metallic grey ("lustré") aspect of these calcschists. It is the abundance of phyllosilicates and graphite, which gives, together with the metamorphism, this characteristic aspect to their schistosity surfaces.

The question of the origin of the Schistes Lustrés has always been problematic, notably because of their close association with metabasites and mantle rocks as well as with continental margin succession. The extreme scarcity of fossils also makes the determination of their age difficult

(e.g. Termier 1902; Staub 1942a). Since the emergence of plate tectonics, the question of the continental or oceanic nature of the bedrock on which the Schistes Lustrés were deposited has been extensively debated among Alpine geologists. The idea that both cases could exist, or even coexist, appeared early on and have been proposed by different authors (e.g. Staub 1942b; Lemoine 1953, 1964, 1967, 1971; Elter 1971; Bearth 1976; Bourbon et al. 1979; Caby 1981; Lemoine and Tricart 1986; Fudral et al. 1987; Lagabrielle 1987). However, in several cases the question still remains relevant today as the stratigraphic or tectonic nature of the contact between the Schistes Lustrés and the surrounding units is most often difficult to establish (Lemoine 1971; Michard and Schumacher 1973; Marthaler and Stampfli 1989). Indeed, a strong ductility contrast generally characterizes these interfaces and favors their late movements in the form of local shearing. The difficulties also result from the strong lithological similarities between the Schistes Lustrés of oceanic origin and those originating from continental margins. The contact between such units may be difficult to identify, especially since they are now involved in nappes and have undergone polyphase ductile deformation (e.g. Savary and Schneider 1983).

The present study focuses on the Schistes Lustrés of the Combin zone (Pennine Alps), in the area located NW of the Dent Blanche klippe (Fig. 3.1b; Canton of Valais, Switzerland).

Fig. 3.1 a Map of the Western and Central Alps showing the Schistes Lustrés units; modified after Schmid et al. (2004, 2017), ► Steck et al. (1999, 2015, 2019), Ballèvre et al. (2018, 2020), Beltrando et al. (2010a, 2014), Balestro et al. (2020), Dal Piaz (1999), Bigi et al. (1992), Gouffon (1993), Deville et al. (1992) and the Tectonic map of Switzerland (2005). *A*: Antrona nappe; *Ac*: Accelgio zone; *AF*: Aosta fault; *ALi*: Apenninic Ligurian nappes; *Am*: Ambin massif; *Ar*: Arpont massif; *B*: Breccia nappe; *Bi*: Biella pluton; *Br*: Brusson window; *BT*: Brèches de Tarentaise; *CB*: Pancherot - Cime Bianche - Bettaforca Series; *Ch*: Chenaillet unit; *CN*: Cheval Noir Flysch; *Dr*: Dranses nappe; *DS*: Dronero-Sampeyre unit; *Em*: Monte Emilius unit; *Ga*: Gastern massif; *Ge*: Gets nappe; *GI*: Gazzo-Isoverde unit; *Gr*: Graies Alps; *GR*: Glacier-Rafray unit; *Gu*: Gurnigel nappe; *HF*: Helminthoid Flysch; *La*: Lanzo massif, *LA*: Ligurian Alps; *LTF*: Lis-Trana fault; M: Money unit; *MF*: Mont Fort nappe; *MV*: Monviso massif; *Ni*: Niesen nappe; *NVa*: Northern Vanoise massif; *Or*: Orobic nappes; *Pg*: Portjengrat nappe; *Pi*: Pillonet unit; *R*: Ruitor unit; *RC*: Roche des Clots unit; *Ro*: Rochebrune unit; *S*: Stockhorn nappe; *Sa*: Saane nappe; *SaM*: Subalpine Molasse; *SC*: Sion-Courmayeur zone; *Si*: Simme nappe; *SM*: Siviez-Mischabel nappe; *SVa*: Southern Vanoise massif; *T*: Traversella pluton; *Ta*: Tavetsch massif; *TL*: Tonale Line; *Ts*: Tsaté nappe; *V*: Voirons nappe; *Vo*: Voltri massif; *Vs*: Valsavarenche unit; *ZH*: Zone Houillère; *ZS*: Zermatt-Saas Fee nappe. **b** Map of the Schistes Lustrés of the Combin zone and surrounding units across the Bagnes, Dix, Hérens and Anniviers valleys in SW Switzerland, and the Ollomont valley and Valpelline in NW Italy; bedrock map compiled after own data and the maps of Moix and Stampfli (1980), Escher (1988), Allimann (1990), Rey (1992), Kramar (1997), Burri et al. (1998), Baillifard (1998), Steck et al. (1999), Favre (2000), Marthaler et al. (2008a, 2020a), Sartori et al. (2011), Sartori and Epard (2011), Glassey (2013) and Geocover (Swisstopo). The individualized "Tracuit - Aig. Rouges z. / Cornet U." groups together the Tracuit - Aiguilles Rouges zone with the Cornet Unit; limits after Marthaler et al. (2020b, fig. 16) and Manzotti et al. (2021, fig. 7), slightly modified. DB_M: Dent Blanche Mesozoic; SM_M: Siviez-Mischabel Mesozoic; ZH_M: Zone Houillère Mesozoic; ZH_P: Zone Houillère Paleozoic; *AR*: Aiguilles Rouges d'Arolla.

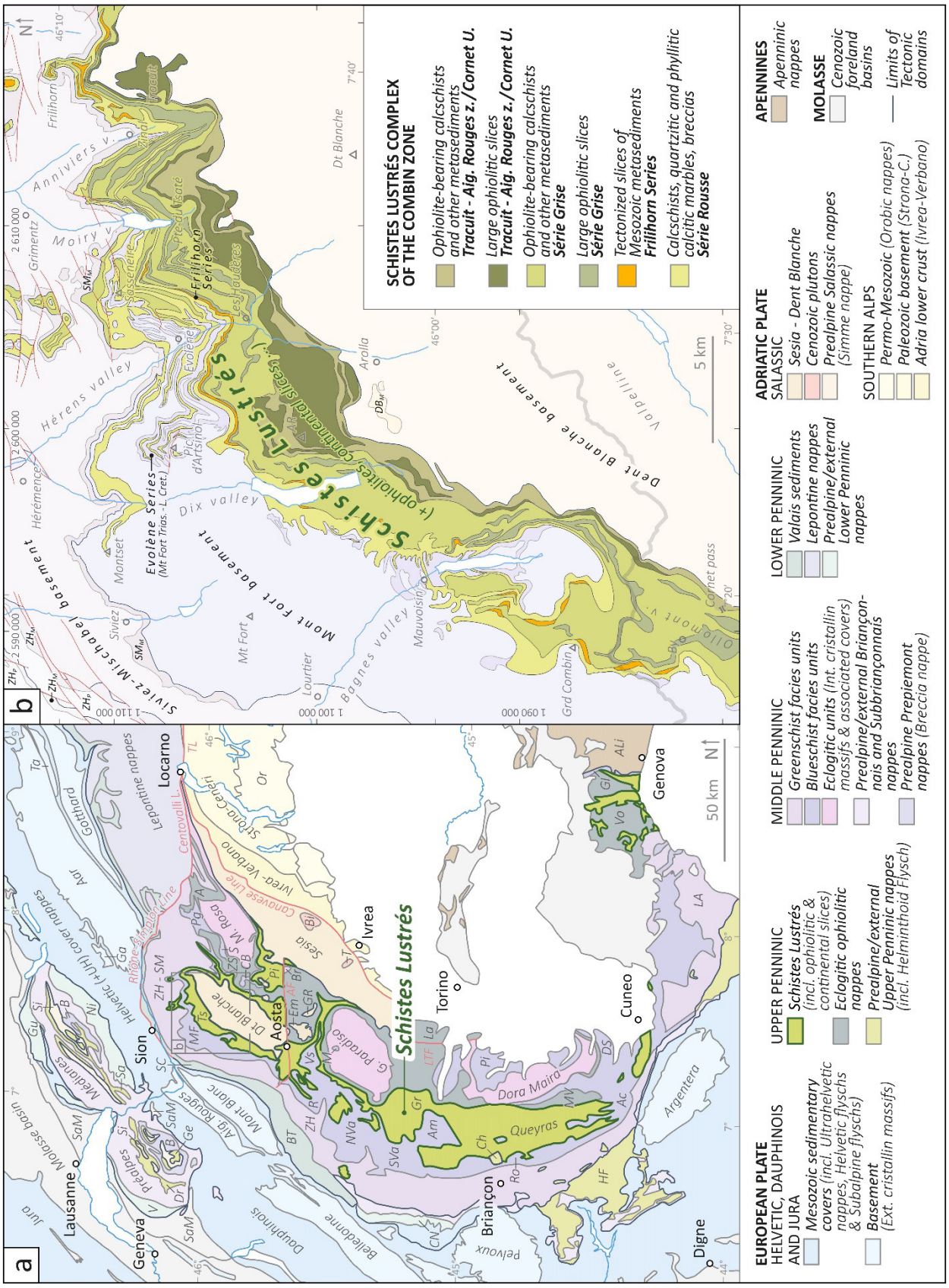
a
b
Lausanne
Geneva
Sion
Locarno
Aosta
Ivrea
Torino
Cuneo
Genova
Briançon
Digne
Schistes Lustrés
Mont Fort basement
Dent Blanche basement
Siviez - Mischabel basement
Schistes Lustrés Complex
(+ ophiolites, Continental slices)
Evolène Series
Frilihorn Series
Tracuit
Arolla
Hérens valley
Dix valley
Bagnes valley
Mauvoisin
Grd Combin
Cornet pass
Dt Blanche
Anniviers v.
Moiry v.
Grimentz
Montset
Siviez
Mt Fort
Lourtier
Evolène
Pic d'Artsinol
Les Haudères
Frilihorn
Tracuit
Arolla
Volpelline
Ollomont v.
5 km
50 km
SCHISTES LUSTRÉS COMPLEX OF THE COMBIN ZONE
Ophiolite-bearing calcschists and other metasediments Tracuit - Aig. Rouges z./Cornet U.
Large ophiolitic slices Tracuit - Aig. Rouges z./Cornet U.
Ophiolite-bearing calcschists and other metasediments Série Grise
Large ophiolitic slices Série Grise
Tectonized slices of Mesozoic metasediments Frilihorn Series
Calcschists, quartzitic and phyllitic calcitic marbles, breccias Série Rousse
EUROPEAN PLATE
HELVETIC, DAUPHINOIS AND JURA
Mesozoic sedimentary covers (incl. Ultrahelvetic nappes, Helvetic flyschs & Subalpine flyschs)
Basement (Ext. cristallin massifs)
UPPER PENNINIC
Schistes Lustrés (incl. ophiolitic & continental slices)
Eclogitic ophiolitic nappes
Prealpine/external Upper Penninic nappes (incl. Helminthoid Flysch)
MIDDLE PENNINIC
Greenschist facies units
Blueschist facies units
Eclogitic units (Int. cristallin massifs & associated covers)
Prealpine/external Briançonnais and Subbriançonnais nappes
Prealpine Prepiemont nappes (Breccia nappe)
LOWER PENNINIC
Valais sediments
Lepontine nappes
Prealpine/external Lower Penninic nappes
ADRIATIC PLATE
SALASSIC
Sesia - Dent Blanche
Cenozoic plutons
Prealpine Salassic nappes (Simme nappe)
SOUTHERN ALPS
Permo-Mesozoic (Orobic nappes)
Paleozoic basement (Strona-C.)
Adria lower crust (Ivrea-Verbano)
APENNINES
Apenninic nappes
MOLASSE
Cenozoic foreland basins
Limits of Tectonic domains

3.2. Geological setting

3.2.1. The Schistes Lustrés in the nappe stack of the Pennine Alps

The metasediments and ophiolitic remnants constituting the Schistes Lustrés complex originated from the Mesozoic Piemont-Liguria basin and its margins. This basin, which constituted the main branch of the Alpine Tethys, was a slow-spreading small oceanic domain, resulting from the rifting between the European and Adriatic plates (e.g. Lemoine and Trümpy 1987; Lagabrielle and Lemoine 1997; Stampfli et al. 2002; Le Breton et al. 2021; Manatschal et al. 2022). Oceanization of the basin is attested since the Bajocian (Elter et al. 1966; Bill et al. 2001; Manatschal and Müntener 2009) and continued at least until the Kimmeridgian (e.g. Bill et al. 1997; Rubatto et al. 1998; Schaltegger et al. 2002; Decrausaz et al. 2021). The progressive closure of the Alpine Tethys starting in the Late Cretaceous (e.g. Caron et al. 1989; Gasinski et al. 1997; Stampfli et al. 1998; Skora et al. 2009; Rubatto et al. 2011), led to the accretion and incorporation of ophiolitic slivers and associated oceanic sediments into the orogenic prism (e.g. Lagabrielle 1987; Marthaler and Stampfli 1989; Stampfli and Marthaler 1990; Stampfli et al. 1998), and finally to the Cenozoic Alpine collision (e.g. Escher and Beaumont 1997; Schmid et al. 2017; Candiotti et al. 2021).

In the nappe stack of the Pennine Alps, the ophiolitic units derived from the Piemont-Liguria basin show two types of contrasting tectono-metamorphic evolution (e.g. Kienast 1973; Dal Piaz 1974; Ernst and Dal Piaz 1978; Merle and Ballèvre 1992; Ballèvre and Merle 1993; Negro et al. 2013). (i) The structurally lower ophiolitic units (Zermatt-Saas Fee, Antrona, and Lanzo) show eclogite facies paragenesis (e.g. Bearth 1967a; Pfeifer et al. 1989; Bucher et al. 2005, 2019; Angiboust et al. 2009; Dragovic et al. 2020) with local UHP relics in Zermatt-Saas Fee (e.g. Reinecke 1991, 1998; Forster et al. 2004; Groppo et al. 2009; Frezzotti et al. 2011, 2014) and a predominance of ophiolites over metasediments. (ii) The structurally upper ophiolite-bearing unit, the *Tsaté nappe* (Sartori 1987; Escher 1988; Marthaler and Stampfli 1989),

or *Combin zone s.str.* (e.g. Dal Piaz 1971; Bearth 1976; Caby 1981), corresponds to the Schistes Lustrés complex. It is dominated by metasediments and shows greenschist facies paragenesis with blueschist-facies relics (e.g. Caby 1981; Bousquet et al. 2004; Manzotti et al. 2021; cf. chap. 3.2.3.1). The lithologies and metamorphic paragenesis of (ii) are similar to those of the Schistes Lustrés of the French Western Alps (e.g. Agard et al. 2001; Plunder et al. 2012).

At its top, the Schistes Lustrés complex of the Combin zone is in tectonic contact with the Paleozoic basement of the Sesia and Dent Blanche nappes (Adriatic margin; e.g. Manzotti et al. 2014, 2017; Angiboust et al. 2014; Kirst 2017; Kirst and Leiss 2017). At its base, it rests on different tectonic units (Fig. 3.1): (i) the Zermatt-Saas Fee nappe (Piemont domain), in the internal part of the belt (Ballèvre et al. 1986; Bucher et al. 2004a; Dal Piaz et al. 2015b); (ii) the Siviez-Mischabel nappe (Briançonnais domain), north of Zermatt, as well as in the Turtmann and Anniviers valleys and on the right side of the Hérens valley (e.g. Hermann 1913; Bearth 1953a, 1978; Sartori 1987, 1990; Scheiber et al. 2013); (iii) the Evolène Series, cover of the Mont Fort nappe (Prepiemont domain; Marthaler 1984; Escher 1988; Pantet et al. 2020), NW of the Dent Blanche klippe; or (iv) directly on the Paleozoic basement of the Mont Fort nappe, if the Evolène Series is absent.

3.2.2. Subdivisions in the Schistes Lustrés complex of the Combin zone

After the first definition of the Combin zone by Argand (1909), as a composite tectonic unit grouping together all the Mesozoic metasediments outcropping between the basements of the Grand St-Bernard and Dent Blanche nappes, more specific studies of its Schistes Lustrés complex (*Combin zone s.str.*) were carried out, for example by Staub (1942b, 1942a, 1942c), Witzig (1948), Zimmermann (1955), Dal Piaz (1965, 1971), Bearth (1967a, 1978) and Caby (1981). Further detailed studies of these Schistes Lustrés, in the area located north of the Dent Blanche klippe, allowed to individualize different lithological and tectonic units within this complex

(Marthaler and Escher in Masson et al. 1980; Marthaler 1981, 1984; Escher and Masson 1984; Sartori 1987; Escher 1988; Escher et al. 1988; Fig. 3.2).

We describe them below, from top to bottom.

(1) The upper unit is mainly formed of basic and ultrabasic rock bodies reaching pluri-km sizes, associated with calcschists. This unit corresponds with the Tracuit zone (Zimmermann 1955; Escher and Masson 1984; Sartori 1987), defined in the eastern part of the study area, and with the ophiolites and associated metasediments of the Aiguilles Rouges d'Arolla (Aiguilles Rouges-Zone and Hochpenninikum höhern Schuppen, Witzig 1948; Série ophiolitique s.s., Kunz 1988; Aiguilles Rouges and Mont de l'Etoile Ophiolites, Decrausaz et al. 2021). In the following, we will use the term *Tracuit - Aiguilles Rouges zone* to refer to this unit.

(2) The intermediate Schistes Lustrés unit is usually designated by the term *Série Grise* (Marthaler 1984). It is composed mostly of calcschists and other oceanic metasediments, mixed with ophiolitic lenses, which are usually smaller than those of the previous unit.

(3) A thin unit of Mesozoic metasediments derived from a continental margin (0.1 - 20 m thick) punctuates the base of the Série Grise as discontinuous and often strongly tectonized slices. It constitutes the upper and outer digitation of the *Faisceau Vermiculaire* of Argand (1916a, 1916b; Escher and Masson 1984). North of the Dent Blanche klippe, its thickness is often below one meter and its maximum thickness (20 m) is reached at the Frilihorn (Fig. 3.1b), the summit that gave its name to this unit (Hermann 1913; Marthaler 1984; Stampfli and Marthaler 1990; Sartori and Marthaler 1994).

(4) The lower Schistes Lustrés unit, called the *Série Rousse* (Marthaler and Escher in Masson et al. 1980; Marthaler 1981), consists mainly of calcitic marbles rich in detrital material and of calcschists. The Schistes Lustrés of this unit show a near continental margin affinity

contrasting with that of the upper units, reflected in particular by the local presence of breccia levels with dolomitic clasts and by a marked quartzitic detrital component.

In the original definition of the Tsaté nappe (Sartori 1987), only the two upper units above, i.e. the Série Grise and the Tracuit (- Aiguilles Rouges) zone, were included in this nappe (Fig. 3.2). The two lower units (Série Rousse and Frilihorn) were attributed to the underlying Mont Fort nappe (e.g. Escher 1988; Escher et al. 1988; Allimann 1990; Deville et al. 1992).

Marthaler and Stampfli (1989) and Stampfli and Marthaler (1990) evidenced the similarities between the Tsaté nappe and modern accretionary prisms, both showing a structure composed of superimposed slices involving sediments and ophiolites. These similarities, together with the identification of large-scale unconformities at the base of the Série Rousse, led to propose the inclusion of the Série Rousse as a basal slice to the Tsaté nappe and to reinterpret the nature of the basal contact of these series as tectonic (Escher et al. 1993; Sartori and Marthaler 1994). Further evidence for local fluid circulation along the basal contact of the Série Rousse was highlighted by an isotopic profile carried out across this contact (Kramar 1997). This evidence reinforced the hypothesis of the affiliation of the Série Rousse to the Tsaté nappe, since then accepted and adopted by all subsequent authors (e.g. Escher et al. 1997; Steck et al. 1999; Tectonic map of Switzerland 2005). According to this redefinition, the Tsaté nappe would correspond to a stack of tectonic slices, grouping together all the Schistes Lustrés of the Combin zone (Fig. 3.2).

The different lithologies constituting the Schistes Lustrés north of the Dent-Blanche klippe are described in the following chapter. It gathers the necessary elements that allow the distinction of the different series or units defined in the literature. The new data are based on detailed mapping and tectonostratigraphic observations of key areas.

Authors		Sartori 1987	Escher et al. 1988 (=Escher et al. 1987) Escher 1988 Marthaler & Stampfli 1989 Sartori 1990	Allimann 1987 Allimann 1990 Deville et al. 1992	Stampfli & Marthaler 1990	Sartori & Marthaler 1994 Escher et al. 1993 Escher et al. 1994 Escher et al. 1997 Sartori et al. 2006 Negro et al. 2013	Steck et al. 1999/2001 Tectonic map of Switzerland 2005 Burri et al. 1998/1999 Marthaler et al. 2008 Gabus et al. 2008 Sartori et al. 2011 Sartori & Epard 2011 Dal Piaz et al. 2015	Scheiber et al. 2013	Angiboust et al. 2014	Marthaler et al. 2020	Manzotti et al. 2021	Proposed interpretation in this study	Authors	
Units/Series													*Units/Series*	
Schistes Lustrés complex of the Combin zone	***Tracuit and Aiguilles Rouges***	***Tsaté*** *nappe:* ***Tracuit*** *zone*	***Tsaté*** *nappe:* ***Tracuit - Aig. Rouges*** *zone or* ***Tracuit + Aig. Rouges*** *zone*	***Tsaté*** *nappe*	***Tsaté*** *nappe:* ***Tracuit + Aig. Rouges*** *zone* *(early incorporation in a accretionary prism)*	***Tsaté*** *nappe*	***Tsaté*** *nappe*	***Tsaté*** *nappe*	***Tsaté*** *complex:* ***Low-T*** *unit*	***Tsaté*** *nappe:* ***Lower T.*** *slice*	***Combin*** *zone:* ***Cornet*** *Unit*	***Tsaté*** *nappe:* ***Tracuit - Aig. Rouges*** *zone / **Cornet** Unit* *(Lower metamorphic grade unit)*	***Tracuit and Aiguilles Rouges***	*Schistes Lustrés complex of the Combin zone*
	Série Grise	***Tsaté*** *nappe:* ***Série Grise***	***Tsaté*** *nappe:* ***Série Grise***		***Tsaté*** *nappe:* ***Série Grise*** *(early incorporation in an accretionary prism)*				***Tsaté*** *complex:* ***Medium-T*** *unit*	***Tsaté*** *nappe:* ***Higher T.*** *slice*	***Combin*** *zone:* ***By*** *Unit*	***Tsaté*** *nappe:* ***Série Grise*** *(Higher metamorphic grade unit)*	***Série Grise***	
	Frilihorn Series	***Mont Fort*** *nappe*	***Mont Fort*** *nappe*	***Mont Fort*** *nappe*	***Frilihorn*** *nappe* *(early incorporation in an accretionary prism)*	***Frilihorn*** *nappe*	***Frilihorn*** *nappe*	***Frilihorn*** *«nappe» (Siviez-Mischabel detached cover)*		***Frilihorn*** *nappe*		***Frilihorn*** *slices* *(possible internal Mont Fort nappe)*	***Frilihorn Series***	
	Série Rousse				***Mont Fort*** *Upper Cretaceous* *(early incorporation in an accretionary prism)*	***Tsaté*** *nappe*	***Tsaté*** *nappe*	***Tsaté*** *nappe*	***Tsaté*** *complex:* ***High-T*** *unit*	***Tsaté*** *nappe:* ***Higher T.*** *slice*	***Mont Fort*** *nappe*	***Mont Fort*** *nappe*	***Série Rousse***	
Evolène Series					***Mont Fort*** *nappe*	***Cimes Blanches*** *nappe*	***Cimes Blanches*** *nappe*	***Cimes Blanches*** *«nappe» (Siviez-Mischabel detached cover)*	*not mentionned*	***Sasseneire*** *nappe*			***Evolène Series***	
Mont Fort basement						***Mont Fort*** *nappe*	***Mont Fort*** *nappe*	***Mont Fort*** *nappe*	***Mont Fort*** *nappe*	***Mont Fort*** *nappe*			***Mont Fort basement***	

Fig. 3.2 Tectonic attributions of the studied units/series between successive previous authors and this study.

3.2.3. Lithologies of the Schistes Lustrés complex of the Combin zone

3.2.3.1. Ophiolite-bearing Schistes Lustrés and associated lithologies

We will describe the different lithologies of the ophiolite-bearing Schistes Lustrés of the Combin zone independently of the tectonic subdivisions detailed in the previous chapter, because the same lithologies are present in these different subdivisions. The ophiolitic material can be incorporated in these Schistes Lustrés as levels or lenses of variable sizes, or as a sand-sized or thinner detrital component.

Calcschists

The calcschists of the ophiolite-bearing Schistes Lustrés of the Combin zone generally display a greyish and sometimes greenish tint, which may turn to russet for the levels that are the richest in calcite (Fig. 3.3a). The characteristic metallic gray appearance of their schistosity surfaces is due to the abundance of phyllosilicates and graphite.

Their mineralogy is generally composed of calcite, quartz, muscovite, chlorite, albite and pyrite, ± tourmaline, apatite, ankerite, zircon, rutile, pyrite and various oxides (e.g. Marthaler et al. 2008b, 2020b). Metamorphic parageneses are mostly typical of greenschist facies, but early blueschist facies parageneses are attested by the local preservation of relics of garnets, Mg-chloritoid and phengite (Burri et al. 1999; Bousquet et al. 2004, 2008), of carpholite pseudomorphs (Pfeifer et al. 1991); and of lawsonite pseudomorphs and aragonite inclusions in titanite (Manzotti et al. 2021). The local presence of fuchsite (Vogel 1995; Manzotti et al. 2021), reflects the presence of chromium in these sediments and seems to confirm their oceanic origin. Lithologies are variable and can evolve towards phyllitic and quartzitic marbles, as well as towards black shales, which are often compared to the *Palombini* shales from the Apennines (e.g. Marthaler and Stampfli 1989). In the Tsaté nappe, such dark shales and associated calcschists have been grouped together as the Garda Bordon Formation, which is supposedly of

Early to "mid"-Cretaceous age (Marthaler et al. 2020b). Rhythmic alternations of shales and decimetric beds of quartzitic calcarenites, locally showing graded bedding, have been, for their part, grouped together as the Fêta d'Août Formation (Viredaz 1979; Marthaler et al. 2020b). This formation is attributed to the Early Cretaceous by analogy with the Replatte formation of the Western Alps (Lemoine and Tricart 1986).

Relics of planktic foraminifera have been described in several localities of the Série Grise (Marthaler 1981, 1984; and unpublished diploma theses from: Savary 1982; Schneider 1982; Besson 1986; Du Bois and Looser 1987; Kunz 1988). They generally come from the levels that are the richest in calcite in this unit. The strong rheological contrast between these levels and the surrounding calcschists, as well as a diagenetic replacement as Fe-carbonate (usually referred to as ankerite), seem to have allowed a local preservation of these forms, despite the intensity of deformation and recrystallization. The forms described mostly recall *Rotalipora* sp., or more rarely *Marginotruncana* sp., corresponding to Cenomanian and Turonian-Santonian age ranges, respectively (e.g. Peryt et al. 2022). Forms of the same types have also been described in various localities of the Schistes Lustrés of the Western Alps (Lemoine et al. 1984; Marthaler et al. 1986; Deville 1987; Fudral et al. 1987) and Corsica (Meresse et al. 2012).

Volcanosedimentary arkoses

Volcanosedimentary levels are found in several locations in the Schistes Lustrés of the Combin zone (e.g. Kunz 1988; Decrausaz et al. 2021; Fig. 3.3b). Kunz (1988) describes in particular volcanosedimentary arkoses at the contact between the ophiolite bodies intercalated in the Schistes Lustrés and the overlying calcschists and black shales. The gradual transition between these lithotypes seems to indicate an original stratigraphic contact of the sediments on their ophiolitic bedrock. Volcanosedimentary levels are also described in the Schistes Lustrés of the Western Alps

(e.g. Lagabrielle and Polino 1985), in particular gabbroic arenites (Le Mer et al. 1986) and basaltic sands (Lagabrielle 1987).

Calcitic marble levels

Several meters to tens of meters thick levels of calcitic marbles and breccias are observed in the ophiolite-bearing Schistes Lustrés of the Combin zone (Staub 1942c; Burri et al. 1998, 1999; Marthaler et al. 2020b). Marbles containing serpentinite clasts, and sometimes abundant epidote, are locally found in stratigraphic contact with ophicarbonates and ophiolitic lenses (Vogel 1995; Marthaler et al. 2020b; Decrausaz et al. 2021; Figs. 3.3c-d). Such levels are also described in the Schistes Lustrés of the Western Alps and Corsica (e.g. Lemoine et al. 1970; Lagabrielle et al. 2015). Their strong analogies with limestones containing ophiolitic clasts of the Upper Penninics of Graubünden in which Weissert (1975) observed *Calpionella*, and with the *Calpionella* limestones of the supra-ophiolitic sediments of the Apennines and Corsica (Abbate and Sagri 1970; Andri and Fanucci 1973), makes their attribution to the latest Jurassic / earliest Cretaceous very likely.

Manganese-bearing quartz micaschist beds

In different localities, metric levels of manganese-bearing quartz micaschists, classically interpreted as metaradiolarites, are intercalated in the Schistes Lustrés of the Combin zone (Staub 1942c; Hagen 1948; Witzig 1948; Bearth and Schwandler 1981; Caby 1981; Ayrton et al. 1982; Marthaler 1984; Burri et al. 1999; Marthaler et al. 2020b). Spessartine is common and is sometimes accompanied by other manganese minerals or mineralizations (e.g. Baldelli et al. 1983; Ansermet and Meisser 2012; Marthaler et al. 2020b). Piemontite, accompanied by braunite and Mn-garnets, have been observed in such levels near the Chanrion hut in the Bagnes valley (Burri et al. 1999; Fig. 3.3e). In the Schistes Lustrés of the Western Alps,

similar quartzschist levels have yielded radiolarians of Callovian to Middle Kimmeridgian age (De Wever and Caby 1981; Deville 1987; De Wever et al. 1987).

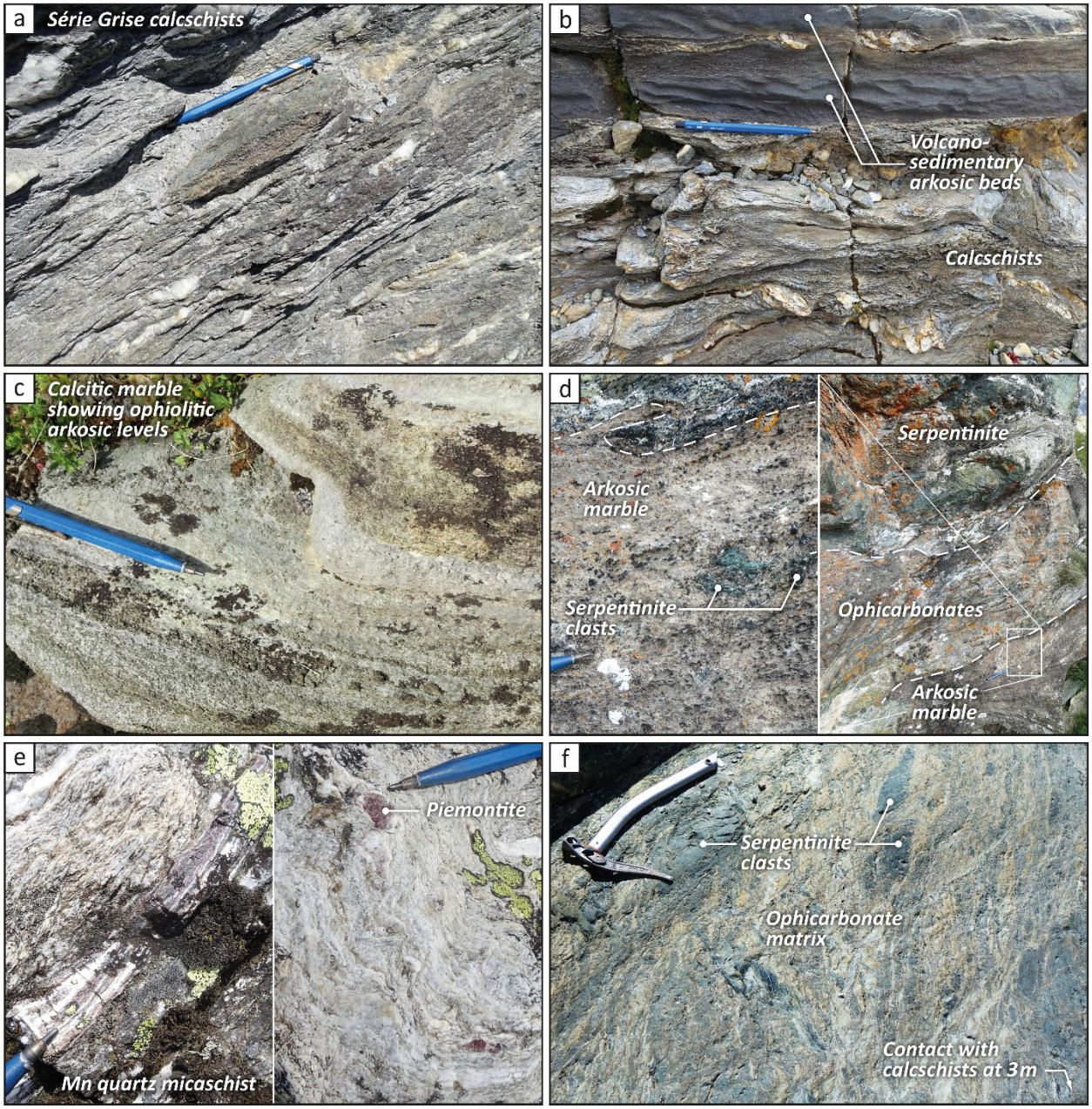

Fig. 3.3 Lithologies of the ophiolite-bearing Schistes Lustrés of the Combin zone. **a** Characteristic aspect of the Série Grise calcschists; Les Haudères [2'604'860/1'104'050]. **b** Graded beds of greenish to violaceous volcanosedimentary arkose interbedded in calcschists; Adlerflüe [2'620'290/1'110'560], Turtmann valley. **c** Decimetric level of greenish calcitic marble outcropping at a few meters from a plurihectometric-long ophiolitic lens (serpentinites, metabasites) of the Série Grise. Detrital mm-sized grains of ophiolitic material are visible under the pencil; Chanrion hut area [2'595'195/1'087'695], Bagnes valley. **d** Arkosic calcitic marble at the contact of a hectometric-long serpentinite lens. Note the presence of cm-serpentinite clasts and the green color of the ophiolitic arkosic detritus; 3 m from Fig. c. **e** Quartzmicaschists levels (1-2 m thick) interpreted as metaradiolarites (Staub 1942c; Burri et al. 1999) and locally rich in piemontite (sometimes associated to braunite); Chanrion hut area [2'595'165/1'087'700]; Mn-garnets and blue amphiboles are visible in the same level, 200 m to the NNW. **f** Serpentinite breccia observed at the contact between calcschists of the Série Grise and a plurihectometric serpentinite lens marking the contact with the Série Rousse; Giétro [2'594'360/1'094'290], Bagnes valley.

Meta(ultra-)basites

Among the ophiolitic intercalations in the Schistes Lustrés of the Combin zone, metabasites are the most abundant. Their chemistry is generally of MORB type (Dal Piaz et al. 1981; Beccaluva et al. 1984; Decrausaz et al. 2021) and their parageneses (epidote + albite + chlorite + titanite ± actinolite/tremolite ± phengite ± apatite ± calcite; e.g. Angiboust et al. 2014; Marthaler et al. 2020b; Decrausaz et al. 2021) are typical of the greenschist facies. An early, largely retromorphosed, blueschist facies paragenesis (Na-amphiboles, garnets, etc.) is locally preserved (e.g. Dal Piaz and Ernst 1978; Ayrton et al. 1982; Sperlich 1988; Martin and Cortiana 2001; Angiboust et al. 2014).

The metabasalts (prasinites, ovardites) form levels of very variable thickness, ranging from a few decimeters to several hundred meters. Pillow lava structures have been recognized in several locations in the Combin zone (e.g. Dal Piaz 1971; Kunz 1988; Decrausaz et al. 2021). Basaltic breccias have been described, particularly at the contact with the underlying ultramafic rocks (e.g. Caby 1981).

The metagabbros can form plurikilometric bodies, as for example in the region of the Tracuit alp; and at the Aiguilles Rouges d'Arolla (Fig. 3.1b), where they have been dated at 154.9 ± 2.6 Ma and 155.5 ± 2.8 Ma (U-Pb on zircon, LA-ICP-MS; Decrausaz et al. 2021).

The most common ultrabasites in the Combin zone are serpentinites. They are intercalated as lenses that can reach plurikilometric dimensions. Their mineralogy is dominated by antigorite, generally accompanied by magnetite and tremolite (Angiboust et al. 2014). The borders of the lenses can be enriched with talc, antigorite, magnesite and dolomite (Pfeifer and Serneels 1988; Angiboust et al. 2014). Serpentinite breccias can be observed locally at the top of these lenses, in contact with the metasediments, and probably result from continued Jurassic rifting (Vogel 1995; Decrausaz et al. 2021; Fig. 3.3f).

3.2.3.2. Frilihorn Series

In the study area, north of the Dent Blanche klippe, the thin and discontinuous Frilihorn Series is mostly reduced to a few tens of cm of strongly tectonized carbonate rocks. Where the series are the thickest and least deformed, different types of Mesozoic metasediments can be recognized (e.g. Hermann 1913; Witzig 1948; Marthaler 1984; Allimann 1990; Sartori 1990). Dolomites constitute the dominant lithology. They are observed in particular at the Bail de l'Ardzentière [2'594'200/1'093'000] in the Bagnes valley (Besson 1986) and NE of Molignon [2'605'540/1'104'600] in the Hérens valley. Calcitic marbles are also common, they are generally clear colored, relatively pure and form notably the 15 m cliff of the summit of the Frilihorn (Marthaler 1984). Thin layers of dolomitic breccias intercalated within this level can be observed there. This same level can be followed through the Arpettes pass towards the Turtmann glacier (cf. Tectonic panorama from Hermann 1913), which it crosses at an altitude of 2700 m, until the NE face of the Adlerflüe, where it forms a clearly visible 10 m thick band of white calcitic marbles. There, a level of breccia, already indicated by Sartori (1990), is present at its base. The mm- to cm-sized clasts are mostly dolomitic and the matrix consists of a dark calcitic marble. Similar breccias are also observed SE of L'Ata Gieute [2'604'625/1'104'755] in the Hérens valley, where they surround a 3 m thick dolomitic level. In the study area, quartzites are very rare in this unit. A 20 cm thick level of micaceous quartzite is nevertheless present near the top of the Frilihorn, intercalated between the marbles of the upper cliffs and russet calcschists covering the summit itself. These calcschists, which contain dolomitic clasts at their base (Marthaler 1984), as well as similar calcschists and russet phyllitic marbles from a few other outcrops, are also attributed to the Frilihorn Series (Marthaler 1984; Sartori 1987; Allimann 1990).

3.2.3.3. Série Rousse

The Série Rousse consists of calcschists, phyllitic and quartzitic marbles, dark shales and thin conglomeratic layers, forming the base of the Schistes Lustrés complex of the Combin zone (e.g. Marthaler 1984; Marthaler et al. 2020b). Its thickness can reach several hundred meters. The calcschists of these series are generally poorer in phyllosilicates than those of the ophiolite-bearing Schistes Lustrés, whereas the levels of calcitic marbles are more abundant and thicker. The name Série Rousse (Marthaler and Escher in Masson et al. 1980) comes from the frequent russet colored patina, typical of the sediments of these series (Figs. 3.4a-c). It is due to the presence of iron oxides, associated with the detrital quartz content, and iron carbonates (e.g. ankerite) in the carbonaceous levels. The tint of the patina contrasts with the glossy metallic gray tint of the schistosity surfaces resulting from the abundance of graphite and white micas in these sediments (Fig. 3.4a). The mineralogy is typically composed of calcite, quartz, white micas, albite, graphite and pyrite (often idiomorphic) ± chlorite, titanite and zircons. Clasts, mostly dolomitic (Figs. 3.4c- d), appear in some levels (Marthaler et al. 2008b, 2020b). Lawsonite pseudomorphs and garnet relics can be observed locally (Besson 1986; P. Manzotti pers. com.).

Relics of planktic foraminifera, diagenetically transformed into in Fe-Mg carbonates, have been described in several locations in the Série Rousse (Marthaler 1981, 1984; and unpublished diploma theses from: Pilloud and Sartori 1981; Schneider 1982; Crespo 1984; Besson 1986; Schmid 1988; Salamin 1989). The described micropaleontologic content presents forms that essentially ascribe to *Rotalipora* sp. (of Cenomanian-type), with a few bicarinate forms indicating a Turonian to "early Senonian" (i.e. Coniacian-Santonian) age (Marthaler 1981, 1984), for the younger parts of the series.

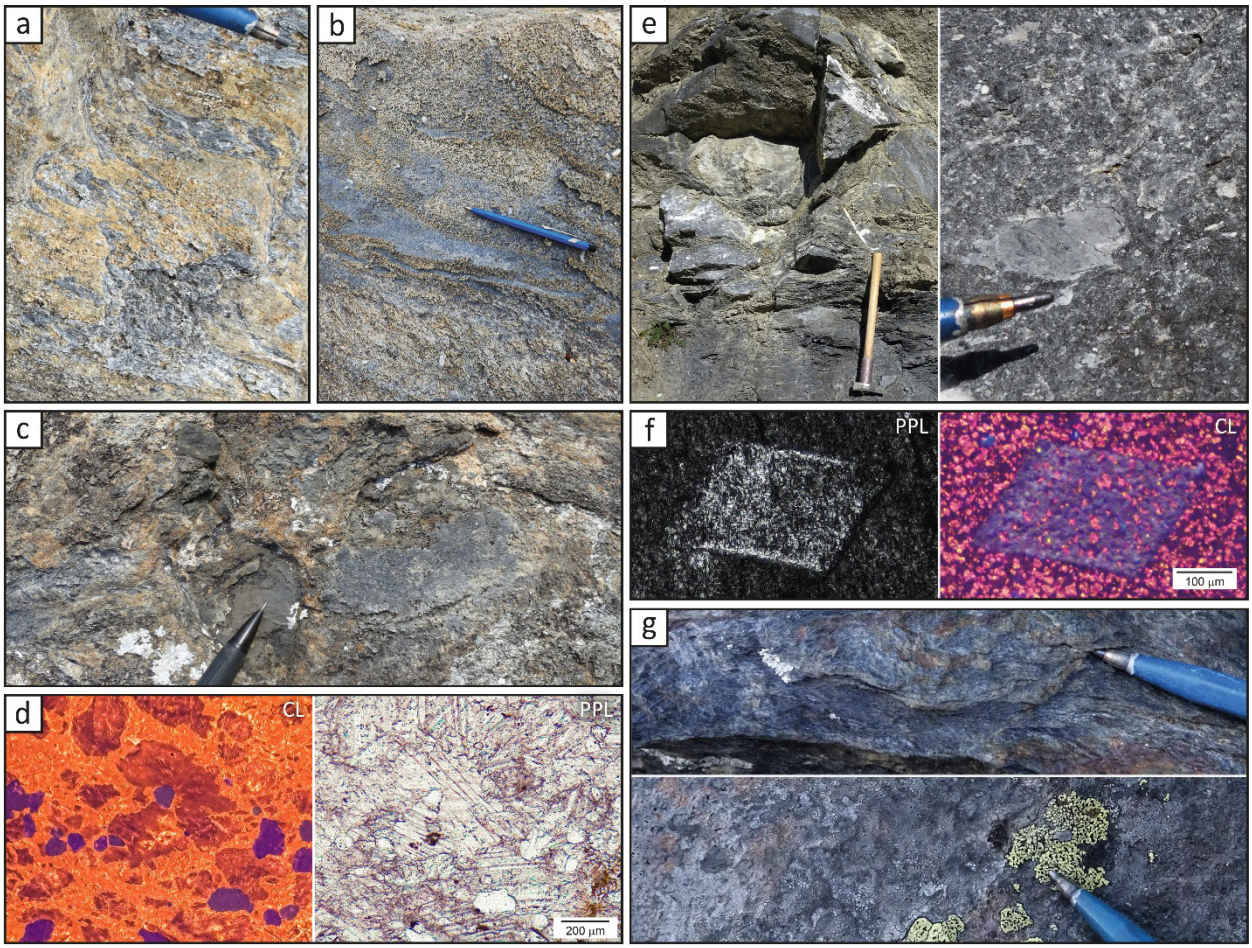

Fig. 3.4 Lithologies of the Série Rousse. **a** Typical glossy metallic grey appearance of the schistosity surfaces of the Série Rousse calcschists; Meina pass [2'599'280/1'105'330], Hérens valley. **b** Alternating grey calcitic marble and russet calcschist levels in the Série Rousse; dolomitic clasts are visible in the same outcrop; Rochers du Bouc [2'595'210/1'099'620], Dix valley. **c** Centimetric clasts in the Série Rousse, mainly formed by dolomites (pencil), limestones and minor quartzschists (out of the picture); Pic d'Artsinol [2'598'770/1'107'050]. **d** Microscopic aspect of a quartzitic marble from the base of the Série Rousse. CL: cathodoluminescence; PPL: plane polarized light. Well sorted rounded detrital quartz grains appear in violet in CL; dolomitic grains show mauve to dull orange colors; overgrowth (probably burial) cements are bright orange; zoning and/or dark rims are discordant with respect to the twinning (PPL) and could represent original variations of Mn^{2+} incorporation; Pic d'Artsinol [2'599'170/1'108'585]. **e** Dark levels of calcschists, calcitic marbles and dolomitic breccia (close-up picture) from the Série Rousse; La Tour [2'605'440/1'104'770], Hérens valley. **f** Rhombohedral automorph mineral observed in various thin sections of dark micritic calcitic marbles of the Série Rousse. Raman spectra indicate feldspar; Pic d'Artsinol [2'598'700/1'108'400]. Similar rhombohedron resulting from the silicification of automorph dolomite crystals are described in dark micrites of the "mid"-Cretaceous Joux Verte Fm. of the Breccia nappe (Dall'Agnolo 1997). **g** Dark non-carbonated schists outcropping 20 m above the base of the Série Rousse at La Vieille [2'602'800/1'105'540], Hérens valley.

3.3. Methods

3.3.1. Field observations and mapping

This study was based essentially on an extensive geological field work conducted over five consecutive seasons. A relatively large-scale approach was favored (studied area extending through the Bagnes, Dix, Hérens, Anniviers and Turtmann valleys; Fig. 3.1b), while the level of detail of the observations was adapted to the interest and quality of the outcrops.

3.3.2. Cathodoluminescence (CL)

Cathodoluminescence, or the emission of photons in the visible range of the electromagnetic spectrum under cathodic excitation, is a technique routinely used in mineralogy and sedimentary petrography, as it may enable to distinguish patterns of trace elements remaining undetectable under classical optical microscopy. CL depends on the presence of activator ions, which are stimulated to emit light when bombarded with energetic electrons, or on the presence of quencher ions. In carbonates, the best-known activator is Mn^{2+}. Bivalent iron (Fe^{2+}) is the most important quencher ion (e.g. Machel et al. 1991). In metasediments showing advanced calcite recrystallization, CL can allow to highlight the presence of microfossils or to distinguish sedimentary structures, no longer recognizable under classical optical microscopy.

CL images were obtained at the University of Lausanne using a Technosyn 8200 MkII mounted on an Olympus BH-2 microscope, and operated at 15-20 kV and 0.4-0.5 mA with an unfocused cold cathode electron beam under a He atmosphere at 0.2 torr.

3.3.3. Raman Spectroscopy of Carbonaceous Material (RSCM)

Raman graphite thermometry is based on the progressive transformation of organic matter into graphite with increasing temperature. As this transformation is considered to be irreversible, the structural organization of the carbonaceous material (CM) records the maximum temperature reached during metamorphism (Wopenka and Pasteris 1993; Beyssac et al. 2002, 2003a). Beyssac et al. (2002) obtained a linear correlation between the peak temperature and the structural organization of CM (RSCM method). This method enables the determination of the peak temperature in the range of 330-650 °C with an absolute accuracy of ± 50 °C. Relative uncertainties on peak temperature may however be much smaller (e.g. Beyssac et al. 2004; Wiederkehr et al. 2011; Negro et al. 2013; Angiboust et al. 2014).

Raman spectroscopy was performed at the University of Lausanne using a HR Raman-FTIR spectrometer from HORIBA Scientific, an integrated Raman microprobe consisting of an Olympus BX41 confocal microscope coupled to an 800 mm focal-length spectrograph. A 532.12 nm frequency doubled Nd-YAG continuous wave laser was focused on the sample. The power of the laser at the surface of the sample was 9 mW. Analytical procedures from Beyssac et al. (2002, 2003b) were followed closely while also taking into account the recommendations reported in Beyssac and Lazzeri (2012): measurements were carried out on polished thin sections, and CM was systematically analyzed below a transparent adjacent mineral, most often quartz. The sampled volume was a few μm^3 using a 100× objective. The Raman signal was collected in backscattered mode. Analyses were carried out using a grating of 1800 grooves/mm, a 150 μm slit aperture and a 150 μm hole. Spectra were recorded in extended scanning mode (1100-1800 cm^{-1}) using the LabspecTM v.4.15 software and an acquisition time of 2×40 s. The spectrometer was calibrated with a silicon standard before each session. Spectra were acquired in 12-35 different spots on each sample. They were processed using the PeakFit v4.12 software. A linear baseline correction was applied using systematically the same parameters (2^{nd} derivative zero linear correction, tolerance 0.5%, zero negative correction). Peaks D1 (~1350 cm^{-1}), G (~1510 cm^{-1}) and D2 (~1620 cm^{-1}) were systematically fitted, peak D3 (~1510 cm^{-1}) was fitted additionally when present. Spectra which could not be fitted with r^2 coef. ≥ 0.995 (PeakFit variance analysis), were rejected. For each sample, temperatures calculated from 10-16 spectra (using equations from Beyssac et al. 2002) were averaged to obtain the peak temperature value.

3.4. New lithological observations

3.4.1. Série Rousse

3.4.1.1. Lithological descriptions and successions

Series devoid of ophiolitic material

Following our observations, the Série Rousse is systematically devoid of ophiolitic material. A metric level of prasinites, intercalated in the calcschists between the SE side of the village of Evolène and the vicinity of the Sasseneire summit, has however been assigned to these series by some authors (Allimann 1987, 1990; Marthaler et al. 2020b) and would represent the only ophiolitic occurrence attributed to these series. According to our interpretation, these ophiolite-bearing calcschists do not belong to the Série Rousse, but to the overlying Série Grise, forming a pinched syncline in this area (Fig. 3.1b). Indeed, associated to these prasinites, ultrabasic rocks can also be observed locally, and in particular, a lens of several meters long of talcschists described by Gerlach (1861), Pfeifer et al. (2011) and Marthaler al. (2020b). Serpentinite lenses of a few cm are associated to the talcschists at point [2'605’040/1'106’260]. Additionally, the calcschists hosting these ophiolitic intercalations are significantly richer in phyllosilicates than those of the surrounding Série Rousse. Our RSCM data (cf. chap. 3.6) point to the presence of a tectonic contact located between these calcschists and the adjacent Série Rousse.

Thickness of the series

The Série Rousse shows large variations in thickness. It reaches several hundred meters in several sectors of the study area (e.g. in the Dix valley), but can be reduced locally to a few tens of meters, as in the thin band bordering the frontal folds of the Mont Fort nappe, east of the village of Evolène (Fig. 3.1b). These important thickness reductions can be partly of tectonic origin (strongly stretched fold limbs), but can locally also have a stratigraphic origin (cf. chap. 3.7.1.2).

Quartz-phyllitic calcitic marbles and calcschists

At the base of the Série Rousse, the lithologies are frequently massive and contain less micas over the first few meters, or sometimes several tens of meters. They generally consist of calcitic, quartzitic and phyllitic marbles. Detrital quartz, which can be very abundant, is either disseminated in the calcareous matrix, or occurs as size-sorted rounded grains of a few tens of hundreds µm size; it is sometimes accompanied by dolomitic grains of arenitic size (Fig. 3.4d). These basal lithologies are locally conglomeratic (cf. chap. 3.5.1.2). The clasts are mostly made of dolomites and limestones (Fig. 3.4c), sometimes of quartzite or gneiss; their size is millimetric to centimetric, sometimes metric.

The micaceous component increases upwards in the series, which is dominated by calcschists in its upper part. Calcite remains however more abundant in the calcschists of the Série Rousse than in those of the overlying ophiolite-bearing Série Grise.

Dark calcschists and marbles, black schists

Dark layers are interbedded at the base of the Série Rousse in several localities of the study area. They are formed of dark, micaceous and graphitic calcschists, which alternate with dark calcitic marbles and local breccias (Fig. 3.4d). Such layers form the base of the Série Rousse, for example, in the area of Mauvoisin in the Bagnes valley [2'592'810/1'094'670; 2'593'490/1'093'710]; and of the Pic d'Artsinol [2'598'660/1'108'430; 2'599'150/1'108'360], St-Christophe [2'605'700/ 1'105'190], La Tour [2'605'440/1'104'770] and La Vieille [2'602'680/1'105'660; 2'602'800/ 1'105'530] in the Hérens valley. In the last locality, dark calcschists, about 20 m thick, are overlain by black siliceous and non-carbonaceous schists (Fig. 3.4f; Marthaler et al. 2020b). These authors note the analogy between these siliceous schists and those of the Joux Verte Fm. from the Breccia nappe in the Chablais Prealps (Dall'Agnolo 1997, 2000), dated by planktic foraminifera from the "mid"-Cretaceous (late Barremian - middle Turonian). The Joux Verte Fm. shows different levels

of dark pelites, correlated at the scale of the Breccia basin and corresponding, according to Dall'Agnolo (1997, 2000), to "mid"-Cretaceous global anoxic events (e.g. Jenkyns 1980; Erbacher and Thurow 1997). The dark basal levels of the Série Rousse also show microscopic facies analogies with those of the Joux Verte Fm. In particular, dark mottled micrites contain rhombohedral automorph silicates of a few hundred µm size (Fig. 3.4f; Raman spectra indicate feldspar), strongly reminiscent of silicified dolomite rhombohedra described by Dall'Agnolo (1997, p. 177) in similar dark micrites containing radiolarians and echinoderm remains. The dark micrites of the base of the Série Rousse also contain locally abundant circular siliceous elements of homogeneous ca. 100 µm size that may correspond to radiolarians and possible echinoderm remains (Figs. 3.5d, f, g; cf. next paragraph).

3.4.1.2. Microfauna descriptions

Thin sections of about forty samples of the Série Rousse were examined under the microscope for the detection of microfossil relics. The study under transmitted light (TL) having proven unsuccessful, it was completed by a cathodoluminescence (CL) examination. It allowed the detection of higher Mn^{2+} trace element concentrations in microfossil relics than in the surrounding sediment, despite the high degree of recrystallization. This method allowed the identification of different biogenic features within a few samples, that were particularly spared from the intense regional deformation.

Samples from the base of the Série Rousse north of the Pic d'Artsinol

Some samples collected at the base of the Série Rousse, close to the summit of the Rionde de Vendes [2'599'170/1'108'585], show little deformation, and hence, relatively well-preserved sedimentary features (Fig. 3.5a). The very competent lithologies of these levels and of the underlying polygenic breccias of the Evolène Series, have probably contributed to this unusual preservation. These samples consist of phyllitic and quartzitic calcitic marbles, containing mm- to

cm-sized clasts of dolomite, quartz, pelagic limestone and quartzschist. Different biogenic features are observed in the thin section of Fig. 3.5a.

The matrix contains some rare dark (TL and CL) round elements of ± 200 µm size, showing regular round openings filled with carbonate of dull orange CL-emission. We interpret these features as originally pyritized and now oxidized holothurian skeletal elements (Fig. 3.5b; a similar form was found in the sample of Fig. 3.5c, few meters above). In the matrix of the first sample, some dolomitic laminae most probably represent reworked echinoderm remains (Fig. 3.5d). Particular shapes of the dark rims (CL) actually suggest stereomes of crinoid ossicles. As both crinoids and holothurians have existed throughout the Mesozoic from shallow shelf to deeper marine environments, they are not age diagnostic, but are, nevertheless, indicative of a higher nutrient environment in their source area, perhaps on an outer slope. Pyrite is preserved in some thin sections and the pyritization of echinoderm remains is common in nutrient-rich paleoenvironments.

Some mm- to cm-sized disrupted clasts of pelagic limestone show preserved lamination and organic matter. These clasts show two distinct lithologies in original sedimentary contact, which can be followed across adjacent fragments (Fig. 3.5a): a lighter grey micrite; and a dark grey, mottled micrite rich in carbonaceous material (confirmed by Raman). The mottles are in fact flattened flakes that could represent original faecal pellets. The borders of the pelagic limestone clasts are fuzzy, suggesting penecontemporaneous reworking into a pebbly sandstone. In CL, the two pelagic lithologies show uniform mauve colors with some blue specks (disseminated biogenic quartz?) and rare bright yellow-orange lens-shaped structures that could represent fossil remains. The mauve color of the pelagic matrix (e.g. Fig. 3.5e) indicates a mixture of the intrinsic blue (± 410 nm) calcite CL, with very low (< 1 ppm) Mn^{2+} orange (600 nm) activation, while the

possible fossil remains contain > 10 ppm of Mn^{2+}. The orange colored intraclast of Fig. 3.5e shows bright yellow outlines (CL) that strongly suggest a double-keeled planktic foraminifera.

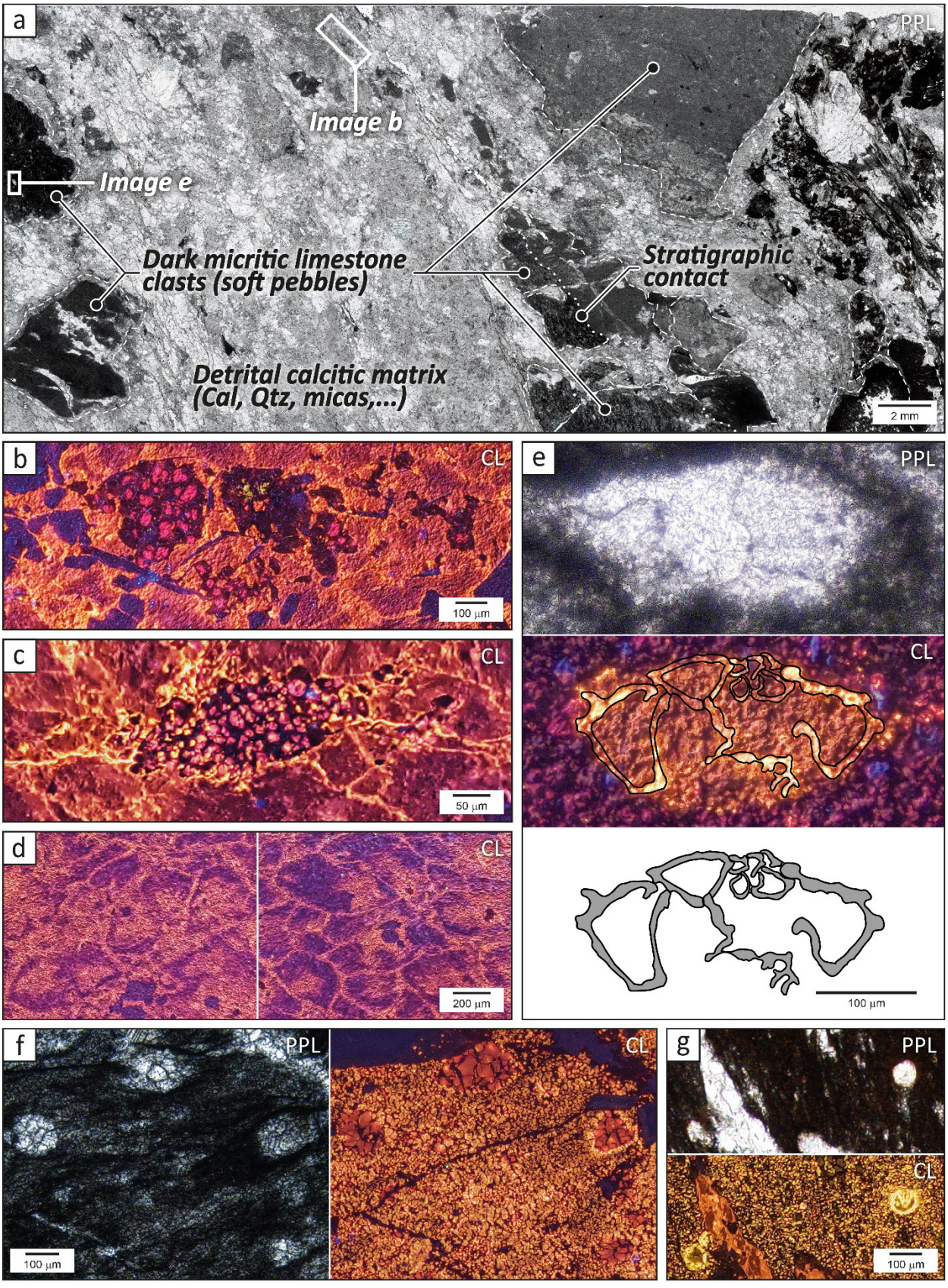

◄ **Fig. 3.5** Potential microfauna observed in Série Rousse samples. CL: cathodoluminescence; PPL: plane-polarized light. **a** Thin section from a conglomerate of the very base of the Série Rousse; Pic d'Artsinol [2'599'170/1'108'585]; sampled a few meters from Fig. 3.8a. The thickness of the conglomeratic level does not exceed 2 m; the mm- to cm-sized clasts are mainly made of dolomites and limestones; a gradual transition is observed to the overlying typical calcschists of the Série Rousse. In comparison with the intense strain generally observed in other samples of the Série Rousse, strain is locally exceptionally low, which allows the preservation of some microfauna that is generally entirely destructed elsewhere. Rounded borders of the clasts could suggest an incomplete diagenesis of the clasts, before their reworking into the conglomerate. **b** Holothuroidea fragments from the matrix of the conglomerate in the same thin-section. **c** Holothuroidea fragment from arenitic calcschist of the Série Rousse, sampled few meters above. **d** Probable reworked echinoderm remains; shapes of the dark rims (CL) suggest stereomes of crinoid ossicles. **e** Probable planktic foraminifera observed as intraclast in a rounded, dark micritic limestone pebble. The form may correspond to Globotruncana neotricarinata, Petrizzo, Falzoni and Premoli Silva (2011) indicating an age range from Campanian to earliest Maastrichtian for the rounded clast. In order to preserve the observed form, the polishing protocol was not fully completed on this thin section. **f, g** Potential radiolarian from a dark micritic limestone element from the base of the Série Rousse; fuzzy borders of the forms could indicate a partial infill of the sediment inside the pores of radiolarian tests; Evolène [2'606'105/1'109'340].

This form suggests a low trochospiral test with a convex spiral side and two equidistant keels, parallel to the coiling axis and separated by a narrow band. Chambers of the last whorl are inflated and trapezoidal on the umbilical side, with an apparent third keel. Such a description would correspond to *Globotruncana neotricarinata* Petrizzo, Falzoni and Premoli Silva (2011). This species has, according to Petrizzo et al. (2011), a diachronous first appearance ranging from the late Santonian (Exmouth Plateau, NE Australia) to the base of the Campanian (Bottacione, Umbria, Italia). It disappears within the *Gansserina ganseri* Zone, which reaches the earliest Maastrichtian. Hence, a Campanian to earliest Maastrichtian age range for the pelagic limestone clasts can be inferred. This age is thus slightly younger than the one deduced from the foraminifera described in the Série Rousse so far (cf. chap. 3.2.3.3). Unfortunately, this finding cannot be confirmed for now with more material. A Campanian maximum age of the Série Rousse must remain a working hypothesis.

Sample from a micritic limestone clast from the Série Rousse NE of Evolène

A sample from a meter-sized clast of micritic limestone, included at the very base of the Série Rousse, SW of the Sasseneire in the Hérens valley [2'606'105/1'109'340], shows in thin section numerous circular features, white in TL, of a homogeneous size of about 100 µm (Figs. 3.5f-g). Their color contrasts strongly with the very dark color of the rock (micritic limestone transformed into calcitic marble). The observation of these features in CL allows to highlight chemical variations between their internal part (appearing orange red; Fig. 3.5f CL), their border

(appearing bright yellow; Figs. 3.5f-g) and the surrounding sediment. Their shape, size, distribution in the sediment and the aspect of their borders (appearing fuzzy in TL and discontinuous in CL; Figs. 3.5f-g), suggest that these forms correspond to radiolarians. These border aspects could reflect their porous nature and the partial filling of these pores by the surrounding sediment.

3.4.2. Mauvoisin marbles

Massive, slightly detrital siliceous calcitic marbles (Fig. 3.6) form the bedrock of the Série Rousse in several sectors of the study area. They are best developed in the area of the Mauvoisin dam, where they reach several hundred meters in thickness (Fig. 3.7a). On the 1:25'000 geological map (Burri et al. 1998, 1999), they are referred to as « unité de Mauvoisin », one of the tectonic units defined in the Tsaté nappe by these authors. We propose to use the term *Mauvoisin marbles* to designate this lithostratigraphic formation.

These characteristic siliceous calcitic marbles can be recognized in other zones of the studied area, in particular in the Hérens valley, where they form massive cliffs, well exposed under the villages of La Sage and Villa. In this zone, the best outcrops can be observed south of the hamlet of La Tour, at that of L'Ata Gieute, at Plan Tsardon [2'603'250/1'105'680], at La Vieille [2'602'680/1'105'660] and at La Noûva [2'600'320/1'107'300; 2'600'260/1'107'840].

The characteristic facies of the Mauvoisin marbles is a massive, quartzitic and slightly phyllitic calcitic marble in decimetric to metric beds, showing millimetric to pluricentimetric thick siliceous bands, often standing out in relief on outcrop surfaces (Figs. 3.6a-c).

The mineralogy is composed of calcite, quartz, white mica, albite, chlorite, graphite and oxides ± epidote, tourmaline, apatite and titanite; in the siliceous levels, quartz can constitute more than 80% of the rock (Burri et al. 1999). Locally, millimetric to centimetric clasts are present; they are mainly made of dolomites and limestones (Fig. 3.6d). In places, these clasts can be relatively

abundant and a few levels of breccia, generally matrix supported and sometimes slightly graded, are visible (Fig. 3.6e). The siliceous banded calcitic marbles described above may also evolve into very siliceous and massive calcitic marbles in some areas.

Although these different levels have sometimes been grouped together with the overlying Schistes Lustrés (e.g. Gouffon and Burri 1997; Burri et al. 1998, 1999), or more specifically with the Série Rousse (Allimann 1990; Steck et al. 1999), their massive aspect and their calcite- and quartz-rich composition clearly distinguish them from these units (cf. Sartori and Marthaler 1994).

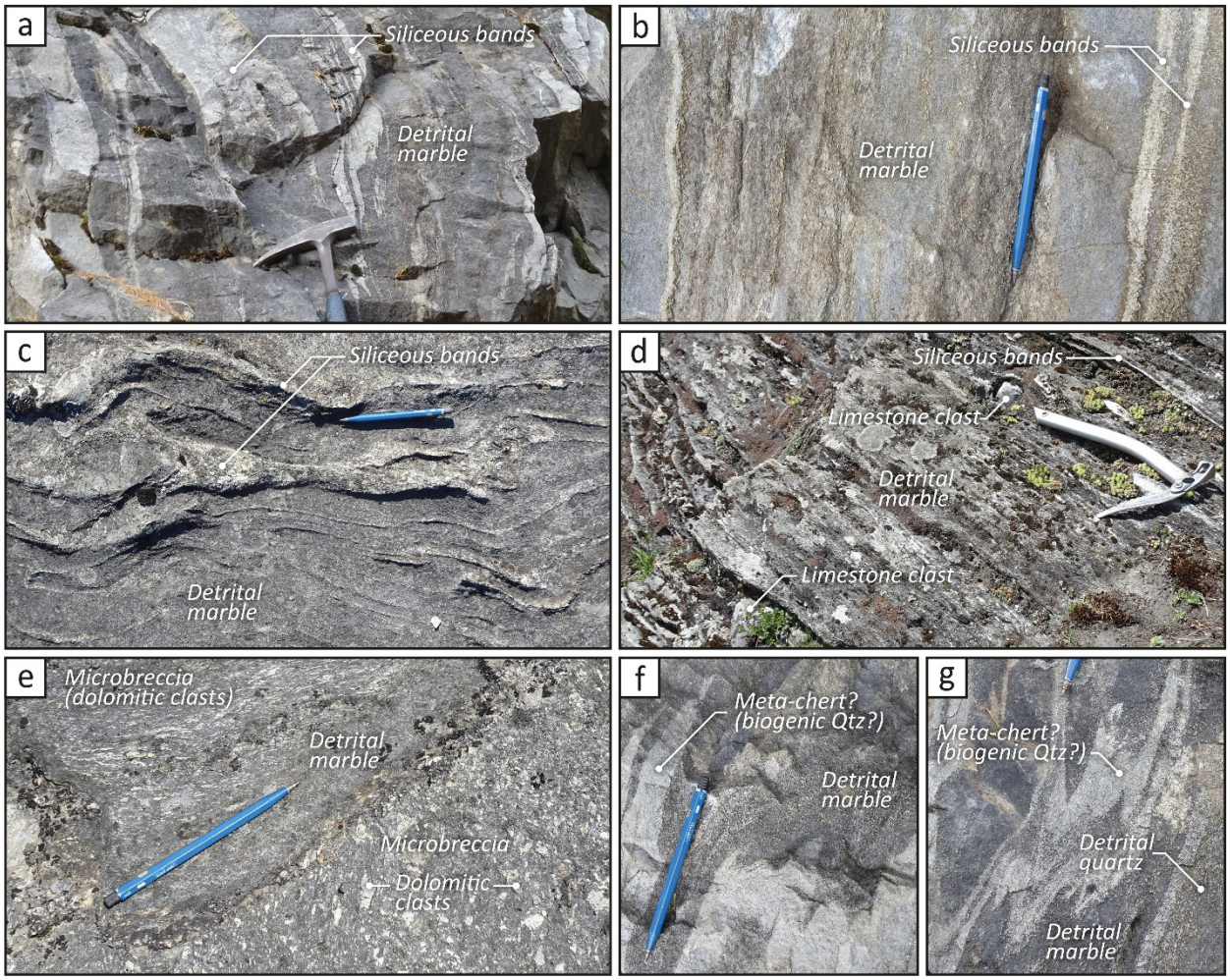

Fig. 3.6 Characteristic facies of the Mauvoisin marbles. **a, b** Slightly detrital calcitic marble with siliceous mm-cm thick bands; Mauvoisin [2'592'650/1'094'510]. **c** Similar lithology at La Tour [2'605'310/1'104'860], Hérens valley. **d** Detrital calcitic marble with mm-cm thick siliceous bands and sparse cm-dm thick limestone clasts (dolomitic clasts appear out of the picture); Giétro [2'593'690/1'092'930], Bagnes valley. **e** Alternating layers of detrital calcitic marble and dolomitic microbreccia; 10 m from Fig. c. **f, g** Details of the outcrops of Figs. a-b. In g: sharp borders are observed at the contact between the siliceous bands and the surrounding marble, whereas a progressive transition is visible to the more carbonaceous inner parts of these bands. As this characteristic is typical of cherts that are not fully silicified in their inner parts, it supports the biogenic nature of these siliceous bands.

No fossils have been found in the Mauvoisin marbles. Some authors have proposed an Early Jurassic age for part of these levels (Sartori and Marthaler 1994; Burri et al. 1999; Marthaler et al. 2020b), by analogy with some facies of the Briançonnais Lower Jurassic. Marthaler et al. (2020b) also note analogies between the siliceous banded calcitic marbles from La Vieille [2'602'680/1'105'660] and lithologies of the Bonave Fm. from the Breccia nappe in the Prealps, which have been dated by *Calpionella* from latest Jurassic / Early Cretaceous (Dall'Agnolo 1997, 2000). Sartori et al. (2006, fig. 18) suggest the same correlation for similar white marbles, overlying the polygenic breccias of the Pic d'Artsinol area.

Our observations throughout the study area confirm the clear analogy between the dominant facies of the Mauvoisin marbles (slightly micaceous siliceous marbles with mm-cm thick siliceous bands) and those described in the Bonave Fm. In particular, the following similarities can be noted. (i) Layers of graded breccias, with clast sizes up to a few cm, occur at various levels of the Bonave Fm. (Dall'Agnolo 1997, 2000), similar to those observed in the Mauvoisin marbles (Fig. 3.6e). (ii) In the Mauvoisin marbles, some siliceous bands show sharp external borders and locally a progressive passage towards a less siliceous internal part (Fig. 3.6f), arguing for a biogenic origin of silica, diagenetically concentrated in replacement chert bands. They could thus correspond to metamorphic equivalents of the characteristic siliceous levels and cherts of the Bonave Fm. (iii) In the upper levels of the Bonave Fm., the cherts and siliceous levels become less abundant and a more diffuse silicification of the limestone is observed, while the detrital component and the frequency of marly interlayers increase (Dall'Agnolo 2000). A similar facies evolution can be observed, e.g. at Mauvoisin along the road between the hotel and the base of the dam. A transition is observed here from facies showing sharply individualized siliceous bands (Figs. 3.6a-b), to massive, almost non-bedded, very siliceous calcitic marbles [2'592'740/1'094'350], that are surrounded by thin layers of micaceous calcschists.

The marked similarities between the Mauvoisin marbles and the lithologies of the Bonave Fm. thus suggest a Late Jurassic to Early Cretaceous age for the Mauvoisin marbles. They would therefore constitute the youngest levels of the Evolène Series.

3.5. Description of the contacts

3.5.1. Basal contact of the Série Rousse

3.5.1.1. Basal unconformity

In the study area, the Série Rousse systematically overlies the Paleozoic basement of the Mont Fort nappe or its Lower Triassic to Lower Cretaceous autochthonous cover (the Evolène Series; cf. Pantet et al. 2020). In the region of Evolène, of the Sasseneire and of Moiry (Fig. 3.1b), the Série Rousse envelops the frontal folds of the Evolène Series and forms to the east highly stretched isoclinal folds, which can to be followed up to the Turtmann and Matter valleys (Sartori 1987, 1990; Marthaler et al. 2008a).

The map in Fig. 3.1b shows that the Série Rousse lies either on the Evolène Series, or alternately directly on the Paleozoic basement of the Mont Fort nappe. This second case is observed in several sectors of the normal limb of this nappe, e.g. in the Col du Vasevay and La Sâle area in the Bagnes valley (Fig. 3.7; Gerlach 1871), in the Lac des Dix area, and in part of its reverse limb (between Evolène and the Montset). Our detailed mapping shows that it actually overlies different levels of the Mont Fort basement and of the Evolène Series (Fig. 3.7); levels whose ages probably range from Ordovician (Gauthiez et al. 2011) to Early Cretaceous (cf. chap. 3.4.2). The basal contact of the Série Rousse over the Mont Fort nappe is therefore characterized by a major unconformity.

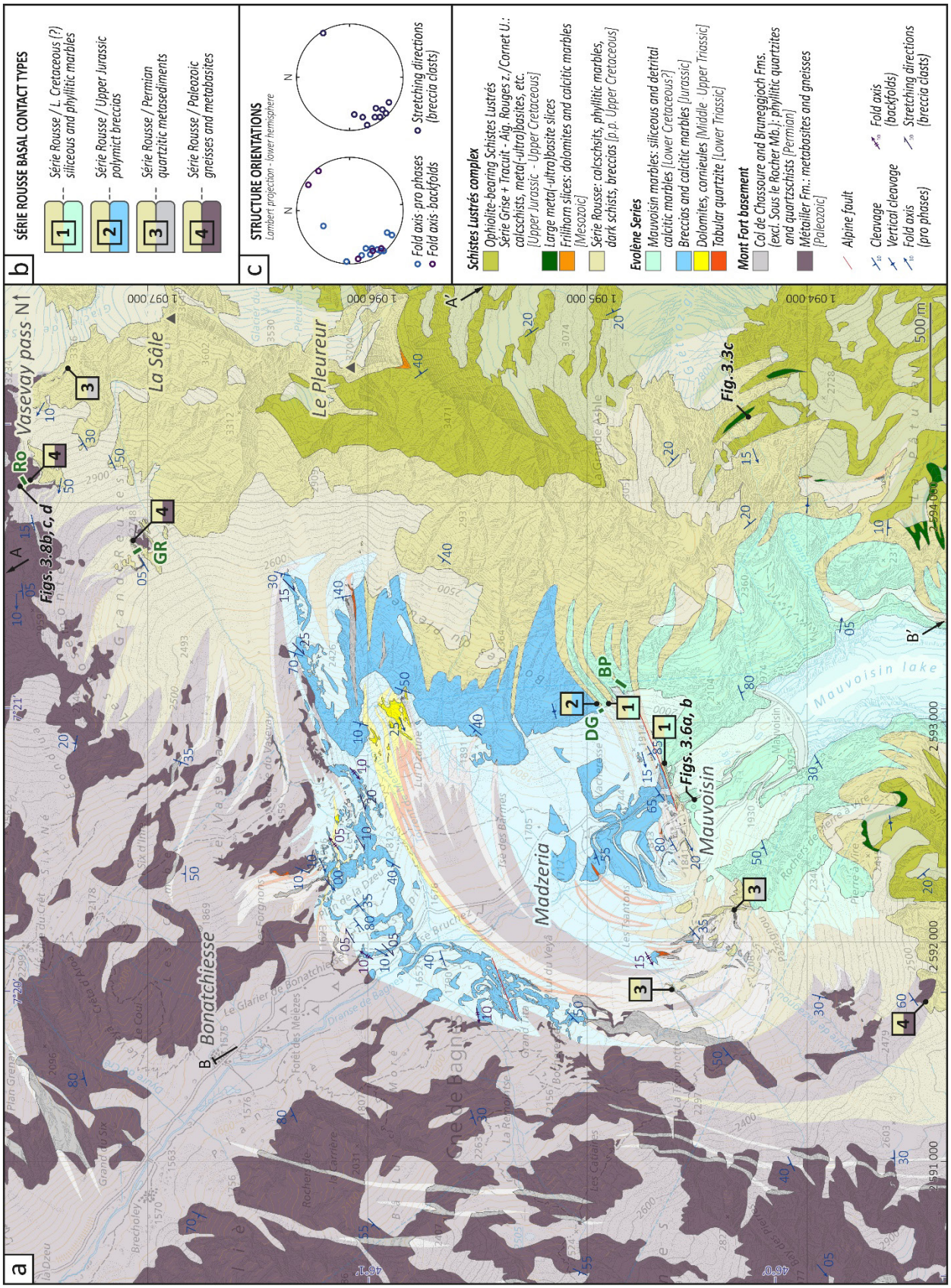

Fig. 3.7 a Detailed geological map of the Mauvoisin area, Bagnes valley; after observations from this study and maps from Baillifard (1998), Burri et al. (1998), Steck et al. (1999) and Dal Piaz et al. (2015b). Topographic base ©Swisstopo 2016; contour intervals: 20 m. 1, 2, 3, 4 refer to Fig. b; Locations of the cross-sections of Fig. 3.11a are indicated by A, A', B, B'; *Fig.x* refer to pictures from other figures; locations of the stratigraphic columns of Fig. 3.11b are indicated in green. **b** Types of basal contacts of the Série Rousse in the area covered by the map. **c** Fold axis and stretching directions in the area covered by the map.

3.5.1.2. Deformation along the contact: localized shearing due to rheological contrasts and locally unsheared contact

A strong rheological contrast often characterizes the contact between the Série Rousse and the underlying levels of the Mont Fort basement and Evolène Series. Indeed, lithologies constituting the Mont Fort nappe are mostly rheologically strong (e.g. gneisses and metabasites of the Paleozoic basement; breccias, dolomites and quartzites of the Evolène Series), whereas most of the lithologies of the Série Rousse are rich in phyllosilicates and are rheologically weak. These contrasting competences frequently lead to a local shearing of the contact.

However, along the sections of the contact where the base of the Série Rousse is itself composed of rheologically strong lithologies (quartzitic marbles, conglomerates), no hint of particular shearing can be detected at the contact (cf. Figs. 3.8a, e, f).

These observations indicate that the basal contact of the Série Rousse over the Mont Fort nappe does not correspond to a major tectonic contact.

3.5.1.3. Basal conglomerates

A conglomeratic level is locally observed at the base of the Série Rousse. Its thickness can reach a few meters, e.g. west of the Vasevay pass in the Bagnes valley (Figs. 3.7, 3.8b), where it was already mentioned by Hagen (1951). Most often its thickness is limited to a few tens of centimeters, or a few centimeters only (Figs. 3.8e-f). Although these conglomerates can be observed in many localities in the study area (Fig. 3.8i), they are most often absent.

The matrix of these conglomerates is of the same composition as the overlying calcschists of the Série Rousse. A gradual transition can be observed between the conglomerates and the calcschists, by progressive increase of the proportion of matrix. These conglomerates are generally polymict. The clasts mostly consist of dolomites, limestones and pure or phyllitic quartzites, sometimes of prasinites/ovardites. Locally, clasts made of breccias (dolomitic clasts and calcareous matrix) can

also be observed (Fig. 3.8d). The presence of these breccia elements and the abundance of phyllosilicates and detrital quartz in the matrix distinguish these conglomerates from the polymict breccias of the Evolène Series of presumed Late Jurassic age (cf. chap. 2.4), even if these two formations are sometimes directly in contact (e.g. Fig. 3.8a). The discovery of a form probably corresponding to a *Globotruncana* sp. in a clast of this basal conglomerate of the Série Rousse (cf. chap. 3.4.1.2), as well as the various presumed relics of *Rotalipora* sp. and bicarinate planktic foraminifera observed in the matrix of other levels of the Série Rousse (cf. chap. 3.2.3.3), would indicate a Late Cretaceous age for these conglomerates.

In different zones of the study area, a correlation can be established between the nature of the clasts of the basal conglomerate of the Série Rousse and the underlying rocks of the Mont Fort nappe. For example, west of the Vasevay pass (Fig. 3.7), the Série Rousse is in contact with Paleozoic metabasites of the Mont Fort basement (Métailler Fm.) and its basal conglomerate contains here numerous clasts of identical lithology (Figs. 3.8b-c). Such a relationship can also be observed near the Col des Roux, where the base of the Série Rousse is locally formed by a conglomerate-rich in decimetric clasts of pure quartzites, identical to the Tabular Quartzites of the Evolène Series, underneath the contact (Fig. 3.8e). On the other hand, no clast observed in this conglomerate consists of a rock that does not form the Evolène Series or the basement of the Mont Fort nappe (such as e.g. granites or serpentinites).

Fig. 3.8 Conglomerates and hardground from the basal contact of the Série Rousse. **a** Contact between a polymict conglomerate forming the base of the Série Rousse (russet phyllitic and quartzitic calcitic matrix) and a polymict (Upper Jurassic?) breccia from the Evolène Series. The conglomeratic base of the Série Rousse is only of a few meters thick. A gradual transition is observed with the overlying calcschists of the same series. Rionde de Vendes [2'599'180/1'108'600], Dix valley. **b** Overturned contact between the Mont Fort Paleozoic basement (Métailler Fm.) and a polymict conglomerate forming the base of the Série Rousse and gradually passing to the typical calcschists of these series (base of the outcrop); Col du Vasevay [2'594'090/1'097'560], Bagnes valley. **c** Close-up view on locally abundant green elements of the basal conglomerate; their lithology is identical to that of the overlying Paleozoic metabasites of the Métailler Fm. **d** Close-up view on clasts of the same conglomerate made of dolomites, limestones and breccias (dolomitic clasts, calcitic matrix). **e** Basal conglomerate of the Série Rousse showing dm-sized clasts made of the same lithology than the adjacent Tabular Quartzites of the Evolène Series; Col des Roux [2'595'580/1'102'090], Dix valley. **f** Oxidized crust (hardground) marking the base of the Série Rousse over a light grey (Upper Jurassic?) calcitic marble of the Evolène Series; the dolomitic clast visible at the very base of the Série Rousse shows a rounded shape indicative of the locally low strain and the absence of particular shearing along the contact (the clast is truncated orthogonally to its elongation), as well as the rolling of the clast; Pic d'Artsinol area [2'599'250/1'107'940]. **g** Basal hardground of the Série Rousse; same location. **h** Oxidized clasts (reworked hardground) observed in the Série Rousse basal conglomerate; Pic d'Artsinol area [2'600'115/1'105'950]; [2'600'210/1'105'840]; [2'600'100/1'105'965]. **i** Occurrences of the basal conglomerate and basal hardground of the Série Rousse (map from Fig. 3.1b). ▶

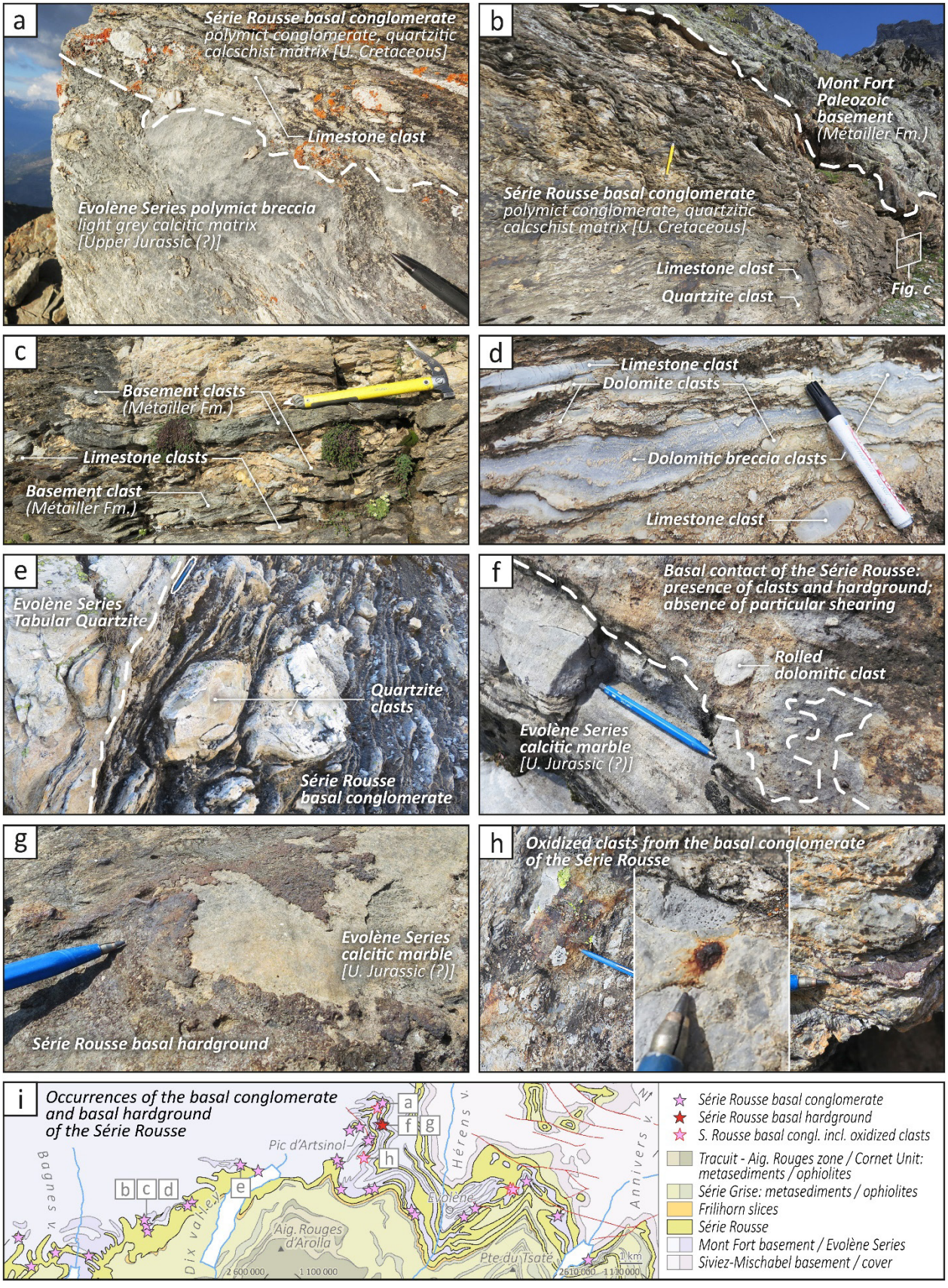
a
Série Rousse basal conglomerate
polymict conglomerate, quartzitic calcschist matrix [U. Cretaceous]
Limestone clast
Evolène Series polymict breccia
light grey calcitic matrix
[Upper Jurassic (?)]
b
Mont Fort Paleozoic basement
(Métailler Fm.)
Série Rousse basal conglomerate
polymict conglomerate, quartzitic calcschist matrix [U. Cretaceous]
Limestone clast
Quartzite clast
Fig. c
c
Basement clasts
(Métailler Fm.)
Limestone clasts
Basement clast
(Métailler Fm.)
d
Limestone clast
Dolomite clasts
Dolomitic breccia clasts
Limestone clast
e
Evolène Series
Tabular Quartzite
Quartzite clasts
Série Rousse
basal conglomerate
f
Basal contact of the Série Rousse:
presence of clasts and hardground;
absence of particular shearing
Rolled
dolomitic clast
Evolène Series
calcitic marble
[U. Jurassic (?)]
g
Evolène Series
calcitic marble
[U. Jurassic (?)]
Série Rousse basal hardground
h
Oxidized clasts from the basal conglomerate
of the Série Rousse
i
Occurrences of the basal conglomerate
and basal hardground
of the Série Rousse
a
f g
h
b c d
e
Pic d'Artsinol
Bagnes v.
Dix valley
Hérens v.
Evolène
Aig. Rouges d'Arolla
Pte du Tsaté
Annivers v.
2 600 000
1 100 000
2610 000
1 km
Série Rousse basal conglomerate
Série Rousse basal hardground
S. Rousse basal congl. incl. oxidized clasts
Tracuit - Aig. Rouges zone / Cornet Unit: metasediments / ophiolites
Série Grise: metasediments / ophiolites
Frilihorn slices
Série Rousse
Mont Fort basement / Evolène Series
Siviez-Mischabel basement / cover

On the contrary, the clasts made of breccias (calcitic matrix, dolomitic clasts), observed in this conglomerate at some localities (e.g. Fig. 3.8d), are particularly typical of the Evolène Series. These observations thus argue for a deposition of the Série Rousse in the immediate vicinity of the rocks constituting the present-day Mont Fort nappe.

On some outcrops preserved from a too strong deformation, it is possible to note the rounded shape of some clasts of the conglomerate (e.g. Fig. 3.8f), which is indicative of rolling of the clasts (mechanical abrasion) and argues for a formation of the conglomerate in a context of stratigraphic onlap on a relief.

These different observations thus clearly indicate the stratigraphic nature of the basal contact of the Série Rousse over the Mont Fort nappe.

3.5.1.4. Basal hardground

Strongly oxidized crusts of a few mm thickness are locally observed at the basal contact of the Série Rousse (Figs. 3.8f-g), on top of Jurassic breccias of the Evolène Series, or of calcitic marbles that would constitute their distal equivalents. Locally, these crusts mostly cover the basal surface of the Série Rousse. We interpret them as corresponding to a hardground. Strongly oxidized mm- to dm-sized clasts are locally observed in the basal conglomerate of the Série Rousse and would correspond to a reworking of such crusts (Fig. 3.8h). The presence of this hardground suggests a significant stratigraphic gap and confirms the stratigraphic nature of the basal contact of the Série Rousse.

3.5.2. Upper contact of the Série Rousse with ophiolite-bearing Schistes Lustrés and Frilihorn slices

Thin discontinuous tectonized slices of the Frilihorn Series (Triassic-Jurassic/Cretaceous; cf. chap. 3.2.3.2) frequently mark the contact between the Série Rousse and the overlying ophiolite-bearing Série Grise (Figs. 3.9a-c). They rarely exceed a few meters in thickness,

but can be present along the contact for several kilometers. Such slices are also observed in the same tectonic position, south of the study area, in the Ollomont valley (P. Manzotti and M. Ballèvre, oral communication) and in the Rhèmes valley (Adatte et al. 1992). Where the Frilihorn slices are absent or hidden by recent deposits, the contact between the Série Rousse and the Série Grise may be difficult to identify. The presence in the calcschists of ophiolitic lenses, of ophiolite-derived detrital material, or locally of fuchsite, sometimes allows the identification of the Série Grise, but the contact is often difficult to follow due to the presence of numerous isoclinal folds (Fig. 3.9c).

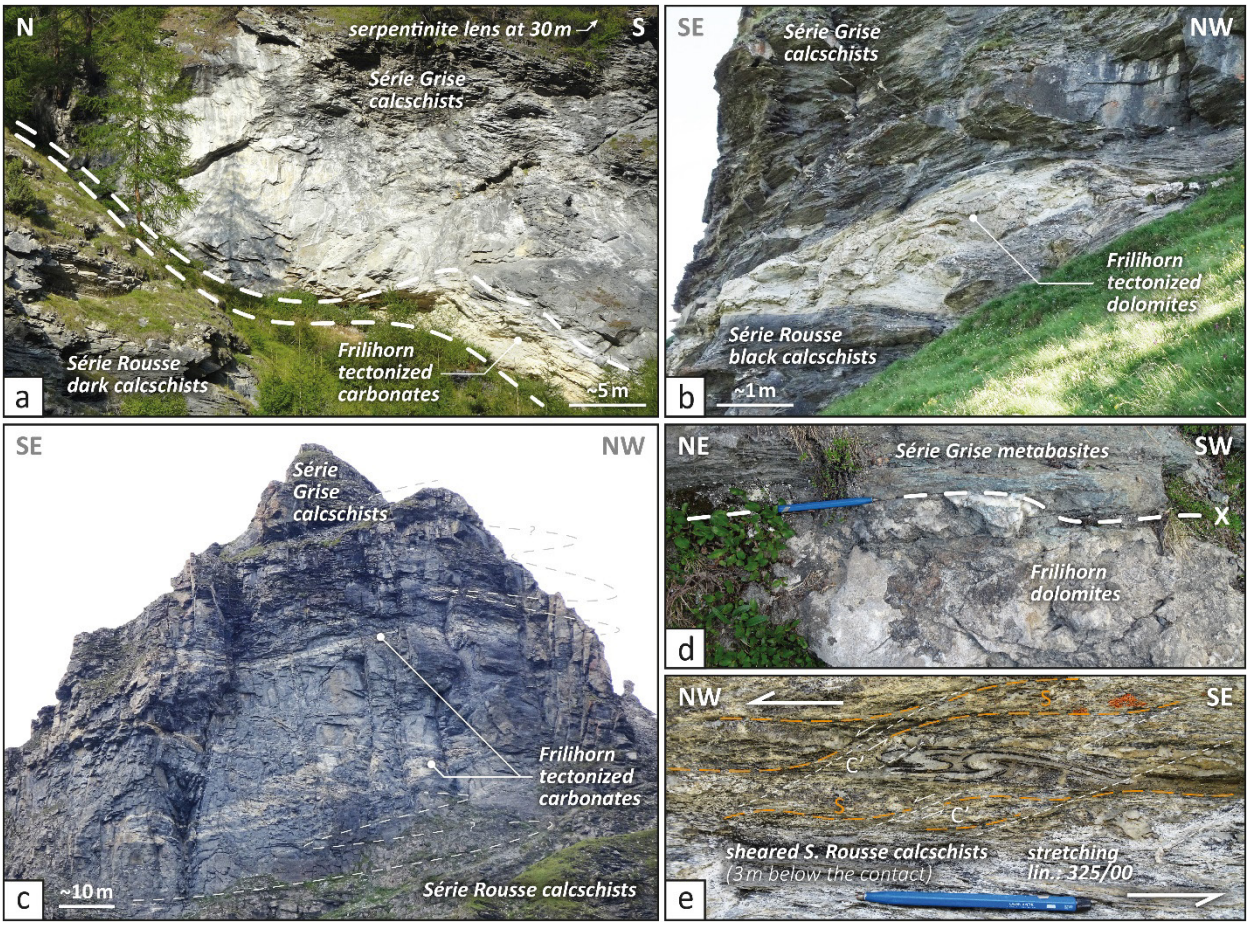

Fig. 3.9 Upper contact of the Série Rousse with the ophiolite-bearing Série Grise and the Frilihorn slices. **a** Tectonized Frilihorn carbonates (partly dolomitic) marking the contact between the Série Rousse and the Série Grise; La Sage [2'606'330/1'105'640], Hérens valley. **b** Frilihorn dolomitic boudins along the same contact; Plan Tsardon [2'603'410/1'105'470], Hérens valley. **c** Thin Frilihorn tectonized and folded bands (polyphase folding of a single band); Meina pass area [2'599'360/1'104'680], Hérens valley. **d** Sharp contact between Frilihorn dolomites and Série Grise metabasites; the Série Rousse is outcropping a few meters below; Palantse de la Cretta west face [2'600'990/1'104'380], Hérens valley. **e** Strongly sheared Série Rousse calcschists, 3 m below its upper contact with the Série Grise; the outcrop is parallel to the marked stretching lineation; asymmetric folds and C' structures indicate a top to the NW shear-sense; S: schistosity; C': extensional shear bands; Mel de la Niva [2'601'850/1'105'750], Hérens valley.

Deformation is generally extremely strong in the vicinity of the contact. It is demonstrated in particular by the intense stretching and boudinage observable in the Frilihorn slices (e.g. Figs. 3.9a-b). North of the Dent Blanche klippe, these slices are systematically affected by an intense shearing and are locally reduced to only a few dm-thick tectonized and highly fractured carbonates (e.g. Figs. 3.9b-c). An intense shearing is also observable within the calcschists directly surrounding the contact (e.g. Fig. 3.9e).

The contact is also characterized by the local abundance of quartz veins, that are more than 50 cm thick in several localities (e.g. [2'599'320/1'104'600], [2'601'700/1'105'640], [2'602'800/1'105'510]) and reach a thickness exceeding 1 m at point [2'601'010/1'104'460], SW of the Palantse de la Cretta in the Hérens valley.

Our observations thus confirm the tectonic nature of the upper contact of the Série Rousse with the ophiolite-bearing Schistes Lustrés, as postulated by all previous authors.

The question of the importance of this tectonic contact, in particular whether it corresponds to a major tectonic contact marking a nappe boundary, or even a tectonic domain boundary (Upper/Middle Penninic Domains), as proposed, for example, by Escher (1988); or whether it is a contact of lesser importance, internal to the Tsaté nappe as proposed, for example, by Sartori and Marthaler (1994), will be discussed in chap. 3.7.3.

3.6. Raman graphite Thermometry

RSCM analyses conducted by Negro et al. (2013), Angiboust et al. (2014), Decrausaz et al. (2021) and Manzotti et al. (2021) reveal significant variations in RSCM temperatures (cf. Beyssac et al. 2002), within the Schistes Lustrés of the Combin zone (Fig. 3.10c). In order to better characterize the variability of RSCM temperatures between the different units and series of this Schistes Lustrés complex (cf. chap. 3.2.2) and in particular between the Série Rousse and the

Série Grise, additional samples were analyzed during this study (Table 3.1). Sampling was concentrated on a limited area (Hérens valley sector; Fig. 3.10a) in order to avoid possible biases related to regional variations in the intensity of metamorphism. In addition, four samples were collected in the Mauvoisin area (Bagnes valley), in order to compare our results with previous studies and better characterize the regional variability of the RSCM temperatures within the different studied units (Fig. 3.10c). Two samples (AP2007 and AP2080) were intentionally collected in close proximity to samples from previous studies (CO0712 from Negro et al. 2013 and #62 from Angiboust et al. 2014, for AP2007; CO092 from Negro et al. 2013 for AP2080). The comparison between the RSCM temperature obtained for these samples show that RSCM temperature values are comparable between our study and these previous studies (values overlap within a 2σ error range for both locations).

Examination of the entire set of RSCM temperatures then available for the samples located in the Série Rousse and the Série Grise shows that no significant difference in temperature exists between these two series. Indeed, in the Hérens valley, these temperatures range from 408 ± 27 °C to 467 ± 23 °C for the Série Rousse (mean val. = 430 ± 20 °C; n = 10) and from 411 ± 17 °C to 466 ± 29 °C for the Série Grise (mean val. = 441 ± 16 °C; n = 8); in the Bagnes valley, between 457 ± 14 °C and 494 ± 7 °C for the Série Rousse (mean val. = 477 ± 15 °C; n = 7) and between 461 ± 4 °C and 487 ± 23 °C for the Série Grise (mean val. = 475 ± 9 °C; n = 8); the few values available in the Anniviers valley (incl. the Moiry valley) range between 441 ± 12 °C and 451 ± 5 °C for the Série Rousse (mean val.= 447 ± 5 °C; n = 3) and between 437 ± 14 °C and 458 ± 16 °C for the Série Grise (mean val.= 446 ± 10 °C; n = 5); see Additional file 3.2 for details.

These data show, however, a significant variation in RSCM temperatures between the different sectors of the study area. The amplitude of this variation is equivalent for the Série Rousse and the Série Grise. This regional variation of the peak temperatures can be explained by differences in tectonic positions (Figs. 3.14a, b). Indeed, the most external sectors, characterized by a shallower

burial depth, such as those of the Hérens and Anniviers valleys, show lower temperatures than the more internal ones, which are characterized by higher burial depths, such as the Bagnes valley. The dense data set obtained for the Hérens valley (Additional file 3.3) allows to quantify the distribution and variability of the RSCM temperatures through the whole Schistes Lustrés complex in this sector (Figs. 3.10a, b).

Table 1 RSCM Temperatures data

Series	Sample nb.	Thin section nb.	Coordinates (MN95)		Calculated Temperatures (Beyssac et al. 2002)					
			X	Y	Measur. nb.[1]	Min. T [°C][1]	Max. T [°C][1]	STD (σ)[1]	Conf. Int.[1,2]	Mean T [°C][1]
Hérens valley										
SR	AP16035	S6-5	2'599'230	1'105'410	13	388	445	19	11	416
SR	AP16036	S5-14	2'599'230	1'105'410	16	365	448	27	14	408
SR	AP16055	S6-18	2'599'170	1'108'585	12	381	501	32	20	460
SR	AP17007	S6-1	2'599'786	1'106'673	10	381	457	22	15	423
SR	AP17017	S5-17	2'605'156	1'106'891	15	400	435	12	7	420
SR	AP17040	S5-8	2'605'156	1'106'888	15	389	467	21	12	427
SR	AP17C4	S6-10	2'605'303	1'107'142	12	396	486	24	15	423
SR	AP1907	S7-6	2'603'082	1'105'740	13	411	473	21	13	439
SR	AP2091	S9-3	2'602'061	1'108'060	13	380	458	18	11	414
SR	AP2032	S9-5	2'605'443	1'104'767	11	431	513	23	16	467
SG	AP17009	S5-15	2'605'004	1'106'290	16	397	458	18	10	436
SG	AP17036	S5-9	2'605'228	1'106'869	13	412	507	29	17	466
SG	AP19001	S7-1	2'605'385	1'103'175	15	388	507	32	18	435
SG	AP19003	S7-5	2'604'862	1'104'049	15	424	495	23	13	446
SG	AP1910	S7-3	2'602'498	1'105'612	13	417	465	15	9	442
SG	AP1912	S8-14	2'603'410	1'105'465	14	416	511	26	15	450
SG	AP2080	S9-2	2'604'400	1'103'220	12	391	451	17	11	411
TAR/C	AP2083	S9-1	2'604'255	1'100'215	11	326	373	13	9	354
Bagnes valley										
SR	AP1925	S7-2	2'594'349	1'094'318	12	437	537	33	21	483
SR	AP1926	S9-6	2'594'217	1'094'242	11	436	541	31	21	459
ES	AP15014	S1-17	2'591'951	1'095'923	14	418	549	31	18	484
ES	AP2007	S8-7	2'592'654	1'094'496	13	433	541	34	20	480

See Additional file 1 for detailed measurements and calculations data. SR: Série Rousse; SG: Série Grise; TAR/C: Tracuit - Aig. Rouges zone / Cornet Unit; ES: Evolène Series

[1] Retained measurements (spectra that could be fitted with $r^2 \geq 0{,}995$)

[2] Confidence interval (Student Law): 1-α = 95%

Fig. 3.10 Geothermometry by Raman spectroscopy of carbonaceous material (RSCM) in the Schistes Lustrés and adjacent lithologies across Hérens valley and surrounding areas of SW Switzerland and NW Aosta valley (IT). **a** RSCM temperatures [°C] across Hérens valley: data from this study (circles) compared with available data from the literature (squares and triangles); background map from Fig. 3.1b. **b** RSCM temperatures [°C] across Hérens valley plotted on a geological cross-section constructed through the area (modified after Escher 1988; Escher et al. 1988, 1993, 1994); location indicated in Fig. a. **c** RSCM temperatures [°C] at regional scale: literature data (squares, pentagons and triangles) and data from this study (circles); background map from Fig. 3.1b (SE zone modified after Steck et al. 1999, 2015; Dal Piaz et al. 2015b). **d** RSCM temperatures [°C] from Figs. a-b (Hérens valley) plotted against the distance of the outcrops to the contact between the Série Rousse (SR) and the Série Grise (SG); distances are calculated orthogonally to the mean local orientations of the structures (cf. Additional file 3.3); °T error bars: 1σ; Dist. error bars: 75%. ▶

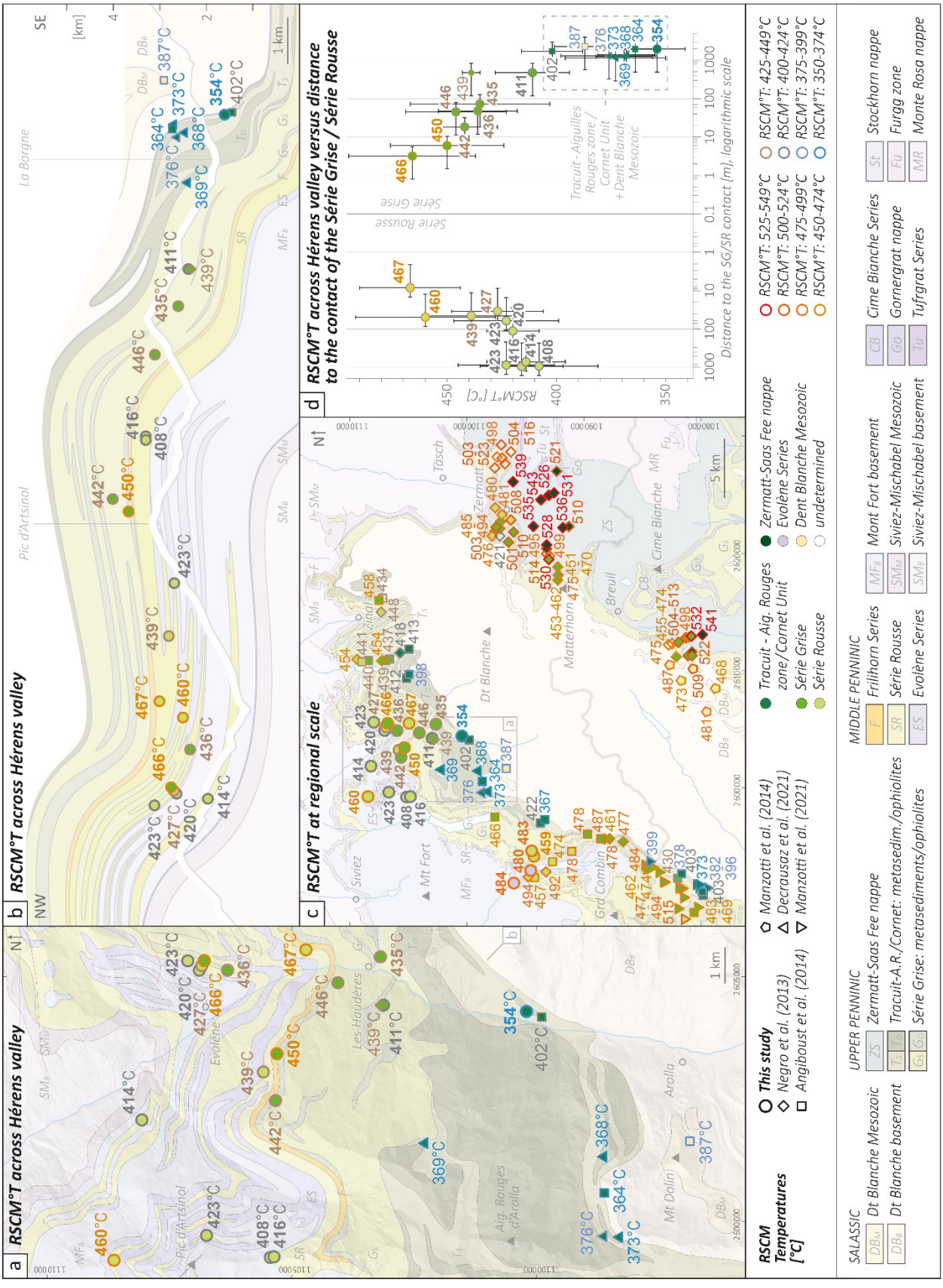
a RSCM°T across Hérens valley
b RSCM°T across Hérens valley
c RSCM°T at regional scale
d RSCM°T across Hérens valley versus distance to the contact of the Série Grise / Série Rousse
RSCM Temperatures [°C]
This study
Negro et al. (2013)
Angiboust et al. (2014)
Manzotti et al. (2014)
Decrausaz et al. (2021)
Manzotti et al. (2021)
Tracit - Aig. Rouges zone/Cornet Unit
Série Grise
Série Rousse
Zermatt-Saas Fee nappe
Evolène Series
Dent Blanche Mesozoic
undetermined
RSCM°T: 525-549°C
RSCM°T: 500-524°C
RSCM°T: 475-499°C
RSCM°T: 450-474°C
RSCM°T: 425-449°C
RSCM°T: 400-424°C
RSCM°T: 375-399°C
RSCM°T: 350-374°C
SALASSIC
Dt Blanche Mesozoic
Dt Blanche basement
UPPER PENNINIC
Zermatt-Saas Fee nappe
Tracuit-A.R./Cornet: metasedim./ophiolites
Série Grise: metasediments/ophiolites
MIDDLE PENNINIC
Frilihorn Series
Série Rousse
Evolène Series
Mont Fort basement
Siviez-Mischabel Mesozoic
Siviez-Mischabel basement
Cime Blanche Series
Gornergrat nappe
Tufgrat Series
Stockhorn nappe
Furgg zone
Monte Rosa nappe

The samples providing the highest RSCM temperatures are those from the immediate vicinity of the contact between the Série Rousse and the Série Grise. The maximum RSCM temperatures are identical for both series (467 ± 23 °C for the Série Rousse and 466 ± 29 °C for the Série Grise) and are obtained from the samples located closest to this contact (< 10 m). Figure 3.10d displays the distribution of RSCM temperatures as a function of their distance from the contact between the Série Rousse and the Série Grise. An increase in temperatures centered on this contact can be clearly evidenced.

The relative influence of factors that control the processes of crystallization and recrystallization of organic matter during metamorphism and rock deformation is still not fully established and quantified (e.g. Nakamura et al. 2017; Beyssac et al. 2019). Nevertheless, the following causes can be suspected to be responsible for the particular distribution of RSCM temperature evidenced through the contact between the Série Rousse and the Série Grise. (i) A local temperature increase along an Alpine thrust. (ii) Recrystallization of the organic material facilitated by fluid flow in the contact zone; and/or (iii) by more intense deformation in the contact zone. These different hypotheses are not mutually exclusive and are all compatible with a contact of tectonic nature, as suggested by previous studies (cf. chap. 3.2.2) and the observations of the previous chapter (3.5.2). Regarding the first hypothesis, a temperature increase associated to faulting and shearing along ductile shear zones has been documented in numerous natural examples, at various scales and magnitudes of temperature variations (e.g. Nicolas et al. 1977; Scholz 1980; England and Molnar 1993; Leloup and Kienast 1993; Nabelek et al. 2001; Stipp et al. 2002; Petroccia et al. 2022). The mechanism of shear heating (or strain heating) and their resulting thermal anomalies, associated both with brittle and ductile deformation, have been extensively studied through thermomechanical modeling (e.g. Molnar and England 1990; Leloup et al. 1999; Nabelek et al. 2001; Burg and Gerya 2005; Duprat-Oualid et al. 2015; Schmalholz and Duretz 2015; Aharonov and Scholz 2018; Mako and Caddick 2018; Kiss et al. 2019).

The thermal anomaly pattern evidenced by our study across the thrust surface and adjacent areas is compatible, in term of amplitude and spatial extension, with the results of the recent thermomechanical modeling studies from Mako and Caddick (2018) and Kiss et al. (2019), for example. The respective influences of strain and fluid flow on graphite (re)crystallization, as evoked in the second and third hypotheses, are poorly constrained for natural settings and geological time scales. Both parameters seem, however, to influence and enhance graphitization kinetics as shown by laboratory experiments (e.g. Ross and Bustin 1990; Bustin et al. 1995; Beyssac et al. 2003a; Nakamura et al. 2017) and some natural examples (e.g. Luque et al. 1998; Luque and Rodas 1999; Kirilova et al. 2018; Wang et al. 2019; Petroccia et al. 2022). Regardless of the mutual influence of the factor(s) controlling the evidenced distribution of the RSCM temperatures measured across the Hérens valley, these results emphasize the importance of the tectonic contact of the Série Grise on the Série Rousse and reinforce the observations and conclusions of chap. 3.5.2.

The Schistes Lustrés samples from the Hérens valley with the lowest RSCM temperatures are from metasediments associated with the large ophiolitic masses of the Tracuit - Aiguilles Rouges zone (Figs. 3.10a, c; Decrausaz et al. 2021, fig. 2). The RSCM temperatures of these samples range from 354 ± 13 °C to 402 ± 14 °C, they are therefore significantly lower than those of both Série Grise and Série Rousse in the same area, which together range there from 408 ± 27 °C to 467 ± 23 °C. This contrast in RSCM temperature is of the same order as that described by Manzotti et al. (2021) between the Cornet Unit (373 ± 13 °C - 403 ± 9 °C) and the By Unit (462 ± 12 °C - 515 ± 23 °C) in the Ollomont valley (IT). The Cornet Unit is located in the direct continuation of the Tracuit - Aiguilles Rouges zone, in an identical tectonic position (Fig. 3.1b). These two units are therefore probably equivalent. The Low-T slice (360-410 °C) of the Tsaté complex highlighted by Angiboust et al. (2014) in this same region (without being mapped) also likely corresponds to these units.

3.7. Discussion

3.7.1. Evolène Series - Série Rousse succession compared to stratigraphic series from the Prealps and Western Alps

The detailed observations along the basal contact of the Série Rousse presented in chap. 3.5.1 clearly suggest the stratigraphic nature of this contact, as pointed out in particular by the local identification of a basal conglomerate and a basal hardground, and by the absence of any hint of particular shearing across various sections of the contact. The interpretation of this contact as stratigraphic, as already proposed by e.g. Escher (1988; cf. Fig. 3.2), clarifies various points concerning the evolution of the Prepiemont domain (cf. Lemoine 1961; chap. 2.2), which are discussed below. In particular, the study of the facies distribution within the Série Rousse and the underlying formations of the Mont Fort basement and Evolène Series provides interesting insights regarding the Cretaceous paleogeographic and sedimentological evolution of the Prepiemont domain and the tectonic correlations between the Prepiemont units outcropping in the Pennine Alps and those transported in the Prealps.

3.7.1.1. Characteristic successions of siliceous limestones and black detrital limestones

Different local stratigraphic columns showing the lithological successions outcropping on both sides of the basal contact of the Série Rousse are presented in Fig. 3.11b for the Mauvoisin area (Bagnes valley); and in Fig. 3.12b for the Hérens valley area. A well-developed conglomerate or hardground is observed at the base of the Série Rousse, when the underlying Evolène Series is devoid of Mauvoisin marbles (e.g. Fig. 3.11b: Sa and Ro logs; Fig. 3.12b: MB, RV and SN logs).

Fig. 3.11 a Geological cross-sections through the Mauvoisin area, Bagnes valley; modified after Argand(1911), Witzig (1948), ► Hagen (1951), Gouffon and Burri (1997), Burri et al. (1999); locations on Fig. 3.7a; A [2'593'530/1'097'900]; A' [2'596'320/1'093'260]; B [2'591'460/1'096'700]; B' [2'594'410/1'091'790]; locations of the stratigraphic columns of Fig. b are indicated in green. **b** Characteristic lithostratigraphic successions through the base of the Série Rousse across the study area; scales differ between the stratigraphic columns (grey strokes represent ca. 20 m); triangles indicate breccia levels; circles, conglomerates; black points, detrital quartz; black dashes, dark calcschists; black lines, black schists. Stratigraphic columns acronyms and coordinates: PV [2'594'390/1'097'950] - [2'594'400/1'097'970], tectonically overturned; Sa [2'594'555/1'097'430] - [2'594'580/1'097'430]; Ro [2'594'110/1'097'570] - [2'594'090/1'097'560], tectonically overturned, pictures Figs. 3.8b-d; GR [2'593'780/1'097'055] - [2'593'780/1'097'045], tectonically overturned; DG [2'593'050/1'094'945] - [2'593'065/1'094'930], tectonically overturned; BP [2'593'130/1'094'830] - [2'593'160/1'094'860]; EG [2'593'710/1'092'930] - [2'593'615/1'092'930], tectonically overturned, Fig. 3.6d from the lower part of the profile. **c** Proposed pre-orogenic restoration (Late Cretaceous) of the cross-section of Fig. a; approximate pre-orogenic locations of the lithostratigraphic successions of Fig. b are indicated in green.

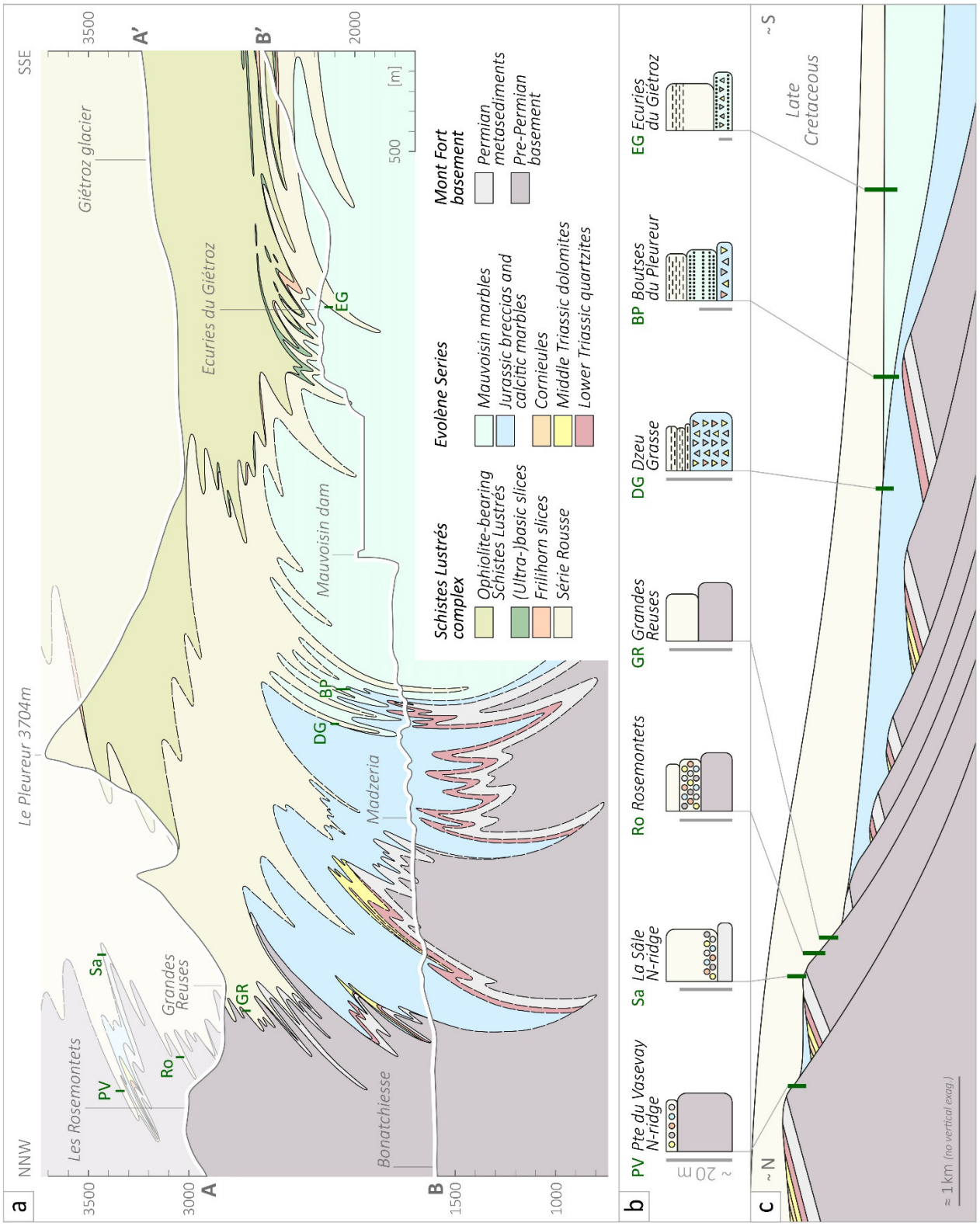
a
NNW
SSE
Le Pleureur 3704m
Les Rosemontets
Grandes Reuses
Giétroz glacier
Ecuries du Giétroz
Mauvoisin dam
Madzeria
Bonatchiesse
PV
Ro
Sa
GR
DG
BP
EG
A
A'
B
B'
3500
3000
2000
1500
1000
500
[m]
Mont Fort basement
Permian metasediments
Pre-Permian basement
Evolène Series
Mauvoisin marbles
Jurassic breccias and calcitic marbles
Cornieules
Middle Triassic dolomites
Lower Triassic quartzites
Schistes Lustrés complex
Ophiolite-bearing Schistes Lustrés
(Ultra-)basic slices
Frilihorn slices
Série Rousse
b
PV Pte du Vasevay N-ridge
Sa La Sâle N-ridge
Ro Rosemontets
GR Grandes Reuses
DG Dzeu Grasse
BP Boutses du Pleureur
EG Ecuries du Giétroz
20 m
c
~ N
~ S
Late Cretaceous
≈ 1 km (no vertical exag.)

This suggests a marked sedimentation gap, that should span from the Late Jurassic to the Late Cretaceous.

On the other hand, when the Série Rousse rests on the Mauvoisin marbles, its basal part generally includes dark levels, rich in phyllosilicates and organic matter (e.g. Fig. 3.11b: DG, BP and EG logs; Fig. 3.12b: Ts, Vi, PT and SC logs). Good examples of such successions can be observed near the Mauvoisin Hotel at [2'592'710/1'094'620] and [2'592'820/1'094'650]; and in the Hérens valley, in the vicinity of La Vieille (Fig. 3.12, Vi log; Marthaler et al. 2020), near the St-Christophe chapel (Fig. 3.12, SC log) and SE of La Tour between [2'605'290/1'104'860] and [2'605'460/1'104'760] (Figs. 3.4e, 3.6c, 3.6e). These successions, characterized by the superposition of light-colored siliceous calcitic marbles, with quartzitic mm-cm thick levels, attributed to the Mauvoisin marbles (cf. chap. 3.4.2), surmounted by dark calcschists or detrital calcitic marbles of the Série Rousse (cf. chap. 3.4.1.1), recall the stratigraphic superposition of the Bonave Fm. (Upper Tithonian - Valanginian/Barremian) and the glauconite-bearing Joux Verte Fm. (Upper Barremian - Middle Turonian) described in the Breccia nappe of the Chablais Prealps (Dall'Agnolo 1997, 2000; Fig. 3.13a).

Fig. 3.12 **a** Bedrock map of the Evolène area (Hérens valley); compiled after data from this study and existing maps (Moix and Stampfli 1980, 1981; Schneider 1982; Escher 1988; Allimann 1990; Kramar 1997; Steck et al. 1999; Sartori and Epard 2011; Glassey 2013; Marthaler et al. 2020a; Swisstopo Geocover); background altitude model ©Swisstopo; locations of the stratigraphic columns of Fig. b are indicated in green. **b** Characteristic lithostratigraphic successions through the base of the Série Rousse along the Hérens valley; scales differ between the stratigraphic columns (grey strokes represent ca. 20 m); triangles indicate breccia levels; circles, conglomerates; black points, detrital quartz; black dashes, dark calcschists; black lines, black schists; brown line, hardground. Stratigraphic columns acronyms and coordinates: Co [2'600'850/1'108'710], tectonically overturned, cf. Allimann (1990); Be [2'605'485/1'108'880]-[2'605'510/1'108'870], cf. Glassey 2013; MB [2'605'260/1'107'190] - [2'605'320/1'107'130]; RV [2'605'130/1'106'900] - [2'605'180/1'106'880]; Ts [2'600'050/1'107'940] - [2'599'790/1'107'790]; Vi [2'602'710/1'105'660] - [2'602'800/1'105'520], tectonically overturned, Fig. 3.4g from the center of the profile; PT [2'602'950/1'105'540] - [2'603'415/1'105'460], Fig. 3.9b from the top of the profile; SC [2'605'545/1'105'230] - [2'605'740/1'105'185]; SN [2'599'285/1'107'975] - [2'599'290/1'107'895], Figs. 3.8f-g from the center of the profile; MP [2'599'250/1'105'470] - [2'599'235/1'105'450]. **c** Pre-orogenic restoration attempt, reproducing lithological contacts and successions observed and reported in Fig. a-b. ▶

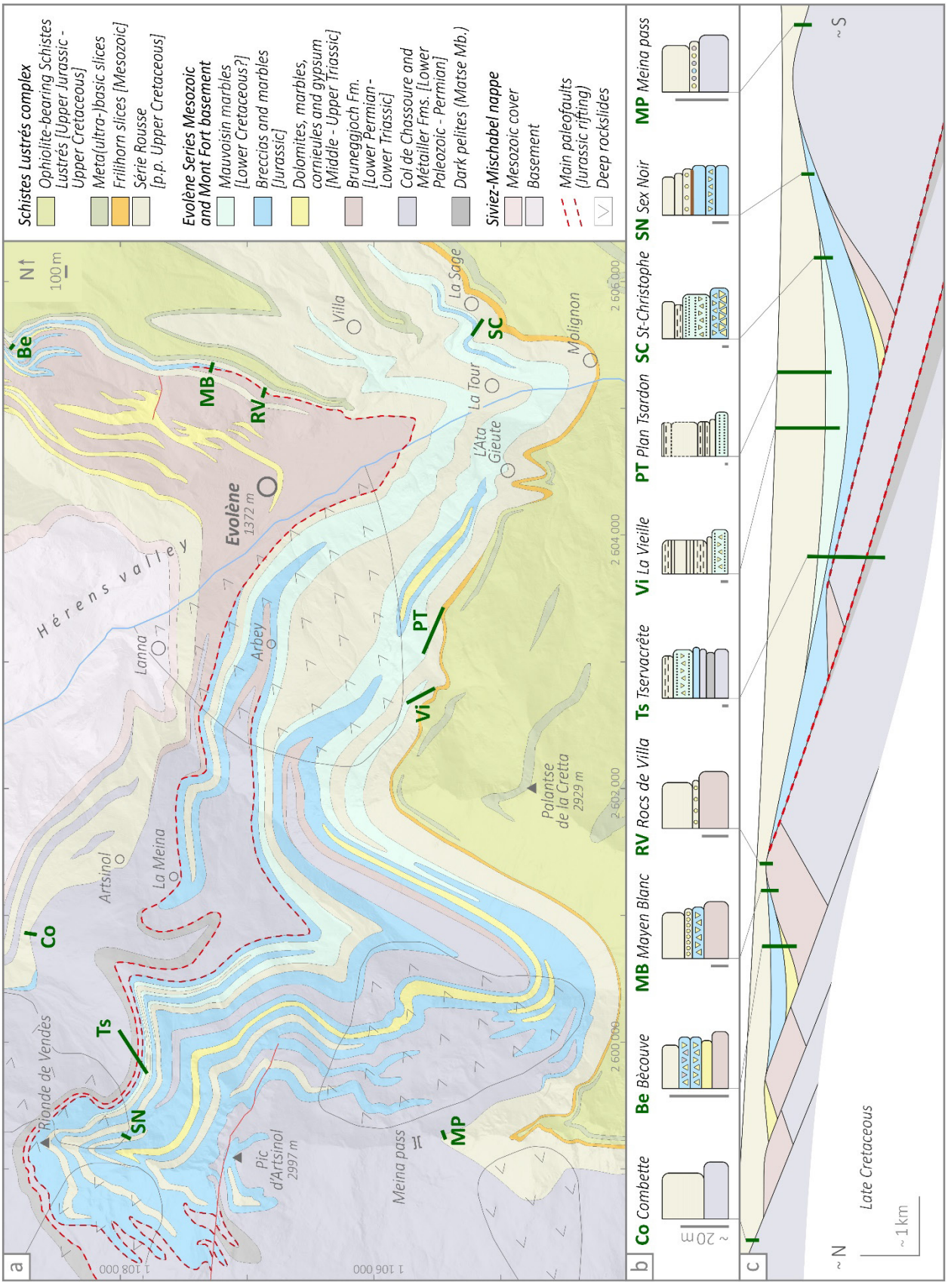
Schistes Lustrés complex
Ophiolite-bearing Schistes Lustrés [Upper Jurassic - Upper Cretaceous]
Meta(ultra-)basic slices
Frilihorn slices [Mesozoic]
Série Rousse [p.p. Upper Cretaceous]
Evolène Series Mesozoic and Mont Fort basement
Mauvoisin marbles [Lower Cretaceous?]
Breccias and marbles [Jurassic]
Dolomites, marbles, cornieules and gypsum [Middle - Upper Triassic]
Bruneggjoch Fm. [Lower Permian - Lower Triassic]
Col de Chassoure and Métailler Fms. [Lower Paleozoic - Permian]
Dark pelites (Matse Mb.)
Siviez-Mischabel nappe
Mesozoic cover
Basement
Main paleofaults (Jurassic rifting)
Deep rockslides
a
N
100 m
Hérens valley
Evolène
1372 m
Arbey
Lanna
Artsinol
La Meina
Rionde de Vendès
Pic d'Artsinol
2997 m
Meina pass
Palantse de la Cretta
2929 m
Villa
La Sage
La Tour
L'Ata
Gleute
Molignon
Be
MB
RV
SC
Co
Ts
SN
Vi
PT
MP
2 606 000
2 604 000
2 602 000
2 600 000
1 108 000
1 106 000
b
Co Combette
Be Bècouve
MB Mayen Blanc
RV Rocs de Villa
Ts Tservacrête
Vi La Vieille
PT Plan Tsardon
SC St-Christophe
SN Sex Noir
MP Meina pass
~ 20 m
c
~ N
~ S
Late Cretaceous
~ 1 km

In the Briançonnais domain s.l. (incl. Prepiemont), the stratigraphic succession of light-colored and massive limestones (or breccias with light-colored limestone matrix of the same age), of cherty light-colored pelagic limestones, and of darker phyllitic and sometimes anoxic limestones, is in fact very characteristic of the superposition of Upper Jurassic, Lower Cretaceous and "mid"-Cretaceous levels (Bourbon et al. 1979). Such successions can be observed in many and less metamorphosed and deformed stratigraphic successions of the Western and Central Alps, e.g. in the Plastic Median Prealps (e.g. Plancherel et al. 2020), the Roche des Clots Series (e.g. Lemoine et al. 1978), or the Chabrière Series (Lemoine and Tricart 1986).

The characteristic superposition of these facies on different sections of the contact between the Evolène Series and the Série Rousse constitutes therefore another strong argument to consider this contact as stratigraphic.

3.7.1.2. Stratigraphic comparison with the Breccia nappe in the Prealps

The stratigraphy of the Breccia nappe in the Prealps (Fig. 3.13a; e.g. Lugeon 1896; Chessex 1959; Weidmann 1972; Dall'Agnolo 1997, 2000; Plancherel et al. 1998) shows very strong similarities with the entire Evolène Series. These similarities have been pointed out several times in the literature (Joukowsky 1907; Escher 1988; Kramar 1997; Sartori et al. 2006; Marthaler et al. 2008b, 2020b; Glassey 2013). It has recently been discussed in detail by Pantet et al. (2020), who highlight a strong correlation between these two stratigraphic successions.

The correlations proposed here between the Bonave Fm. and the Mauvoisin marbles (upper part of the Evolène Series), and between the Joux Verte Fm. and the lower part of the Série Rousse, further strengthen the correlation between the Breccia nappe and the whole Mesozoic series associated to the Mont Fort nappe (Fig. 3.13).

The few differences between these two stratigraphic successions are minor. The absence of Lower and Middle Triassic levels in the Prealps is simply explained by the detachment of the stratigraphic

successions above the Carnian evaporites (Caron in Debelmas 1970; Weidmann 1972). Differences also appear concerning the thickness of the Jurassic and Cretaceous levels between the two stratigraphic columns of Fig. 3.13. They are however not really significant, since these synthetic columns only indicate maximum thicknesses, whereas considerable thickness variations are observable within the series themselves for these levels (Dall'Agnolo 1997, 2000; Figs. 3.7, 3.11, 3.12).

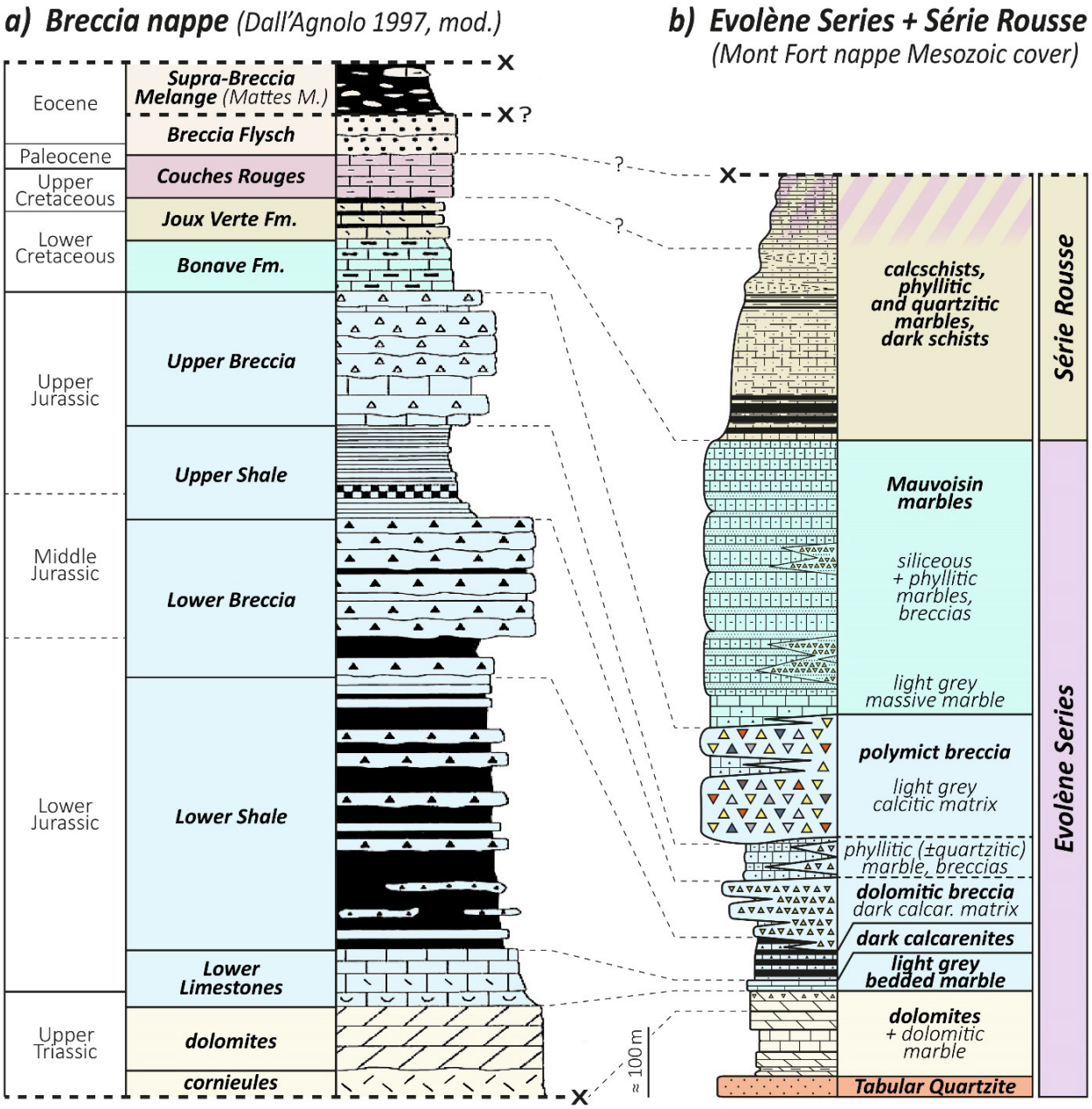

Fig. 3.13 a Synthetic stratigraphic columns of the Breccia nappe in the Prealps (modified after Dall'Agnolo 1997), compared to **b** the Evolène Series and Série Rousse superimposed synthetic stratigraphic columns (modified after Kramar 1997; Sartori et al. 2006; Pantet et al. 2020); complete stratigraphic successions of the series are represented, widespread local stratigraphic gaps are ignored.

Regarding the Breccia nappe, these thickness variations are mainly of stratigraphic origin, whereas for the units associated with the Mont Fort nappe, their origin is not only stratigraphic, but also partly tectonic, given the strong Alpine deformation affecting these units. Finally, another difference between the two columns concern the flysch and the melange (Suprabrekzienmelange / Mélange Supra-Brèche; Dall'Agnolo 1997, 2000; Mattes Melange; Plancherel et al. 2020) overlying the stratigraphic series of the Breccia nappe, and for which, no equivalent has been recognized at the top of the Série Rousse. However, the relationship of this melange to the Breccia nappe is possibly tectonic (De Lepinay 1981; Dall'Agnolo 1997) and its potential equivalent at the top of the Série Rousse (as well as the overlying levels) may have been tectonically replaned by the overthrusting of the Upper Penninic units.

Strong stratigraphic similarities can therefore be evidenced between the Breccia nappe in the Chablais Prealps and the ensemble formed by the Evolène Series and the Série Rousse. They lead us to consider this ensemble as a single entity, whose stratigraphic successions extend from the basal Triassic to the Upper Cretaceous at least.

3.7.2. The basal unconformity: progressive infill and sealing of the remnants of the Jurassic fault scarps

The basal contact of the Série Rousse is characterized by an unconformity described in chap. 3.5.1.1. This unconformity has led various authors (Escher et al. 1993; Sartori and Marthaler 1994) to consider this contact as being of a tectonic nature. All our observations however consistently show that the contact is primarily stratigraphic (cf. chaps. 3.5.1.2 - 3.5.1.4, 3.7.1) and that the unconformity can be explained by deposition on a paleorelief of former syn-sedimentary faults (Figs. 3.11c, 3.12c), following a model already developed in chap. 2. These syn-sedimentary faults, mostly active during the Jurassic, delimit small basins formed by tilted blocks (half-grabens), whose movement is at the origin of the locally large breccia accumulations observed in the Evolène Series. The thinness of the breccia deposits in the

Série Rousse (in general > 10 cm, never exceeding 3 m) seems to indicate that these faults were no longer active or less active during the Late Cretaceous. A submarine relief formed by the Jurassic fault scarps should have remained, allowing the local erosion of the Evolène Series and of various Paleozoic levels of the Mont Fort basement. The activity of Cretaceous faults or rejuvenation of Jurassic faults during the Cretaceous has nevertheless been documented in other areas of the Alps (e.g. Claudel et al. 1997; Michard and Martinotti 2002, Bertok et al. 2012; Cardello and Mancktelow 2014; Michard et al. 2022).

Our detailed mapping (Figs. 3.7a, 3.12a) shows that the different lithological successions along the basal contact of the Série Rousse (e.g. Figs. 3.11b, 3.12b), as well as their distribution, are compatible with the hypothesis of a progressive filling of such half grabens by the Série Rousse.

For example, the conglomerate, locally present at the base of the Série Rousse, is better developed where the Evolène Series is absent or reduced to a small thickness. Following our restoration attempts of the structures preceding the Alpine collision (Figs. 3.11c, 3.12c), the areas yielding these basal conglomerates would correspond either to areas characterized by the sedimentation of the Série Rousse directly on ancient fault scarps (e.g. Fig. 3.11b, PV, Sa and Ro logs; Fig. 3.12b, MP log), or to the upper parts of tilted blocks (e.g. Fig. 3.12b, MB and SN logs). The area where a hardground is observed and document a large stratigraphic gap (Triassic levels and Mauvoisin marbles missing; Fig. 3.12b, SN log), would correspond, following the restoration attempt of Fig. 3.12c, to the highest part of a tilted-block. Areas where the Série Rousse overlies the Mauvoisin marbles and shows dark facies (e.g. Fig. 3.11b, BP log; Fig. 3.12b, Vi, PT and SC logs) correspond, in contrast, to the depocenters of the half graben basins, where sedimentation continued during the Cretaceous with a smaller stratigraphic gap than in adjacent areas.

The different points discussed above show strong evidences for the onlap and sealing by the Série Rousse, during the Late Cretaceous, of a paleotopography characterized by fault scarps resulting of the Jurassic development and activity of large synsedimentary extensional faults.

The Série Rousse therefore represents the sedimentary continuation of the Evolène Series and should consequently not be considered as an independent allochthonous tectonic unit.

3.7.3. Tectonic limits and units in the Schistes Lustrés complex of the Combin zone

Taken together, our observations thus indicate that the Série Rousse constitutes the youngest part of the autochthonous sedimentary cover of the Mont Fort nappe, rather than a basal slice of the Tsaté nappe. They also show that the upper contact of the Série Rousse with the ophiolite-bearing Schistes Lustrés of the Série Grise is clearly of tectonic nature (cf. chaps. 3.2.2, 3.5.2, 3.6). This contact thus corresponds to an Alpine thrust separating the Tsaté and Mont Fort nappes. According to our interpretation, the contact between these two nappes is therefore not located at the base of the Série Rousse, but at its top. This contact, which corresponds to the major tectonic limit that separates the Upper Penninic ocean-derived units from the continental margin-derived Middle Penninic units, is thus located within the Schistes Lustrés complex of the Combin zone (Figs. 3.2, 3.14).

According to the proposed interpretation, the ensemble constituted by the Evolène Series and the Série Rousse thus forms the relative autochthonous sedimentary cover of the Mont Fort nappe, whereas the Tsaté nappe is restricted to the Série Grise and the Tracuit - Aiguilles rouges zone / Cornet Unit. The thin Frilihorn slices are located at the contact of the two nappes rather than within the Tsaté nappe.

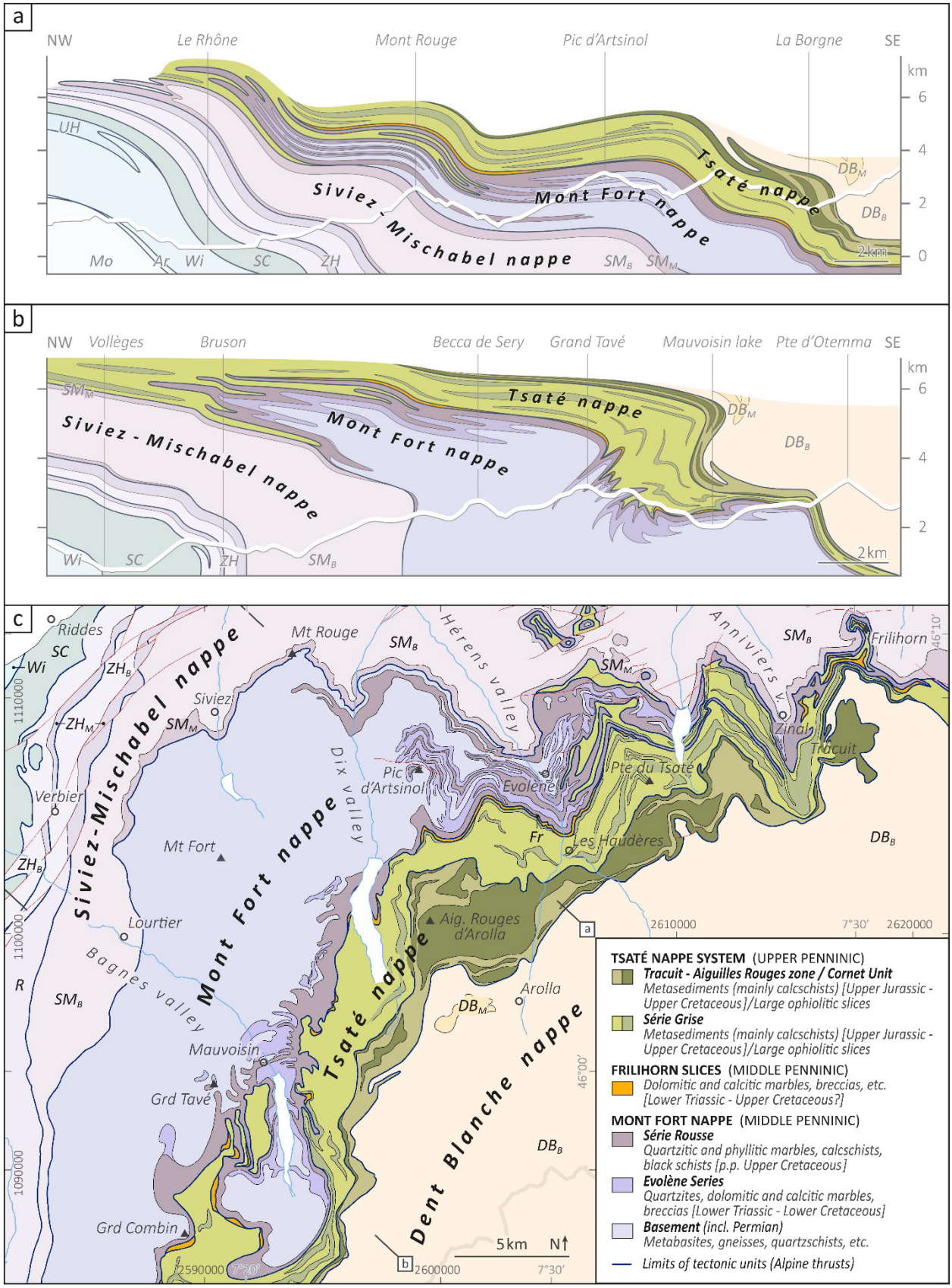

Fig. 3.14 Reinterpreted schematic cross-sections and tectonic map of the studied area; *Ar*: Ardon nappe; DB_B: Dent Blanche basement; *Fr*: Frilihorn slices; *Mo*: Morcles nappe; *R*: Ruitor basement; *SC*: Sion-Courmayeur zone; SM_B: Siviez-Mischabel basement; SM_M: Siviez-Mischabel Mesozoic; *UH*: Ultrahelvetic nappes; *Wi*: Wildhorn nappe; *ZH*: Zone Houillère; ZH_B: Zone Houillère basement; ZH_M: Zone Houillère Mesozoic. **a** Schematic geological cross-section through the Hérens valley; modified after Escher (1988), Escher et al. (1988, 1993, 1994), Schaer (1960); location indicated in Fig. c. **b** Schematic geological cross-section through the Bagnes valley; location indicated in Fig. c. **c** Tectonic map of the upper Bagnes, Dix, Hérens and Anniviers valleys (SW Switzerland); compiled after data from this study and existing maps (see Fig. 3.1b for references).

This interpretation corresponds in fact to the first hypothesis adopted when these different units were defined (Fig. 3.2; Marthaler and Escher in Masson et al. 1980; Marthaler 1981, 1984; Escher and Masson 1984; Sartori 1987; Escher 1988; Escher et al. 1988) and before the subsequent reinterpretation of the tectonic scheme by some of these authors (e.g. Escher et al. 1993; Sartori and Marthaler 1994; cf. chap. 3.2.2).

The interpretation of the tectonic position of the Frilihorn slices, at the base rather than within the Tsaté nappe, is interesting with respect to the questions of the origin and tectonic attribution of these slices. In the studied area, north of the Dent Blanche klippe, all the observed Frilihorn slices are located along the contact between the Série Rousse and the ophiolite-bearing Schistes Lustrés (which is locally redoubled by isoclinal folds; Fig. 3.9c). These observations actually seem hardly compatible with the hypothesis of an Adriatic origin of these slices (e.g. Staub 1942d; Caby et al. 1978; Dal Piaz 1999; Froitzheim et al. 2006; Pleuger et al. 2007; Passeri et al. 2018). It is indeed extremely difficult to imagine a mechanism able to insert slices of Adriatic origin in this position without inserting ophiolite-bearing Schistes Lustrés below these slices. However, a provenance from the Briançonnais s.str. swell and a southward emplacement, as proposed by Scheiber et al. (2013), also seems unlikely to be compatible with the widespread breccia layers observed within the calcitic marbles of these slices (cf. chaps. 3.2.3.2, 3.5.2); and with the top-NW shear sense associated to the main schistosity that is observed in some localities (Fig. 3.9e). According to the observations above, a Prepiemont origin (i.e. derived from the southern distal margin of the Briançonnais s.l. domain; Fig. 3.15b), as proposed for example by Elter (1960, 1972), Dal Piaz (1974), Bearth (1976), Marthaler (1984) and Escher (1988), seems, therefore, more likely. Considering such a Prepiemont origin, two different possibilities concerning the origin and tectonic attribution of the Frilihorn slices could be envisaged: (i) a more distal origin than the Mont Fort nappe on the distal Prepiemont margin, the Frilihorn slices would hence constitute an independent tectonic unit, thrusted along the base of the Tsaté nappe;

(ii) an origin corresponding to the most internal part of the Mont Fort nappe, folded and boudinaged under the Tsaté basal thrust (similarly e.g. to the Helvetic Drône anticline under the Penninic thrust; Steck et al. 1989; Escher et al. 1997; Cardello et al. 2019).

The existence of an Alpine tectonic contact within the ophiolite-bearing Schistes Lustrés (i.e. the Tsaté nappe as redefined above) has been postulated by Angiboust et al. (2014). Its existence has been recently confirmed by Manzotti et al. (2021) based on metamorphic arguments. Indeed, on each sides of this contact in the Ollomont valley (IT), both the RSCM temperatures and the metamorphic paragenesis are strongly contrasted. In this sector, the lower part of the Schistes Lustrés complex (By Unit) shows parageneses characterized by the presence of pseudomorphs after lawsonite, aragonite inclusions in titanites and the local presence of small garnets in quartzitic schists. Its peak P-T conditions are estimated at ca. 16-17 kbar and 460-480 °C. In the Cornet Unit, which represents there the uppermost unit of the Schistes Lustrés complex, the parageneses mentioned above are completely absent and the peak P-T conditions are estimated at ca. 8 ± 1 kbar and 370-400 °C.

According to these authors, the metamorphic evolution is similar between the Cornet Unit and the overlying Dent Blanche nappe. The upper limit of the Schistes Lustrés complex of the Combin zone would therefore not correspond to an important metamorphic limit. The same seems to be true for the lower limit of this complex. Indeed, as highlighted above, this limit is stratigraphic in nature and is internal to the Mont Fort nappe, which is not compatible with a metamorphic limit. Available data concerning the metamorphic evolution of the different units composing this nappe are consistent with this interpretation (Sodic amphiboles, chloritoid, epidotes and HP white micas in the Paleozoic basement; Schaer 1960; Bearth 1963; Thélin et al. 1994; Steck et al. 2001; Bousquet et al. 2004; Evolène Series RSCM°T ranging from 484 ± 31 °C to 480 ± 34 °C, Table 1, Fig. 3.10c; Série Rousse RSCM°T ranging from 408 ± 27 °C to 494 ± 7 °C, Additional file 3.2;

pseudomorphs after lawsonite in the Série Rousse in the Bagnes valley, Besson 1986 and in the Ollomont valley, P. Manzotti, pers. com.). The limit between the Mont Fort and Tsaté nappes (i.e. between the Série Rousse and the Série Grise ± Frilihorn slices), although clearly of tectonic nature, neither corresponds to an important metamorphic limit (cf. chap. 3.6). Contrary to the hypothesis of Angiboust et al. (2014), the intensity of metamorphism does not appear to increase between the middle and basal parts of the Schistes Lustrés complex.

The most important metamorphic boundary in the whole Mont Fort, Tsaté and Dent Blanche nappe stack therefore corresponds to the limit between the Série Grise and the Tracuit - Aiguilles Rouges zone / Cornet Unit. The question of the origin of such a metamorphic discontinuity is beyond the scope of this article and will not be further discussed here.

Although the Schistes Lustrés complex of the Combin zone has been considered by many authors as a single tectonic entity, the above data and discussions show that it is instead composed of different tectonic units, separated by (i) a major tectonic contact that corresponds to the Middle-Upper Penninics limit, separating the lower and middle units of this complex, i.e. the Série Rousse and the Série Grise respectively, and (ii) by a major metamorphic discontinuity, separating the middle from the upper unit of this complex (Tracuit - Aig. Rouges zone / Cornet Unit). It is particularly interesting to note that these two contacts do not correspond to marked lithological limits, they are even sometimes extremely inconspicuous, which may explain why their importance has been underestimated by most authors. In the light of these new data, the structure of the Combin zone is thus comparable to that of the Schistes Lustrés of the Western Alps, also characterized by a tectonic juxtaposition of different units showing distinct metamorphic evolutions (e.g. Fudral et al. 1987; Rolland et al. 2000; Plunder et al. 2012; Agard 2021; Herviou et al. 2022).

3.7.4. Cretaceous-Paleogene sedimentation along the Briançonnais-Prepiemont margin and Piemont basin

The Briançonnais s.str. domain, its hyperextended SE-margin (Prepiemont domain; Lemoine 1961) and the Piemont basin are characterized by a deep-water, clastic, hemipelagic and pelagic sedimentation throughout the Cretaceous (Fig. 3.15). Thus, until the end of this period, these realms remained essentially unaffected by the subduction and the onset of the Alpine collision that started along the Adriatic margin and southern Piemont-Liguria basin at that time. The onset of the convergence is attested since the late Cenomanian to early Turonian by the first Alpine flysch units, containing material of the Adriatic margin and now constituting the Simme nappe (Caron et al. 1989; Gasinski et al. 1997), and by the age of the prograde HP metamorphism starting at ca. 85 Ma in the Adriatic and Piemont derived units of the Pennine Alps (Skora et al. 2009; Rubatto et al. 2011; Manzotti et al. 2014; Regis et al. 2014). Stratigraphic data from the Briançonnais s.l. series in the Swiss Prealps (Fig. 3.15a) show that pelagic to hemipelagic sedimentation extends into the Paleocene in the external part of the Prepiemont domain (Couches Rouges of the Breccia nappe; Dousse 1965; Dall'Agnolo 1997) and into the early Eocene in the Briançonnais s.str. domain (Chenaux Rouges Fm.; Guillaume 1986). It is then relayed by flysch deposition, until middle Eocene (Guillaume 1986; Dall'Agnolo 1997; Hable 1997).

Alpine metamorphism and deformation in the Briançonnais s.l. and surrounding units of the Pennine Alps are dated to the late Eocene, with ages ranging in Western Switzerland between 41-42 Ma for the Piemont domain, 37-40 Ma for the Prepiemont domain and 35-40 Ma for the Briançonnais s.str. domain (e.g. Markley et al. 1998; Gebauer 1999; Angiboust et al. 2014). The sedimentation gaps, sometimes large, revealed at different levels in the Cretaceous and Paleocene of these series (Fig. 3.15a) are interpreted as resulting from the progression of the

lithospheric bulge associated with the progressive subduction of the Piemont domain under the Adriatic plate (Stampfli et al. 1998).

The sedimentary evolution during the Late Cretaceous - Paleogene is less constrained in the internal Prepiemont domain and Piemont domain (corresponding to the domains of deposition of the Série Rousse and Série Grise respectively), given the poor preservation of microfossils in the Pennine Alps and the lack of complete corresponding series in the Prealps. The few biochronological data available indicate a Cenomanian to earliest Maastrichtian minimal age for the Série Rousse (cf. chaps. 3.2.3.3, 3.4.1.2) and a Cenomanian to Santonian minimal age for the Série Grise (cf. chap. 3.2.3.1). The presence of well-developed dark anoxic levels in these series may, in turn, argue for their partly "mid"-Cretaceous age. The ages that can be inferred for these series are thus comparable with those indicated by Dall'Agnolo (1997, 2000; cf. Fig. 3.15a) for the Joux Verte Fm. (late Barremian - middle Turonian) and for the base of the Couches Rouges from the Breccia nappe (Campanian - Paleocene) as well as for the Couches Rouges included in the Mattes Melange (or Supra-Breccia Melange; late Campanian - early Paleocene; Dall'Agnolo 1997, 2000; Plancherel et al. 2020). As the Mattes Melange contains lenses of Couches Rouges and lenses of Helminthoid Flysch and is intercalated between the Breccia nappe and the upper Prealps nappes (Badoux 1962; Caron 1966, 1972; Caron and Weidmann 1967; Dall'Agnolo 1997), the origin of these lenses must therefore correspond either to the internal part of the basin of the future Breccia nappe or to a more internal domain, i.e. to the inner part of the Prepiemont domain or the Piemont domain. Lithological successions unambiguously corresponding to Couches Rouges or flysch units have however not been recognized at the top of the Série Rousse or Série Grise. The lithologies observed in these series differ from the Couches Rouges of the Médianes Prealps and of their metamorphic equivalents of the Barrhorn Series, by systematically higher quartz and organic matter contents (in the Couches Rouges and their metamorphic equivalents, quartz content is usually < 2-5% and CM is very scarce;

Guillaume 1986; Sartori 1990; Dall'Agnolo 1997). The Couches Rouges described in the Breccia nappe and in the Mattes Melange seem however to have a higher detrital input (Dousse 1965; Dall'Agnolo 1997) and could partly correspond to the upper part of the Série Rousse (Figs. 3.13 and 3.15).

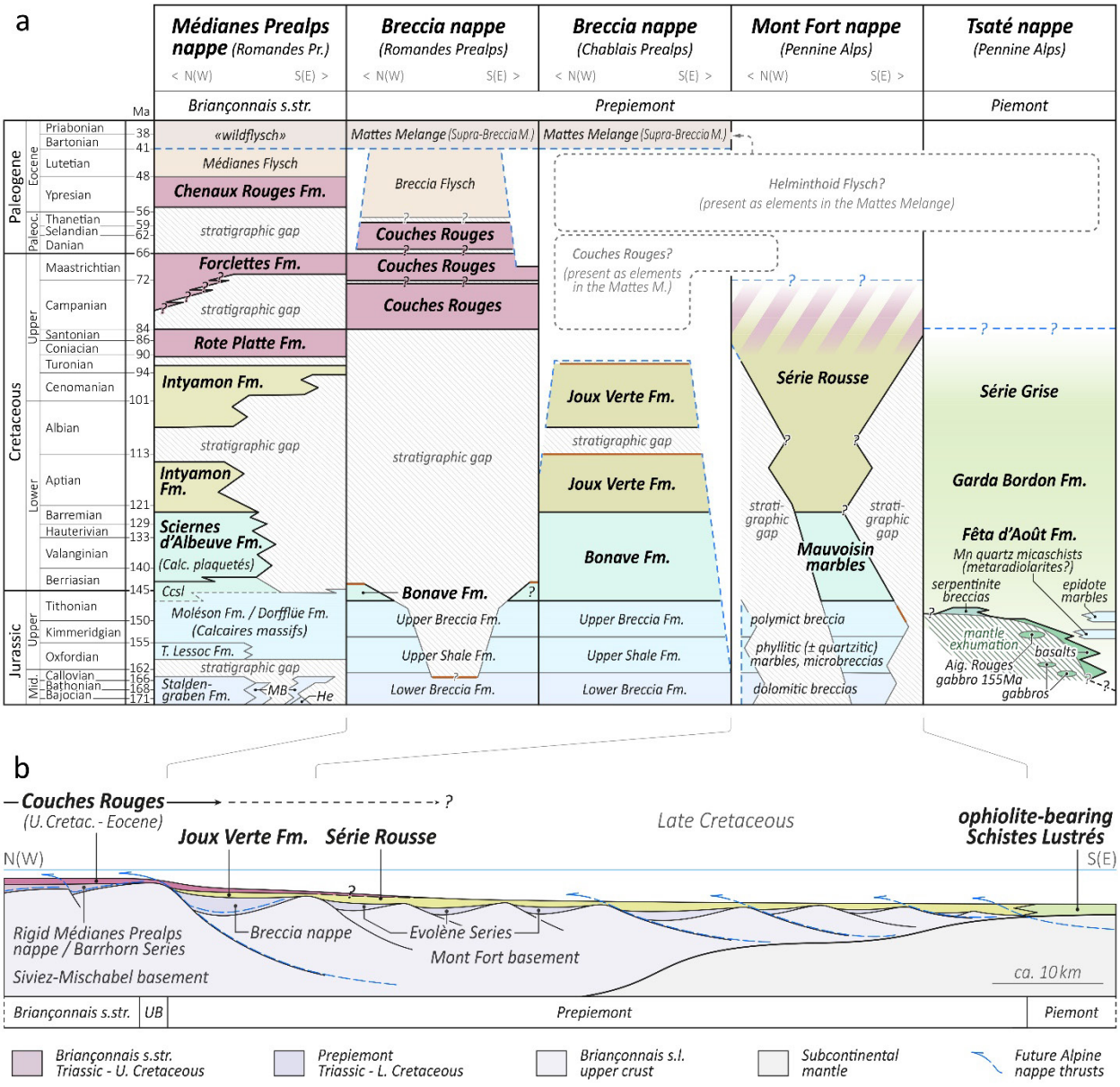

Fig. 3.15 a Correlations between the lithostratigraphic formations of the Breccia, Médianes, Mont Fort and Tsaté nappes (Prealps and Pennine Alps) for the Jurassic, Cretaceous and Paleogene periods; in this representation, only the time-extensions of the formations are indicated, independently of their actual thickness; modified after Dall'Agnolo (1997, 2000); Mosar et al. (1996, fig. 4); Stampfli et al. (1998, 2002); Plancherel et al. (1998, 2020); Decrausaz et al. (2021); Marthaler et al. (2020b); brown lines represent hardgrounds; blue dashed lines indicate probable tectonic contacts; *Ccsl*: Calcaires compacts et sublithographiques; *MB*: Mytilus Beds; *He*: Heiti Fm. **b** Restoration attempt of the South Briançonnais - Prepiemont margin at Late Cretaceous Epoch, before the onset of Alpine deformation in that area; modified after Stampfli and Marthaler (1990); Stampfli et al. (1998, 2002); Mohn et al. (2010); Pantet et al. (2020); *UB*: Ultrabriançonnais domain.

The lithologies of the upper part of these series are also further distinguished from the Breccia Flysch, by the scarcity of graded beds and the non-cyclic character of the sedimentation. It is nevertheless possible that the Couches Rouges and flysch, included as lenses in the Mattes Melange, may have first been deposited at the top of the Série Rousse and/or of the Série Grise, but that these sequences were then locally detached and transported to the Prealps. Such a detachment seems to have affected the Breccia nappe in the Chablais Prealps, where it would have occurred at the level of the of the "mid"-Cretaceous anoxic shales (De Lepinay 1981; Dall'Agnolo 1997). It is reflected by the absence of levels younger than the middle Turonian and by an important unconformity at the top of the internal part of the Breccia nappe.

A general slope from the Briançonnais swell towards the Piemont basin (Fig. 3.15b) is documented by an overall proximal to distal and upward fining of the Cretaceous detrital sediment component. Indeed, during the whole period from the Early Cretaceous to the early Late Cretaceous, the detrital input is significantly larger in the Prepiemont domain than in the Briançonnais s. str. domain (cf. Dall'Agnolo 1997, 2000; Plancherel et al. 2020). While submarine topographic highs of the Briançonnais were sheltered from such a detrital input and were the site of hemipelagic to pelagic sedimentation (which continued until the end of the Couches Rouges deposition), sedimentation in the Prepiemont domain was characterized by an input of quite mature quartz and detrital carbonate sands and episodic breccias intercalations. The presence of large fault scarps in the Prepiemont domain, preserved from the Jurassic extension and exposing both lower Mesozoic and Paleozoic rocks at the seafloor (cf. chap. 3.7.2), are very likely to constitute the main source of this detrital input in the Prepiemont Cretaceous formations.

3.8. Conclusion

Our study shows that the Schistes Lustrés complex of the Combin zone in western Switzerland consists of several lithologically distinct and tectonically independent series.

The lower Schistes Lustrés unit, the Série Rousse, is non-ophiolitic and consists mainly of detrital calcitic marbles and calcschists with continental affinities. We argue that the discontinuity characterizing the basal contact of these series results rather from the passive onlap and progressive sealing of remnants of Jurassic extensional fault scarps, than from a tectonic contact between different slices emplaced in an accretionary prism context, as previously proposed. The stratigraphic nature of the basal contact of the Série Rousse is attested by (i) the occurrence in several sectors of a basal conglomerate, sometimes reworking directly underlying formations of the Mont Fort nappe, (ii) the local preservation of a hardground at the actual base of the series, and (iii) the absence of particular shearing along different sections of the contact.

The Série Rousse therefore belongs to the relative autochthonous Mesozoic cover of the Mont Fort nappe, which it forms together with the Evolène Series (cf. chap. 2), as previously proposed by Escher (1988) for example.

The stratigraphic sequence composed by the superposition of the Evolène Series and the Série Rousse shows very strong similarities with the stratigraphy of the Breccia nappe in the Prealps. The comparison of the Série Rousse with the Breccia nappe, which is better constrained biochronologically, as well as the discovery in the Série Rousse of a form corresponding to *Globotruncana neotricarinata*, allows us to better constrain its age. It probably extends from the middle of the Early Cretaceous (Aptian?) to the Late Cretaceous (Campanian to earliest Maastrichtian?).

The median Schistes Lustrés unit, the ophiolite-bearing Série Grise, overlies the Série Rousse by a tectonic contact corresponding to the Upper/Middle Penninic limit. It is underlined by tectonized slices (Frilihorn Series), whose origin corresponds either to the internal part of the Mont Fort nappe, or to a more internal Prepiemont unit. The performed RSCM analyses show that the recrystallization of the organic matter progressively increases towards this contact. RSCM temperatures calculated in the Hérens valley for samples taken in the immediate vicinity of the contact (< 10 m) reach 467 ± 23 °C for the Série Rousse and 466 ± 29 °C for the Série Grise, whereas the lowest values obtained for both series in this same valley come from the areas most distant from the contact (408 ± 27 °C and 411 ± 17 °C respectively). This temperature increase centered on the contact may reflect a shear heating effect, associated with the intense strain localized along this major tectonic contact.

The upper unit of the Schistes Lustrés complex, the Tracuit - Aiguilles Rouges zone, very likely corresponds to the Cornet Unit individualized by Manzotti et al. (2021) in the Ollomont valley. Our data indicate that the metamorphic limit highlighted by these authors at the base of the Cornet Unit is also found at the base of the Tracuit - Aiguilles Rouges zone. This limit appears as the most important metamorphic discontinuity inside the Mont Fort, Tsaté and Dent Blanche nappe stack.

Although the Schistes Lustrés complex of the Combin zone has been regarded by many authors as a single tectonic entity, our study thus confirms and details that it is instead composed of different tectonic units separated by major metamorphic and/or tectonic contacts.

Our study moreover clearly documents that the Schistes Lustrés consist of both sediments deposited on oceanic crust, which locally show preserved stratigraphic contacts with ophiolitic or serpentinized sub-continental mantle slivers, as well as of sediments still resting stratigraphically on a former hyper-extended continental margin.

Abbreviations

CL: Cathodoluminescence

CM: carbonaceous material

Fm.: Formation

HP: High Pressure

RSCM: Raman Spectroscopy of Carbonaceous Material

RSCM°T: Temperature calculated following RSCM method (peak°T)

TL: transmitted light

UHP: Ultra High Pressure

[Geographic coordinates] refer to the Swiss grid MN95

Supplementary information (see Appendix)

Additional file 3.1: Detailed RSCM°T calculations

Additional file 3.2: Série Rousse and Série Grise mean RSCM°T and series attributions

Additional file 3.3: Hérens valley RSCM°T and distances to the Série Grise / Série Rousse contact

Acknowledgments

The authors would like to thank the following people, who were of great support in carrying out this study: Paola Manzotti and Michel Ballèvre for the numerous discussions regarding the results and interpretations and for the common excursion in the Chanrion area; Yves Gouffon and Stefan Dall'Agnolo for the highly interesting discussions regarding the results and interpretations; Christophe Jossevel, Nicolas Buchs and Martin Robyr for their precious help in the field; Charlotte Ribes for her advices and for accompanying us in the Artsinol and Pointe de Chalune areas; Gianreto Manatschal, Nicolas Dall'Asta and Guilhem Hoareau for the discussions and for accompanying us in the Mauvoisin area; Albrecht Steck for the discussions about the regional

geological structure; Gérard Stampfli for the interesting discussion and outcrops indications; Olivier Reubi for the assistance with Raman spectroscopy; and Youness Zangui for thin sections elaboration. The authors acknowledge the University of Lausanne for funding this work and the Société Académique Vaudoise for the additional financial support. Finally, the authors thank Yves Gouffon and Luca Cardello for their review and for their numerous suggestions that helped to improve the manuscript.

Chapter 4: Structure and stratigraphy of continent-derived metasediment units (Cimes Blanches and Frilihorn) intercalated within the ophiolites around Zermatt: Relations with the Mischabel backfold, Alphubel basement and Mont Fort nappe (Pennine Alps, SW Switzerland and NW Italy)

Abstract

The nature of the mechanisms leading to the imbrication of continental- and oceanic-derived units in collision zones is a long standing and, in several cases, still debated subject in geology. The studied area around Zermatt (SW Switzerland and NW Italy) exhibits some classic examples of such imbrications. In particular, the units called *Cimes Blanches* and *Frilihorn* or *Faisceau Vermiculaire*, consist of a set of thin but widely-extending bands of continent-derived metasediments intercalated at different levels in the thick complex of ophiolites and oceanic metasediments exposed over this region. Despite the very wide variety of mechanisms that have been invoked to explain such intercalations and the complex tectonic architecture of this area, no real consensus has been reached within the geological community concerning these questions.

We present new data concerning the structure and stratigraphy of the different bands constituting the Faisceau Vermiculaire in the area surrounding Zermatt and, in particular, in the Täschalpen sector, where the Faisceau Vermiculaire is locally in contact with basement units forming the Mischabel backfold and the Alphubel anticline.

Our lithological and stratigraphic observations allow: (i) to confirm the presence in the Faisceau Vermiculaire of widespread breccias, for the most part of probable Lower to Upper Jurassic age, that are intensely stretched and therefore locally difficult to recognize; (ii) to confirm the interpretation of the first authors suggesting the stratigraphic nature of the contacts between

the Faisceau Vermiculaire and the overlying non-ophiolitic, p.p. Upper Cretaceous, calcschists (Série Rousse), which constitute the lower part of the Schistes Lustrés of the Combin zone; (iii) to confirm the existence of a strong contrast in the Jurassic to Cretaceous/Paleogene stratigraphic sequences between the autochthonous cover of the Siviez-Mischabel nappe (Barrhorn Series, Briançonnais s.str.) and the series formed by the Faisceau Vermiculaire and Série Rousse, which is characteristic of a sedimentation in a deeper basin (Prepiemont basin) with an important clastic and detritic input; (iv) to interpret the contact of the Faisceau Vermiculaire and the Série Rousse with the basement forming the Alphubel anticline east of Zermatt, as a stratigraphic contact; the locally discordant character of this contact is interpreted as the result of the activity of synsedimentary Jurassic normal paleofaults; (v) to confirm the widely accepted interpretation concerning the tectonic nature of the contact separating the Faisceau Vermiculaire and the Série Rousse from the basement forming the hinge of the Mischabel backfold; this basement is separated from the one forming the Alphubel anticline by a deep early syncline, involving ophiolites of the Tsaté nappe, the eastward prolongation of this syncline in the Mischabel massif is potentially important but hidden by the moraines and glaciers.

We propose a new tectonic scheme for the structure of the Faisceau Vermiculaire and adjacent units. It involves an early northward folding of the Faisceau Vermiculaire together with the Série Rousse and ophiolitic Schistes Lustrés of the Tsaté nappe, followed by major backfolding responsible for the southward emplacement of these units above the HP Zermatt-Saas and Monte Rosa nappes. With respect to the Siviez-Mischabel and Tsaté nappes, our tectonic study at regional scale shows that the ensemble formed by the Alphubel basement, the Faisceau Vermiculaire and the Série Rousse share an identical tectonic position with the Mont Fort nappe outcropping north and west of the Dent Blanche klippe. Based on tectonic and stratigraphic arguments, we propose that the Alphubel basement, the Faisceau Vermiculaire and the Série Rousse form together the eastern prolongation of the Mont Fort nappe, in the lower limb of the Mischabel backfold.

4.1. Introduction

The mechanisms leading to the imbrication of continental and oceanic derived units in collision zones is a long standing and, in several cases, still debated subject in geology.

This study focuses on the region surrounding Zermatt (SW Switzerland and NW Italy), in the central zone of the Alpine Arc (Fig. 4.1), which exhibits some of the most classic examples of such imbrications in Alpine geology. In particular, a set of thin but widely-extending bands formed by metasediments of continental origin are intercalated at different levels in the thick complex of ophiolites and oceanic metasediments exposed over this region. The existence of these bands is known to geologists since the 19th century (e.g. Gerlach 1869, 1871, 1883) and have been described and mapped in detail since the beginning of the 20th century by Emile Argand who grouped them under the name of *Faisceau Vermiculaire* (Argand 1908, 1909, 1911, 1916a, 1923). Since then, several names have been used to designate specific parts, levels or zones of the Faisceau Vermiculaire between the northern Aosta valley and SW Valais, the main ones being: *complesso triassico basale* (Dal Piaz 1965); *série du Frilihorn* (Marthaler 1984; Escher and Masson 1984; Sartori 1987); *Frilihorn nappe* (Escher et al. 1993); *Pancherot - Cime Bianche - Bettaforca Unit* (Dal Piaz 1988); *série des Cimes Blanches* (Vannay and Allemann 1990); and *Cimes Blanches nappe* (Escher et al. 1993; Sartori and Marthaler 1994).

These intercalations of the Faisceau Vermiculaire continent-derived metasediments within calcschists and slivers of oceanic crust around Zermatt have been extensively studied during the last century. A very wide variety of mechanisms have been invoked to explain them. The main one are: (a) stratigraphic succession in natural chronological order (Giordano 1869); (b) high amplitude isoclinal folding involving continent-derived metasediments, calcschists and ophiolites, with a vergence towards the external part of the Alpine arc, followed by backfolding (i.e. having a vergence towards the internal part of the arc), also of large

amplitude (e.g. Argand 1911, 1920, 1934); (c) tectonic superposition of large composite units including basal continent-derived metasediments and upper parts formed by calcschists and ophiolites, followed by later backfolding (e.g. Staub 1942b; Güller 1947; Iten 1948; Bearth 1953b, 1964a, 1976); (d) early tectonic emplacement towards the external part of the belt of calcschists and ophiolites on top of the partly sheared off sedimentary cover of the downgoing continental margin, and later major retro-transport and backfolding of the whole on top of the lower ophiolitic units (Ellenberger 1953); (e) early detachment of the sedimentary cover from portions of the subducting continental margin, followed by polyphased folding of variable vergence and later backfolding (e.g. Sartori 1987, 1990; Steck 1989; Sartori et al. 1989; Vannay and Allemann 1990; Escher et al. 1993, 1997); (f) shallow depth offscraping, and stacking within an accretionary wedge, of slivers derived either from the continental margins, or oceanic crust and basin (Marthaler and Stampfli 1989; Stampfli and Marthaler 1990); (g) hyper-extension of the continental margin during Jurassic rifting, leading to the formation of continent-derived detachment allochthons inside the oceanic domain, and subsequent occurrence of small continental units pinched within the oceanic units in the Alpine nappe stack (Dal Piaz 1999; Beltrando et al. 2014; Dal Piaz et al. 2015a; Passeri et al. 2018); (h) emplacement of thin continent-derived sheared slices inside the ophiolitic units, along crustal scale shear zones showing a complex history and reactivations with opposite shear senses (e.g. Cartwright and Barnicoat 2002; Reddy et al. 2003; Forster et al. 2004; Groppo et al. 2009; Kirst 2017; Kirst and Leiss 2017); (i) emplacement of continent-derived detached sedimentary slivers at the interface between two distinct ophiolitic units by early thrusting and shearing (extraction), directed towards the external part of the belt (Froitzheim et al. 2006, 2019; Pleuger et al. 2007); (j) backshearing and backfolding allowing the emplacement of sheared off continent-derived sedimentary blocks and lenses inside the ophiolites and calcschists complex (Scheiber et al. 2013); (k) diachronous juxtaposition and underplating of slices detached at different depth along the Alpine subduction

interface (Angiboust et al. 2014); (l) early delamination and thrusting of continent-derived subducting sedimentary flakes towards the internal part of the belt, over the ophiolitic units, followed by polyphased thrusting, folding and backfolding (Steck et al. 2015). Despite the impressive number of studies addressing these questions, and the many and various hypotheses that have been proposed to explain the complex tectonics of this zone, it appears that no real consensus has been reached within the geological community concerning these questions, which still are regularly addressed in the literature.

The present study mainly focuses on questions concerning the structure and stratigraphy of the different bands constituting the Faisceau Vermiculaire in the area surrounding Zermatt and, in particular, in the Täschalpen sector (Fig. 4.1). At this location, the Faisceau Vermiculaire is locally in contact with Paleozoic basement; the question of the nature of these contacts constitutes also an important aspect of the study. Relationships between these last units and those studied in the two previous main chapters of this manuscript (Evolène Series, Série Rousse, Frilihorn Series and Mont Fort basement), on the other side of the Dent Blanche klippe, are also discussed. Finally, questions regarding the initiation and progressive development of backfolds are briefly discussed in regard to the new data and constraints resulting from this study.

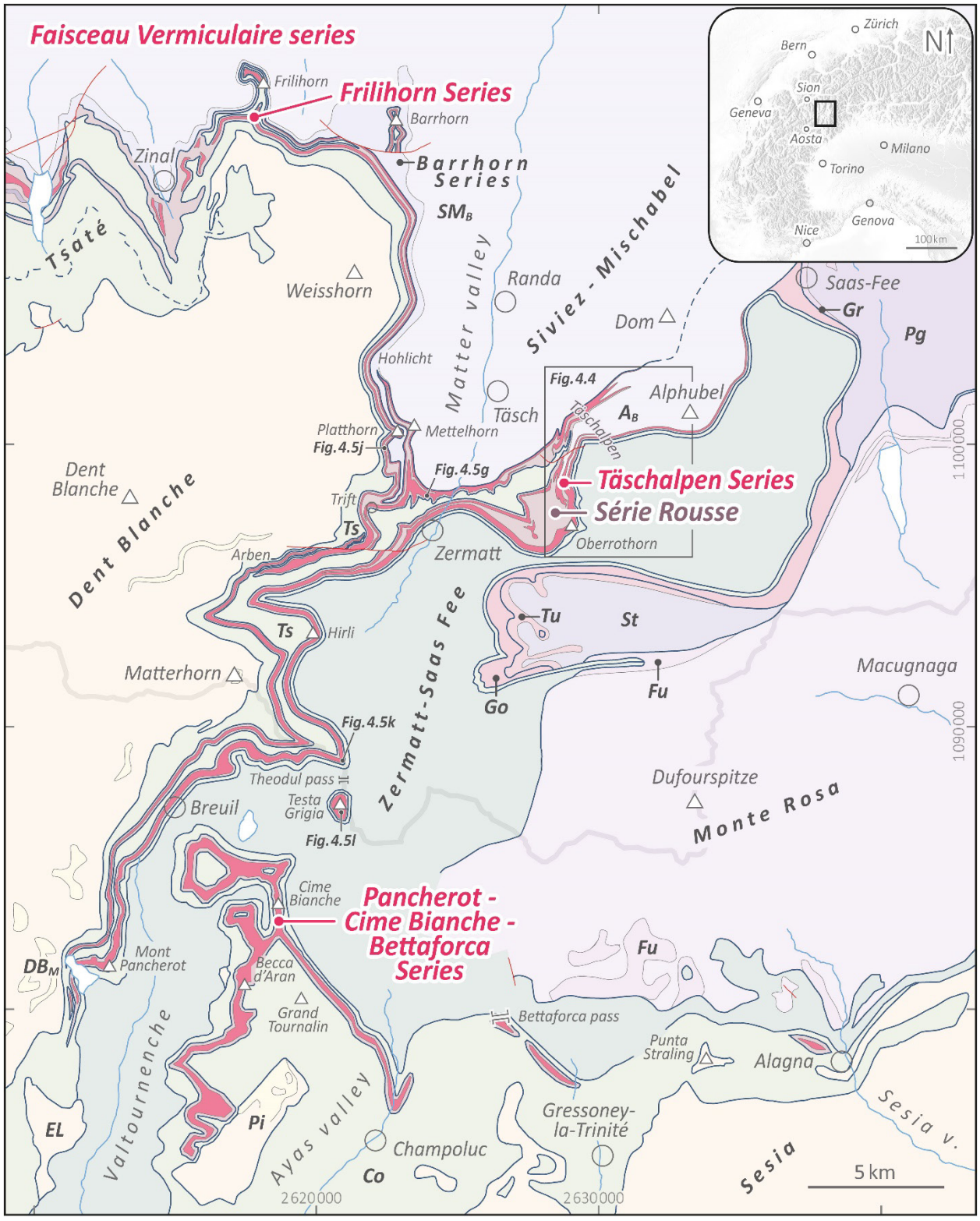

Fig. 4.1 Tectonic map of the upper Matter valley and NW Aosta valley showing the intercalations of (i) the continent-derived Faisceau Vermiculaire Permian-Jurassic series (incl. Pancherot - Cime Bianche - Bettaforca, Frilihorn, etc.) and (ii) of the non ophiolitic Schistes Lustrés of the Série Rousse, inside the ophiolitic Tsaté nappe (or Combin zone s.str.). After Argand (1908), Güller (1947), Bearth (1953a, 1964b, 1967a, 1973), Martin (1982), Crespo (1984), Sartori (1987), Escher (1988), Girard (1995), Steck et al. (1999, 2015), Bucher et al. (2003a), Marthaler et al. (2008a, 2020a), Dal Piaz et al. (2015b) and observations from this study. A_B: Alphubel pre-Permian basement; *Co*: Combin zone s.str. (=Tsaté nappe); DB_M: Dent Blanche Mesozoic; *EL*: Etirol-Levaz unit; *Fu*: Furgg Series; *Go*: Gornergrat nappe; *Gr*: Grundberg Series; *PG*: Portjengrat basement; *Pi*: Pillonet unit; SM_B: Siviez-Mischabel basement; *St*: Stockhorn basement; *Tu*: Tuftgrat Series.

4.2. Geological setting

Overviews concerning the development of the Alpine chain and of the Pennine Alps in particular are given in the first two main chapters of this manuscript. Below, we will concentrate on the description of the units studied in the present chapter and those directly surrounding them, in the area around Zermatt (upper Matter valley and NE Aosta valley).

The complex nappe stack constituting this area includes both: (i) units derived from the Paleozoic basements and Mesozoic covers of each of the two continental margins (European - Briançonnais s.l. margin and Adriatic margin) which bordered the Piemont Basin (Alpine Tethys) to the north and to the south, respectively, during the Mesozoic; as well as (ii), ophiolites and oceanic meta-sediments derived from the basin itself.

The uppermost unit of this nappe stack is the Adriatic margin-derived klippe of the Dent Blanche nappe (e.g. Lugeon and Argand 1905a; Argand 1911; Diehl et al. 1952; Ballèvre et al. 1986), or Dent Blanche Tectonic System (Manzotti et al. 2014, 2017), showing Alpine metamorphic imprint at the transition between the greenschist- and blueschist-facies conditions (Manzotti et al. 2020), and rooting into the eclogitic Sesia zone (e.g. Dal Piaz et al. 1972; Compagnoni 1977; Giuntoli and Engi 2016) which forms the southeastern part of the area (Fig. 4.1). The other units including basement in this area are derived from the European - Briançonnais s.l. continental margin. From an internal to an external position, they consist of: the Monte Rosa nappe (e.g. Bearth 1952; Pawlig and Baumgartner 2001; Kramer 2002; Steck et al. 2015; Vaughan-Hammon et al. 2021; Luisier et al. 2022); the Stockhorn nappe (Escher et al. 1988; Steck et al. 2001, 2015; Kramer 2002) ; the Portjengrat nappe (e.g. Kramer 2002; Masson 2002; Steck et al. 2015); and the Siviez-Mischabel nappe (e.g. Bearth 1963, 1964a; Escher 1988; Sartori 1990; Genier et al. 2008; Scheiber et al. 2013, 2014). Alpine metamorphic imprint in these units varies from HP/UHP eclogite facies

in the Monte Rosa to (HP) greenschist facies in the Siviez-Mischabel nappe (cf. references here above; Steck et al. 2001, 2015; Bousquet et al. 2004). Ophiolites and oceanic meta-sediments derived from the Piemont basin form a complex stack of folded slivers revealing two distinct types of metamorphic evolution (Kienast 1973; Dal Piaz 1974; Ernst and Dal Piaz 1978; Merle and Ballèvre 1992; Ballèvre and Merle 1993; Negro et al. 2013): the lower units (Zermatt-Saas Fee and Antrona) display eclogite-facies paragenesis (e.g. Bearth 1967a; Pfeifer et al. 1989; Bucher et al. 2005, 2019; Angiboust et al. 2009; Dragovic et al. 2020) with a local UHP relic (e.g. Reinecke 1991, 1998; Forster et al. 2004; Groppo et al. 2009; Frezzotti et al. 2011, 2014), whereas the upper unit, the Tsaté nappe (Sartori 1987; Escher 1988; Marthaler and Stampfli 1989) or Combin zone s.str (e.g. Dal Piaz 1971; Bearth 1976; Caby 1981), displays greenschist-facies paragenesis with blueschist-facies relics (e.g. Caby 1981; Desmons et al. 1999; Bousquet et al. 2004; Manzotti et al. 2021).

The studied continent-derived metasediments constituting the different bands of the *Faisceau Vermiculaire* (Argand 1916b, 1916a), are intercalated at various levels within the Schistes Lustrés and ophiolites of the Tsaté nappe and close to its basal limit with the Zermatt-Saas Fee nappe (Figs. 4.1, 4.2). They are mainly formed of quartzites, dolomites, and various marbled and/or highly tectonized carbonates (e.g. cornieules). The ages of these metasediments are mostly interpretative, classical age attributions range from Permian to Jurassic (e.g. Güller 1947; Bearth 1976). The slopes located directly north of Zermatt (Fig. 4.2) correspond to the sector of the hinge of the Mischabel backfold (Studer 1851; Argand 1911). In this area, it is possible to count up to twenty of superimposed bands of the Faisceau Vermiculaire, between the top of the ophiolites of the Zermatt-Saas Fee nappe and the base of the Dent Blanche nappe (Argand 1916a). They are interspersed and folded with the non-ophiolitic Schistes Lustrés of the Série Rousse (cf. chap. 4.3.2) and with the ophiolites and ophiolite-bearing Schistes Lustrés of the Tsaté nappe.

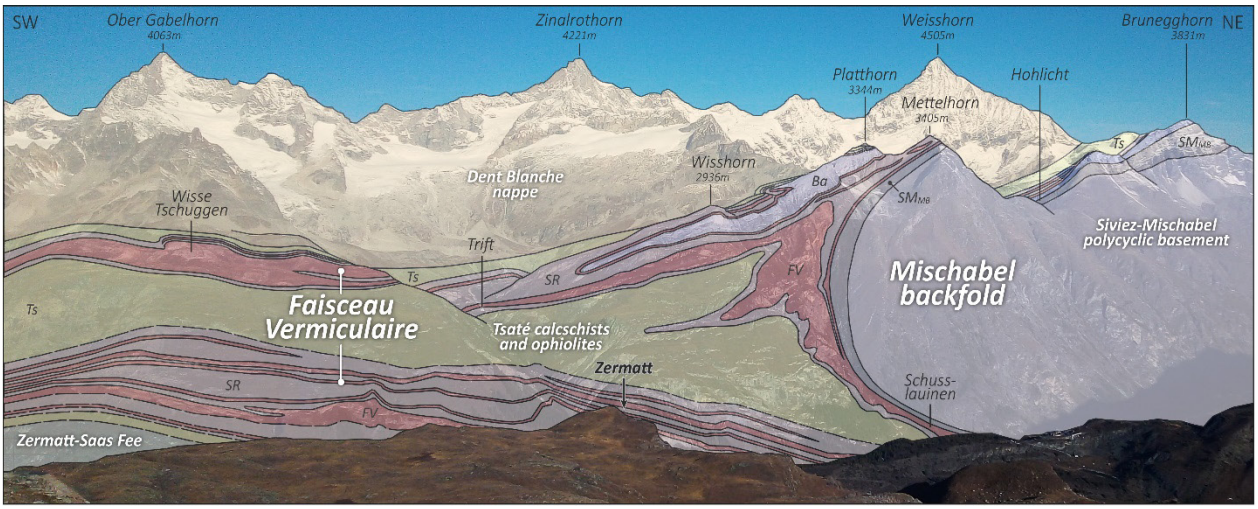

Fig. 4.2 Structure of the Faisceau Vermiculaire superimposed bands of Permian-Jurassic continental metasediments and associated Série Rousse calcschists above Zermatt, in the area of the hinge of the Mischabel backfold; and relations with the Tsaté, Dent Blanche, Zermatt-Saas Fee and Siviez-Mischabel nappes. Picture taken from the Gornergrat area (C. Jossevel); geological limits after Argand (1908), Bearth (1953a, 1964b), Wilson (1978), Crespo (1984) and Sartori (1987); *Ba*: Barrhorn Series (Siviez-Mischabel autochthonous Mesozoic cover); *FV*: Faisceau Vermiculaire; SM_{MB}: Siviez-Mischabel monocyclic basement; *SR*: Série Rousse calcschists; *Ts*: Tsaté nappe.

The thickness of the different bands forming the Faisceau Vermiculaire rarely exceeds a few tens of meters and is frequently reduced to a few meters or tens of cm (Fig. 4.3a). In some sectors, generally corresponding to fold hinges, their thickness can reach a few hundred meters (e.g. Fig. 4.2). Despite their reduced thickness, these bands show remarkable extensions. The thickest ones can be followed almost continuously, except for a few zones covered by Quaternary deposits, from the Täschalpen sector to the NE of Zermatt, up to the crests of the upper Valtournenche and Ayas valleys, and are found even further to the SE around the Bettaforca pass and up to Alagna (Fig. 4.1). Further south, the Faisceau de Cogne in southern Aosta valley (e.g. Hermann 1925, 1928; Elter 1972; Beltrando et al. 2008, 2009; Loprieno and Ellero 2021) and the Faisceau de Prariond in the Vanoise massif (e.g. Ellenberger 1958; Polino and Dal Piaz 1978; Deville 1987; Deville et al. 1992), in a tectonic position similar to that of the Faisceau Vermiculaire, represent most likely its southern equivalents.

In most of the recent studies, the Faisceau Vermiculaire is subdivided into two distinct tectonic units. The Frilihorn nappe groups the structurally higher bands of the Faisceau Vermiculaire that

are interspersed within the Tsaté nappe, whereas the structurally lower bands, located near the basal contact of the Tsaté nappe over the Zermatt Saas zone, are linked to the Cimes Blanches nappe (e.g. Escher et al. 1993, 1997; Steck et al. 1999, 2015). These last bands are intercalated exactly at the contact between the Zermatt-Saas Fee and Tsaté nappes, but are structurally higher. Indeed, metabasites devoid of eclogite-facies imprint (even as relict) have been identified between the lowermost bands of the Faisceau Vermiculaire and the Zermatt-Saas Fee eclogites in different localities of the Valtournenche and Ayas valley, where they are referred to as Lower Combin Unit (Ballèvre et al. 1986; Cortiana et al. 1998; Bucher et al. 2004a; Dal Piaz et al. 2015b; Passeri et al. 2018). Metabasites devoid of eclogitic imprint have also been described in an identical tectonic position around Zermatt, in the sectors of the Oberrothorn (Bearth 1973) and Täschalpen (Cartwright and Barnicoat 2002).

In the area surrounding Täschalpen, the Faisceau Vermiculaire is composed of numerous bands which are partly folded together with the basement of the Alphubel Lappen (Staub 1942d; Güller 1947; Müller 1983), later described as the Alphubel fold (Steck 1989; Sartori et al. 1989), and tectonically linked to the Siviez-Mischabel nappe (e.g. Escher 1988; Steck 1989; Steck et al. 1999, 2015). In this area, the distinction between the Frilihorn and Cimes Blanches units according to the criteria described above is unclear (cf. Fig. 4.1; Steck et al. 1999). For this reason, we will rather use the term Täschalpen Series to refer to the whole set of bands constituting the Faisceau Vermiculaire in this sector.

The question of the paleogeographic origin of the continent-derived metasediments forming the Faisceau Vermiculaire remains controversial. The first hypothesis proposed (Argand 1909, 1911, 1916b) was a northern origin. It has been later followed by many authors invoking a provenance from the Briançonnais (s.l.) margin (e.g. Sartori 1987; Vannay and Allemann 1990; Escher et al. 1997; Sartori et al. 2006; Steck et al. 2015), or more specifically from the

Briançonnais swell (e.g. Ellenberger 1953; Scheiber et al. 2013), or from the Prepiemont domain (i.e. the distal part of the Briançonnais s.l. margin; e.g. Elter 1960, 1972; Dal Piaz 1974; Bearth 1976; Dal Piaz and Ernst 1978; Escher and Masson 1984; Marthaler 1984; Escher 1988; Deville et al. 1992). The hypothesis of a southern origin (Staub 1942d; Güller 1947; Iten 1948) has been later followed by several authors, proposing either an origin from the distal Adriatic margin (e.g. Caby et al. 1978; Caby 1981; Froitzheim et al. 2006, 2019; Pleuger et al. 2007), or from Adriatic margin-derived extensional allochthons (Lower Austroalpine outliers; e.g. Dal Piaz 1999; Dal Piaz et al. 2001, 2015a; Beltrando et al. 2014; Passeri et al. 2018).

4.3. Lithologies and stratigraphy of the Faisceau Vermiculaire and Série Rousse

4.3.1. Faisceau Vermiculaire series

In several sectors of the investigated area, the study of the stratigraphy of the metasediments forming the Faisceau Vermiculaire is fastidious, because of the intense deformation of these units. Those are frequently reduced to thin, extremely stretched and boudined bands (Fig. 4.3a), sometimes less than a meter thick, where only the presence of dolomites (often partly transformed into cornieules; cf. Masson 1972), and/or of quartzites can be identified.

Nevertheless, the deformation affecting the Faisceau Vermiculaire shows strong regional variations and some sectors of particularly low strain allow interesting. This is the case in particular for the area directly south of the Mischabel backfold, between the Schusslauinen and the Täschalpen (Figs. 4.1 and 4.4), where the strong rheological contrast between the Paleozoic basement and the Mesozoic sediments, allows the preservation of a lower strain sector in the hinge zone of this large open backfold. In this area, some of the bands forming the Faisceau Vermiculaire reach thicknesses of several tens of meters (e.g. Figs. 4.3b, i; 4.5b, d), up to a hundred meters with well-developed stratigraphic series, involving quartzschists, phyllitic and tabular quartzites,

dolomites, calcareous marbles and breccias (e.g. Figs. 4.3b-c). It is described below and compared to the successions at other localities in the Faisceau Vermiculaire. The general stratigraphic succession described below is found in almost all the different bands and series of the Faisceau Vermiculaire. Nevertheless, local successions are most often reduced compared to this complete succession. Depending on the area, these reductions may be tectonic (boudinage, shearing) or stratigraphic (e.g. sedimentary gaps; cf. chap. 4.6.1).

Fig. 4.3 Lithologies of the Faisceau Vermiculaire Permian-Jurassic series and of the Série Rousse non- ophiolitic Schistes Lustrés (p.p. Upper Cretaceous). **a** Typical aspect of a highly stretched band of the Faisceau Vermiculaire and associated Série Rousse calcschists; Adlerflüe [2'620'460/1'110'670], Turtmann valley. **b** Stratigraphic succession of Lower Triassic Tabular Quartzite, Lower Triassic dolomites and banded calcareous marbles showing dolomitic elements (Jurassic?), in the Täschalpen Series from the Faisceau Vermiculaire; Bru [2'629'460/1'100'880], Täschalpen. **c** Stratigraphic contact between the Permian phyllitic quartzite ("Verrucano") and the Tabular Quartzite attributed to the Lower Triassic; Rinderberg [2'629'860/1'100'290], Täschalpen. **d** Phyllitic quartzite with cm-sized quartz clasts ("Verrucano" facies) attributed to the Permian; Sommertschuggen [2'628'945/1'098'630], Täschalpen. **e** Polymict breccia of the Täschalpen Series with light grey calcareous matrix and clasts locally dominated by dolomites. These breccias are attributed to the Upper Jurassic by comparison with the stratigraphic succession of the Breccia nappe of the Prealps. Sommertschuggen [2'628'840/1'098'560]. **f** Similar polymict breccia from the Cime Bianche Series of the Faisceau Vermiculaire; Col Sud des Cimes Blanches [2'618'630/1'084'180]. **g**, **h** Polymict breccia of the Täschalpen Series showing Lower Triassic Tabular Quartzite clasts and Permian "Verrucano" clasts, in addition to the dolomites and limestones clasts; Sommertschuggen, g: [2'628'970/1'098'650]; h: [2'628'720/1'098'540]. **i** Stratigraphic sequence observed in the Täschalpen Series and Série Rousse (tectonically overturned). From top to bottom: Lower Triassic Tabular Quartzites, Middle to Upper Triassic dolomites, microbreccias (Jurassic?) and Série Rousse calcschists (p.p. Upper Cretaceous); Rotbach [2'629'440/1'101'240]. **j** Typical aspect of the Série Rousse calcschists; Bru [2'629'560/1'101'030], Täschalpen. **k** Stratigraphic contact between a polymict breccia of the Faisceau Vermiculaire attributed to the Jurassic and the Série Rousse calcschists showing cm dolomitic clasts at the contact. Schusslauinen [2'624'280/1'098'110], Zermatt. **l** Série Rousse calcschists showing a conglomeratic basal level (Jurassic limestones are outcropping 2 m below on the right); Rinderberg [2'629'660/1'100'155], Täschalpen. ▶

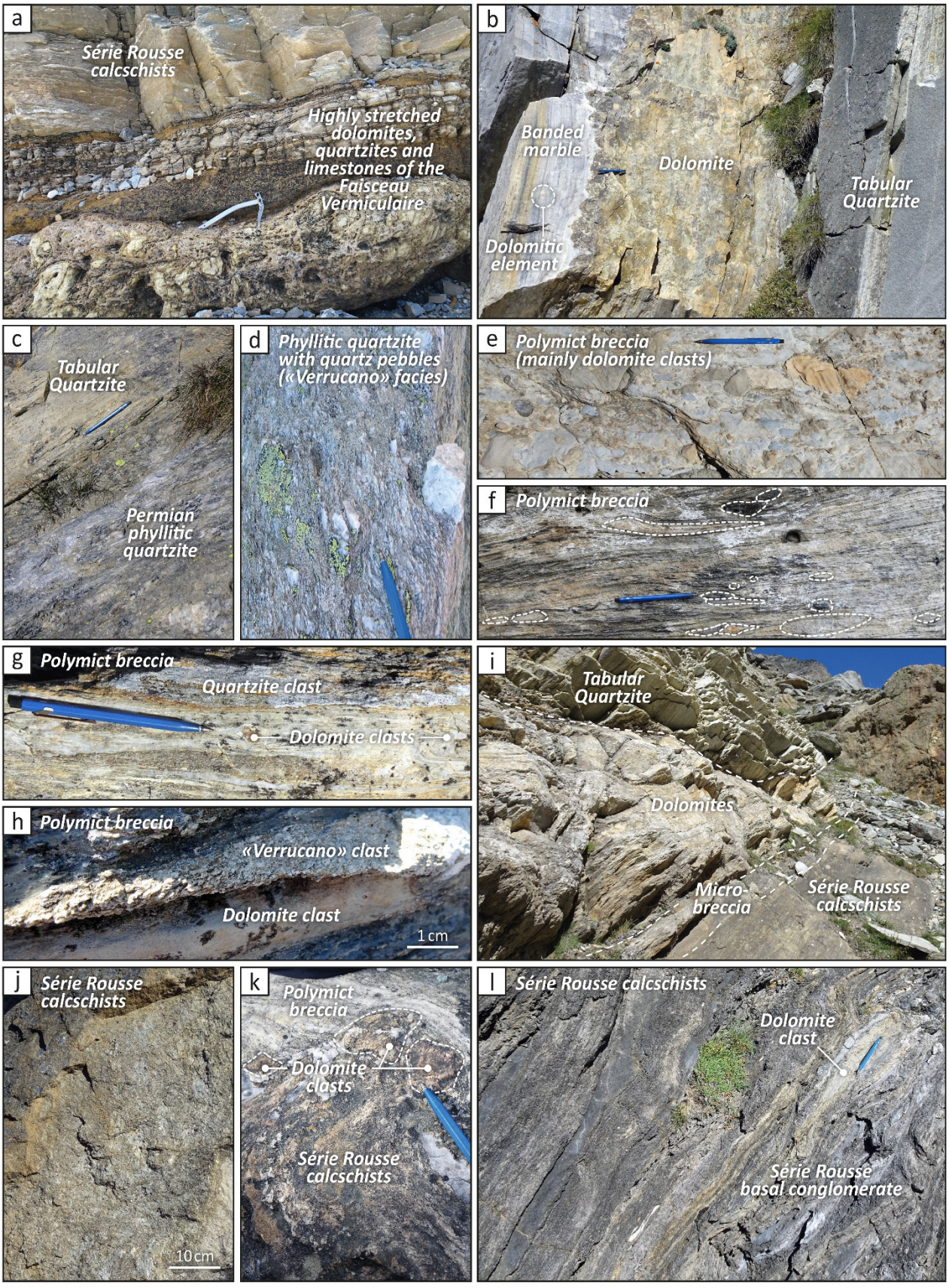
a
Série Rousse calcschists
Highly stretched dolomites, quartzites and limestones of the Faisceau Vermiculaire
b
Banded marble
Dolomite
Tabular Quartzite
Dolomitic element
c
Tabular Quartzite
Permian phyllitic quartzite
d
Phyllitic quartzite with quartz pebbles («Verrucano» facies)
e
Polymict breccia (mainly dolomite clasts)
f
Polymict breccia
g
Polymict breccia
Quartzite clast
Dolomite clasts
h
Polymict breccia
«Verrucano» clast
Dolomite clast
1 cm
i
Tabular Quartzite
Dolomites
Micro-breccia
Série Rousse calcschists
j
Série Rousse calcschists
10 cm
k
Polymict breccia
Dolomite clasts
Série Rousse calcschists
l
Série Rousse calcschists
Dolomite clast
Série Rousse basal conglomerate

4.3.1.1. Quartzites

The quartzschists and phyllitic quartzites are mainly composed of quartz, generally in sub-mm grains, white micas and minor chlorite, marking the penetrative cleavage, albite and K-feldspar; accessory minerals include apatite, zircon, calcite, chlorite, tourmaline, epidote, rutile and other oxides (e.g. Girard 1995; Bucher et al. 2004a; Passeri et al. 2018). At Täschalpen, especially on the left (SW) side of the valley, the quartzites have a thickness of a few tens of meters. Identical lithologies at the base of the Pancherot - Cime Bianche - Bettaforca Series in the upper Valtournenche are one hundred meters thick (cf. Passeri et al. 2018). These quartzschists and phyllitic quartzite are classically assigned to Permian (e.g. Güller 1947; Bearth 1953a, 1976). Some of these levels are characterized by the presence of abundant cm-sized, sometimes pinkish, quartz pebbles (Fig. 4.3d), which is commonly found in the Upper Permian levels of the units derived from the Briançonnais s.l. and often referred to as «Verrucano» (e.g. Jäckli 1950; Trümpy 1966; Genier et al. 2008) and attributed to the Bruneggjoch Fm. (Sartori 1990, Sartori et al. 2006).

At their top, the phyllitic quartzites decrease in mica content and gradually turn into pure white quartzites in centimetric beds (Figs. 4.3b-c) classically referred to as Tabular Quartzites or "Tafelquartzite" in German. This formation and the gradual transition from the phyllitic quartzites are observed in numerous localities in the Faisceau Vermiculaire. They are very similar to those observed at the top of the Bruneggjoch Fm. in the Siviez-Mischabel nappe (e.g. Sartori 1990; Genier et al. 2008) and in the Mont Fort nappe (e.g. Allimann 1987, 1990; cf. chap. 4.2.4.2), and described as the Sous le Rocher Member (Sartori et al. 2006). In the Faisceau Vermiculaire, the Tabular Quartzites reach a maximum thickness of a few tens of meters, partly resulting of duplications by isoclinal folding.

4.3.1.2. Dolostones and associated limestones

Dolostones, sometimes associated with carbonaceous marbles, stratigraphically overly the quartzites (e.g. Figs. 4.3b, i). Dolostones show different facies: either massive, dm-bedded and light-colored, with a russet or brownish patina (Fig. 4.3b); to fine-grained, laminated, dark-colored facies, sometimes with whitish patina (Vannay and Allemann 1990; Passeri et al. 2018). They are made up to 90% of dolomite, associated with calcite, phlogopite and white mica ± talc and Mg-chlinochlore (Bucher et al. 2004a). No fossils have been found in the dolomitic levels of the Faisceau Vermiculaire, but the comparison with less deformed and fossil-bearing series of the Alps and Prealps suggests a Middle to Late Triassic age (e.g. Sartori 1987; Vannay and Allemann 1990; Passeri et al. 2018).

In several sectors, light-colored, thin-bedded and laminated calcareous marbles are intercalated within the dolomitic levels, or locally form their base; they are usually referred to the Middle Triassic (e.g. Sartori 1987; Vannay and Allemann 1990; Passeri et al. 2018). Remnants of corals and crinoids have been observed by Bucher et al. (2004a) in similar marbles from the Arben area, west of Zermatt (Fig. 4.1).

In several places, the dolostones and marbles of the Faisceau Vermiculaire are partly replaced by cornieules. The presence of gypsum is mentioned by Bearth (1976) within cornieules levels in the Oberrothorn area, east of Zermatt.

The presence of an upper yellow quartzite level, as described by Passeri et al. (2018) on the Pancherot and Becca d'Aran successions in the Valtournenche and interpreted as representing the Upper Triassic, was not observed in any of the outcrops studied in this work. High amplitude isoclinal folds have however been identified in many sectors (e.g. Figs. 4.4, 4.5a) and locally induce duplications of the Lower Triassic Tabular Quartzite level. The unpublished detailed studies of the Pancherot and Eastern upper Valtournenche areas from Dentan and

Menthonnex (1990) and Allemann and Vannay (1987), respectively, indicate that such high-amplitude recumbent isoclinal folds are affecting the whole series in both Pancherot and Becca d'Aran sectors and could therefore be responsible of such duplications.

The thickness of the Triassic carbonates in the Faisceau Vermiculaire series reach locally several tens of meters, but the thickest outcrops show duplications resulting from Alpine folding.

4.3.1.3. Breccias and associated limestones

Well recognizable breccias have been described in multiple localities throughout the Faisceau Vermiculaire (e.g. Figs. 4.3e-h; Güller 1947; Bearth 1953b, 1973, 1976; Dal Piaz 1965, 1974; Sartori 1987, 1990; Vannay and Allemann 1990; Dal Piaz et al. 2015a). However, because of the strong deformation, breccias are frequently difficult to recognize. Highly elongated clasts could be mistaken for thin-bedded sedimentary alternations. For this reason, the quantity of breccias in the Faisceau Vermiculaire series is probably most often drastically underestimated.

These breccias show very variable facies, all intermediates are observable between: (i) monogenic dolomitic breccias with a dolomitic matrix (e.g. Bearth 1976; Vannay and Allemann 1990; Bucher et al. 2004a); (ii) breccias made of dolomitic clasts and dark calcarenitic matrix (e.g. Bearth 1976); (iii) polymict breccias with a calcareous matrix and clasts made of different types of dolomites, limestones, sometimes of tabular quartzite (Fig. 4.3g) and, locally, also of Permian quartzschists (Fig. 4.3h); and (iv) breccias with a quartz- and phyllosilicates-rich calcareous matrix and clasts mainly consisting of dolomites and limestones (Fig. 4.3l; cf. chap. 4.3.2). The size of their respective clasts ranges from a few mm to several tens of cm.

Some of the monomict dolomitic breccias could correspond to the Upper Triassic intraformational breccias (Vannay and Allemann 1990; Bucher et al. 2004a), that have been described, for example, in the Briançonnais units of the Prealps (e.g. Baud et al. 2016) and of the Western Alps (e.g. Mégard-Galli 1972; Mégard-Galli and Faure 1988). The other types of breccias have most

often been referred to the Lower or Middle Jurassic (e.g. Güller 1947; Bearth 1976; Sartori 1987; Vannay and Allemann 1990). They actually show strong similarities with, for example, the breccias dated from the Early to Middle Jurassic of the Prepiemont-derived Breccia nappe of the Prealps (attested ages from Sinemurian to Bathonian; Weidmann 1972; Stampfli and Marthaler 1990; Plancherel et al. 1998), and of the Adriatic-derived Mont Dolin Series of the Pennine Alps (Hagen 1948; Weidmann and Zaninetti 1974; Ayrton et al. 1982). However, the presence of Upper Jurassic breccias in the Breccia nappe of the Prealps (dated from Late Oxfordian to Early Tithonian; Chessex 1959; Plancherel et al. 1998) and in the Evolène Series (cf. chap. 2.4), which both show stratigraphic series very similar to that of the Faisceau Vermiculaire, suggests that some of the breccias described here are also Late Jurassic in age.

Various types of calcareous marbles, with a more or less important detritic component (quartz, phyllosilicates, dolomitic grains, etc.), are associated with the breccias. All intermediates are observable between the breccias described above and dark calcarenites or relatively massive light-colored limestones. As they are closely associated with the breccias, they are most often also referred to the Jurassic (Bearth 1976; Sartori 1987; Vannay and Allemann 1990).

4.3.1.4. Paleogeographic aspects

As mentioned above, the question of the paleogeographic origin of the Faisceau Vermiculaire is still controversial. The abundance of breccias in the upper part of the series seems to clearly indicate an origin in the distal domain of a continental margin (e.g. Bearth and Schwandler 1981). As thick breccia deposits are found both in the distal Adriatic margin (e.g. in the Mont Dolin Series; Hagen 1948; Weidmann and Zaninetti 1974; Ayrton et al. 1982) and in the distal Briançonnais margin, i.e. the Prepiemont domain (e.g. in the Breccia and Mont Fort nappes; cf. chap. 4.2), the abundance of breccias in the Faisceau Vermiculaire is, however, not itself indicative of its paleogeographic origin.

The presence of well-developed Permian and Tabular Quartzites at the base of the Faisceau Vermiculaire distinguishes this series from that of the Adriatic margin-derived Mesozoic Roisan Series, where such levels seem to be absent or extremely limited (Ballèvre et al. 1986; Dal Piaz et al. 2015a; Ciarapica et al. 2016). Such Permian and Early Triassic quartzitic facies are however found at the base of the Adriatic margin-derived Mont Dolin Series (Hagen 1948; Ayrton et al. 1982; Burri et al. 1999), where their thickness reaches several meters, or tens of meters locally (Hagen 1948). Comparing the thicknesses of these Permian and Lower Triassic quartzitic levels between the different tectonic units of the Pennine Alps, it appears that these thicknesses decrease between: (i) the Zone Houillère and Siviez-Mischabel nappe (representing the proximal domain of the southern Briançonnais margin in the studied transverse section), where these levels are up to several hundred meters thick (e.g. Sartori et al. 2006); (ii) the Mont Fort nappe (representing the distal Briançonnais margin, i.e. the Prepiemont Domain, in this transverse section), where the Permian levels reach thicknesses of several hundred meters in the frontal part and the overturned limb of the nappe, but where the Tabular Quartzites are significantly thinner than in the previous domain and do not exceed a few tens of meters in thickness (cf. chap. 4.2.4); and (iii) the above mentioned cover units of the distal Adriatic margin, where these levels are absent or do not exceed a few meters in thickness in most localities. The thickness of these levels in the Faisceau Vermiculaire, although not clearly indicative of a paleogeographic origin, is best compared among the above-mentioned thicknesses, to that observed in the Mont Fort nappe.

Finally, the presence of Triassic limestone levels in the Faisceau Vermiculaire may recall the facies of the Briançonnais (s.l.) Triassic, where limestone levels are particularly well developed (e.g. Trümpy 1960; Mégard-Galli and Baud 1977; Baud et al. 2016). As for the Permian and Lower Triassic levels, the thickness of the Middle and Upper Triassic levels also shows a marked decrease in thickness between the proximal and distal domains of the southern Briançonnais margin (cf. chap. 4.2.2). The thicknesses of these levels in the Faisceau Vermiculaire seem to

compare better with those observed in the Mont Fort nappe than in the Zone Houillère and Siviez-Mischabel nappe.

4.3.2. Basal non-ophiolitic calcschists associated with the Faisceau Vermiculaire: the Série Rousse

At the base of the Schistes Lustrés overlying the different bands of the Faisceau Vermiculaire, levels devoid of ophiolites and, on average, richer in carbonates and detrital inputs are systematically observed. The existence of such levels at the base of the Schistes Lustrés has already been observed and described by Güller (1947), Iten (1948) and Bearth (1967a, 1973, 1976). These basal levels mainly consist of calcschists with a brownish to russet patina (Figs. 4.3i-l), often rich in detritic quartz grains. Their mineralogy consists of calcite, quartz, white micas, chlorite, albite, pyrite, graphite, Fe-carbonates, titanite, tourmaline, clinozoisite, apatite and oxides. Potential relics of planktonic foraminifera constituted of Fe-carbonates have been described by Crespo (1984) and would indicate a Late Cretaceous age for some of these levels.

The basal contact of these ophiolite-devoid russet calcschists with the metasediments of the Faisceau Vermiculaire most of the time appears as a clean contact without hints of particular shearing (e.g. Figs. 4.3i, k) and has been interpreted as stratigraphic by numerous authors (Güller 1947; Iten 1948; Bearth 1973, 1976; Chadwick 1974; Escher and Masson 1984; Sartori 1987, 1990; Dal Piaz 1988; Escher 1988; Escher et al. 1988; Sartori et al. 1989; Vannay and Allemann 1990; Gasco and Gattiglio 2011). Our observations fully confirm this interpretation. Furthermore, mm to cm dolomitic clasts are locally observed within the calcschists along this basal contact (Fig. 4.3k). In some outcrops, the base of the calcschists is even formed by a polymict breccia with a matrix of calcschists and decimetric clasts of dolomites and limestones (Fig. 4.3l; Güller 1947, Iten 1948, Bearth 1973, 1976). This breccia level of the base of the calcschists do not exceed a few tens of cm in thickness, locally it reaches a few meters. Upwards, these breccias rapidly evolve to standard non-ophiolitic russet calcschists, by a progressive decrease in

clast content (Fig. 4.3l). The local occurrence of such a basal conglomerate reinforces the hypothesis of the stratigraphic nature of this contact.

Lithologies very similar to these non-ophiolitic russet calcschists are found both in the upper part of the Roisan Series (Ciarapica et al. 2016) and north of the Dent Blanche klippe, where they are referred to as the Série Rousse (Marthaler and Escher in Masson et al. 1980; Marthaler 1984) and have been interpreted as forming the upper part of the autochthonous cover of the Mont Fort nappe (e.g. Escher 1988; chap. 3.7). Relics of planktonic foraminifera have been described in various localities of the Série Rousse (e.g. Marthaler 1981, 1984; cf. chaps. 3.2.3.3, 3.4.1.2) and indicate a Late Cretaceous age (Cenomanian - Campanian?).

The attribution of the non-ophiolitic russet calcschists from the area of Zermatt to the Série Rousse has been proposed by Sartori (1987). The cartographic continuity of the Série Rousse from the Hérens valley, where it rests on top of the Triassic - Lower Cretaceous cover of the Mont Fort nappe and its Paleozoic basement (cf. chap. 3), through the upper Turtmann valley, to the area of Zermatt, has then been mapped by Escher (1988). Our observations confirm that the Série Rousse outcropping north of the Dent Blanche klippe (cf. chap. 3.4.1) is in every point identical to the above described non-ophiolitic russet calcschists from the area of Zermatt. Following the interpretation of Sartori (1987), Escher (1988) and Escher et al. (1988), they will be referred to as Série Rousse below.

4.4. Phases of deformation affecting the Faisceau Vermiculaire

4.4.1. Hinge zone of the Mischabel backfold

In the area of Zermatt, the Faisceau Vermiculaire shows a complex structure (Figs. 4.1, 4.2) resulting from successive ductile phases of folding. The most distinctive structure of the area is the Mischabel backfold (Studer 1851; Argand 1911). Its hinge zone, at the level of the basement,

is well exposed on the left side of the Matter valley between Zermatt and Täsch and is more than 1500 m high. In this area, between the Schusslauinen and the Wisshorn, the metasediments of the Faisceau Vermiculaire form a remarkable fold cascade resulting of the interference pattern between early isoclinal folds and disharmonic open to tight folds associated to the Mischabel backfold (e.g. Figs. 4.2, 4.6; Argand 1911; Güller 1947; Bearth 1964a, 1967b; Sartori 1987, 1990; Escher et al. 1997; Steck et al. 2015).

In this sector, where the deformation of the Faisceau Vermiculaire is lower than in the surrounding areas because of the strong rheological contrast with the adjacent Paleozoic basement, two distinct phases of isoclinal folds can be recognized macroscopically (e.g. Milnes et al. 1981; Mazurek 1986; Steck 1989; Lebit et al. 2002). As these two phases are most of the time not distinguishable on the field and form together the dominant schistosity, they will be jointly referred to as "nappe emplacement and early folding phases".

In the hinge area, the axis of the Mischabel backfold plunges to the W/SW with an angle of 20°-25° (Fig. 4.6; Lebit et al. 2002).

4.4.2. Täschalpen area

Because of the axial plunge of the Mischabel backfold, the prolongation of the structures towards the NE of the hinge zone, such as in the Täschalpen area, corresponds to the overturned limb of this fold. In this area, the Faisceau Vermiculaire is folded around the basement forming the Alphubel Lappen (Staub 1942d; Güller 1947; Müller 1983), or Alphubel fold (Figs. 4.4, 4.6; Steck 1989, Sartori et al. 1989). A deep syncline, constituted of Schistes Lustrés and of different bands of the Faisceau Vermiculaire, separates the basement forming the Alphubel fold, of that forming the hinge of the Mischabel backfold (Figs. 4.4, 4.6). This complex syncline has been called the Rotbach syncline by Steck (1989). Its continuation to the NE of the Täschalpen is hidden

by the moraines and glaciers covering the most part of this area (Fig. 4.4), making both the direction of its continuation and its amplitude difficult to estimate.

The fold affecting the Alphubel basement was first interpreted as a second order fold of the same phase as the Mischabel backfold (e.g. Staub 1942d; Güller 1947; Martin 1982; Müller 1983). The detailed study of the successive phases of deformation in the area of Zermatt and Täschalpen, by Steck and collaborators, led to the interpretation of the Alphubel fold as an early fold, prior to the Mischabel phase, locally refolded during this phase (Steck 1989; Sartori et al. 1989; Steck et al. 1989). Our observations fully confirm this interpretation.

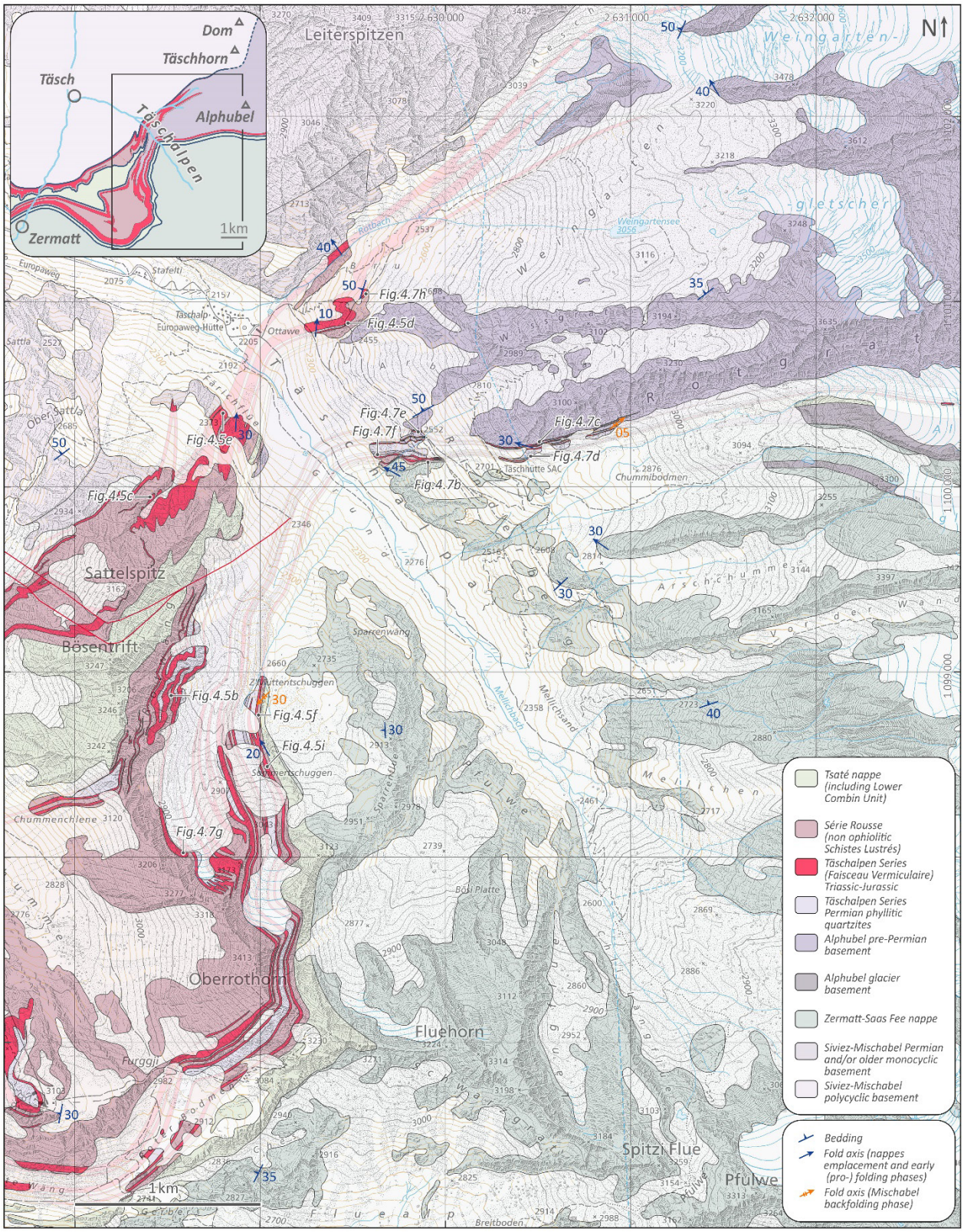

Fig. 4.4 Geological map of the Täschalpen area; after Güller (1947); Bearth (1953a, 1964b, 1967b, 1973); Martin (1982); Escher (1988); Ganguin (1988); Girard (1995); Steck et al. (1999, 2015) and observation from this study; Basemap ©Swisstopo.

On the left (SW) side of the Täschalpen valley, outcrops of pre-Permian basement mark the continuation of the basement fold of the Alphubel (Figs. 4.4, 4.5a). These outcrops are found in particular at the SE extremity of the Färichflüe, and in the Sommertschuggen area (e.g. around the point [2'628'960/1'098'580]; Girard 1995). In the Sommertschuggen area, the pre-Permian basement forms the core of a thin and extremely stretched isoclinal anticline and is surrounded by Permian phyllitic quartzites and Mesozoic metasediments of the Täschalpen Series and the Série Rousse. Several other similar thin and stretched anticlines are visible throughout the left side of the valley, between the east face of the Oberrothorn and the north face of the Sattelspitz (Figs. 4.4, 4.5a). Most of their anticlinal cores are formed by Permian phyllitic quartzites (e.g. Fig. 4.5b). These stretched isoclinal anticlines constitute most likely frontal digitations of the Alphubel fold. Observations of the hinges associated to these folds show that they are coeval with the dominant schistosity (e.g. Fig. 4.5e).

Fig. 4.5 a Structure of the Faisceau Vermiculaire, Série Rousse and Alphubel basement in the Täschalpen area. Isoclinal folds affecting the Permian-Jurassic levels of the Faisceau Vermiculaire (Täschalpen Series), the Série Rousse and the Tsaté nappe are visible in the south-east faces of the Oberrothorn and Bösentrift and in the north face of Sattelspitz. These folds are in turn refolded by open to tight folds of the Mischabel phase showing asymmetric "z" geometries compatible with the overturned limb of the Mischabel backfold (visible in the background). Picture taken from the base of the Alphubel glacier [2'631'860/1'100'270]. A_B: Alphubel pre-Permian basement; *Ba*: Barrhorn Series (Siviez-Mischabel Mesozoic); *LC*: Lower Combin Unit; SM_B: Siviez-Mischabel basement; *SR*: Série Rousse; *ZS*: Zermatt-Saas Fee nappe; b-l: location of next pictures. **b** Hectometric fold of the Bösentrift east face showing an interference pattern between early isoclinal folds (blue) and later close to tight lower amplitude folds attributed to the Mischabel phase (orange). Asymmetric "z" geometries of the folds are compatible with the overturned limb of the Mischabel backfold (cf. Fig. a). **c** Enlargement of Fig. a (Sattelspitz N face) highlighting folds of the Mischabel phase affecting the light-colored early phase isoclinal anticline formed by the metasediments of the Täschalpen Series. **d** Isoclinal early phase anticline at Täschalpen [2'629'450/1'100'880] showing a core of Permian quartzschists surrounded by Triassic and Jurassic carbonates of the Täschalpen Series and calcschists of the Série Rousse; the dominant schistosity is parallel to the axial plane. **e** Early phase isoclinal folds hinges in tabular quartzites at Täschalpen [2'628'800/1'100'380]. **f** Open to tight folds affecting basal levels of the Série Rousse in the Z'Muttentschuggen area [2'629'000/1'098'760]. Contrary to the early phase isoclinal folds of Figs. d and e, no penetrative schistosity is visible parallel to the axial surfaces of these folds, only a poorly developed crenulation can be distinguished locally. Asymmetric "z" geometries of the folds are compatible with the overturned limb of the Mischabel backfold. **g** Open fold of the Mischabel phase affecting limestones of the Faisceau Vermiculaire in the area of the hinge of the Mischabel backfold; Schusslauinen [2'624'000/1'098'100]. Slickensides can be observed in the bedding (+ dominant schistosity) surfaces on both limbs of the fold, they show opposite sense between the two limbs and are indicative of flexural slip folding mechanism; location on Fig.4.1. **h** Slickensides from the vertical limb of the fold in Fig. g. **i** Limestone clast from a breccia of the Täschalpen Series deformed as a sigma-clast and indicating a top-N shear sense (associated to the dominant schistosity); the outcrop surface is parallel to the stretching directions of the clasts; Sommertschuggen area [2'629'040/1'098'450]. **j** Early quartz vein parallel to the main schistosity in calcschists of the Série Rousse, showing domino-type boudins indicating a top-NNE shear sense; the outcrop is parallel to the stretching lineation (020/25); Platthorn area [2'622'490/1'099'870]; location on Fig. 4.1. **k** Domino-type boudins in a dolomitic level of marbles from the Faisceau Vermiculaire and indicating a top-NE shear sense. The outcrop is parallel to the stretching lineation (215/10); Theodulhorn [2'620'950/1'088'670]; location on Fig. 4.1. **l** Dolomitic clasts from the base of the Série Rousse (top) and marbles of the Faisceau Vermiculaire (bottom), deformed as sigma-clasts and indicating a top-SE shear sense. The outcrop is parallel to the stretching lineation (310/20); c' shear bands are visible in the same outcrop and indicate a top-SE shear sense as well; Testa Grigia [2'620'860/1'087'040]; location on Fig. 4.1. ►

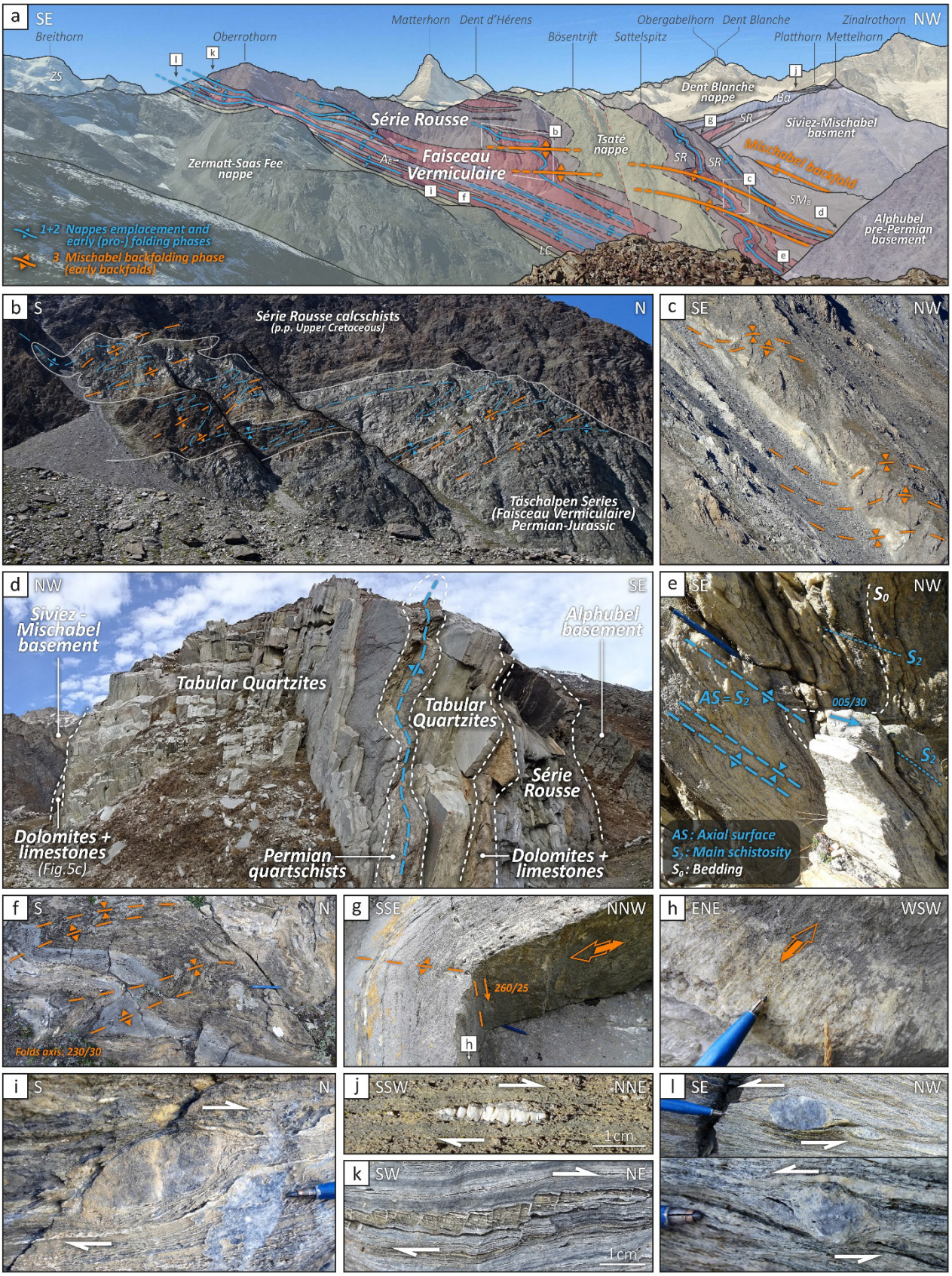
a
SE
NW
Breithorn
Oberrothorn
Matterhorn
Dent d'Hérens
Bösentrift
Obergabelhorn
Sattelspitz
Dent Blanche
Platthorn
Mettelhorn
Zinalrothorn
ZS
Dent Blanche nappe
Série Rousse
Faisceau Vermiculaire
Tsaté nappe
Zermatt-Saas Fee nappe
Siviez-Mischabel basment
Mischabel backfold
Alphubel pre-Permian basement
1+2 Nappes emplacement and early (pro-) folding phases
3 Mischabel backfolding phase (early backfolds)
b
S
N
Série Rousse calcschists
(p.p. Upper Cretaceous)
Täschalpen Series
(Faisceau Vermiculaire)
Permian-Jurassic
c
SE
NW
d
NW
SE
Siviez - Mischabel basement
Alphubel basement
Tabular Quartzites
Tabular Quartzites
Série Rousse
Dolomites + limestones
(Fig.5c)
Permian quartschists
Dolomites + limestones
e
SE
NW
S_0
S_2
$AS = S_2$
005/30
S_2
AS : Axial surface
S_2 : Main schistosity
S_0 : Bedding
f
S
N
Folds axis: 230/30
g
SSE
NNW
260/25
h
ENE
WSW
i
S
N
j
SSW
NNE
1cm
k
SW
NE
1cm
l
SE
NW

Pinched isoclinal folds involving pre-Permian basement, Permian quartzites and Mesozoic metasediments of the Täschalpen Series and of the Série Rousse are also found on the right side of the valley, on both limbs of the Alphubel fold (Fig. 4.4). They are characterized by steeply dipping axial surfaces and are also coeval with the dominant schistosity (e.g. Fi. 4.5d). They are interpreted as second order folds associated to the Alphubel antiform.

These stretched isoclinal folds from the Täschalpen area are refolded by open to tight folds with subhorizontal axial surfaces (e.g. Figs. 4.5a-c) that are not associated with a penetrative schistosity, in contrast with the earlier isoclinal folds. Only a poorly developed cleavage is sometimes observable in the hinges of these later folds, parallel to their axial surfaces (e.g. Fig. 4.5f). These interference patterns are identical to those observed in the hinge zone of the Mischabel backfold. There, early isoclinal folds, which are in continuity with those of Täschalpen, are refolded by open to tight folds of the Mischabel phase, which are also devoid of penetrative schistosity associated to their axial surfaces (Fig. 4.5g). The above-described late open to tight folds of the Täschalpen area, are thus interpreted as equally corresponding to the Mischabel phase. In the slopes between the Oberrothorn and the Sattelspitz, these folds show typical asymmetric "z" geometries (Figs. 4.5a-c, f) that are compatible with geometries expected for second order folds of the overturned limb of the Mischabel backfold.

4.4.3. Phases of deformation at regional scale

The same type of interference patterns between early extremely stretched isoclinal folds coeval to the dominant schistosity and later folds associated to the Mischabel phase are recognized in the Faisceau Vermiculaire and in the surrounding Schistes Lustrés, in the whole upper Matter valley (e.g. Fig. 4.6; Mazurek 1986; Sartori 1987; Steck 1989; Lebit et al. 2002; Bucher et al. 2004a; Steck et al. 2015) and in the northern Aosta valley (e.g. Vannay and Allemann 1990; Bucher et al. 2004a; Pleuger et al. 2007, 2008).

The folds associated to the Mischabel phase show a WSW-ENE mean axial direction, while most of the measured directions are comprised between SW-NE and SE-NW (Fig. 4.6; Steck 1989; Vannay and Allemann 1990). Early isoclinal folds, associated to the dominant schistosity, show more variable axial directions. NW-SE to N-S axial directions are frequent for these folds (Fig. 4.6; Steck 1989), and could possibly correspond to their original dominant orientation, while directions parallel to those of the Mischabel phase could represent later local reorientations. Stretching directions associated to the early isoclinal folds and the dominant schistosity show a mean NNW-SSW orientation.

Early folds associated to the dominant schistosity are systematically isoclinal throughout the study area. The geometries of the folds associated to the Mischabel phase, affecting the Faisceau Vermiculaire, are much more variable. Open folds associated to the Mischabel phase, showing slickensides indicative for flexural slip folding mechanism (Figs. 4.5g-h), are observed in the cascade of disharmonic folds affecting the Faisceau Vermiculaire, directly south of the basement hinge of the Mischabel backfold. Southward, further away from the hinge zone, geometries of the folds associated to the Mischabel phase progressively evolve to tight folds, showing a semi-ductile deformation style, with slightly bent or kinked micas and nucleation of secondary quartz, calcite and chlorite, but without development of a penetrative schistosity (Mazurek 1986). In southern part of the area, where the Combin zone s.l. is pinched between the Sesia zone and the Zermatt-Saas Fee and Monte Rosa nappes, folds associated to the Mischabel phase evolve to isoclinal folds (e.g. Müller 1983; Mazurek 1986; Steck et al. 2015).

A second phase of backfolding, subsequent to the Mischabel phase, affected the whole nappe stack of the Pennine Alps. It resulted in the formation of the crustal-scale Vanzone antiform, which axial trace runs through the southern Monte Rosa nappe (e.g. Argand 1911; Milnes et al. 1981; Steck et al. 2015). In the area surrounding Zermatt, macroscopic structures associated to

the Vanzone phase are inconspicuous at the outcrop scale. Late kink folds from the Täschalpen area are attributed to this phase by Müller (1983). The main effect of the Vanzone phase in the area of Täschalpen and Zermatt consists of a major tilting of the structures towards the NW.

Fig. 4.6 Structure of the Faisceau Vermiculaire and surrounding units around Zermatt. Bedrock map compiled after Argand (1908), ► Güller (1947), Bearth (1953a, 1964b, 1967a, 1973), Wilson (1978), Martin (1982), Crespo (1984), Sartori (1987), Ganguin (1988), Girard (1995), Steck et al. (1999, 2015), Bucher et al. (2003a) and observations from this study.

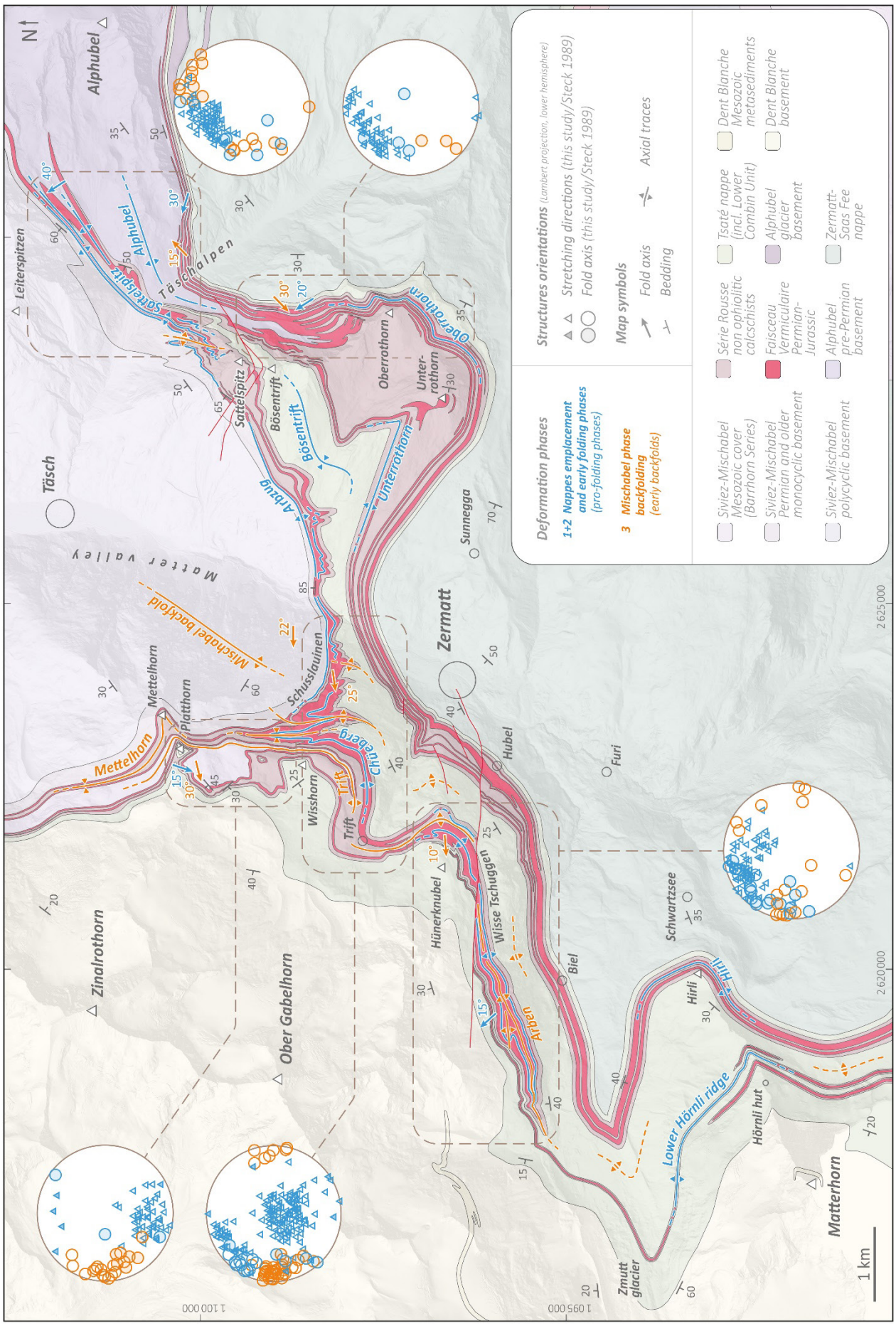
N
Alphubel
Leiterspitzen
Täschalpen
Alphubel
Sattelspitz
Sattelspitz
Bösentrift
Bösentrift
Oberrothorn
Unterrothorn
Oberrothorn
Unterrothorn
Täsch
Matter valley
Alphubel
Sunnegga
Zermatt
Mischabel backfold
Schussiaui
Mettelhorn
Platthorn
Mettelhorn
Trift
Trift
Chiebergg
Wisshorn
Hubel
Furi
Hünerknubel
Wisse Tschuggen
Biel
Schwartzsee
Hirli
Hirli
Zinalrothorn
Ober Gabelhorn
Arbola
Lower Hörnli ridge
Hörnli hut
Matterhorn
Zmutt glacier
1 km
Structures orientations (Lambert projection, lower hemisphere)
Stretching directions (this study/Steck 1989)
Fold axis (this study/Steck 1989)
Map symbols
Fold axis
Axial traces
Bedding
Deformation phases
1+2 Nappes emplacement and early folding phases (pro-folding phases)
3 Mischabel phase backfolding (early backfolds)
Série Rousse non ophiolitic calcschists
Tsaté nappe (incl. Lower Combin Unit)
Dent Blanche Mesozoic metasediments
Faisceau Vermiculaire Permian-Jurassic
Alphubel glacier basement
Dent Blanche basement
Alphubel pre-Permian basement
Zermatt-Saas Fee nappe
Siviez-Mischabel Mesozoic cover (Barrhorn Series)
Siviez-Mischabel Permian and older monocyclic basement
Siviez-Mischabel polycyclic basement
2 625 000
2 620 000
1 095 000
1 100 000

4.4.4. Macroscopic shear sense indicators

Macroscopic markers indicating local shear sense are frequently observed in the metasediments of the Faisceau Vermiculaire and of the Série Rousse across the whole studied area. They mainly consist of rigid objects such as dolomitic clasts deformed within a more viscous matrix (made e.g. of calcschists or limestones) and of c'-type shear bands, systematically observed in sections oriented perpendicular to the schistosity and parallel to the stretching direction (deduced e.g. from the stretching direction of the clasts or from strain shadows).

In the Faisceau Vermiculaire, the Série Rousse and the directly surrounding units, stretching directions associated to the dominant schistosity, although showing some dispersion, are mostly oriented NW-SE to N-S throughout the upper Matter valley and northern Aosta valley (Fig. 4.6; Steck 1989; Reddy et al. 2003; Pleuger et al. 2007; Steck et al. 2015; Kirst 2017; Kirst and Leiss 2017).

Shear senses deduced from macroscopic markers in the Faisceau Vermiculaire and the Série Rousse are, however, not constant across this area. In the sector of the Täschalpen, observed markers constantly indicate a top-N(NW) shear sense (e.g. Fig. 4.5i). The same shear sense is also observed in different sector between Zermatt and the Platthorn (e.g. Fig. 4.5j; top-NNE shear sense), further south in the Theodulhorn (Fig. 4.5k; top-NE shear sense), and locally in the continuation of the Série Rousse north of the Dent Blanche klippe (e.g. Fig. 3.9e). In the sector of Testa Grigia (Fig. 4.1), the observed shear-sense markers all indicate top-SE shearing (e.g. Fig. 4.5l). A top-SE shear sense is also reported by Reddy et al. (2003) in the Cime Bianche unit in Valtournenche. Top-S macroscopic shear indicators are also reported by Scheiber et al. (2013) in the NW continuation of the Faisceau Vermiculaire (Frilihorn Series) in the Anniviers valley. Kirst and Leiss (2017) report both top-NW and top-SE macroscopic

shear sense markers for calcschists from the Combin zone, surrounding the Faisceau Vermiculaire, in the Lago di Cignana area.

These few data concerning macroscopic shear sense markers clearly indicate that such data are difficult to interpret when not associated to detailed structural studies at both microscopic and macroscopic scales. Such detailed studies have been carried in different sectors of the Faisceau Vermiculaire and surrounding units, for example by Reddy et al. (2003), Pleuger et al. (2007, 2009), Kirst and Leiss (2017). The results of these studies are discussed in chapter 4.6.3.

4.5. Contacts of the Faisceau Vermiculaire with the surrounding units between Täschalpen and Zermatt

In the area between the Täschalpen and Zermatt, the different bands forming the Faisceau Vermiculaire alternately rest in contact with different units: with the Permian and older monocyclic basement of the Siviez-Mischabel nappe in the northern part of the area; with the pre-Permian basement forming the Alphubel fold (or Alphubel Lappen; cf. chap. 4.4.2) to the east; and with the ophiolitic units (Zermatt-Saas Fee nappe / Lower Combin Unit) to the south of the zone. In addition, an important syncline formed of calcschists and ophiolites of the Tsaté nappe (Bösentrift syncline; Fig. 4.6) penetrates between the bands of the Faisceau Vermiculaire from the west. We detail below our observations concerning the contacts of the Faisceau Vermiculaire with each of these units.

4.5.1. Contacts of the Faisceau Vermiculaire with the ophiolitic units

According to our observations, the Permian to Jurassic metasediments of the Faisceau Vermiculaire are never in direct contact with the ophiolites in this area. They are systematically separated by at least a few meters to several tens of meters of non-ophiolitic calcschists of the Série Rousse. It is the case both within the Bösentrift syncline (Fig. 4.6; e.g. SW of Färichflüe,

Fig. 4.4) and below the southernmost band of the Faisceau Vermiculaire, which is outcropping close to the contact with the Zermatt-Saas Fee eclogites (e.g. Sommertschuggen and NW-Rinderberg areas; Figs. 4.4, 4.7a-b).

In this last locality, metabasalts devoid of eclogite-facies imprint are also intercalated between the Faisceau Vermiculaire (and underlying Série Rousse) and the eclogite-facies ophiolites and calcschists of the Zermatt-Saas Fee nappe. These metabasalts have been described by Cartwright and Barnicoat (2002), who attributed them to the Combin zone. According to these authors, they show a relict blueschist facies mineralogy, composed of mm-sized garnet porphyroblasts, blue-green amphiboles, Ca-rich clinozoisite, paragonite and probable pseudomorphs after lawsonite (corresponding to a P-T estimate of 451 ± 23 °C and 1240 ± 38 MPa), strongly retrogressed to greenschist facies assemblages. Compared to the underlying eclogites of the Zermatt-Saas Fee nappe (for which P-T estimates of 591 ±39 °C at 1820 ± 190 MPa and 577 ± 47 °C at 1760 ± 220 MPa were obtained), the relict blueschist facies assemblage of the above-described metabasalts differ by the notably less sodic composition of the amphiboles and the absence of omphacite (Cartwright and Barnicoat 2002). Our observations show that, only a few meters away from these non-eclogitic metabasalts, in the other side of a small valley covered by Quaternary deposits, garnet porphyroblasts up to 1 cm size are abundant in the calcschists forming the south side of this depression (e.g. at point [2'629'980/1'100'130]). As cm-sized garnet porphyroblasts are frequent within calcschists and metabasites of the Zermatt-Saas Fee nappe (e.g. Bearth 1967a; Cartwright and Barnicoat 2002; Bucher et al. 2005), while garnets are rarely observed in the Tsaté nappe (Combin zone s.str.) and generally do not exceed 1 mm in diameter (e.g. Burri et al. 1999; Bucher et al. 2004a; Manzotti et al. 2021), we attribute the calcschists of the southern side of this small valley to the Zermatt-Saas Fee nappe and place the upper contact of this unit along this depression (Figs. 4.4, 4.7a-b). This interpretation is supported by

the occurrence of eclogite-facies metabasalts in the directly surrounding area described by Cartwright and Barnicoat (2002).

Metabasalts devoid of eclogitic imprint, associated with calcschists, have also been described in a same tectonic position, east of Roter Bodmen, by Bearth (1973), and later by Girard (1995), in the whole area between Roter Bodmen and Sommertschuggen (topographic names indicated in Fig. 4.4). These metabasalts are located in the direct prolongation of those studied by Cartwright and Barnicoat (2002) at Rinderberg, also in a position between the lowermost band of the Faisceau Vermiculaire and the eclogite-facies metabasites and associated lithologies of the Zermatt-Saas Fee nappe. In contrast with the metabasalts outcropping in a lower position in the Zermatt-Saas Fee nappe, these metabasalts (prasinites) are characterized by a clearer, green color, the absence of omphacite and the scarcity of garnets, Na-amphiboles and pseudomorphs after lawsonite (Girard 1995).

As these metabasalts devoid of eclogitic imprint from the Täschalpen and Oberrothorn areas show an identical tectonic position and very similar parageneses and metamorphic imprint to that of the Lower Combin Unit, evidenced and described in the Valtournenche and Ayas valley (Ballèvre et al. 1986; Cortiana et al. 1998; Bucher et al. 2004a; Dal Piaz et al. 2015b; Passeri et al. 2018), we propose to attribute these metabasalts and associated calcschists from the upper Matter valley to this Lower Combin Unit. Further investigations are required to confirm the continuity of this unit between the upper Valtournenche and Oberrothorn areas.

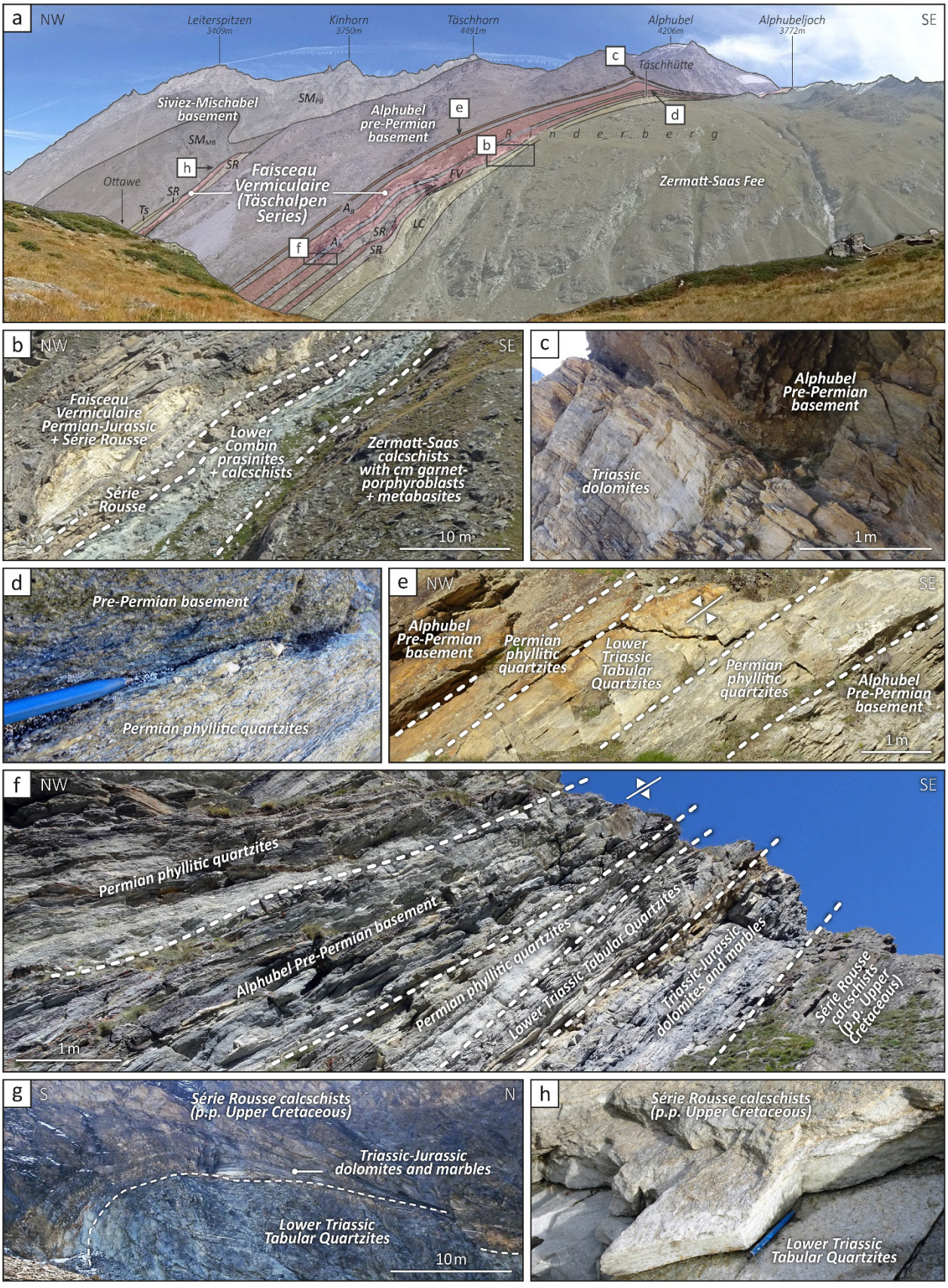
a
NW
SE
Leiterspitzen
3409m
Kinhorn
3750m
Täschhorn
4491m
Alphubel
4206m
Alphubeljoch
3772m
Täschhütte
Siviez-Mischabel basement
Alphubel pre-Permian basement
Faisceau Vermiculaire (Täschalpen Series)
Zermatt-Saas Fee
Ottawe
b
NW
SE
Faisceau Vermiculaire Permian-Jurassic + Série Rousse
Lower Combin prasinites + calcschists
Zermatt-Saas calcschists with cm garnet-porphyroblasts + metabasites
Série Rousse
10 m
c
Alphubel Pre-Permian basement
Triassic dolomites
1m
d
Pre-Permian basement
Permian phyllitic quartzites
e
NW
SE
Alphubel Pre-Permian basement
Permian phyllitic quartzites
Lower Triassic Tabular Quartzites
Permian phyllitic quartzites
Alphubel Pre-Permian basement
1m
f
NW
SE
Permian phyllitic quartzites
Alphubel Pre-Permian basement
Permian phyllitic quartzites
Lower Triassic Tabular Quartzites
Triassic-Jurassic dolomites and marbles
Série Rousse calcschists (p.p. Upper Cretaceous)
1m
g
S
N
Série Rousse calcschists (p.p. Upper Cretaceous)
Triassic-Jurassic dolomites and marbles
Lower Triassic Tabular Quartzites
10m
h
Série Rousse calcschists (p.p. Upper Cretaceous)
Lower Triassic Tabular Quartzites

◄ **Fig. 4.7** Contacts of the Faisceau Vermiculaire Permian-Jurassic series (Täschalpen Series) with the Alphubel Pre-Permian basement, the Série Rousse calcschists and the Lower Combin Unit in the Täschalpen area. **a** Right (NE) side of the Täschalpen valley; picture from Z'Muttentschuggen area; geological limits after Güller (1947), Bearth (1964b), Steck et al. (1999) and data from this study; A_B: Alphubel Pre-Permian basement; *FV*: Faisceau Vermiculaire Permian-Jurassic Series (Täschalpen Series); *LC*: Lower Combin Unit (Tsaté nappe); SM_{MB}: Siviez-Mischabel monocyclic basement; SM_{PB}: Siviez-Mischabel polycyclic basement; *SR*: Série Rousse calcschists; *Ts*: Tsaté nappe; b-h: location of next pictures. **b** Lower contact of the Faisceau Vermiculaire in the Rinderberg area, on top of the Lower Combin Unit and underlying Zermatt-Saas Fee nappe. **c** Sharp contact between Alphubel Pre-Permian albitic gneisses and Triassic dolomites of the Täschalpen; Täschhütte area [2'630'510/1'100'250]. **d** Contact between Pre-Permian albitic gneisses of the Alphubel basement and Permian phyllitic quartzites forming the base of the Täschalpen Series; Täschhütte area [2'630'440/1'100'150]. **e** Syncline formed by Lower Triassic Tabular Quartzites of the Täschalpen Series, stratigraphically surrounded on both sides by Permian phyllitic quartzites and Pre-Permian albitic gneisses of the Alphubel basement; Rinderberg [2'629'860/1'100'300]. **f** Pinched anticlinal core of Pre-Permian Alphubel albitic gneisses surrounded by Permian phyllitic quartzites and showing to the right, a stratigraphic sequence (tectonically overturned) with Lower Triassic Tabular Quartzites, Triassic-Jurassic dolomites and marbles, and calcschists of the Série Rousse (p.p. Upper Cretaceous); Rinderberg [2'629'610/1'100'170]. **g** Anticlinal hinge showing a preserved stratigraphic sequence between Lower Triassic Tabular Quartzites, thin Triassic-Jurassic dolomites and marbles, and Série Rousse calcschists; Rotwäng [2'628'560/1'098'050]. **h** Contact between Série Rousse calcschists (p.p. Upper Cretaceous) and the Lower Triassic Tabular Quartzite of the Täschalpen Series; Bru area [2'629'560/1'101'040].

4.5.2. Contacts of the Faisceau Vermiculaire with the Siviez Mischabel basement in the hinge of the Mischabel backfold

The Faisceau Vermiculaire (and associated Série Rousse) are in direct contact with the Permian and older monocyclic basement forming the hinge of the Mischabel backfold from the Mettelhorn to the Rotbach valley, NE of Täschalpen (Figs. 4.4, 4.6; Güller 1947; Bearth 1964a, b; Sartori 1987). Throughout this area, the contact is mostly covered by Quaternary deposits, from which only patches of intensely strained carbonates and cornieules are emerging. Only a few outcrops allow detailed observations of the contact. They were described by Staub (1942d) and particularly by Güller (1947) who highlighted the tectonic nature of the contact, characterized by intense strain, the presence of a plurimeter thick level of crushed carbonates and cornieules, and locally by the direct contact between an overturned stratigraphic sequence of the Faisceau Vermiculaire Triassic levels and the Permian and older monocyclic basement forming the hinge of the Mischabel backfold. The first descriptions of this contact by Argand (1909, 1916a), actually already mention the "abnormal" nature of this contact and refer to the Faisceau Vermiculaire as "detached" from the Grand Saint Bernard nappe. Our observations confirm this interpretation, which was equally adopted and confirmed by e.g. Iten (1948), Sartori (1987), Escher (1988) and Steck et al. (2015).

Moreover, the Faisceau Vermiculaire is clearly distinct from the Mesozoic cover of the Siviez-Mischabel nappe (the Barrhorn Series), which extends to the Wisshorn and Trift area (Fig. 4.6), north of Zermatt. They are distinct by both the nature of the contact with the Paleozoic basement and the stratigraphy of the series (e.g. Staub 1942d; Güller 1947; Sartori 1987, 1990; Steck et al. 2015). This last point is discussed in chapter 4.6.5.

4.5.3. Contact of the Faisceau Vermiculaire with the basement forming the Alphubel fold (Alphubel basement)

The contact of the Faisceau Vermiculaire and the Série Rousse with the pre-Permian basement forming the Alphubel fold (or Alphubel Lappen; cf. chap. 4.4.2) is exposed on both limbs of this fold in the NE side of the Täschalpen valley, as well as in SE-Färichflüe and Sommertschuggen areas, in the SW side of the valley (Figs. 4.4, 4.7).

Contrary to the contact with the Permo-Carboniferous metasediments forming the hinge of the Mischabel backfold described above, this contact does not show uniform or constant characteristics across the area and, in particular, various lithologies of the Faisceau Vermiculaire and the Série Rousse are alternately observed in direct contact with the Alphubel Pre-Permian basement. For example, a direct and sharp contact, between the Pre-Permian basement and levels of Triassic dolomites from the Faisceau Vermiculaire, is visible NW of Rinderberg, at point [2'629'870/1'100'250], and is well exposed in the slopes above the Täsch hut (Fig. 4.7c). Crushed carbonates and cornieules are in turn in direct contact with the same basement a few hundred meters further east (e.g. [2'630'820/1'100'320], [2'630'850/1'100'300]). This pre-Permian basement is instead in contact with the Série Rousse calcschists in the SE of Färichflüe (Fig. 4.4), and at Bru (Sartori et al. 1989; e.g. around the point [2'629'510/1'100'860], although the exact contact is masked by Quaternary deposits in this area). Sharp contacts with phyllitic quartzschists (Permian) are also visible in several locations (e.g. Fig. 4.7d). The discordant character of this contact, as well as the contrast between the large amount of outcrops of pre-Permian basement

in the NE side of the Täschalpen valley and their scarcity in the SW side of the valley, which is dominated by calcschists, lead to interpret this contact as tectonic (Güller 1947; Bearth 1964b; Martin 1982; Sartori et al. 1989).

Further observations however show that the contact of the Alphubel pre-Permian basement with the Faisceau Vermiculaire (and the Série Rousse) locally appears as concordant, i.e. showing a lithological succession characteristic of a continuous stratigraphic sequence. This is for example the case NW of Rinderberg (Fig. 4.7e), where a level of Tabular Quartzites (1.5 m thick) shows progressive contacts on both sides with phyllitic quartzites and Verrucano-facies quartzites (0.5-1.5 m thick), which show in turn, unsheared contacts with the pre-Permian basement visible on both sides of the outcrop. As all the contacts observed in this outcrop appear as stratigraphic, this succession is interpreted as a pinched isoclinal syncline with a core belonging to the Faisceau Vermiculaire (Täschalpen Series) and a rim formed by the Alphubel pre-Permian basement. Another lithological succession outcropping at the base of the cliffs, NW of Rinderberg (Fig. 4.7f), shows a 2 m thick level of pre-Permian basement (gneisses and albitic Paleozoic metabasites), surrounded on both sides by Permian phyllitic quartzites. To the right, these phyllitic quartzites (~ 1 m thick) progressively turn to pure Tabular Quartzites attributed to the Early Triassic (~ 1 m thick), which are in contact with dolomites and marbles (Triassic-Jurassic; ~ 2 m thick), which in turn, surmount several meters of non-ophiolitic calcschists of the Série Rousse (p.p. Upper Cretaceous). Like for the previous outcrop, all the contacts are clean, do not show particular shearing and appear as stratigraphic. This outcrop thus most likely corresponds to an anticline, whose core is formed by a pinched level of Alphubel pre-Permian basement and whose overturned (right) limb is formed by the Täschalpen Series and the Série Rousse. The lithological succession exposed on this outcrop would then correspond to a stratigraphic sequence extending at least from the Upper Paleozoic to the Upper Cretaceous.

The contact between the Alphubel pre-Permian basement and the Faisceau Vermiculaire is therefore characterized by a large-scale unconformity, and shows both discordant sections (where various levels are juxtaposed across the contact, without chronological continuity), and local concordant sections, where lithological successions across the contact appear as chronologically continuous and stratigraphic. The interpretation of these seemingly contradictory observations is discussed below.

4.6. Discussion

4.6.1. Nature of the contact between the Faisceau Vermiculaire (and Série Rousse) with the Alphubel basement

Different outcrops exposing the contact between the Faisceau Vermiculaire (Permian-Jurassic Täschalpen Series) and the pre-Permian basement forming the Alphubel fold (e.g. Figs. 4.7c-f) show that this contact, at least locally, was not affected by an intense Alpine shearing, as it would be expected along a major tectonic contact separating two different tectonic units (which corresponds to the interpretation of most of the authors; this contact even corresponds to the limit between two tectonic domains, according to several authors; cf. chap. 4.2). Clean contacts, devoid of particular shearing and appearing as stratigraphic, are actually locally observable between: (i) the pre-Permian basement and the Permian phyllitic quartzites (e.g. Figs. 4.7d-e); (ii) these phyllitic quartzites and the pure Tabular Quartzite (e.g. Figs. 4.3c, 4.5d, 4.7e-f); (iii) the Tabular Quartzite and the Triassic dolomites (e.g. Figs. 4.3i, 4.7f-g); (iv) these dolomites and the Triassic-Jurassic marbles and breccias (e.g. Figs. 4.3b, 4.7f); and finally (v), between different levels of the Täschalpen Series and the Série Rousse (e.g. Figs. 4.3i, 4.3k, 4.7f, 4.7h; cf. chap. 4.3.2). No intercalation of ophiolite-bearing calcschists or of ophiolites is observable along this contact. These different local observations are very unlikely to be compatible with a large detachment and translation of both the Täschalpen Series and

the Série Rousse, with respect to the Alphubel pre-Permian basement. The occurrence of local lithological successions appearing as concordant and stratigraphic across the contact, as described in the previous chapter (4.5.3; Figs. 4.7d-f), corroborate this interpretation.

This contact is, however, marked by a large-scale unconformity, and along the contact, both discordant and concordant sections (in a stratigraphic point of view) are alternately observable (cf. chap. 4.5.3). As discussed in chapters 2 and 3 of the present manuscript, for contacts affecting the Mont Fort nappe in the Bagnes, Dix and Hérens valleys, such a configuration could be properly explained if the contact locally corresponds to synsedimentary paleofaults. The discordant sections of the contact would then represent the paleofaults themselves, while the concordant sections would represent preserved stratigraphic successions from the footwalls and hanging walls.

Our observations in the Täschalpen area are compatible with this interpretation. In particular, the levels of coarse polymict breccia observed in the Täschalpen Series (e.g. Figs. 4.3e-h), containing clasts up to several tens of cm made of various lithologies most probably ranging from Permian to Lower Jurassic, are actually indicative of a deposition at the immediate vicinity of high amplitude active faults. The similarities existing between these breccias and those of the Breccia nappe in the Prealps (whose ages range from Sinemurian to Early Tithonian; e.g. Chessex 1959; Weidmann 1972; Stampfli and Marthaler 1990; Plancherel et al. 1998), both in term of facies and of stratigraphic position (cf. chap. 4.3.1.3), suggest a Jurassic age for the main activity of these paleofaults. The presence of Jurassic high amplitude normal paleofaults (e.g. Fig. 4.8a) could explain not only the unconformity observable at the contact between the Täschalpen Series and the Alphubel pre-Permian basement, but also the unconformity that can be evidenced at the base of the Série Rousse in this area. Indeed, the Série Rousse alternately rests on different levels of the Täschalpen Series (e.g. on Triassic to Jurassic carbonates in Figs. 4.3i, 4.7f-g; and on

Lower Triassic Tabular Quartzite in Fig. 4.7h), although its basal contact clearly appears as stratigraphic (cf. chap. 4.3.2). Considering a margin geometry such as the one outlined in Fig. 4.8a, the stratigraphic deposition of the Série Rousse directly on top of the Lower Triassic Tabular Quartzite (e.g. Fig. 4.7h) could represent a stratigraphic sequence typical of the upper parts of tilted blocks. The same stratigraphic sequence is observed, for example, in the Mont Fort nappe, east of Evolène (Rocs de Villa succession; Fig. 3.12).

Other observations from the Täschalpen area, concerning the relative thicknesses of the limbs of early isoclinal folds affecting the Täschalpen Series, can also be explained considering the presence of synsedimentary normal faults. Different outcrops in the area show early folds, coeval to the dominant schistosity, which are characterized by thicker sedimentary successions in their (original) overturned limbs than in their (original) normal limbs (e.g. Fig. 4.5a; and the asymmetrical anticline with the core formed of Permian quartzschist around point [2'628'920/1'100'340] in Färichflüe, Fig. 4.4; as these folds were later overturned during the Mischabel phase, their original normal limbs are now overturned, and inversely). As layers are generally thinner in the overturned limbs of folds due to the more intense stretching, the observation of those thicker (original) overturned limbs may seem counterintuitive. Such fold geometries are however likely to result from the folding of a sequence affected by synsedimentary faults, when fold hinges develop close to the summit of tilted blocks, with axial surfaces subparallel to the paleofaults (Fig. 4.8; e.g. Dolivo 1982; Epard 1990; Krayenbuhl and Steck 2009; Bellahsen et al. 2012; Boutoux et al. 2016).

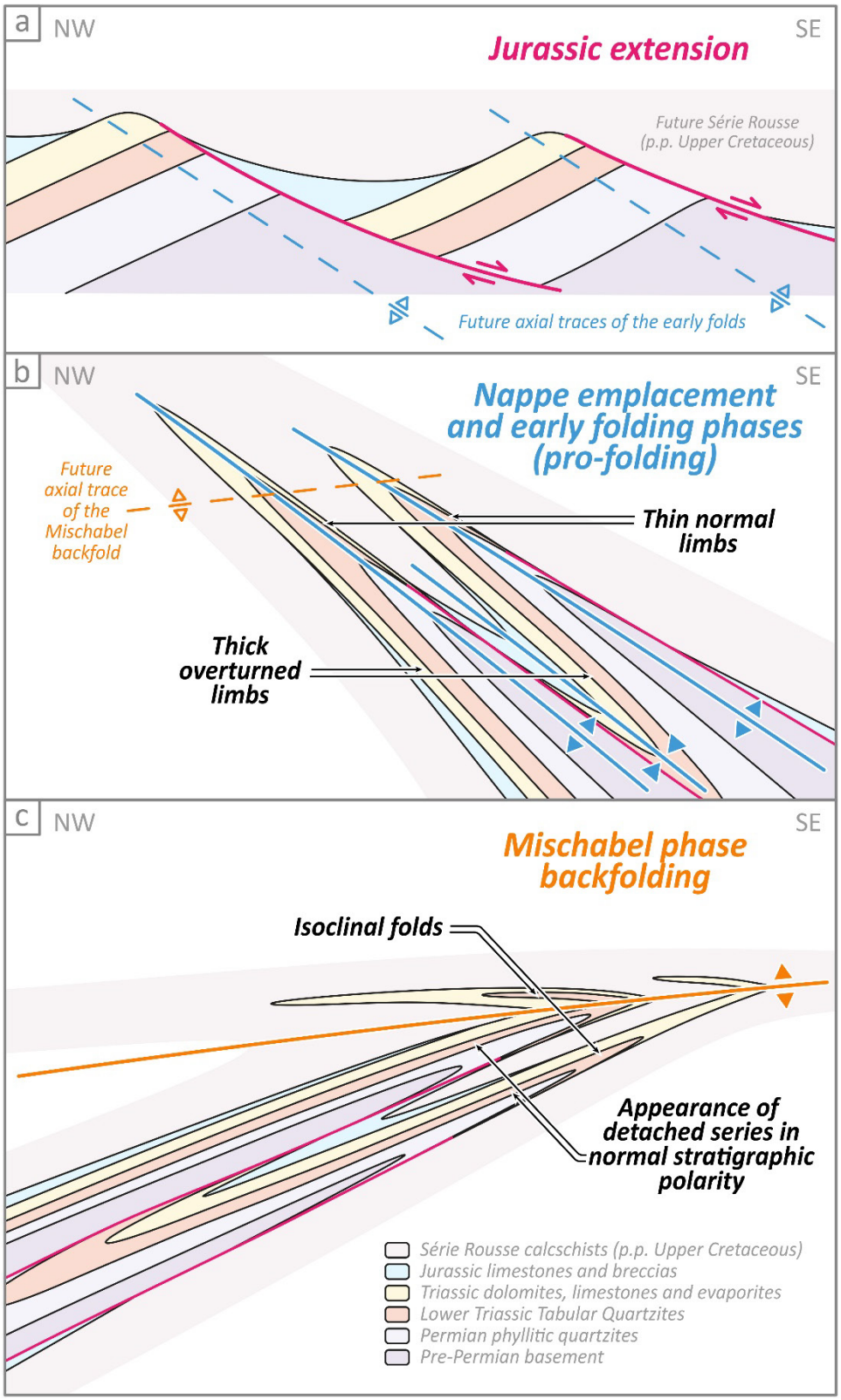

Fig. 4.8 Schematic sketches representing the polyphase folding of an initial configuration consisting of tilted blocks and half-grabens, in order to illustrate the different structures observed in the Faisceau Vermiculaire between the Täschalpen and Cimes Blanches areas. **a** In the proposed model, hinges of the early pro-vergent folds are localized within the summit zones of the tilted blocks. **b** Folds resulting from such an initial configuration would be strongly asymmetrical, with thicker sedimentary successions in the overturned limbs (which may seem counterintuitive, as the layers are generally thinner in the overturned limb of the folds due to the more intense stretching). **c** Due to the polyphase deformation and the assumed asymmetry of the early folds, the resulting configuration of the inverted limb of the backfold may be confused with a detached (thrusted) series showing a normal polarity, while the isoclinal nature of the early folds is clearly recognizable when looking at the area of their frontal hinges.

According to these observations, the Täschalpen Series would thus most likely constitute the autochthonous sedimentary cover, of the pre-Permian basement forming the Alphubel anticline. As all the different bands forming the Faisceau Vermiculaire seem to have direct connections with those of the Täschalpen Series (Figs. 4.1, 4.6), the Alphubel anticline (and its potential western extension at depth under the Combin zone) could thus correspond to the root zone of the whole Faisceau Vermiculaire series.

There are, however, some caveats regarding this hypothesis. (i) It is not possible to exclude a more eastern (and/or internal) origin than the Alphubel basement for the two lowermost anticlines involving the Täschalpen Series and cores of pre-Permian basement. Indeed, the existence of potential synclinal hinges connecting these two lowermost anticlines to the Alphubel basement cannot be attested due to the presence of Quaternary deposits and glaciers covering the contacts, east of Täschalpen (Fig. 4.4). These two anticlines could thus be linked either to the Alphubel basement or be linked to (or derived from) more internal units, such as the Gornergrat, Stockhorn or Portjengrat, for example. (ii) Some outcrops partly formed by highly stretched continental basement are found east of the Täschalpen in the border of the Alphubel glacier, out of the studied zone (they are referred to as Alphubel glacier basement on Fig. 4.4). As these outcrops have never been studied in detail, and as their contacts with the surrounding units are mostly hidden by the ice and moraines, their tectonic position and relations with the surrounding units are unclear. Their tectonic position however seems to be structurally lower than that of the basement forming the Alphubel anticline (and that of the Faisceau Vermiculaire), and appears to be located at the top, or within, the Zermatt-Saas Fee nappe. Such a position could correspond to that of, for example, the Etirol-Levaz, Châtillon, and/or Theodul Glacier units (e.g. Kienast 1983; Ballèvre et al. 1986; Dal Piaz 1999; Dal Piaz et al. 2001, 2015a; Weber and Bucher 2015; Fassmer et al. 2016; Bucher et al. 2020; Bucher and Stober 2021).

4.6.2. Relations between the Alphubel basement and the Siviez-Mischabel nappe

Based on the above observations and discussions, the metasediments of the Faisceau Vermiculaire and the Série Rousse thus appear to be in stratigraphic contact with the pre-Permian basement forming the Alphubel anticline (chaps. 4.5.3, 4.6.1), but in tectonic contact with the Permian and older monocyclic basement forming the hinge of the Mischabel backfold (chap. 4.5.2). In turn, the Permian metasediments of the Siviez-Mischabel nappe are stratigraphically overlaid by the Mesozoic Barrhorn Series on the normal limb of the Mischabel backfold, from the area of Hohlicht (Figs. 4.1, 4.2; Steck et al. 1999), to the north of the Barrhorn summits (Fig. 4.1; Sartori 1990).

Important stratigraphic differences are observable between the Barrhorn Series and the series formed by the Faisceau Vermiculaire and Série Rousse succession. These differences, already noted by Staub (1942d), Güller (1947) and Bearth and Schwandler (1981), mainly concern (i) the presence in the Faisceau Vermiculaire of locally abundant breccias and limestone levels reminiscent of the Lower Jurassic facies of the Prepiemont and Austroalpine series, whereas such lithologies are almost absent in the Barrhorn Series; and (ii) the differences between the younger levels of the Barrhorn Series and the Série Rousse, as quartzitic calcschists reminiscent of those of the Série Rousse are almost absent in the Barrhorn Series, whereas the metamorphic equivalent of the Couches Rouges of the Prealps and the dark Eocene Flysch, which form the upper part of the Barrhorn Series (e.g. Ellenberger 1953; Sartori 1990), do not seem to be represented in the Série Rousse. These stratigraphic differences in the post-Triassic sequences between the Barrhorn Series and the sequence formed by the succession of the Faisceau Vermiculaire and Série Rousse are too important to represent lateral facies changes inside a continuous sedimentary basin.

In its present position, the basement forming the Alphubel anticline could be separated from that forming the hinge of the Mischabel backfold by an important tectonic discontinuity. Indeed, the complex Rotbach syncline (Steck 1989; cf. chap. 4.4.2), anterior to Mischabel backfolding phase

and involving ophiolites of the Tsaté nappe, is deeply embedded between these two basements structures. The amplitude of this discontinuity is however difficult to assess, as the prolongation of the Rotbach syncline NE of Täschalpen is hidden by the moraines and glaciers, and as, further to the NE, a direct contact between two different basement units would be difficult to highlight inside the Mischabel massif. For these reasons, the existence of a possible (major?) tectonic limit, between the basement forming the hinge of the Mischabel backfold (Siviez-Mischabel basement), and the one forming the Alphubel anticline (associated with the Faisceau Vermiculaire series and Série Rousse), has to be considered.

The individualization of the Alphubel basement from the basement forming the northern part of the Mischabel massif (i.e. Täschhorn, Dom, etc.) has previously been proposed by Staub (1942d) and Güller (1947), who individualized the "Alphubellappen" (or "Alphubel Keil"), from the "Dom-Täschhorn-Keil", and by Müller (1983), who distinguished the "Alphubel-Lappen" as a subunit of the Siviez-Mischabel nappe, mainly for structural reasons.

4.6.3. Structure of the Faisceau Vermiculaire and its relations with the Mischabel and Vanzone folds

4.6.3.1. General structure of the Faisceau Vermiculaire and Combin zone

An interpretation of the structure of the Faisceau Vermiculaire and Combin zone for the area surrounding Zermatt is given in the bedrock and axial traces maps of Fig. 4.6 and in the cross-sections of Fig. 4.9. This interpretation is essentially based on an attempt to synthesize the stratigraphic and structural observations at the outcrop scale, and the analysis of axial traces on bedrock maps compiled from detailed geological maps and data.

Fig. 4.9 a Geological cross-section through the upper Matter valley. The axial traces of early (pro-) folding phases (blue) are folded by later backfolds of the Mischabel phase (orange); A [2'615'030/1'094'070], A' [2'620'610/1'087'450], B [2'619'540/1'103'570], B' [2'629'180/1'092'120]; locations on Fig. 4.10a. *An*: Antrona zone; A_B: Alphubel pre-Permian basement; *DB*: Dent Blanche nappe; *Fu*: Furgg zone; *Go*: Gornergrat nappe; *Po*: Portjengrat nappe; SM_M: Siviez-Mischabel Mesozoic cover; SM_{MB}: Siviez-Mischabel monocyclic basement; SM_{PB}: Siviez-Mischabel polycyclic basement; *St*: Stockhorn basement; *Tu*: Tuftgrat Series; *ZH*: Zone Houillère; *ZS*: Zermatt-Saas Fee nappe. **b** Geological cross-section through the Pennine Alps between the Rhône valley and Sesia valley, modified after Steck et al. 2015; location on Fig. 4.10b. ▶

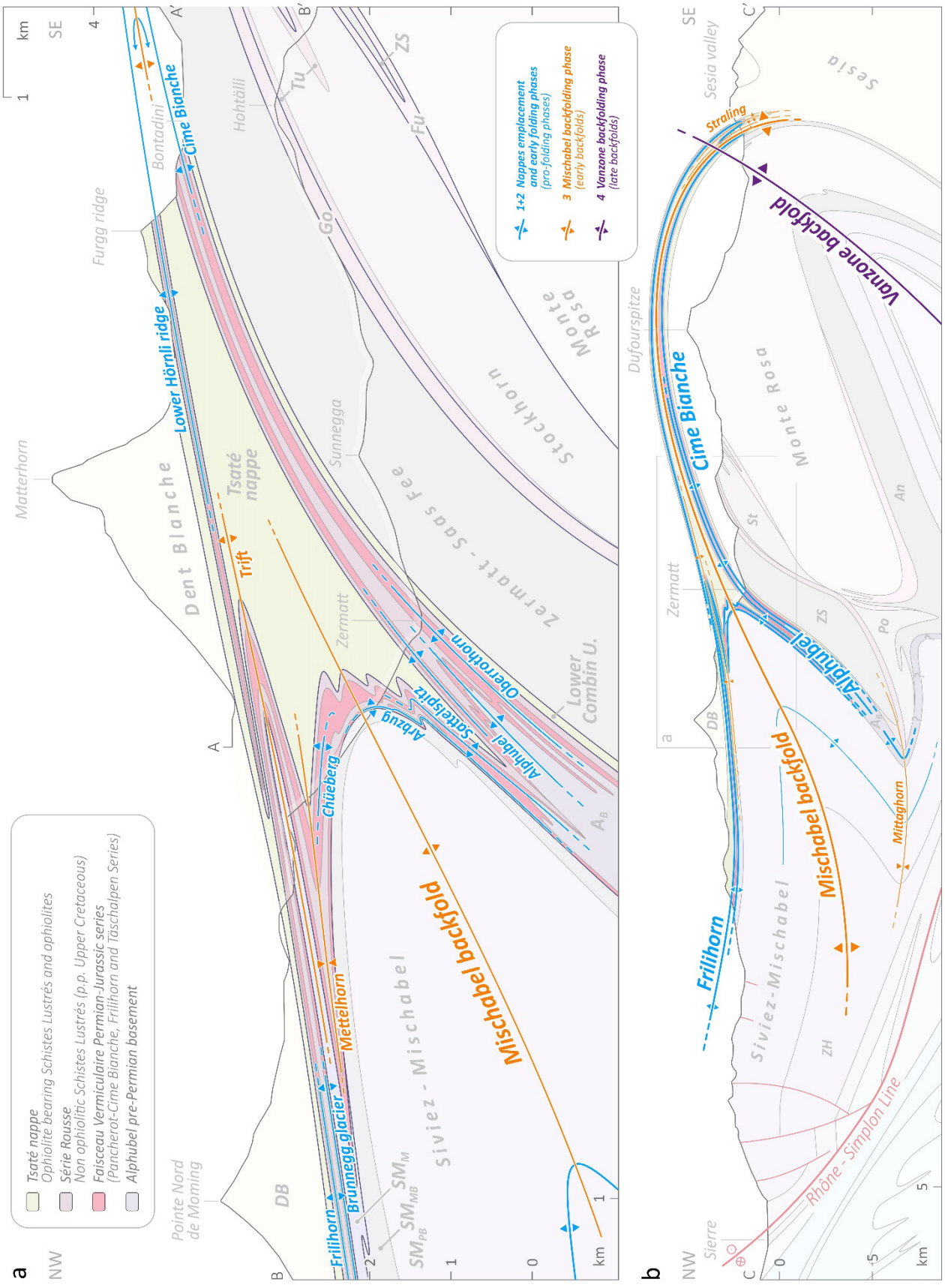
a
b
NW
SE
km
Tsaté nappe
Ophiolite bearing Schistes Lustrés and ophiolites
Série Rousse
Non ophiolitic Schistes Lustrés (p.p. Upper Cretaceous)
Faisceau Vermiculaire Permian-Jurassic series
(Pancherot-Cime Bianche, Frilihorn and Täschalpen Series)
Alphubel pre-Permian basement
1+2 Nappes emplacement and early folding phases (pro-folding phases)
3 Mischabel backfolding phase (early backfolds)
4 Vanzone backfolding phase (late backfolds)
Matterhorn
Dent Blanche
Lower Hörnli ridge
Furgg ridge
Bontadini
Cime Bianche
Hohtälli
Tsaté nappe
Trift
Sunnegga
Zermatt
Stockhorn
Monte Rosa
Zermatt - Saas Fee
Lower Combin U.
Obertorthorn
Sattelspitz
Arbzug
Alphubel
Chüeberg
Mettelhorn
Brunnegg glacier
Frilihorn
Mischabel backfold
Siviez - Mischabel
Pointe Nord de Moming
DB
Dufourspitze
Sesia valley
Straling
Vanzone backfold
Monte Rosa
Siviez-Mischabel
Mischabel backfold
Mittaghorn
Rhône - Simplon Line
Sierre

The proposed tectonic scheme involves: a first stage of deformation associated with the developments of high amplitude, N/NW vergent, folds (pro-movements) that corresponds to the individualization and emplacement of the nappes, followed by a second stage of deformation with S/SE vergent folds (retro-movements), including the high amplitude Mischabel early backfold and the later crustal-scale Vanzone open backfold.

According to this interpretation, the Faisceau Vermiculaire is rooted on the Alphubel basement (or eventually on a more internal Prepiemont-derived basement unit, for its lowermost part; cf. chap. 4.6.1). The formation of the different highly strained bands of the Faisceau Vermiculaire and their folding within the Schistes Lustrés and ophiolites of the Combin zone (incl. the Tsaté nappe and Lower Combin Unit), are interpreted to occur during the early N/NW-vergent (pro-) movements. The whole nappe stack would then be strongly refolded during the Mischabel backfolding phase. With the development of the Mischabel backfold, the Faisceau Vermiculaire would be displaced and sheared towards the S/SE. As the Faisceau Vermiculaire is mainly located in the lower limb of the Mischabel backfold, it would be almost entirely overturned during this phase. Following Argand (1911, 1916a) and Steck et al. (2015), we interpret hinges in the Combin zone and the Faisceau Vermiculaire in the area of Alagna and Punta Straling as associated to the main hinges of the Mischabel backfold (Figs. 4.1, 4.9b). The very thin bands from the Faisceau Vermiculaire that are intercalated in the upper part of the Combin zone, as the meter-thick bands outcropping on the lower section of the Hörnli ridge of the Matterhorn (Argand 1909; Müller 1984; Bucher et al. 2003a; Figs. 4.6, 4.9), are interpreted as representing the prolongation in the upper limb of the Mischabel backfold, of the thicker lower bands of the Faisceau Vermiculaire belonging to the lower limb of this fold. The later development of the crustal-scale Vanzone open backfold is responsible for the tilting towards the N of the structures in the northern part of the area and for their folding (of very large amplitude) in the hinge zone located in the Monte Rosa massif. A significant thinning of the structures in the sectors corresponding to the

limbs of the Vanzone fold (Fig. 4.9) is likely to occur during this phase, and would concern in particular the rheologically weaker metasedimentary units, such as the Combin zone (including the Faisceau Vermiculaire).

The proposed structural interpretation is compatible with the main results of the detailed structural studies carried out by Reddy et al. (2003), Pleuger et al. (2007, 2009) and Kirst and Leiss (2017), in different parts of the Faisceau Vermiculaire and surrounding units in the Italian side of the area. These different studies all provided microstructural evidences for top-(N)NW shearing during synkinematic greenschist facies recrystallisation. Neutron texture goniometry on quartzites from the Faisceau Vermiculaire show that, during this phase, top-(N)NW-directed rotational component of shear was small and that pure shear was the dominant deformation mechanism (Pleuger et al. 2007; Kirst and Leiss 2017). The microstructural studies of Reddy et al. (2003) and Pleuger et al. (2007, 2009) show that this phase clearly predates a later top-SE shearing phase, characterized by a strong rotational shear component, and that locally almost completely reworked earlier structures. This later top-SE shearing is associated with the Mischabel phase by Pleuger et al. (2007, 2009). The macroscopic shear sense markers observed around Zermatt (Figs. 4.5i-k; chap. 4.4.4), indicating foreland-directed shearing, are interpreted as being associated with the early foreland-directed phase evidenced in the Italian side of the belt by the above-mentioned authors. The top-SE macroscopic shear sense indicators observed in the area located further south of Zermatt (e.g. at Testa Grigia; Fig. 4.5l) are interpreted to be associated with later backfolding, locally overprinting earlier structures in the areas where the Combin zone is thinner and the Mischabel fold tighter (Fig. 4.9).

The internal structure of the different bands forming the Faisceau Vermiculaire locally clearly corresponds to hyper-stretched recumbent isoclinal anticlines. Such an isoclinal internal structure is observable, for example, in the area of the Cime Bianche and Gran Sometta (Vannay and

Allemann 1990), at the Bettaforca pass (Gasco and Gattiglio 2011), in the Hirli summit (Müller 1984) and in the lower Hörnli ridge (Argand 1909). Isoclinal anticlinal hinges are visible, for example, in the E faces of the Oberrothorn, Sattelspitz and Bösentrift (Figs. 4.5a-b, 4.7g; Güller 1947), at the base of the thick band of Arben (Güller 1947, fig. 15) and in the NE face of the Grand Tournalin (Allemann and Vannay 1987; Ellis et al. 1989). These isoclinal folds are often strongly asymmetrical (cf. chap. 4.6.1; Fig. 4.8) and the thinner limbs are regularly reduced to a hyper stretched level of crushed carbonates, sometimes less than one meter thick (e.g. Fig. 4.5d), which may give locally the appearance of a detached series (Fig. 4.8c).

The tectonic scheme proposed here appears to be actually very close to that proposed by Argand (e.g. 1911, 1916a) concerning the first order scheme. The main differences concern: (i) our more detailed descriptions of the structures in the sector of the overturned limb of the Mischabel backfold, and a more detailed description of the links between the Faisceau Vermiculaire and the Paleozoic basement in this sector; (ii) our proposition to subdivide Argand's Grand St-Bernard nappe into two different tectonic subunits in the sector of the overturned limb of the Mischabel backfold; and (iii) the detailed structure of the Faisceau Vermiculaire in the Zmutt valley, west of Zermatt, as we propose to link the thick band of the Faisceau Vermiculaire outcropping in Arben to that of Chüeberg (Fig. 4.6), following Sartori (1987) and Steck et al. (1999, 2015), contrary to Argand who linked the band of Arben to that of the lower Hörnli ridge. Following our interpretation, the continuation of the band of the lower Hörnli ridge, in the northern side of the Zmutt valley, corresponds to the meter-thick levels of quartzite and cornieules that are locally observable inside the Schistes Lustrés and ophiolites above the thick principal band of the Faisceau Vermiculaire in Arben (Mazurek 1986, fig. 2; Bucher et al. 2003a) and in the Wisse Tschuggen (e.g. [2'621'220/1'096'360], Crespo 1984; [2'621'660/1'096'640]).

4.6.3.2. Local structures

Different interpretations have been proposed concerning the phase of deformation attributed to some specific folds in the area located directly north and west of Zermatt. It concerns in particular the fold in the southern part of the Barrhorn Series, whose frontal hinge is outcropping just above Trift, called Trift anticline by Sartori (1987), and its associated lower syncline, whose axial trace runs through the level of Série Rousse forming the summit of the Mettelhorn, which has been called Platthorn syncline by Sartori (1987) and is referred to as Mettelhorn syncline here (Figs. 4.2, 4.6, 4.9a). These folds have classically been attributed to the Mischabel phase (Argand 1909, 1911, 1916a; Staub 1942d; Güller 1947; Ellenberger 1953; Bearth 1967b; Müller 1983; Mazurek 1986; Bucher et al. 2004a). According to the interpretation of Crespo (1984), Sartori (1987) and Steck (1989), these folds would however be older than the Mischabel phase, as their axial trace would be refolded by folds of the Mischabel phase in the sector of Arben. A detailed structural study would be necessary to confirm this interpretation, and to exclude that the axial trace of the Trift fold would rather be linked to the late open folds of the sector of Arben (as proposed in Figs. 4.6, 4.9a) than to the earlier isoclinal folds observed in this sector, as proposed by Crespo (1984), Sartori (1987) and Steck (1989).

In the Barrhorn area, in the upper Turtmann valley, recent glacial retreat allows the observation of new outcrops of dolomites, marbles, quartzites and cornieules located at the top of the Barrhorn Series and forming the base of the Série Rousse, east of the Adlerflüe (Fig. 4.10a), just above the small lake that formed at the front of the Brunegg glacier. These metasediments form a 15 m thick highly strained level, surmounting the dark Eocene Flysch of the uppermost syncline of the Barrhorn Series (Barr syncline; Sartori 1987, 1990). The basal contact of this level, with the Flysch, is masked by the lake. This level is in turn directly overlaid by the Série Rousse (Fig. 4.3a). Sartori (1990) describes the direct prolongation of this level 300 m to the NW, as well as in other sectors of the upper Turtmann and Matter valleys. He proposes an origin either from the

Barrhorn Series or from a more internal unit, for this tectonized level. The polished surfaces of the new outcrops allow to observe the presence of metric levels of breccias, composed of a light-colored calcareous matrix and clasts made of dolomites and limestones, up to 30 cm in size at point [2'620'490/1'110'670]. They alternate with decimetric beds of dolomites, and quartzites. Cornieules are also present at the top of this level (Fig. 4.3a). The presence of such breccias, not observed anywhere else in the Barrhorn Series, as the tectonic position of this level, strongly suggest its attribution to the Faisceau Vermiculaire. We interpret this level, corresponding to the *Brunegg glacier* axial trace in Figs. 4.9-4.10, as the prolongation to the north of the most external band of the Faisceau Vermiculaire of the area of Zermatt. This external band, partly made of cornieules, is in direct contact with the Permian and/or older monocyclic basement levels of the Siviez-Mischabel nappe in the hinge of the Mischabel backfold (e.g. Güller 1947; Bearth 1964b; *Arbzug* axial trace in Figs. 4.6, 4.9, 4.10) and is also found further west around the Trift anticline (Fig. 4.6; Argand 1908; Bearth 1964b; Crespo 1984).

4.6.4. Relations of the Alphubel basement, Faisceau Vermiculaire and Série Rousse with the Mont Fort nappe

As evidenced in chapter 4.6.1, the Alphubel basement, the Faisceau Vermiculaire and the Série Rousse appear to form together a coherent tectonic unit, separated from the Siviez-Mischabel nappe by an important discontinuity (chap. 4.6.2). Its structural position with respect to both the Siviez-Mischabel and Tsaté nappes, when considered at regional scale (Fig. 4.10), appears to be identical to that of the Mont Fort nappe (such as described in chap. 3.7.3). The Alphubel basement and most part of the Faisceau Vermiculaire are located in the overturned limb of the Mischabel backfold, whereas north and west of the Dent Blanche klippe (e.g. in the Hérens valley), the position of the Mont Fort nappe corresponds to the normal limb of this fold (Fig 4.11). In addition to sharing an identical tectonic position, the Mont Fort nappe and the ensemble formed by the Alphubel basement, the Faisceau Vermiculaire and the associated Série Rousse show

identical stratigraphic successions, both regarding lithologies and stratigraphic sequences (cf. chap. 4.3), and the presence of large unconformities and important local stratigraphic gaps which are best interpreted as resulting from the activity of synsedimentary paleofaults (cf. chaps. 2.6, 3.7.2, 4.5.3, 4.6.1). For these reasons, we propose that the Alphubel basement, the Faisceau Vermiculaire and associated Série Rousse constitute together the eastern prolongation of the Mont Fort nappe. This nappe would be folded obliquely around the Mischabel backfold, so that to the north and to the west of the Dent Blanche klippe, its position corresponds to the normal limb of the backfold, while to the east it corresponds to its overturned limb (Figs. 4.10, 4.11). The prolongation of the hinge of the Mischabel backfold (at the level of the Paleozoic basement) reappears to the SW, on the other side of the Dent Blanche axial depression and Aosta fault, to form the Valsavaranche backfold (Fig. 4.10b; e.g. Lugeon and Argand 1905b; Argand 1911; Hermann 1925, 1928; Bucher et al. 2003b, 2004b). Due to this axial direction, the hinge of the Mischabel backfold is not outcropping north and west of the Dent Blanche klippe. It is located in a more internal position under the Dent Blanche nappe and Combin zone (e.g. Argand 1911; Hermann 1925; Steck et al. 1997). Between the northernmost outcrops of the Mont Fort pre-Permian basement in the Hérens valley and westernmost outcrops of the Alphubel pre-Permian basement in the Täsch valley, the proposed connection is hidden by the Dent Blanche and Tsaté klippe (Figs. 4.10, 4.11). However, the Série Rousse outcrops continuously (except for small sectors covered by ice and moraines) from the Täsch valley, where it is associated with the Faisceau Vermiculaire and the Alphubel basement, through the Matter, Turtmann and Anniviers valleys, to the Hérens and Bagnes valleys, where it rests in stratigraphic contact with the Evolène Series and western Mont Fort nappe (Figs. 4.1, 4.10; Sartori 1987, 1990; Escher 1988). The connection between the Faisceau Vermiculaire in the east and the Evolène Series in the west is also almost continuous through the Matter, Turtmann and Anniviers valleys, along the thin

bands interpreted as extremely stretched and partly boudinaged isoclinal anticlines that are referred to as *Brunegg glacier* and *Frilihorn* axial traces in Fig. 4.10a.

It is interesting to note that this connection has already been proposed by Argand (1911) and drawn on his 1:500'000 tectonic map and associated cross-sections. The affiliation of the Faisceau Vermiculaire to the Mont Fort nappe (together with the Série Rousse) has later been proposed by Escher and Masson (1984), Sartori (1987, 1990), Escher (1988) and Escher et al. (1988). However, contrary to our hypothesis, these authors didn't include the Alphubel basement into the Mont Fort nappe but rather into the underlying Siviez-Mischabel nappe. A different tectonic scheme was then proposed by some of these authors, stating that most of the Permian-Jurassic metasediments overlapping the Mont Fort basement to the west were linked to the Faisceau Vermiculaire to form together the Cimes Blanches nappe, but detached both from the underlying Mont Fort basement and from the overlying Série Rousse (Escher et al. 1993, 1997; Sartori and Marthaler 1994; Steck et al. 1999, 2001). On the other hand, Müller (1983) already noted the similarities between the Alphubel basement and the Métailler Paleozoic (now linked to the Mont Fort nappe) regarding their tectonic positions and relations to the Combin zone.

Fig. 4.10 Axial traces of the successive folding phases affecting the Mont Fort and Alphubel basements and associated Mesozoic series (Evolène Series and Faisceau Vermiculaire series); *AR*: Aiguilles Rouges massif; *An*: Antrona zone; *Ba*: Barrhorn Series; *Bi*: Biella pluton; *Co*: Combin zone s.str. (= Tsaté nappe); *DB*: Dent Blanche nappe; DB_M: Dent Blanche Mesozoic; DB_B: Dent Blanche basement; *Em*: Monte Emilius unit; *ES*: Evolène Series; *GP*: Grand Paradis massif; *He*: Helvetic and Ultrahelvetic nappes; *IV*: Ivrea-Verbano zone; *Le*: Lepontine nappes; *M*: Money unit; *MB*: Mont Blanc massif; *MF*: Mont Fort nappe; MF_B: Mont Fort basement; *MP*: Médianes Prealps; *Or*: Orobic nappes; *Pg*: Portjengrat nappe; *R*: Ruitor unit; *SC*: Sion-Courmayeur zone; *SCe*: Strona-Ceneri zone; *Se*: Sesia zone; SM_M: Siviez-Mischabel Mesozoic; SM_B: Siviez-Mischabel basement; *SM - ZH*: Siviez-Mischabel nappe and Zone Houillère; *SR*: Série Rousse; *T*: Traversella pluton; *Ts*: Tsaté nappe; *Va*: Valsavarenche unit; *ZS*: Zermatt-Saas Fee nappe; A-A', B-B' and C-C' indicate the location of the cross-sections of Fig. 9. **a** Axial traces, fold axis and stretching directions in the upper Hérens, Anniviers, Turtmann, Matter and Valtournenche valleys; Basemap after Argand (1908), Güller (1947), Bearth (1953a, 1964b, 1967a, 1973), Milnes et al. (1981), Crespo (1984), Sartori (1987, 1990), Escher (1988), Allimann (1990), Girard (1995), Steck et al. (1999, 2015), Bucher et al. (2003a), Marthaler et al. (2008a, 2020a), Dal Piaz et al. (2015b) and data from this study. **b** Axial traces at regional scale (SW Switzerland and NW Italy); basemap modified after Schmid et al. (2004, 2017), Steck et al. (1999, 2015, 2019), Ballèvre et al. (2018, 2020), Beltrando et al. (2010a, 2014), Balestro et al. (2020), Bigi et al. (1992), Gouffon (1993), Deville et al. (1992) and the Tectonic map of Switzerland (2005). ▶

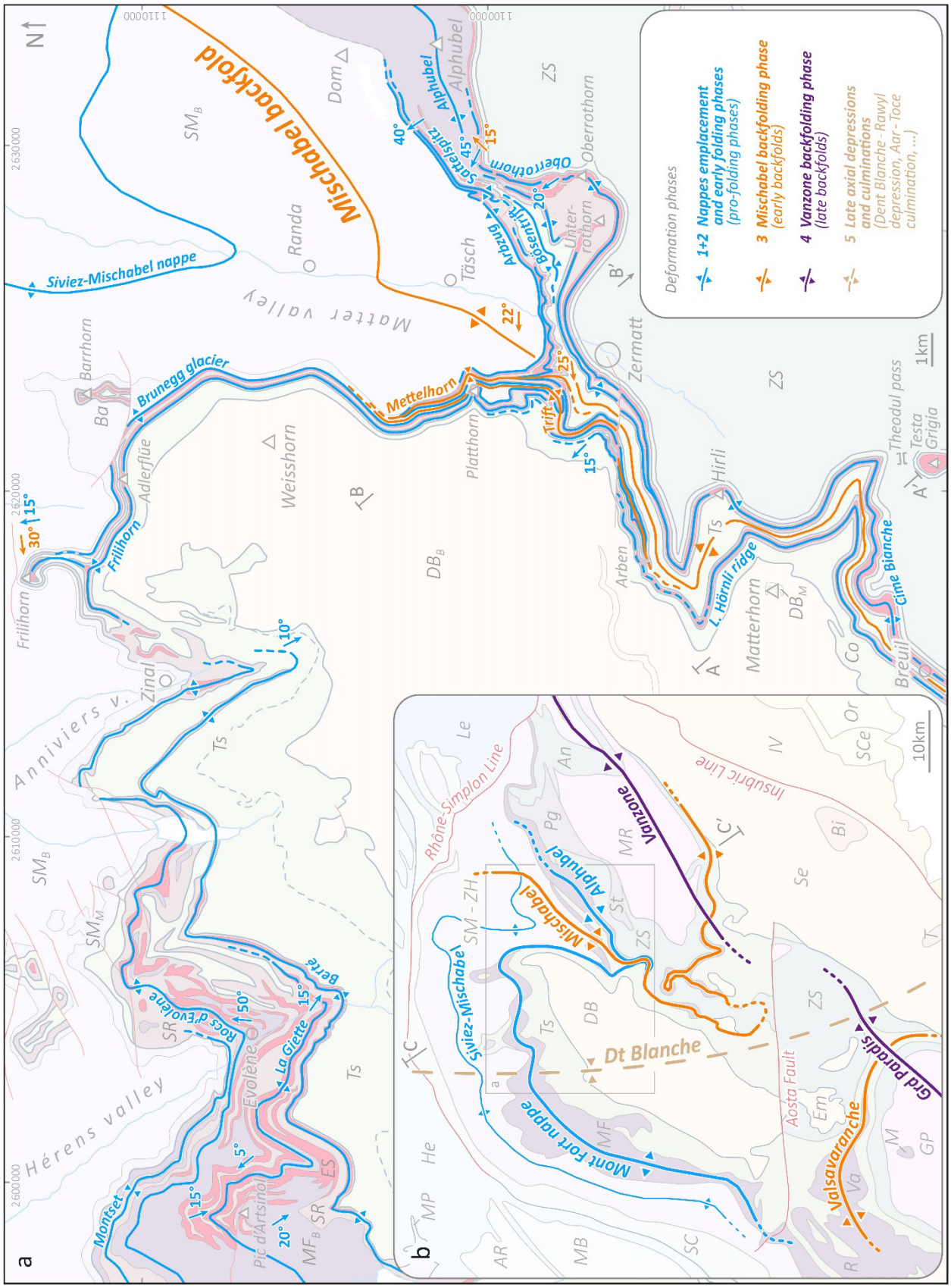
Deformation phases
1+2 Nappes emplacement and early folding phases (pro-folding phases)
3 Mischabel backfolding phase (early backfolds)
4 Vanzone backfolding phase (late backfolds)
5 Late axial depressions and culminations (Dent Blanche - Rawyl depression, Aar - Toce culmination, ...)
Mischabel backfold
Siviez-Mischabel nappe
Matter valley
Brunegg glacier
Mettelhorn
Trift
Alphubel
Schalligrat
Athbalg
Gässenfirst
Oberrothorn
Unter-rothorn
Zermatt
Theodul pass
Testa Grigia
Hörnli ridge
Cime Bianche
Breuil
Matterhorn
Arben
Hirli
Platthorn
Weisshorn
Barrhorn
Brunegg
Adlerflue
Frilihorn
Zinal
Anniviers v.
Hérens valley
Evolène
Roc d'Evolène
La Giette
Bertie
Montsec
Pic d'Artsinol
Randa
Täsch
Dom
1km
10km
a
b
A
A'
B
B'
C
C'
Rhône-Simplon Line
Insubric Line
Vanzone
Mischabel
Alphubel
Siviez-Mischabel
Mont Fort nappe
Dt Blanche
Aosta Fault
Grd Paradis
Valsavaranche

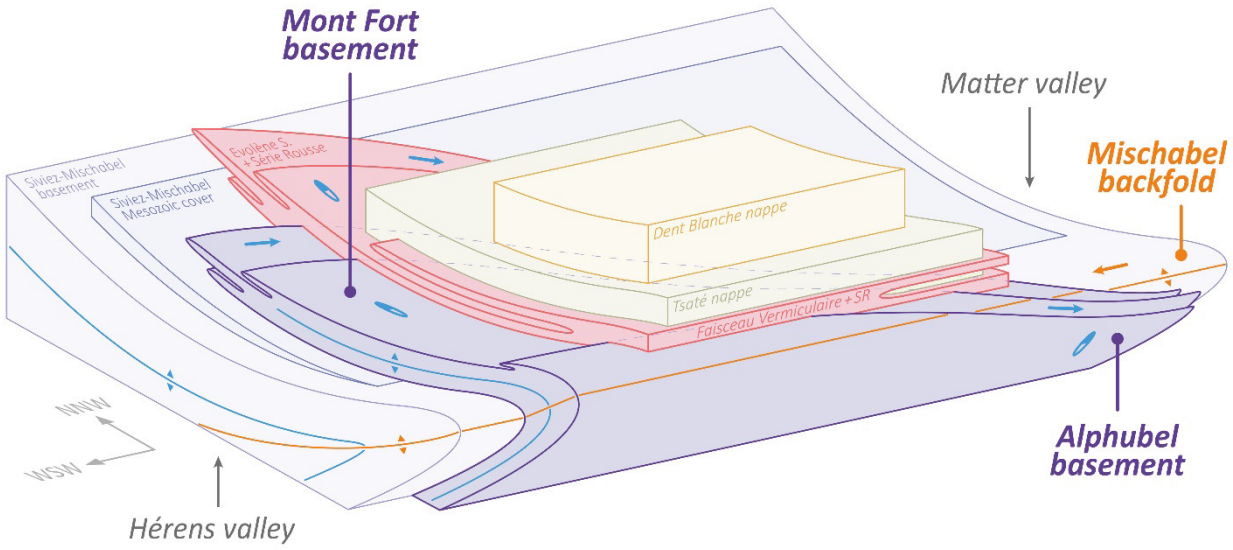

Fig. 4.11 Schematic block-diagram representing the oblique folding of the Mont Fort - Alphubel basement around the Mischabel backfold. The left side of the block-diagram corresponds to the geometry of the nappe stack in the Hérens valley, whereas its right side corresponds to the Matter valley. Note that the connection between the Mont Fort and Alphubel basements is not outcropping due to the presence of the Dent Blanche (+Tsaté) klippe (cf. Fig. 4.10). Arrows represent fold axis directions; ellipses, stretching directions; orange colors correspond to the Mischabel backfolding phase, blue colors correspond to the nappes emplacement and early (pro-) folding phases; *SR*: Série Rousse.

4.6.5. Constraints from the stratigraphic sequences of the Faisceau Vermiculaire and Barrhorn series on the Briançonnais-Prepiemont paleomargin evolution

Some characteristic lithological successions observable, within the Faisceau Vermiculaire and associated Série Rousse, the Barrhorn Series (Siviez-Mischabel autochthonous cover), and across their contacts with the underlying basements, have been reported in Figs. 4.12a-b. The study of these lithological successions provides interesting clues regarding the structure of the Jurassic-Cretaceous southern paleomargin of the Briançonnais s.l. domain, for this transect.

As already mentioned in chapter 4.6.2, the stratigraphic sequences observed in the ensemble formed by the Faisceau Vermiculaire series and the Série Rousse show strong discrepancies with those observed in the Barrhorn Series (Staub 1942d; Güller 1947; Bearth 1964b, 1976;

Sartori 1987, 1990; Steck et al. 2015). While stratigraphic sequences from the Barrhorn Series are typical of the Briançonnais domain (e.g. Ellenberger 1952, 1953, 1958; Escher 1988; Sartori 1990), those from the Faisceau Vermiculaire and Série Rousse are typical of the Prepiemont domain (e.g. Escher and Masson 1984; Escher 1988).

The Barrhorn Series is characterized by large stratigraphic gaps in the Triassic-Jurassic sequence, resulting from an Early to Middle Jurassic erosion and emersion and attested by metabauxites representing paleokarstic infill (Sartori 1990; Schöllihorn profile, Fig. 4.12b). In the whole series, Lower Jurassic levels are completely missing (e.g. Ellenberger 1952; Bearth 1980; Sartori 1990). The stratigraphic gap is less important in the northern sector of the Barrhorn Series (e.g. Stellijoch and Barr profiles, Fig. 4.12a-b), where Upper Triassic levels (locally containing gypsum) are partly preserved from the erosion (Sartori 1990), and where sedimentation most probably starts again since the Middle Jurassic as levels similar to the Mytilus Beds from the Prealps and Vanoise series are observed in this sector (Ellenberger 1952, 1953; Sartori 1990). The stratigraphic gap is gradually more important to the south, forming a large-scale unconformity, clearly highlighted by Sartori (1990, fig. 19). In the southernmost outcrops of the Barrhorn Series above Zermatt, in the slopes of the Platthorn and Wisshorn for example, the Upper Jurassic marble directly onlaps the Lower Triassic Tabular Quartzite (Sartori 1990; Platthorn profile, Fig. 4.12b). Another stratigraphic gap is observed at the top of the Upper Jurassic marble. In the northwestern part of the Barrhorn Series, this marble is overlapped by a local mm ferruginous crust and by an Upper Albian to Lower Cenomanian dark marble (Complexe schisteux intermédiaire; Sartori 1990; Barr profile, Fig. 4.12b). Elsewhere in the Barrhorn Series, the Upper Jurassic marble is directly overlaid by an orange to greenish micaceous marble constituting the metamorphic equivalent of the Couches Rouges (Ellenberger 1953; Sartori 1990), which ages extend from the Turonian to the Ypresian in the Médianes Prealps (Guillaume 1986). A dark Flysch forms the top of the Barrhorn Series, its age is most likely Eocene (Ellenberger 1952, 1953; Sartori 1990).

The stratigraphic sequences from the central and northern parts of the Barrhorn Series are typical of the Briançonnais swell (Briançonnais s.str. domain), whereas the stratigraphic sequences of the southern part of the series show similarities with some sequences described in the Gummfluh area in the Swiss Prealps (Hürlimann et al. 1996), and particularly with the Ultrabriançonnais domain of the French-Italian Alps (e.g. Lefèvre and Michard 1976; Lefèvre 1982; Lemoine et al. 1986; Michard et al. 2022).

Stratigraphic sequences observed in the different bands of the Faisceau Vermiculaire and associated Série Rousse systematically contrast with those of the Barrhorn Series. While breccia levels of probable Jurassic age (cf. chap. 4.3.1.3) are widespread in the Faisceau Vermiculaire series, they are completely absent in the Barrhorn Series (Fig. 4.12b). In this series, there is also no equivalent of the dark calcarenites with mm-cm dolomitic clasts that are observed in various localities in the Faisceau Vermiculaire (Güller 1947; Bearth 1976; Sartori 1990; Färichflüe and Becca d'Aran profiles, Fig. 4.12), and show strong analogies with the Sinemurian to Aalenian "Schistes inférieurs" of the Breccia nappe. Another major difference between these series is the abundance of cornieules levels in the Faisceau Vermiculaire (locally associated with gypsum; Bearth 1976), whereas these lithologies are almost absent in the Barrhorn Series. An exception is observed in the northernmost outcrops of the series, where these levels escaped the Early to Middle Jurassic erosion, which was less deep in this sector (Sartori 1990). Finally, quartzitic calcschists similar to those of the Série Rousse are not developed in the Barrhorn Series, while conversely, equivalent of the metamorphic Couches Rouges and of the dark Eocene Flysch do not seem to be present in the Série Rousse. The sedimentation in the Faisceau Vermiculaire and Série Rousse during the Jurassic and Cretaceous thus appears as locally more continuous than in the Barrhorn Series, with the presence of presumably widespread Upper Triassic and Lower Jurassic levels. It is also characterized by an important detritic and clastic input that is completely missing in the Barrhorn Series during these periods. The stratigraphic sequences observed in the Faisceau

Vermiculaire and Série Rousse are however extremely variable, and locally, unconformities and large stratigraphic gaps are also documented (chap. 4.6.1; e.g. Bru profile, Fig. 4.12b).

From the area of Hohlicht (Fig. 4.12a), southward and eastward towards the Mischabel massif, the Barrhorn Series is progressively completely absent on the top of the Siviez-Mischabel basement. Between the Mettelhorn and the Weingarten glacier, east of Täschalpen, this basement is in direct contact with the Faisceau Vermiculaire and Série Rousse (cf. chap. 4.5.2). In this sector, the upper part of the basement is formed of quartzitic and micaceous metasediments, locally graphitic, that are attributed to the Permian and/or Carboniferous depending on the authors (e.g. Argand 1908; Bearth 1964b; Steck et al. 2015). Quartzites similar to those of the base of the Bruneggjoch Fm. (Late Permian to earliest Triassic; Sartori 1990; Sartori et al. 2006) are not observed in this sector.

A possibility to explain such a complete lack of the Mesozoic and latest Permian levels in this sector is to interpret it as representing the remnant of an important Jurassic normal fault that would have separated the Siviez-Mischabel basement and Barrhorn Series from the Alphubel basement and the overlying Faisceau Vermiculaire and Série Rousse (Hohlicht-Mischabel paleofault; Fig. 4.12c). As a direct contact is observable in this sector between the Siviez-Mischabel basement and the Faisceau Vermiculaire and Série Rousse, without the intercalation of another tectonic unit in between, such as the Tsaté nappe which is intimately folded with the Série Rousse, Faisceau Vermiculaire and Evolène Series in other sectors (Figs. 4.4, 4.6, 4.10), it is likely that the Siviez-Mischabel basement, the Série Rousse and the Faisceau Vermiculaire have already been juxtaposed before the Alpine nappe stacking.

The restoration of the southern Briançonnais-Prepiemont continental paleomargin derived from the interpretation of this contact as an important Jurassic normal fault is fully consistent with the observed variations in the stratigraphic sequences across the Barrhorn Series, Faisceau

Vermiculaire and Série Rousse (Figs. 4.12b-c). This interpretation allows to explain the stratigraphic variations within the Barrhorn Series, which evolves towards the very lacunary sequence observed in the southernmost outcrops of the series (Platthorn profile, Fig. 4.12), interpreted as the upper part of the necking domain of the paleomargin (e.g. Sutra and Manatschal 2012; Peron-Pinvidic et al. 2019). It also explains the abrupt disappearance of the Mesozoic series in the Hohlicht area (Fig. 4.12a), which is interpreted as corresponding to the summit of the paleofault scarp. The stratigraphic sequences observed in the Faisceau Vermiculaire and Série Rousse are interpreted as representing sedimentation in a deeper basin, where sediments, and in particular breccias, were deposited during the emersion characterizing the Briançonnais swell at Early to Middle Jurassic Time. The variability of the stratigraphic sequences formed by the Faisceau Vermiculaire and Série Rousse, the local identification within these series of large stratigraphic gaps, affecting sectors of relatively small extension, as well as the importance in the Série Rousse of the detritic input, argue for the sedimentation of these series in a basin formed by half grabens and tilted blocks. The stratigraphic sequences observed in the Faisceau Vermiculaire and Série Rousse therefore argue for an origin of these series in the hyperextended domain of a distal continental margin (e.g. Mohn et al. 2010; Haupert et al. 2016; Ribes et al. 2019).

According to this interpretation, the Hohlicht-Mischabel paleofault would represent a major Jurassic normal fault separating the Briançonnais swell (Briançonnais s.str. and Ultrabriançonnais domains) from the Prepiemont basin. The contrasting and characteristic stratigraphic successions observed in the footwall and hanging wall of this presumed paleofault would indicate that it corresponded to a first order discontinuity inside the southern Briançonnais s.l. Jurassic margin, comparable to the mega fault-scarps described and studied by Ribes et al. (2019). Such major discontinuities could correspond to an abrupt thinning of the continental crust, which can typically vary from 30 ± 5 km in the necking domain to only 10 ± 5 km in the hyper-extended domain (e.g. Sutra and Manatschal 2012; Haupert et al. 2016; Ribes et al. 2019).

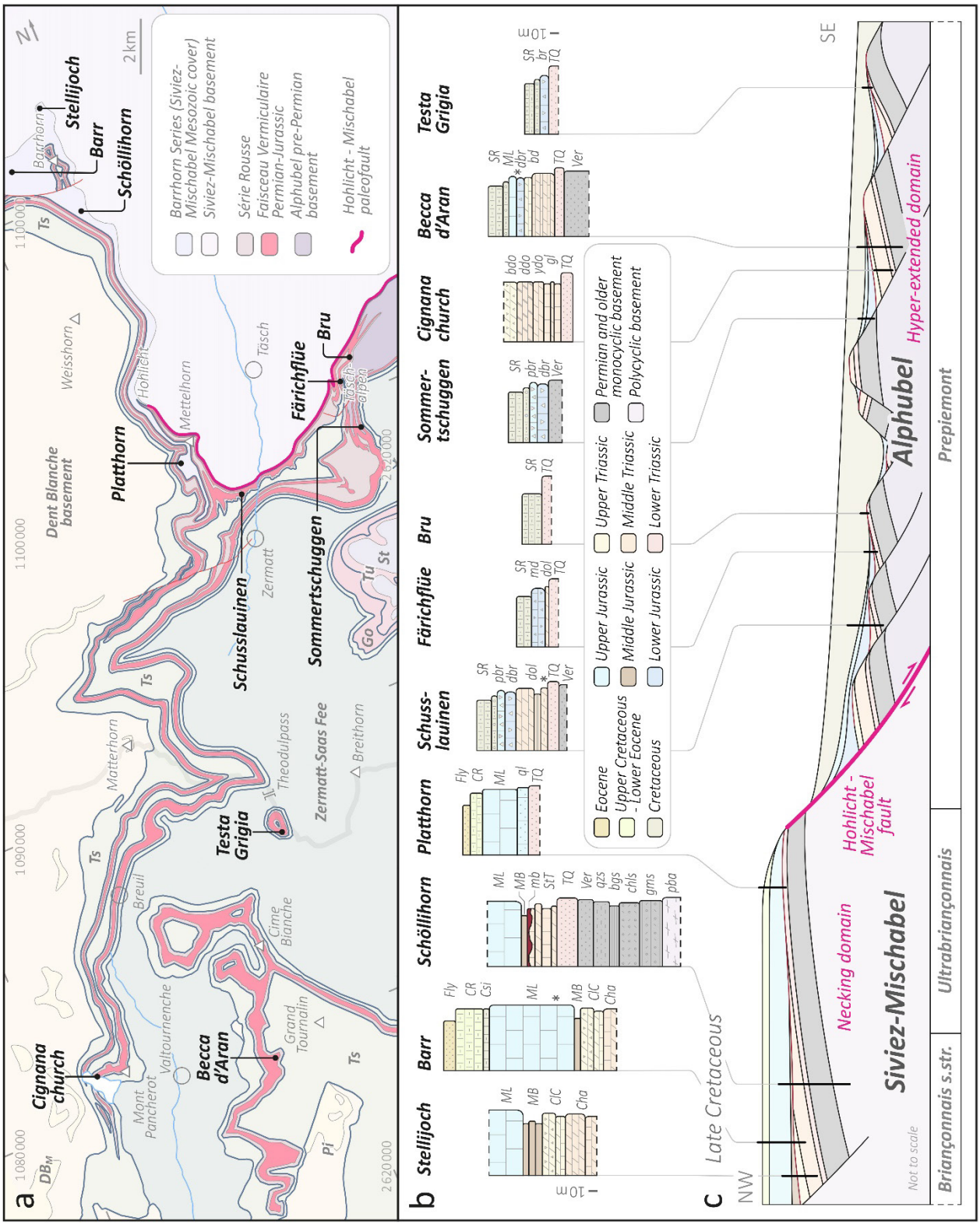
a
b
c
Cignana church
Becca d'Aran
Testa Grigia
Platthorn
Schusslauinen
Sommertschuggen
Färichflüe
Bru
Stellijoch
Barr
Schöllihorn
Dent Blanche basement
Barrhorn Series (Siviez-Mischabel Mesozoic cover)
Siviez-Mischabel basement
Série Rousse
Faisceau Vermiculaire
Permian-Jurassic
Alphubel pre-Permian basement
Hohlicht - Mischabel paleofault
Eocene
Upper Cretaceous - Lower Eocene
Cretaceous
Upper Jurassic
Middle Jurassic
Lower Jurassic
Upper Triassic
Middle Triassic
Lower Triassic
Permian and older monocyclic basement
Polycyclic basement
Late Cretaceous
NW
SE
Necking domain
Hohlicht - Mischabel fault
Siviez-Mischabel
Alphubel
Hyper-extended domain
Not to scale
Briançonnais s.str.
Ultrabriançonnais
Prepiemont

◄ **Fig. 4.12** Stratigraphic profiles across the Barrhorn and Faisceau Vermiculaire series and associated basements (Siviez-Mischabel and Alphubel respectively) through the Matter valley and Valtournenche. **a** Profile locations: Stellijoch [2'623'220/1'112'940; 2'623'110/1'113'100]; Barr [2'620'590/1'111'510; 2'621'740/1'111'400]; Schöllihorn [2'623'650/1'110'140; 2'623'110/1'109'680]; Platthorn [2'622740/1'099800; 2'622'670/1'099'950]; Schusslauinen [2'624'100/1'098'200; 2'624'260/1'098'090]; Färichflüe [2'628'880/1'100'380; 2'628'830/1'100'370; Bru [2'629'550/1'101'030; 2'629'580/1'101'060]; Sommertschuggen [2'628'990/1'098'640; 2'628'980/1'098'650]; Testa Grigia [2'620'890/1'086'980; 2'620'860/1'087'040]; Cignana church [2'611'590/1'081'510; 2'611'600/1'081'570]; Becca d'Aran [2'617'240/1'079'770; 2'617'740/1'079'920]; DB_M: Dent Blanche Mesozoic; *Go*: Gornergrat nappe; *Pi*: Pillonet unit; *St*: Stockhorn basement; *Ts*: Tsaté nappe; *Tu*: Tuftgrat Series; basemap: cf. Fig. 1. **b** Stratigraphic profiles: Stellijoch, Barr and Schöllihorn profiles after data from Sartori (1990); Platthorn, Schusslauinen, Färichflüe, Bru, Sommertschuggen and Testa Grigia profiles after data from this study; Cignana church profile after Dentan and Menthonnex (1990) and data from this study; Becca d'Aran profile after Passeri et al. (2018), modified according to our observations. Local level duplications due to isoclinal folding (*) are not represented. Age attributions are partly hypothetical. *bd*: bedded dark and light colored dolostones and marbles; *bdo*: brecciated dolomites; *bgs*: black graphitic schists; *br*: breccia (calcareous matrix, dolomitic and dolomitic limestone cm clasts); *Cha*: metamorphic equivalent of the Champcella (Wiriehorn) Fms.; *chls*: chlorite-schists and metabasites; *ClC*: metamorphic equivalent of the Clôt la Cime Fm.; *CR*: metamorphic Couches Rouges; *Csi*: Complexe schisteux intermédiaire; *dbr*: breccia with dolomitic clasts; *pbr*: polymict breccia; *ddo*: dark dolomites; *dol*: dolomites; *Fly*: flysch; *gl*: grey marbled limestone (St-Triphon Limestone?); *gms*: graphitic micaschist; mb: metabauxite (paleokarst); MB: metamorphic Mytilus Beds; md: marbles with discontinuous dolomitic layers (probable stretched breccias); *ML*: metamorphic Upper Jurassic Massive Limestones; *pba*: polycyclic basement (amphibolites, gneisses,...); *ql*: quartzitic limestone; *qzs*: Permian quartzschists; *StT*: metamorphic equivalent of the St-Triphon Fm.; *SR*: Série Rousse (incl. local conglomeratic base); *TQ*: Tabular Quartzite; *Ver*: Permian «Verrucano»; *ydo*: yellow dolomites. **c** Margin restoration attempt at Late Cretaceous Time, before the onset of Alpine deformation in that area; Black strikes indicate approximate the pre-orogenic locations of the profiles of Fig. b; brown strikes represent Early to Middle Jurassic erosion levels.

4.6.6. Mischabel and Vanzone backfold development and proposed relations with the European - Briançonnais (s.l.) paleomargin structure

Backfolds are structuring the overall tectonic architecture of the Western Alps and in particular of the Pennine Alps, where their importance have been highlighted notably by Argand (1911, 1916b, 1920) and Hermann (1925, 1928), and more recently by Klein (1978), Milnes et al. (1981), Müller (1983), Steck (1984, 1990, 2008), Ballèvre and Merle (1993), Escher and Beaumont (1997), Kramer (2002), Keller et al. (2005), Pleuger et al. (2007, 2008) and Steck et al. (2015) for example.

Backfold development starts in the Late Eocene to Early Oligocene in the Pennine Alps. The dating of these structures is partly based on indirect data and is therefore subject to interpretation, hence the discrepancies sometimes appearing between the ages proposed by the different authors. Ages proposed for the development of the Mischabel backfolding range between 40 and 30 Ma (e.g. Barnicoat et al. 1995; Cartwright and Barnicoat 2002; Pleuger et al. 2008; Scheiber et al. 2013; Steck et al. 2015; Kirst 2017; Kirst and Leiss 2017). For the SW prolongation of the Mischabel backfold in the French-Italian Alps, an age range from 35-31 Ma has been proposed for the development of the Valsavaranche backfold (and associated Ruitor backfold; Bucher 2003; Bucher et al. 2004b; Schmid et al. 2017).This first backfolding phase shortly follows the NW-directed emplacement of the Siviez-Mischabel nappe, dated at 41-36 Ma (40Ar/39Ar ages of synkinematically grown micas; Markley et al. 1998, 2002), and is partly coeval to the ongoing NW-directed movements (Escher and Beaumont 1997; Markley et al. 1998; Bucher et al. 2004b; Scheiber et al. 2013; Schmid et al. 2017). Proposed development age for the Vanzone backfold is in the 35-10 Ma interval (Pettke et al. 1999; Keller et al. 2005; Pleuger et al. 2007, 2008; Steck 2008; Steck et al. 2015; Kirst 2017; Kirst and Leiss 2017). The initiation of backfold development in the Penninic units is coeval to a period of major changes in the evolution of the Alpine orogen. It is characterized by the development of crustal-scale transpressional shear zones,

such as the Insubric line (ductile shearing at least during the 32-25 Ma time interval; e.g. Schmid al. 1989; Steck and Hunziker 1994; Steck et al. 2013) and the Rhône-Simplon line (active since c.a. 35 Ma; e.g. Steck 1990; Mancktelow 1992; Steck and Hunziker 1994; Steck et al. 2015), associated with a southwestward movement of the entire Pennine Alps (and Graian Alps) nappe pile (e.g. Gouffon 1993; Gouffon and Burri 1997; Bistacchi et al. 2000; Egli and Mancktelow 2013; Schmid et al. 2017). These movements are associated with magmatism along the Insubric line, with the emplacement of the mantle-derived 42-21 Ma Bergell, Biela and Traversella plutons (e.g. von Blackenburg 1992; Berger et al. 1996; Kapferer et al. 2012; Ji et al. 2019) and with 42-5 Ma aplite and pegmatite dykes (e.g. Romer et al. 1996; Schärer et al. 1996; Rubatto et al. 2009; Bergomi et al. 2015). This period is also characterized by a rapid uplift and cooling of the Pennine and Lepontine Alps (e.g. Hurford et al. 1991; Hunziker et al. 1997; Bistacchi et al. 2001; Steck et al. 2013) and the overfilling of the foreland basins corresponding to the transition from flysch to molasse sedimentation at ca. 30 Ma (e.g. Schroeder and Ducloz 1955; Homewood and Lateltin 1988; Sinclair and Allen 1992; Schlunegger and Kissling 2015). Following this period, a later phase of backfold development (incl. e.g. the Glishorn, Berisal and Evêque backfolds) affected the more external Lower Penninic and Helvetic nappes (e.g. Steck 1984, 2008; Escher et al. 1994; Steck et al. 1997). Their development is estimated to occur during the ca. 15-5 Ma time interval (e.g. Steck and Hunziker 1994; Steck 2008; Krayenbuhl and Steck 2009) and is likely to be more or less coeval with the end of the activity along the basal thrusts of the Helvetic nappes at ca.15-10 Ma (Crespo-Blanc et al. 1995; Kirschner et al. 1996).

The tectonostratigraphic reconstructions proposed in this work tend to indicate a possible link between the localization of the first backfolds developing within the orogenic wedge and the structure of the southern European - Briançonnais s.l. paleomargin. Indeed, the hinge of the

Mischabel backfold developed on a position interpreted as constituting a possible first order discontinuity regarding the crustal thickness of this paleomargin (cf. chap. 4.6.5; Figs. 4.13a-b).

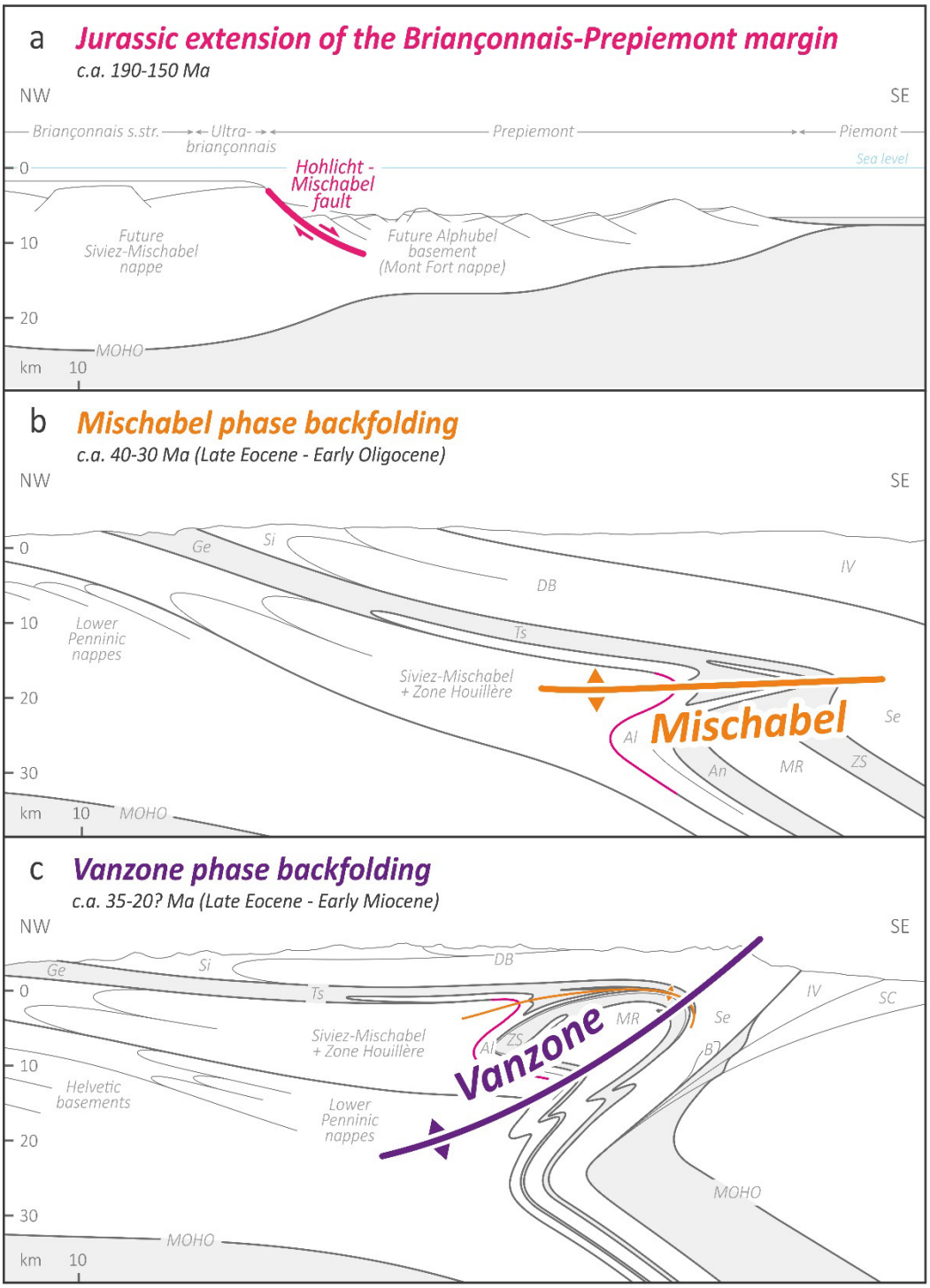

Fig. 4.13 Schematic restoration attempts of (**a**) the Briançonnais-Prepiemont margin after the Jurassic extension, and (**b, c**) of Alpine early backfolding phases, for the Pennine Alps transect; b and c modified after Steck (2008) and Steck et al. (2015); *Al*: Alphubel / Mont Fort nappe; *An*: Antrona zone; *B*: Biella pluton; *DB*: Dent Blanche Tectonic system; *Ge*: Gets nappe; *IV*: Ivrea-Verbano zone; *MR*: Monte Rosa nappe; *SC*: Strona-Ceneri zone; *Se*: Sesia zone; *Si*: Simme nappe; *Ts*: Tsaté nappe; *ZS*: Zermatt-Saas Fee nappe.

Contrary to the later crustal-scale Vanzone backfold, which is affecting the entire nappe stack (Figs. 4.9b, 4.13c), the earlier Mischabel backfolding phase only developed in the Grand St-Bernard nappe system and overlying units, and do not affect lower units such as Lower Penninic and Helvetic nappes. It is shown in particular by the studies of Milnes et al. (1981) and Steck (e.g. 1984, 2008; Steck et al. 2015), which indicate that the axial traces of the Mischabel backfold and associated lower Mittaghorn syncline do not cross the Rhône-Simplon ductile shear zone. These particular positions and structural characteristics of the Mischabel phase backfolds may indicate their possible development in response to the subduction, and incorporation in the accretionary wedge, of the thicker and more buoyant continental crust from the proximal domain of the Briançonnais s.l. margin.

This hypothesis is consistent with the short time interval separating the development of the Mischabel backfold from the subduction and prograde metamorphism of the Siviez-Mischabel nappe. Indeed, the Mischabel backfold developed during Late Eocene to earliest Oligocene, in the 40-30 Ma time range (cf. last paragraph), whereas the Eocene Flysch, stratigraphically deposited on top of the Barrhorn Series, predates subduction. Microfossils in the equivalent flysch from the Médianes Prealps indicate a Lutetian age (Caron et al. 1980; Fig. 3.15). As for the NW-directed emplacement of the Siviez-Mischabel nappe, it is dated at 41-36 Ma (Markley et al. 1998, 2002), an age that partly overlaps with the one inferred for the development of the Mischabel backfold. Our hypothesis is also consistent with the contrasting metamorphic imprint existing between the Siviez-Mischabel nappe and the more internal Mont Fort nappe. The Siviez-Mischabel nappe system shows a greenschist facies Alpine metamorphic imprint (e.g. Thélin et al. 1994; Steck et al. 2001; Bousquet et al. 2004) with HP-greenschist facies paragenesis described in Al-rich metasediments from the Barrhorn Series (estimated P-T: 3-8 kbar, 400-450 °C; Sartori 1990; Chopin et al. 2003). In the Mont Fort nappe, the presence in the Paleozoic basement of glaucophane (locally abundant), chloritoid, epidote, garnet and HP white micas

(e.g. Wegmann 1922; Argand 1934; Vallet 1950; Bearth 1963; Thélin et al. 1994; Steck et al. 2001, fig. 1) argue for epidote-blueschist facies conditions (Bousquet et al. 2004). Pseudomorphs after lawsonite have been described in in the Série Rousse in Ollomont valley (P. Manzotti, pers. com.) and the Bagnes valley (Besson 1986). Raman spectroscopy on graphite from metasediments of the Mesozoic cover of the nappe (Evolène Series and Série Rousse) indicates peak temperatures of 410-490 °C (cf. chap. 3.6).

The proposed hypothesis concerning the development of the earlier backfolds corroborates the hypothesis from Groppo et al. (2009; see also Beltrando et al. 2010b) who proposed to explain the Late Eocene decrease of the thermal gradient at the subduction zone evidenced in the Zermatt-Saas Fee nappe by the "locking" of the Alpine subduction in response to the arrival in the subduction zone of the buoyant Briançonnais block. It also corroborates the more general assumption of Escher and Beaumont (1997) and Beaumont et al. (1996) concerning the direct link proposed between incorporation of thicker continental crust into the subduction zone and the initiation of backfolding and the development of a doubly-vergent orogenic wedge. Compared to the slab breakoff model that has been frequently invoked to explain backfold formation (e.g. von Blanckenburg and Davies 1995, 1996; Sinclair 1997; Bergomi et al. 2015; Schlunegger and Kissling 2015), the proposed model allows to explain both: the development of multiple successive backfolding phases (such as the Mischabel, Vanzone and Glishorn-Berisal phases) related to the complex structure and multiple thickness variations of the subducting paleomargin; and the out-of-sequence development of the backfolds in the Central and Western Alps.

4.7. Conclusion

This study focuses on the structure, contacts and stratigraphy of the Permian-Jurassic Faisceau Vermiculaire series (incl. Cime Blanches and Frilihorn) and associated non-ophiolitic p.p. Upper Cretaceous calcschists (Série Rousse), which are both intercalated within the ophiolitic units in the area around Zermatt. It allows to revise several tectonic and paleogeographic attributions and to present a new tectonic model for the area.

Our lithological and stratigraphic observations allow: (i) to confirm the presence in the Faisceau Vermiculaire of widespread breccias, for the most part of probable Early to Late Jurassic age, that are intensely stretched and therefore locally difficult to recognize; (ii) to confirm the interpretation of the first authors suggesting the stratigraphic nature of the contacts between the Faisceau Vermiculaire and the overlying non-ophiolitic, p.p. Upper Cretaceous, calcschists of the Série Rousse, which constitute the lower part of the Schistes Lustrés of the Combin zone; (iii) to confirm the existence of a strong contrast in the Jurassic to Cretaceous/Paleogene stratigraphic sequences between the autochthonous cover of the Siviez-Mischabel nappe (Barrhorn Series, Briançonnais s.str.) and the series formed by the Faisceau Vermiculaire and Série Rousse, which is characteristic of a sedimentation in a deeper basin with an important clastic and detritic input (Prepiemont series); (iv) to interpret the contact of the Faisceau Vermiculaire and the Série Rousse with the basement forming the Alphubel anticline east of Zermatt, as a stratigraphic contact. The locally discordant character of this contact is interpreted as the result of the activity of synsedimentary Jurassic normal faults.

The Faisceau Vermiculaire and the Série Rousse are however in tectonic contact with the Siviez-Mischabel basement north of Zermatt, and this basement is separated from the one forming the Alphubel anticline by a deep early syncline, involving ophiolites of the Tsaté nappe. The eastward prolongation of this syncline in the Mischabel massif is potentially important but hidden

by the moraines and glaciers. For these tectonic reasons and the stratigraphic observations stated above, the Alphubel basement is most likely separated from the Siviez-Mischabel nappe by a tectonic contact.

We propose a new tectonic scheme for the structure of the Faisceau Vermiculaire and adjacent units. It involves an early northward folding of the Faisceau Vermiculaire together with the Série Rousse and ophiolitic Schistes Lustrés of the Tsaté nappe, followed by major backfolding responsible for the southward emplacement of these units above the HP Zermatt-Saas Fee and Monte Rosa nappes.

The ensemble formed by the Alphubel basement, the Faisceau Vermiculaire and the Série Rousse share an identical tectonic position with respect to the Siviez-Mischabel and Tsaté nappes, and mostly identical stratigraphic sequences, as the Mont Fort nappe outcropping north and west of the Dent Blanche klippe. Therefore, we interpret the Alphubel basement, the Faisceau Vermiculaire and the Série Rousse as the eastern prolongation of the Mont Fort nappe, in the lower limb of the Mischabel backfold.

Finally, the disappearance of the Barrhorn Series north of Zermatt and the complete absence of Upper Permian and younger levels on top of the Siviez-Mischabel basement, from this area to the Mischabel massif in the east, could represent the remnant of a major Jurassic paleofault scarp located between the Briançonnais swell and the Prepiemont basin. This paleofault could correspond to a first order discontinuity of the southern Briançonnais s.l. Jurassic margin. Our study thus seems to highlight some specific links between the structure of the paleomargin and the development of the successive deformation phases, in terms of the location of the nappe boundaries in the early formation of the orogenic wedge, and later, with respect to the location of the first backfolds that develop on a major discontinuity of the paleomargin.

Acknowledgements

I would like to thank Jean-Luc Epard very much for his involvement in this work, for the numerous discussions concerning the results and interpretations, for joining me several times on the field and helping with the writing of the manuscript. I would also like to thank Henri Masson for joining us various times on the field and for his constructive remarks regarding the interpretations, Christophe Jossevel for accompanying me numerous times on the field and for his helpful reflections, Paola Manzotti and Michel Ballèvre for the common field excursions in the Pancherot and Becca d'Aran areas, Yves Gouffon for is constructive and helpful comments that helped to improve the manuscript, Stefan Schmalholz, Lukas Baumgartner and Michel Ballèvre for the very constructive discussions and comments regarding the conditions and timing of the Mischabel backfold development, Martin Robyr for accompanying me in the Toûno and Boudri area and Didier Pantet for accompanying me in the upper Turtmann valley. Finally, I would like to thank Maud Jordan and Alexandra Demers-Roberge for their precious help in improving and correcting the manuscript.

I acknowledge the University of Lausanne for funding this work and the Société Académique Vaudoise for the additional financial support.

Chapter 5: General conclusion

This study, based on a multidisciplinary approach, relying primarily on an extensive fieldwork over a sector covering several Alpine valleys in SW Switzerland, allowed to better constrain the nature of different contacts around the Upper/Middle Penninic boundary. The study allowed in particular to revise some tectonic and paleogeographic attributions and to present a new tectonic model for the area.

This study highlights the difficulties that can be encountered in highly strained domains of mountain belts, in determining the nature of geological contacts. This is particularly true for the discrimination between originally stratigraphic and tectonic contacts, like nappe thrusts. The determination of the nature of the contacts often requires detailed structural studies at various scales (including multi-kilometer scale), especially when contacts separate lithologies of contrasting viscosities. For contacts involving sedimentary series, detailed stratigraphic studies appear as essential. Our study shows that the original nature of contacts initially corresponding to large-scale synsedimentary paleofaults is particularly delicate to identify. Original angular discordances may almost be fully obliterated in highly strained domains as the original obliquity of the fault with respect to bedding most often gradually decreases with strain. Such contacts are characterized by large-scale unconformities and may be confused with low-angle thrusts. The identification of locally preserved concordant stratigraphic sequences appears as key to recognize original stratigraphic contacts. For low-angle normal faults, concordant sections of the contact may however be preserved in much reduced proportions than the discordant sections corresponding to fault scarps. Our study suggests that deformed normal paleofaults, although most often not recognized as such, appear to be widespread in the internal part of the Alpine belt.

Our study of the debated contacts separating the Middle Penninic Mont Fort nappe from the Upper Penninic Schistes Lustrés and ophiolites of the Tsaté nappe, NW of the Dent Blanche klippe

(Fig. 5.1), allows to provide new and detailed data concerning these contacts and to propose well constrained hypothesis regarding their natures and positions. The proposed interpretations concerning these contacts are the following:

· The contact between the Mont Fort Paleozoic basement and the Triassic - Lower Cretaceous Evolène Series is reinterpreted as stratigraphic, as already proposed by Escher (1988). Several sections of this contact are discordant and are interpreted as corresponding to high-amplitude Jurassic normal paleofaults.

· The basal contact of the non-ophiolitic lower Schistes Lustrés forming the Série Rousse, over the Evolène Series and the Mont Fort Paleozoic basement is interpreted as stratigraphic as well. The Série Rousse, together with the Evolène Series, are interpreted as constituting the autochthonous sedimentary cover of the Mont Fort nappe. This interpretation is also in agreement with the tectonic scheme proposed by Escher (1988). The unconformable character of this contact is interpreted as resulting from the passive onlap and progressive sealing of remnants of the Jurassic paleofault scarps.

· The contact between the Série Rousse and the ophiolite-bearing Schistes Lustrés and associated slivers of meta(ultra-)basites is marked by the presence of thin, highly strained, slices of continent-derived metasediments (Frilihorn Series). It is interpreted as representing the major tectonic contact separating the Middle Penninic Mont Fort nappe from the Upper Penninic Tsaté nappe. We propose a redefinition of the Tsaté nappe by excluding the Série Rousse and including only the ophiolite-bearing Schistes Lustrés and associated meta(ultra-)basites. This definition actually corresponds to the first definition of the Tsaté nappe (Sartori 1987).

Fig. 5.1 Reinterpreted tectonic map of the Mont Fort nappe and surrounding units in SW Switzerland and NW Italy. After Argand (1908), Güller (1947), Bearth (1953a, 1964b, 1967a, 1973), Crespo (1984), Sartori (1987), Escher (1988), Allimann (1990), Girard (1995), Burri et al. (1998), Steck et al. (1999, 2015), Bucher et al. (2003a), Marthaler et al. (2008a, 2020a), Dal Piaz et al. (2015b) and own data. The dashed line inside the Tsaté complex marks the limit between two different tectonic units: the Tracuit-Aiguilles Rouges / Cornet Unit and the Série Grise. DB_B: Dent Blanche basement; DB_M: Dent Blanche Mesozoic cover; *EL*: Etirol-Levaz unit; *Fu*: Furgg zone; *Go*: Gornergrat nappe; *MBi*: internal Mont Blanc massif; *Pi*: Pillonet unit; SM_B: Siviez-Mischabel basement; SM_T: Siviez-Mischabel Triassic; *Ts*: Tsaté (= Combin zone s.str.); *To*: Toûno Series; *Wi*: Wildhorn nappe. ►

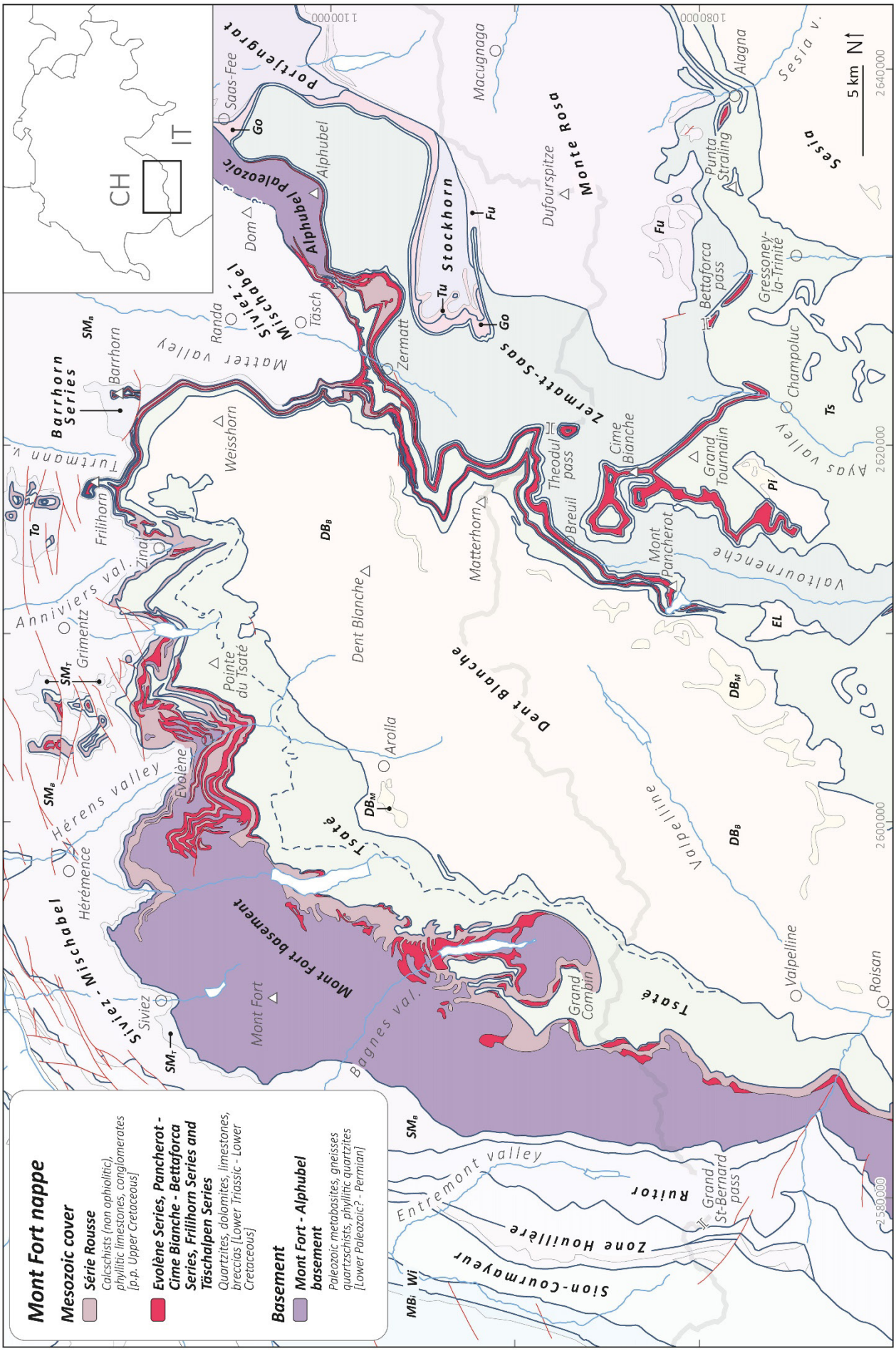
Mont Fort nappe
Mesozoic cover
Série Rousse
Calcschists (non ophiolitic), phyllitic limestones, conglomerates [p.p. Upper Cretaceous]
Evolène Series, Pancherot - Cime Bianche - Bettaforca Series, Frilihorn Series and Täschalpen Series
Quartzites, dolomites, limestones, breccias [Lower Triassic - Lower Cretaceous]
Basement
Mont Fort - Alphubel basement
Paleozoic metabasites, gneisses, quartzschists, phyllitic quartzites [Lower Paleozoic? - Permian]
CH
IT
5 km
N
Portjengrat
Alphubel
Saas-Fee
Macugnaga
Monte Rosa
Dufourspitze
Stockhorn
Zermatt-Saas
Zermatt
Randa
Täsch
Dom
Matter valley
Barrhorn
Barrhorn Series
Weisshorn
Matterhorn
Dent Blanche
Cervinia
Cime Blanche
Grand Tournalin
Mont Pancherot
Breuil
Theodul pass
Bettaforca pass
Gressoney-la-Trinité
Champoluc
Ayas valley
Valtournenche
Punta Straling
Alagna
Sesia v.
Sesia
Turtmann v.
Frilihorn
Zinal
Anniviers val.
Grimentz
Hérens valley
Evolène
Hérémence
Siviez - Mischabel
Siviez
Mont Fort
Pointe du Tsaté
Arolla
Tsaté
Mont Fort basement
Bagnes val.
Grand Combin
Valpelline
Valpelline
Roisan
Entremont valley
Grand St-Bernard pass
Ruitor
Zone Houillère
Sion-Courmayeur
Siviez - Mischabel
Go
Tu
Fu
To
Pi
EL
Ts
SMB
SMT
DBB
DBM
MB
Wi
2600000
2620000
2640000
2580000
1100000
1080000

Our study of the Permian-Jurassic Faisceau Vermiculaire series (including the Pancherot - Cime Bianche - Bettaforca and Frilihorn Series), in the area surrounding Zermatt, and of its contacts with the Paleozoic basement north and east of Zermatt, and with the Schistes Lustrés and ophiolites of the Combin zone and Zermatt-Saas Fee nappe, allows to propose new interpretations regarding the tectonic attribution of the Faisceau Vermiculaire and its structure.

· The contact between the Faisceau Vermiculaire series and the lower non-ophiolitic Schistes Lustrés is interpreted as stratigraphic, as already proposed by Güller (1947) and Bearth (1973) for example. Following Sartori (1987) and Escher (1988), for instance, these basal non-ophiolitic Schistes Lustrés are considered as the direct continuation of the Série Rousse east and south of the Dent Blanche klippe.

· The contact of the Faisceau Vermiculaire and the Série Rousse with the basement forming the Alphubel anticline (Alphubel “Lappen”; e.g. Staub 1942d; Müller 1983) is interpreted as stratigraphic. The locally discordant sections of this contact are interpreted as corresponding to remnants of Jurassic paleofaults.

· Following the interpretation of all recent authors, the contact of the Faisceau Vermiculaire and the Série Rousse with the Siviez Mischabel basement in the hinge of the Mischabel backfold and further east in the area of Täschalpen is considered as tectonic. We interpret this contact as extending NE into the Mischabel massif where it separates the Alphubel basement from the Siviez-Mischabel basement.

· We propose to interpret the ensemble formed by the Alphubel basement, the Faisceau Vermiculaire series and the Série Rousse as the continuation of the Mont Fort nappe, east and south of the Dent Blanche klippe, in the lower limb of the Mischabel backfold. This tectonic

interpretation is close to the one of Argand (e.g. 1911, 1916b), regarding the main outlines of the structural scheme.

· The tectonic map presented in Fig. 5.1 incorporates these different hypotheses. The proposed tectonic scheme is significantly different from those of the more up-to-date published tectonic maps (e.g. Steck et al. 1999, 2015, Tectonic map of Switzerland, 2005; Schmid et al. 2004, 2017). It emphasizes the significance of the Mont Fort nappe in the Penninic nappe stack, extending on both sides of the Dent Blanche klippe. The Mont Fort nappe, derived from the Prepiemont distal margin, constitutes a link between the Briançonnais units and the Piemont ophiolitic units, which appears to be essential for the understanding of the geological structure of the Penninic nappe stack.

References

Abbate, E., & Sagri, M. (1970). The eugeosynclinal sequences. *Sedimentary Geology*, *4*(3–4), 251–340. doi:10.1016/0037-0738(70)90018-7

Adatte, P., Dubas, A., Tache, E., & Strauss, F. (1992). *Géologie et minéralogie du haut Val de Rhêmes (Vallée d'Aoste)* [Travail de diplôme non publié, Université de Lausanne].

Agard, P. (2021). Subduction of oceanic lithosphere in the Alps: Selective and archetypal from (slow-spreading) oceans. *Earth-Science Reviews*, *214*, 103517. doi:10.1016/j.earscirev.2021.103517

Agard, P., Jolivet, L., & Goffé, B. (2001). Tectonometamorphic evolution of the Schistes Lustrés Complex; implications for the exhumation of HP and UHP rocks in the Western Alps. *Bulletin de la Société Géologique de France*, *172*(5), 617–636.

Aharonov, E., & Scholz, C. H. (2018). A Physics-Based Rock Friction Constitutive Law: Steady State Friction. *Journal of Geophysical Research: Solid Earth*, *123*(2), 1591–1614. doi:10.1002/2016JB013829

Allemann, R., & Vannay, J.-C. (1987). *Géologie et pétrographie des unités penniques entre le Valtournanche et le vallon de Cortoz (Val d'Aoste, Italie du Nord)* [Travail de diplôme non publié, Université de Lausanne].

Allimann, M. (1987). La nappe du Mont Fort dans le Val d'Hérens. *Bulletin de la Société Vaudoise des Sciences Naturelles*, *78*(372), 431–444. doi:10.5169/seals-278921

Allimann, M. (1989). Les brèches de la région d'Evolène (Nappe du Mont Fort, Valais, Suisse). *Schweizerische Mineralogische und Petrographische Mitteilungen*, *69*(2), 237–250. doi:10.5169/seals-52791

Allimann, M. (1990). *La nappe du Mont Fort dans le Val d'Hérens (Zone Pennique, Valais, Suisse)* [Thèse de doctorat, Université de Lausanne].

Andri, E., & Fanucci, F. (1973). Osservazioni sulla litologia e stratigrafia del Calcari a Calpionella liguri (Val Graveglia, Val di Vara). *Italian Journal of Geosciences*, *92*(1), 161–192.

Angiboust, S., Agard, P., Jolivet, L., & Beyssac, O. (2009). The Zermatt-Saas ophiolite: the largest (60-km wide) and deepest (c. 70-80 km) continuous slice of oceanic lithosphere detached from a subduction zone? *Terra Nova*, *21*(3), 171–180. doi:10/fvmssm

Angiboust, S., Glodny, J., Oncken, O., & Chopin, C. (2014). In search of transient subduction interfaces in the Dent Blanche–Sesia Tectonic System (W. Alps). *Lithos*, *205*, 298–321. doi:10/f6jzrf

Ansermet, S., & Meisser, N. (2012). *Mines et minéraux du Valais. II Anniviers et Tourtemagne* (Musée de la nature, Sion, Musée cantonal de géologie, Lausanne.). Ayer: Editions Portes-Plumes.

Argand, E. (1908). Carte géologique du massif de la Dent Blanche. Carte géol. spéc. 52. Comm. géol. Suisse.

Argand, E. (1909). L'exploration géologique Alpes pennines centrales. *Bulletin de la Société Vaudoise des Sciences Naturelles*, *45*(166), 217–276. doi:10/gfj2z8

Argand, E. (1911). Les nappes de recouvrement des Alpes Pennines et leurs prolongements structuraux. *Matériaux pour la Carte Géologique de la Suisse [n.s.]*, *31*(1), 1–29.

Argand, E. (1916a). Compte-rendu de l'excursion de la Société géologique suisse à Zermatt les 16, 17 et 18 septembre 1915. *Eclogae Geologicae Helvetiae*, *14*, 192–204. doi:10/gfkwj8

Argand, E. (1916b). Sur l'arc des Alpes occidentales. *Eclogae Geologicae Helvetiae*, *14*, 145–191.

Argand, E. (1920). Plissements précurseurs et plissements tardifs des chaînes de montagnes. *Actes de la Société Helvétique des Sciences Naturelles*, *101*(2), 13–39. doi:10.5169/seals-90310

Argand, E. (1923). La géologie des environs de Zermatt. *Actes de la Société Helvétique des Sciences Naturelles*, *104*(2), 96–110. doi:10.5169/SEALS-90336

Argand, E. (1924). La tectonique de l'Asie. In *Congrès géologique international (XIIIe session), Belgique 1922* (Vol. 1/5, pp. 171–372). Liège: Vaillant-Carmanne.

Argand, E. (1934). La zone pennique. In *Guide géologique de la Suisse. Fasc. III: Introductions générales* (Société Géologique Suisse., pp. 149–189). Basel: Wepf.

Ayrton, S., Bugnon, C., Haarpaintner, T., Weidmann, M., & Frank, E. (1982). Géologie du front de la nappe de la Dent-Blanche dans la région des Monts-Dolins, Valais. *Eclogae Geologicae Helvetiae*, *75*(2), 269–286. doi:10.5169/seals-165231

Baillifard, F.-J. (1998). *Relation socle-couverture au pied du barrage de Mauvoisin* [Travail de diplôme non publié, Université de Lausanne].

Baldelli, C., Dal Piaz, G. V., & Polino, R. (1983). Le quarziti a manganese e cromo di Varenche-St. Barthelemy, una sequenza di copertura oceanica della falda Piemontese. *Ofioliti*, *8*(2), 207–221.

Balestro, G., Nosenzo, F., Cadoppi, P., Fioraso, G., Groppo, C., & Festa, A. (2020). Geology of the southern Dora-Maira Massif: insights from a sector with mixed ophiolitic and continental rocks (Valmala tectonic unit, Western Alps). *Journal of Maps*, *16*(2), 736–744. doi:10.1080/17445647.2020.1824825

Ballèvre, M., Camonin, A., Manzotti, P., & Poujol, M. (2020). A step towards unraveling the paleogeographic attribution of pre-Mesozoic basement complexes in the Western Alps based on U–Pb geochronology of Permian magmatism. *Swiss Journal of Geosciences*, *113*(1), 12. doi:10.1186/s00015-020-00367-1

Ballèvre, M., Kienast, J.-R., & Vuichard, J.-P. (1986). La "nappe de la Dent-Blanche" (Alpes occidentales): deux unités austroalpines indépendantes. *Eclogae Geologicae Helvetiae*, *79*(1), 57–74. doi:10/gfkn7k

Ballèvre, M., Manzotti, P., & Dal Piaz, G. V. (2018). Pre-Alpine (Variscan) Inheritance: A Key for the Location of the Future Valaisan Basin (Western Alps). *Tectonics*, *37*(3), 786–817. doi:10/gdgrkz

Ballèvre, M., & Merle, O. (1993). The Combin fault: compressional reactivation of a Late Cretaceous-Early Tertiary detachment fault in the Western Alps. *Schweizerische Mineralogische und Petrographische Mitteilungen*, *73*(2), 205–227.

Barféty, J.-C., & Gidon, M. (1984). Un exemple de sédimentation sur un abrupt de faille fossile : Le Lias du versant est du massif du Taillefer (Zone dauphinoise, Alpes occidentales). *Revue de géographie physique et de géologie dynamique*, *25*(4), 267–286.

Barféty, J.-C., Gidon, M., Lemoine, M., & Mouterde, R. (1979). Tectonique synsédimentaire liasique dans les massifs cristallins de la zone externe des Alpes occidentales françaises: la faille du col d'Ornon. *Comptes Rendus de l'Académie des sciences Paris*, *(D) 289*, 1207–1210.

Barnicoat, A. C., Rex, D. C., Guise, P. G., & Cliff, R. A. (1995). The timing of and nature of greenschist facies deformation and metamorphism in the upper Pennine Alps. *Tectonics*, *14*(2), 279–293.

Baud, A. (1987). Stratigraphie et sédimentologie des calcaires de Saint-Triphon (Trias, Préalpes, Suisse et France). *Mémoire de Géologie (Lausanne)*, *1*, 326 pp.

Baud, A., Plasencia, P., Hirsch, F., & Richoz, S. (2016). Revised middle Triassic stratigraphy of the Swiss Prealps based on conodonts and correlation to the Briançonnais (Western Alps). *Swiss Journal of Geosciences*, *109*(3), 365–377. doi:10/gcsmn7

Baud, A., & Septfontaine, M. (1980). Présentation d'un profil palinspastique de la nappe des Préalpes médianes en Suisse occidentale. *Eclogae Geologicae Helvetiae*, *73*(2), 651–660. doi:10.5169/seals-164982

Bearth, P. (1952). Geologie und Petrographie des Monte Rosa. *Beiträge zur Geologischen Karte der Schweiz*, *96*, 1–94.

Bearth, P. (1953a). Blatt 535 Zermatt. - Geologischer Atlas der Schweiz 1:25 000, Karte 29.

Bearth, P. (1953b). *Blatt 535 Zermatt. - Geologischer Atlas der Schweiz 1: 25 000, Erläuterungen 29*.

Bearth, P. (1963). Contribution à la subdivision tectonique et stratigraphique du Cristallin de la nappe du Grand-St-Bernard dans le Valais (Suisse). In Société Géologique de France (Ed.), *Livre à la Mémoire du Professeur Paul Fallot. Tome II: L'évolution paléogéographique et structurale des domaines méditerranéens et alpins d'Europe* (pp. 407–418).

Bearth, P. (1964a). *Blatt 1328 Randa. - Geologischer Atlas der Schweiz 1: 25 000, Erläuterungen 43*.

Bearth, P. (1964b). Blatt 1328 Randa. - Geologischer Atlas der Schweiz 1:25 000, Karte 43.

Bearth, P. (1967a). *Die Ophiolithe der Zone von Zermatt-Saas Fee*. Kümmerli & Frey, Bern.

Bearth, P. (1967b). Excursion Nr. 10 Visp-St. Niklaus-Zermatt-Gornergrat. In *Geologischer Führer der Schweiz* (Schweizerischen Geologischen Gesellschaft., Vol. 3, pp. 1465–157). Basel: Wepf & Co.

Bearth, P. (1973). Gesteins- und Mineralparagenesen aus den Ophiolithen von Zermatt. *Schweizerische Mineralogische und Petrographische Mitteilungen*, *53*(2), 299–335. doi:10.5169/SEALS-41387

Bearth, P. (1976). Zur Gliederung der Bündnerschiefer in der Region von Zermatt. *Eclogae Geologicae Helvetiae*, *69*(1), 149–161. doi:10.5169/SEALS-164499

Bearth, P. (1978). Blatt 1308 St. Niklaus. - Geologischer Atlas der Schweiz 1:25 000, Karte 71.

Bearth, P. (1980). *Blatt 1308 St. Niklaus. - Geologischer Atlas der Schweiz 1: 25 000, Erläuterungen 71*.

Bearth, P., & Schwandler, H. (1981). The post-Triassic sediments of the ophiolite zone Zermatt-Saas Fee and the associated manganese mineralizations. *Eclogae Geologicae Helvetiae*, *74*(1), 189–205. doi:10.5169/SEALS-165098

Beaumont, C., Ellis, S., Hamilton, J., & Fullsack, P. (1996). Mechanical model for subduction-collision tectonics of Alpine-type compressional orogens. *Geology*, *24*(8), 675. doi:10.1130/0091-7613(1996)024<0675:MMFSCT>2.3.CO;2

Beccaluva, L., Dal Piaz, G., & Macciotta, G. (1984). Transitional to normal MORB affinities in ophiolitic metabasites from the Zermatt-Saas, Combin and Antrona units, Western Alps: implications for the paleogeographic evolution of the Western Tethyan Basin. *Geologie en mijnbouw*, *63*(2), 165–177.

Bellahsen, N., Jolivet, L., Lacombe, O., Bellanger, M., Boutoux, A., Garcia, S., Mouthereau, F., Le Pourhiet, L., & Gumiaux, C. (2012). Mechanisms of margin inversion in the external Western Alps: Implications for crustal rheology. *Tectonophysics*, *560–561*, 62–83. doi:10.1016/j.tecto.2012.06.022

Beltrando, M., Compagnoni, R., & Lombardo, B. (2010a). (Ultra-) High-pressure metamorphism and orogenesis: An Alpine perspective. *Gondwana Research*, *18*(1), 147–166. doi:10/drb9z2

Beltrando, M., Lister, G., Hermann, J., Forster, M., & Compagnoni, R. (2008). Deformation mode switches in the Penninic units of the Urtier Valley (Western Alps): Evidence for a dynamic orogen. *Journal of Structural Geology*, *30*(2), 194–219. doi:10/bzdbhg

Beltrando, M., Lister, G. S., Forster, M., Dunlap, W. J., Fraser, G., & Hermann, J. (2009). Dating microstructures by the 40 Ar/ 39 Ar step-heating technique: Deformation–pressure–temperature–time history of the Penninic Units of the Western Alps. *Lithos*, *113*(3–4), 801–819. doi:10/b69n5x

Beltrando, M., Manatschal, G., Mohn, G., Dal Piaz, G. V., Vitale Brovarone, A., & Masini, E. (2014). Recognizing remnants of magma-poor rifted margins in high-pressure orogenic belts: The Alpine case study. *Earth-Science Reviews*, *131*, 88–115. doi:10/f5xdvw

Beltrando, M., Rubatto, D., & Manatschal, G. (2010b). From passive margins to orogens: The link between ocean-continent transition zones and (ultra)high-pressure metamorphism. *Geology*, *38*(6), 559–562. doi:10/fcb5j3

Berger, A., Rosenberg, C., & Schmid, S. M. (1996). Ascent, emplacement and exhumation of the Bergell pluton within the Southern Steep Belt of the Central Alps. *Schweizerische Mineralogische und Petrographische Mitteilungen*, *76*(3), 357–382. doi:10.5169/SEALS-57706

Bergomi, M. A., Dal Piaz, G. V., Malusà, M. G., Monopoli, B., & Tunesi, A. (2017). The Grand St Bernard-Briançonnais Nappe System and the Paleozoic Inheritance of the Western Alps Unraveled by Zircon U-Pb Dating. *Tectonics*, *36*(12), 2950–2972. doi:10.1002/2017TC004621

Bergomi, M. A., Zanchetta, S., & Tunesi, A. (2015). The Tertiary dike magmatism in the Southern Alps: geochronological data and geodynamic significance. *International Journal of Earth Sciences*, *104*(2), 449–473. doi:10.1007/s00531-014-1087-5

Bertok, C., Martire, L., Perotti, E., d'Atri, A., & Piana, F. (2012). Kilometre-scale palaeoescarpments as evidence for Cretaceous synsedimentary tectonics in the External Briançonnais Domain (Ligurian Alps, Italy). *Sedimentary Geology*, *251–252*, 58–75. doi:10/fxv8p3

Bertotti, G., Siletto, G. B., & Spalla, M. I. (1993). Deformation and metamorphism associated with crustal rifting: The Permian to Liassic evolution of the Lake Lugano-Lake Como area (Southern Alps). *Tectonophysics*, *226*(1–4), 271–284. doi:10.1016/0040-1951(93)90122-Z

Besson, O. (1986). *Géologie des nappes du Mt Fort et du Tsaté dans le Haut Val de Bagnes (Mauvoisin)* [Travail de diplôme non publié, Université de Lausanne].

Beyssac, O., Bollinger, L., Avouac, J.-P., & Goffé, B. (2004). Thermal metamorphism in the lesser Himalaya of Nepal determined from Raman spectroscopy of carbonaceous material. *Earth and Planetary Science Letters*, *225*(1–2), 233–241. doi:10.1016/j.epsl.2004.05.023

Beyssac, O., Brunet, F., Petitet, J.-P., Goffé, B., & Rouzaud, J.-N. (2003a). Experimental study of the microtextural and structural transformations of carbonaceous materials under pressure and temperature. *European Journal of Mineralogy*, *15*(6), 937–951. doi:10.1127/0935-1221/2003/0015-0937

Beyssac, O., Goffé, B., Chopin, C., & Rouzaud, J. N. (2002). Raman spectra of carbonaceous material in metasediments: a new geothermometer. *Journal of Metamorphic Geology*, *20*(9), 859–871. doi:10/b7p8kx

Beyssac, O., Goffé, B., Petitet, J.-P., Froigneux, E., Moreau, M., & Rouzaud, J.-N. (2003b). On the characterization of disordered and heterogeneous carbonaceous materials by Raman spectroscopy. *Spectrochimica Acta Part A: Molecular and Biomolecular Spectroscopy*, *59*(10), 2267–2276. doi:10.1016/S1386-1425(03)00070-2

Beyssac, O., & Lazzeri, M. (2012). Application of Raman spectroscopy to the study of graphitic carbons in the Earth Sciences. In G. Ferraris, J. Dubessy, M.-C. Caumon, & F. Rull (Eds.), *Raman spectroscopy applied to Earth sciences and cultural heritage* (pp. 415–454). European Mineralogical Union. doi:10.1180/EMU-notes.12.12

Beyssac, O., Pattison, D. R. M., & Bourdelle, F. (2019). Contrasting degrees of recrystallization of carbonaceous material in the Nelson aureole, British Columbia and Ballachulish aureole, Scotland, with implications for thermometry based on Raman spectroscopy of carbonaceous material. *Journal of Metamorphic Geology*, *37*(1), 71–95. doi:10/ggdvjn

Bigi, G., Cosentino, D., Parotto, M., & Sartori, R. (1992). Structural Model of Italy. Florence: S.E.L.C.A.

Bill, M., Bussy, F., Cosca, M., Masson, H., & Hunziker, J. C. (1997). High-precision U-Pb and 40Ar/39Ar dating of an Alpine ophiolite (Gets nappe, French Alps). *Eclogae Geologicae Helvetiae*, *90*(1), 43–54. doi:10.5169/seals-168144

Bill, M., O'Dogherty, L., Guex, J., Baumgartner, P. O., & Masson, H. (2001). Radiolarite ages in Alpine-Mediterranean ophiolites: Constraints on the oceanic spreading and the Tethys-Atlantic connection. *Geological Society of America Bulletin*, *113*(1), 129–143. doi:10.1130/0016-7606(2001)113<0129:RAIAMO>2.0.CO;2

Bistacchi, A., Dal Piaz, G., Massironi, M., Zattin, M., & Balestrieri, M. (2001). The Aosta–Ranzola extensional fault system and Oligocene–Present evolution of the Austroalpine–Penninic wedge in the northwestern Alps. *International Journal of Earth Sciences*, *90*(3), 654–667. doi:10.1007/s005310000178

Bistacchi, A., Eva, E., Massironi, M., & Solarino, S. (2000). Miocene to Present kinematics of the NW-Alps: evidences from remote sensing, structural analysis, seismotectonics and thermochronology. *Journal of Geodynamics*, *30*(1–2), 205–228. doi:10.1016/S0264-3707(99)00034-4

Bonini, M., Sani, F., & Antonielli, B. (2012). Basin inversion and contractional reactivation of inherited normal faults: A review based on previous and new experimental models. *Tectonophysics*, *522–523*, 55–88. doi:10.1016/j.tecto.2011.11.014

Botteron, G. (1961). Etude géologique de la région du Mont d'Or (Préalpes romandes). *Eclogae Geologicae Helvetiae*, *54*(1), 29–106. doi:10.5169/seals-162815

Bourbon, M., Caron, J. M., Lemoine, M., & Tricart, P. (1979). Stratigraphie des schistes lustrés piémontais dans les Alpes cottiennes (Alpes occidentales franco-italiennes): nouvelle interprétation et conséquences géodynamiques. *Compte Rendu. Sommaire des Séances. Société Géologique de France*, *4*, 180–182.

Bousquet, R., Engi, M., Gosso, G., Oberhänsli, R., Berger, A., Spalla, M. I., Zucali, M., & Goffé, B. (2004). Transition from the Western to the Central Alps. In R. Oberhänsli (Ed.), Metamorphic structure of the Alps: explanatory notes to the map 1:100 000. *Mitteilungen der Oesterreichischen Mineralogischen Gesellschaft*, *149*, 145–156.

Bousquet, R., Oberhänsli, R., Goffé, B., Wiederkehr, M., Koller, F., Schmid, S. M., Schuster, R., Engi, M., Berger, A., & Martinotti, G. (2008). Metamorphism of metasediments at the scale of an orogen: a key to the Tertiary geodynamic evolution of the Alps. *Geological Society, London, Special Publications*, *298*(1), 393–411. doi:10.1144/SP298.18

Boutoux, A., Bellahsen, N., Lacombe, O., Verlaguet, A., & Mouthereau, F. (2014). Inversion of pre-orogenic extensional basins in the external Western Alps: Structure, microstructures and restoration. *Journal of Structural Geology*, *60*, 13–29. doi:10/f5t72m

Boutoux, A., Bellahsen, N., Nanni, U., Pik, R., Verlaguet, A., Rolland, Y., & Lacombe, O. (2016). Thermal and structural evolution of the external Western Alps: Insights from (U–Th–Sm)/He thermochronology and RSCM thermometry in the Aiguilles Rouges/Mont Blanc massifs. *Tectonophysics*, *683*, 109–123. doi:10.1016/j.tecto.2016.06.010

Bucher, K., Dal Piaz, G. V., Oberhänsli, R., Gouffon, Y., Martinotti, G., & Polino, R. (2003a). Blatt 1347 Matterhorn. - Geologischer Atlas der Schweiz 1:25 000, Karte 107.

Bucher, K., Dal Piaz, G. V., Oberhänsli, R., Gouffon, Y., Martinotti, G., & Polino, R. (2004a). *Blatt 1347 Matterhorn. - Geologischer Atlas der Schweiz 1: 25 000, Erläuterungen 107*.

Bucher, K., Fazis, Y., de Capitani, C., & Grapes, R. (2005). Blueschists, eclogites, and decompression assemblages of the Zermatt-Saas ophiolite: High-pressure metamorphism of subducted Tethys lithosphere. *American Mineralogist*, *90*(5–6), 821–835. doi:10.2138/am.2005.1718

Bucher, K., & Stober, I. (2021). Metamorphic gabbro and basalt in ophiolitic and continental nappes of the Zermatt region (Western Alps). *Swiss Journal of Geosciences*, *114*(1), 12. doi:10.1186/s00015-021-00390-w

Bucher, K., Weisenberger, T. B., Klemm, O., & Weber, S. (2019). Decoding the complex internal chemical structure of garnet porphyroblasts from the Zermatt area, Western Alps. *Journal of Metamorphic Geology*, *37*(9), 1151–1169. doi:10.1111/jmg.12506

Bucher, K., Weisenberger, T. B., Weber, S., Klemm, O., & Corfu, F. (2020). The Theodul Glacier Unit, a slab of pre-Alpine rocks in the Alpine meta-ophiolite of Zermatt-Saas, Western Alps. *Swiss Journal of Geosciences*, *113*(1), 1. doi:10.1186/s00015-020-00354-6

Bucher, S. (2003). *The Briançonnais units along the ECORS-CROP transect (Italian-French Alps): structures, metamorphism and geochronology* [Ph.D. thesis, University of Basel]. https://edoc.unibas.ch/326/1/DissB_7335.pdf

Bucher, S., Schmid, S. M., Bousquet, R., & Fugenschuh, B. (2003b). Late-stage deformation in a collisional orogen (Western Alps): nappe refolding, back-thrusting or normal faulting? *Terra Nova*, *15*(2), 109-117. doi:10/bpq9xf

Bucher, S., Ulardic, C., Bousquet, R., Ceriani, S., Fügenschuh, B., Gouffon, Y., & Schmid, S. M. (2004b). Tectonic evolution of the Briançonnais units along a transect (ECORS-CROP) through the Italian-French Western Alps. *Eclogae Geologicae Helvetiae*, *97*(3), 321–345. doi:10/ctfsz9

Burg, J.-P., & Gerya, T. V. (2005). The role of viscous heating in Barrovian metamorphism of collisional orogens: thermomechanical models and application to the Lepontine Dome in the Central Alps. *Journal of Metamorphic Geology*, *23*(2), 75–95. doi:10.1111/j.1525-1314.2005.00563.x

Burri, M. (1983). Le front du Grand St-Bernard du val d'Hérens au val d'Aoste. *Eclogae Geologicae Helvetiae*, *76*(3), 469–490. doi:10.5169/seals-165373

Burri, M., Allimann, M., Chessex, R., Dal Piaz, G. V., Della Valle, G., Dubois, L., Gouffon, Y., Guermani, A., Hagen, T., Krummenacher, D., & Looser, M.-O. (1998). Feuille 1346 Chanrion, avec partie nord de la feuille 1366 Mont Vélan. - Atlas géologique de la Suisse 1:25 000, Carte 101.

Burri, M., Dal Piaz, G. V., Della Valle, G., Gouffon, Y., & Guermani, A. (1999). *Feuille 1346 Chanrion, avec partie nord de la feuille 1366 Mont Vélan. - Atlas géologique de la Suisse 1:25 000, Notice explicative 101*.

Bussy, F., Derron, M.-H., Jacquod, J., Sartori, M., & Thélin, P. (1996a). The 500 Ma-old Thyon metagranite: a new A-type granite occurrence in the western Penninic Alps (Wallis, Switzerland). *European Journal of Mineralogy*, *8*(3), 565–576. doi:10.1127/ejm/8/3/056

Bussy, F., Sartori, M., & Thélin, P. (1996b). U-Pb zircon dating in the middle Penninic basement of the Western Alps (Valais, Switzerland). *Schweizerische Mineralogische und Petrographische Mitteilungen*, *76*, 81-84. doi:10.5169/seals-57689

Bussy, F., & von Raumer, J. F. (1994). U–Pb geochronology of Palaeozoic magmatic events in the Mont-Blanc crystalline massif, Western Alps. *Schweizerische Mineralogische und Petrographische Mitteilungen*, *74*, 514–515. doi:10.5169/seals-56355

Bustin, R. M., Rouzaud, J.-N., & Ross, J. V. (1995). Natural graphitization of anthracite: Experimental considerations. *Carbon*, *33*(5), 679–691. doi:10.1016/0008-6223(94)00155-S

Caby, R. (1981). Le Mésozoïque de la zone du Combin en Val d'Aoste (Alpes Graies): Imbrications tectoniques entre séries issues des domaines pennique, austroalpin et océanique. *Géologie Alpine*, *57*, 5–13.

Caby, R., Kienast, J. R., & Saliot, P. (1978). Structure, métamorphisme et modèle d'évolution tectonique des Alpes occidentales. *Rev. Geogr. Phys. Geol. Dyn*, *20*(4), 307–322.

Candioti, L. G., Duretz, T., Moulas, E., & Schmalholz, S. M. (2021). Buoyancy versus shear forces in building orogenic wedges. *Solid Earth*, *12*(8), 1749–1775. doi:10.5194/se-12-1749-2021

Cardello, G. L., Di Vincenzo, G., Giorgetti, G., Zwingmann, H., & Mancktelow, N. (2019). Initiation and development of the Pennine Basal Thrust (Swiss Alps): a structural and geochronological study of an exhumed megathrust. *Journal of Structural Geology*, *126*, 338–356. doi:10/gf7s4s

Cardello, G. L., & Mancktelow, N. S. (2014). Cretaceous syn-sedimentary faulting in the Wildhorn Nappe (SW Switzerland). *Swiss Journal of Geosciences*, *107*(2–3), 223–250. doi:10/gcsmnt

Caron, C., Homewood, P., Morel, R., & van Stuijvenberg, J. (1980). Témoins de la Nappe du Gurnigel sur les Préalpes Médianes: une confirmation de son origine ultrabriançonnaise. *Bulletin de la Société Fribourgeoise des Sciences Naturelles*, *69*(1), 64–79. doi:10.5169/SEALS-308586

Caron, C., Homewood, P., & Wildi, W. (1989). The original Swiss flysch: a reappraisal of the type deposits in the Swiss prealps. *Earth-Science Reviews*, *26*(1–3), 1–45. doi:10.1016/0012-8252(89)90002-0

Caron, J.-M. (1977). Lithostratigraphie et tectonique des schistes lustrés dans les Alpes cottiennes septentrionales et en Corse orientale [Thèse de doctorat, Université Louis Pasteur de Strasbourg]. *Sciences Géologiques. Mémoire*, *48*, 1–330.

Cartwright, I., & Barnicoat, A. C. (2002). Petrology, geochronology, and tectonics of shear zones in the Zermatt-Saas and Combin zones of the Western Alps. *Journal of Metamorphic Geology*, *20*(2), 263-281.

Chadwick, B. (1974). Glaucophane Fabric in the Cover of the Monte Rosa Nappe, Zermatt–Saas Fee, Southwest Switzerland. *Geological Society of America Bulletin*, *85*(6), 907–909. doi:10.1130/0016-7606(1974)85<907:GFITCO>2.0.CO;2

Chenin, P., Manatschal, G., Decarlis, A., Schmalholz, S. M., Duretz, T., & Beltrando, M. (2019). Emersion of Distal Domains in Advanced Stages of Continental Rifting Explained by Asynchronous Crust and Mantle Necking. *Geochemistry, Geophysics, Geosystems*, *20*(8), 3821–3840. doi:10/ggbv83

Chessex, R. (1959). La géologie de la haute vallée d'Abondance, Haute-Savoie (France). *Eclogae Geologicae Helvetiae*, *52*(1), 295. doi:10/gfn43j

Chessex, R. (1995). Tectonomagmatic setting of the Mont Fort nappe basement, Penninic Domain, Western Alps, Switzerland. In Ö. Pişkin, M. Ergün, M. Y. Savaşcin, & G. Tarcan (Eds.), *Proceedings of the International Earth Sciences Colloquium on the Aegean Region, Izmir - Güllück, Turkey* (Vol. 1, pp. 19–35).

Chopin, C., Goffe, B., Ungaretti, L., & Oberti, R. (2003). Magnesiostaurolite and zincostaurolite: mineral description with a petrogenetic and crystal-chemical update. *European Journal of Mineralogy*, *15*(1), 167–176. doi:10.1127/0935-1221/2003/0015-0167

Ciarapica, G., Passeri, L., Bonetto, F., & Dal Piaz, G. V. (2016). Facies and Late Triassic fossils in the Roisan zone, Austroalpine dent blanche and Mt Mary-Cervino nappe system, NW Alps. *Swiss Journal of Geosciences*, *109*(1), 69–81.

Claudel, M.-E., Dumont, T., & Tricart, P. (1997). Une preuve d'extension contemporaine de l'expansion océanique de la Téthys ligure en Briançonnais : les failles du Vallon Laugier. *Comptes Rendus de l'Académie des Sciences Paris, Sciences de la terre et des planètes*, *(IIA) 325*(4), 273–279. doi:10/dcj2bj

Compagnoni, R. (1977). The Sesia-Lanzo zone: high pressure - low temperature metamorphism in the Austroalpine continental margin. *Rendiconti della Società Italiana di Mineralogia e Petrologia*, *33*, 335–374.

Conti, P., Manatschal, G., & Pfister, M. (1994). Synrift sedimentation, Jurassic and Alpine tectonics in the central Ortler nappe (Eastern Alps, Italy). *Eclogae Geologicae Helvetiae*, *87*(1), 63–90. doi:10.5169/seals-167443

Cortiana, G., Dal Piaz, G. V., Del Moro, A., Hunziker, J. C., & Martin, S. (1998). 40Ar-39Ar and Rb-Sr dating of the Pillonet klippe and Sesia-Lanzo basal slice in the Ayas valley and evolution of the Austroalpine-Piedmont nappe stack. *Memorie di Scienze Geologiche*, *50*, 177–194.

Crespo, A. (1984). *Géologie des unités penniques au NW de Zermatt (Valais, Suisse)* [Travail de diplôme non publié, Université de Lausanne].

Crespo-Blanc, A., Masson, H., Sharp, Z., Cosca, M., & Hunziker, J. (1995). A stable and 40Ar/39Ar isotope study of a major thrust in the Helvetic nappes (Swiss Alps): evidence for fluid flow and constraints on nappe kinematics. *Geological Society of America Bulletin*, *107*(10), 1129–1144.

Dal Piaz, G., Cortiana, G., Del Moro, A., Martin, S., Pennacchioni, G., & Tartarotti, P. (2001). Tertiary age and paleostructural inferences of the eclogitic imprint in the Austroalpine outliers and Zermatt–Saas ophiolite, western Alps. *International Journal of Earth Sciences*, *90*(3), 668–684. doi:10/cnd29q

Dal Piaz, G. V. (1965). La formazione mesozoica dei calcescisti con pietre verdi fra la Valsesia e la Valtournenche ed i suoi rapporti strutturali con il ricoprimento Monte Rosa e con la zona Sesia-Lanzo. *Bollettino della Società geologica italiana*, *84*, 67–104.

Dal Piaz, G. V. (1971). Alcune considerazioni sulla genesi delle ofioliti piemontesi e dei giacimenti ad esse associati. *Bollettino della Associaizione Mineraria Subalpina*, *8*(3–4), 365–388.

Dal Piaz, G. V. (1974). Le métamorphisme de haute pression et basse température dans l'évolution structurale du bassin ophiolitique alpino-apenninique (1ère partie: Considérations paléogéographiques). *Bollettino della Società geologica italiana*, *93*(2), 437–467.

Dal Piaz, G. V. (1988). Revised setting of the Piedmont zone in the northern Aosta Valley, Western Alps. *Ofioliti*, *13*(2–3), 157–162.

Dal Piaz, G. V. (1999). The Austroalpine-Piedmont nappe stack and the puzzle of Alpine Tethys. *Memorie di Scienze Geologiche*, *51*(1), 155–176.

Dal Piaz, G. V., Bistacchi, A., Gianotti, F., Monopoli, B., & Passeri, L. (2015a). *Note illustrative della Carta Geologica d'Italia alla scala 1: 50.000, Foglio 070 Monte-Cervino*. Roma: Servizio Geologico d'Italia.

Dal Piaz, G. V., Bistacchi, A., Gianotti, F., Monopoli, B., & Passeri, L. (2015b). Carta Geologica d'Italia alla scala 1: 50.000, Foglio 070 Monte-Cervino. Roma: Servizio Geologico d'Italia.

Dal Piaz, G. V., & Ernst, W. G. (1978). Areal geology and petrology of eclogites and associated metabasites of the Piemonte ophiolite nappe, Breuil-St. Jacques area, Italian Western Alps. *Tectonophysics*, *51*(1), 99-126. doi:10.1016/0040-1951(78)90053-7

Dal Piaz, G. V., Hunziker, J. C., & Martinotti, G. (1972). La Zona Sesia-Lanzo e l'evoluzione tettonico-metamorfica delle Alpi nordoccidentali interne. *Memorie della Società Geologica Italiana*, *11*, 433-466.

Dal Piaz, G. V., Venturelli, G., Spadea, P., & Di Battistini, G. (1981). Geochemical features of metabasalts and metagabbros from the Piemonte ophiolite nappe, Italian Western Alps. *Neues Jahrbuch für Mineralogie. Abhandlungen*, *142*(3), 248–269.

Dall'Agnolo, S. (1997). *Die Kreide und das Tertiär der Brekziendecke in den französischen und schweizerischen Voralpen: Stratigraphie, Sedimentologie und Geodynamik (These Nr. 1146)* [Ph.D. thesis, Universität Freiburg, Schweiz].

Dall'Agnolo, S. (2000). Le Crétacé de la Nappe de la Brèche (Préalpes franco-suisses). Données nouvelles et essai de synthèse stratigraphique et paléogéographique. *Eclogae Geologicae Helvetiae*, *93*(2), 157–174. doi:10.5169/seals-168814

De Lepinay, B. (1981). *Etude géologique de la région des Gets et de Samoëns (Haute Savoie). Les rapports entre les Préalpes du Chablais (nappe de la Brèche et nappe des Gets) et les unités delphino-helvétiques.* [Thèse de doctorat, Université Pierre et Marie Curie, Paris]. https://tel.archives-ouvertes.fr/tel-00635406

de Szepessy Schaurek, A. (1949). *Geologische Untersuchungen im Gd. Combin-Gebiet zwischen Dranse de Bagnes und Dranse d'Entremont* [Ph.D. thesis, ETH Zürich]. https://doi.org/10.3929/ethz-a-000099247

De Wever, P., Baumgartner, P. O., & Polino, R. (1987). Précision sur les datations de la base des Schistes Lustrés postophiolitiques dans les Alpes cottiennes. *Comptes rendus de l'Académie des sciences Paris*, *II* (305), 487–491.

De Wever, P., & Caby, R. (1981). Datation de la base des schistes lustrés postophiolitiques par des radiolaires (Oxfordien-Kimméridgien moyen) dans les Alpes Cottiennes (Saint Véran, France). *Comptes Rendus de l'Académie des Sciences*, *(II) 292*, 467–472.

Debelmas, J. (1955). *Les zones subbriançonnaise et briançonnaise occidentale entre Vallouise et Guillestre (Hautes Alpes) - Alpes françaises* [Thèse de doctorat, Université de Grenoble]. https://hal.archives-ouvertes.fr/tel-00563860

Debelmas, J. (1970). *Guides géologiques régionaux: Alpes (Savoie et Dauphiné)*. Paris: Masson.

Decarlis, A., Beltrando, M., Manatschal, G., Ferrando, S., & Carosi, R. (2017a). Architecture of the Distal Piedmont-Ligurian Rifted Margin in NW Italy: Hints for a Flip of the Rift System Polarity. *Tectonics*, *36*(11), 2388–2406. doi:10/gcr84z

Decarlis, A., Fellin, M. G., Maino, M., Ferrando, S., Manatschal, G., Gaggero, L., Seno, S., Stuart, F. M., & Beltrando, M. (2017b). Tectono-thermal Evolution of a Distal Rifted Margin: Constraints From the Calizzano Massif (Prepiedmont-Briançonnais Domain, Ligurian Alps). *Tectonics*, *36*(12), 3209–3228. doi:10/gcxzvs

Decarlis, A., & Lualdi, A. (2011). Synrift sedimentation on the northern Tethys margin: an example from the Ligurian Alps (Upper Triassic to Lower Cretaceous, Prepiedmont domain, Italy). *International Journal of Earth Sciences*, *100*(7), 1589–1604. doi:10.1007/s00531-010-0587-1

Decrausaz, T., Müntener, O., Manzotti, P., Lafay, R., & Spandler, C. (2021). Fossil oceanic core complexes in the Alps. New field, geochemical and isotopic constraints from the Tethyan Aiguilles Rouges Ophiolite (Val d'Hérens, Western Alps, Switzerland). *Swiss Journal of Geosciences*, *114*(1), 3. doi:10.1186/s00015-020-00380-4

Dentan, P., & Menthonnex, F. (1990). *Etudes géologiques et minéralogiques de la région de Valtournanche (Val d'Aoste, Italie du Nord)* [Travail de diplôme non publié, Université de Lausanne].

Derron, M.-H., Jacquod, J., & Sartori, M. (2006). The Goli d'Aget Member: Early Permian volcanoclastic and volcanic rocks within the Briançonnais Grand St-Bernard Nappe (Valais, Switzerland). *Eclogae Geologicae Helvetiae*, *99*(3), 301–307. doi:10/b4mtwt

Desmons, J., Compagnoni, R., & Cortesogno, L. (1999). Alpine metamorphism of the Western Alps: II. High-P/T. *Schweizerische Mineralogische und Petrographische Mitteilungen*, *79*(1), 111–134. doi:10.5169/SEALS-60201

Deville, E. (1987). *Etude géologique en Vanoise orientale (Alpes occidentales françaises, Savoie). De la naissance à la structuration d'un secteur de la paléomarge européenne et de l'océan téthysien: aspects stratigraphiques, pétrographiques et tectoniques* [Thèse de doctorat, Université de Savoie, Chambéry]. https://tel.archives-ouvertes.fr/tel-00525200

Deville, E., Fudral, S., Lagabrielle, Y., Marthaler, M., & Sartori, M. (1992). From oceanic closure to continental collision: A synthesis of the" Schistes lustrés" metamorphic complex of the Western Alps. *Geological Society of America Bulletin*, *104*(2), 127–139.

Diehl, E. A., Masson, R., & Stutz, A. H. (1952). Contributo alla conoscenza del ricoprimento della Dent Blanche. *Memorie degli Istituti di Geologia e Mineralogia dell'Università di Padova*, *17*, 1–52.

Dolivo, E. (1982). Nouvelles observations structurales au SW du massif de l'Aar entre Visp et Gampel. *Matériaux pour la Carte Géologique de la Suisse*, *157*, 1–84.

Dousse, B. (1965). Géologie des Rochers de Château-d'Oex (Partie orientale). *Matériaux pour la Carte Géologique de la Suisse [n.s.]*, *119*, 1–79.

Dragovic, B., Angiboust, S., & Tappa, M. J. (2020). Petrochronological close-up on the thermal structure of a paleo-subduction zone (W. Alps). *Earth and Planetary Science Letters*, *547*, 116446. doi:10.1016/j.epsl.2020.116446

Du Bois, L., & Looser, M.-O. (1987). *Etudes Géologiques, pétrographiques et géochimiques en Val d'Ollomont (Région autonome de la Vallée d'Aoste), Italie* [Travail de diplôme non publié, Université de Lausanne].

Dumont, T. (1983). *Le chaînon de Rochebrune au Sud-Est de Briançon: évolution paléogéographique et structurale d'un secteur de la Zone Piémontaise des Alpes Occidentales.* [Thèse de doctorat, Université Scientifique et Médicale de Grenoble]. https://tel.archives-ouvertes.fr/tel-00541937

Dumont, T., Lemoine, M., & Tricart, P. (1984). Tectonique synsédimentaire triasico-jurassique et rifting téthysien dans l'unité prépiémontaise de Rochebrune au Sud-Est de Briançon. *Bulletin de la Société Géologique de France*, *(7) 26*(5), 921–933. doi:10.2113/gssgfbull.S7-XXVI.5.921

Duprat-Oualid, S., Yamato, P., & Schmalholz, S. M. (2015). A dimensional analysis to quantify the thermal budget around lithospheric-scale shear zones. *Terra Nova*, *27*(3), 163–168. doi:10.1111/ter.12144

Egli, D., & Mancktelow, N. (2013). The structural history of the Mont Blanc massif with regard to models for its recent exhumation. *Swiss Journal of Geosciences*, *106*(3), 469–489. doi:10/f5mgq3

Ellenberger, F. (1952). Sur l'extension des faciès briançonnais en Suisse, dans les Préalpes médianes et les Pennides. *Eclogae Geologicae Helvetiae*, *45*(2), 285–6.

Ellenberger, F. (1953). La série du Barrhorn et les rétrocharriages penniques. *Comptes rendus hebdomadaires des séances de l'Académie des Sciences Paris*, *236*(2), 218–220.

Ellenberger, F. (1958). Étude géologique du pays de Vanoise [Thèse de doctorat, Université de Paris, 1954]. *Mémoires pour servir à l'explication de la carte géologique détaillée de la France*, 662 pp.

Ellis, A. C., Barnicoat, A. C., & Fry, N. (1989). Structural and metamorphic constraints on the tectonic evolution of the upper Pennine Alps. *Geological Society, London, Special Publications*, *45*(1), 173–188. doi:10.1144/GSL.SP.1989.045.01.09

Elter, G. (1960). La zona Pennidica dell'alta e media Valle d'Aosta e le unitá imitrofe. *Memorie degli Istituti di Geologia e Mineralogia dell'Università di Padova*, *22*, 113.

Elter, G. (1971). Schistes lustrés et ophiolites de la zone piémontaise entre Orco et Doire Baltée (Alpes Graies). Hypothèses sur l'origine des ophiolites. *Géologie Alpine*, *47*, 147–169.

Elter, G. (1972). Contribution a la connaissance du Briançonnais interne et de la bordure piémontaise dans les Alpes Graies nord-orientales et considérations sur les rapports entre les zones du Briançonnais et des Schistes Lustrés. *Memorie degli Istituti di Geologia e Mineralogia dell'Università di Padova*, *28*, 1-20.

Elter, G., Elter, P., Sturani, C., & Weidmann, M. (1966). Sur la prolongation du domaine ligure de l'Apennin dans le Monferrat et les Alpes et sur l'origine de la nappe de la Simme s.l.: des Préalpes romandes et chablaisiennes. *Archives des sciences (Genève)*, *19*(3), 279–384. doi:10.5169/seals-739334

England, P., & Molnar, P. (1993). The interpretation of inverted metamorphic isograds using simple physical calculations. *Tectonics*, *12*(1), 145–157. doi:10.1029/92TC00850

Epard, J. L. (1990). La nappe de Morcles au sud-ouest du Mont-Blanc. *Mémoires de Géologie (Lausanne)*, *8*, 165 pp.

Epard, J.-L., & Escher, A. (1996). Transition from basement to cover: a geometric model. *Journal of Structural Geology*, *18*(5), 533–548. doi:10/dp4336

Epin, M.-E., Manatschal, G., & Amann, M. (2017). Defining diagnostic criteria to describe the role of rift inheritance in collisional orogens: the case of the Err-Platta nappes (Switzerland). *Swiss Journal of Geosciences*, *110*(2), 419–438. doi:10/gbj36k

Erbacher, J., & Thurow, J. (1997). Influence of oceanic anoxic events on the evolution of mid-Cretaceous radiolaria in the North Atlantic and western Tethys. *Marine Micropaleontology*, *30*(1), 139–158. doi:10.1016/S0377-8398(96)00023-0

Ernst, W. G., & Dal Piaz, G. V. (1978). Mineral parageneses of eclogitic rocks and related mafic schists of the Piemonte ophiolite nappe, Breuil-St. Jacques area, Italian Western Alps. *American Mineralogist*, *63*(7-8), 621–640.

Escher, A. (1988). Structure de la nappe du Grand Saint-Bernard entre le val de Bagnes et les Mischabel. *Rapports géologiques du Service hydrologique et géologique national*, *7*, 1–27.

Escher, A., & Beaumont, C. (1997). Formation, burial and exhumation of basement nappes at crustal scale: a geometric model based on the Western Swiss-Italian Alps. *Journal of Structural Geology*, *19*(7), 955-974. doi:10/fh6p64

Escher, A., Escher, J. C., & Watterson, J. (1975). The Reorientation of the Kangâmiut Dike Swarm, West Greenland. *Canadian Journal of Earth Sciences*, *12*(2), 158–173. doi:10.1139/e75-016

Escher, A., Hunziker, J. C., Marthaler, M., Masson, H., Sartori, M., & Steck, A. (1997). Geologic framework and structural evolution of the western Swiss-Italian Alps. In O. A. Pfiffner, P. Lehner, P. Heitzmann, S. Mueller, & A. Steck (Eds.), *Deep structure of the Swiss Alps: results of NRP 20* (pp. 205–221). Basel: Birkhäuser Verlag. doi:10.1007/978-3-0348-9098-4_16

Escher, A., & Masson, H. (1984). Le Cervin: un dessin géologique inédit d'Emile Argand (1929) et son interprétation actuelle. *Travaux du Comité Français d'Histoire de la Géologie*, *(2) 2*(8), 95–127.

Escher, A., Masson, H., & Steck, A. (1987). Coupes géologiques des Alpes occidentales suisses. *Rapports géologiques du Service hydrologique et géologique national*, *2*.

Escher, A., Masson, H., & Steck, A. (1988). Coupes géologiques des Alpes occidentales suisses. *Mémoires de Géologie (Lausanne)*, *2*, 11 pp.

Escher, A., Masson, H., & Steck, A. (1993). Nappe geometry in the Western Swiss Alps. *Journal of Structural Geology*, *15*(3–5), 501–509. doi:10.1016/0191-8141(93)90144-Y

Escher, A., Masson, H., Steck, A., Epard, J.-L., Marchant, R., Marthaler, M., Sartori, M., & Venturini, G. (1994). Coupe tectonique des Alpes de Suisse occidentale. Section des sciences de la terre, Université de Lausanne.

Escher, A., & Watt, W. S. (1976). *Geology of Greenland*. Copenhagen: Grønlands geologiske undersøgelse.

Fassmer, K., Obermüller, G., Nagel, T. J., Kirst, F., Froitzheim, N., Sandmann, S., Miladinova, I., Fonseca, R. O.C., & Münker, C. (2016). High-pressure metamorphic age and significance of eclogite-facies continental fragments associated with oceanic lithosphere in the Western Alps (Etirol-Levaz Slice, Valtournenche, Italy). *Lithos*, *252–253*, 145–159. doi:10/ggd36c

Faure, J.-L., & Mégard-Galli, J. (1988). L'émersion jurassique en Brianconnais: sedimentation continentale et fracturation distensive. *Bulletin de la Société Géologique de France*, *4*(4), 681–692.

Favre, O. (2000). *Etude géologique de la couverture mésozoïque de la Nappe du Mont Fort dans la région du barrage de Moiry (Valais, Suisse)* [Travail de diplôme non publié, Université de Lausanne].

Florineth, D., & Froitzheim, N. (1994). Transition from continental to oceanic basement in the Tasna nappe (Engadine window, Graubünden, Switzerland): evidence for Early Cretaceous opening of the Valais ocean. *Schweizerische Mineralogische und Petrographische Mitteilungen*, *74*(3), 437–448. doi:10.5169/seals-56358

Forster, M., Lister, G., Compagnoni, R., Giles, D., Hills, Q., Betts, P., Beltrando, M., & Tamagno, E. (2004). Mapping of oceanic crust with" HP" to" UHP" metamorphism: The Lago di Cignana Unit (Western Alps). In *Pasquarè G, Venturini C, Groppelli G (eds) Mapping geology in Italy* (Servizio Geologico d'Italia., pp. 279–286). Geological Society of London.

Frezzotti, M. L., Selverstone, J., Sharp, Z. D., & Compagnoni, R. (2011). Carbonate dissolution during subduction revealed by diamond-bearing rocks from the Alps. *Nature Geoscience*, *4*(10), 703–706. doi:10.1038/ngeo1246

Frezzotti, M.-L., Huizenga, J.-M., Compagnoni, R., & Selverstone, J. (2014). Diamond formation by carbon saturation in C–O–H fluids during cold subduction of oceanic lithosphere. *Geochimica et Cosmochimica Acta*, *143*, 68–86. doi:10/gcsgrh

Froitzheim, N., & Eberli, G. P. (1990). Extensional detachment faulting in the evolution of a Tethys passive continental margin, Eastern Alps, Switzerland. *Geological Society of America Bulletin*, *102*(9), 1297-1308. doi:10/cndfss

Froitzheim, N., & Manatschal, G. (1996). Kinematics of Jurassic rifting, mantle exhumation, and passive-margin formation in the Austroalpine and Penninic nappes (eastern Switzerland). *Geological Society of America Bulletin*, *108*(9), 1120–1133. doi:10.1130/0016-7606(1996)108<1120:KOJRME>2.3.CO;2

Froitzheim, N., Pleuger, J., Hauke, M., & Nagel, T. J. (2019). The origin of the Cimes-Blanches Nappe and the tectonic structure of the Penninic Alps. In *14th Emile Argand Conference on Alpine Geological studies (Sion), Abstract Volume* (p. 22).

Froitzheim, N., Pleuger, J., & Nagel, T. J. (2006). Extraction faults. *Journal of Structural Geology*, *28*(8), 1388-1395. doi:10.1016/j.jsg.2006.05.002

Fudral, S., Deville, E., & Marthaler, M. (1987). Distinction de trois ensembles d'unités dans les «Schistes lustrés» compris entre la Vanoise et le Val de Suse (Alpes franco-italiennes septentrionales): aspects lithostratigraphiques, paléogéographiques et géodynamiques. *Comptes Rendus de l'Académie des Sciences Paris*, *(II) 305*(6), 467–472.

Gabus, J. H., Weidmann, M., Bugnon, P.-C., Burri, M., Sartori, M., & Marthaler, M. (2008). Feuille 1287 Sierre. - Atlas géologique de la Suisse 1:25 000, Carte 111.

Galster, F., Cavargna-Sani, M., Epard, J.-L., & Masson, H. (2012). New stratigraphic data from the Lower Penninic between the Adula nappe and the Gotthard massif and consequences for the tectonics and the paleogeography of the Central Alps. *Tectonophysics*, *579*, 37–55. doi:10/f4md22

Ganguin, J. (1988). *Contribution à la caractérisation du métamorphisme polyphasé de la zone de Zermatt-Saas Fee (Alpes valaisannes), (Thèse n° 8731)* [Ph.D. thesis, ETH Zürich]. https://doi.org/10.3929/ethz-a-000541595

Gasco, I., & Gattiglio, M. (2011). Geological map of the upper Gressoney Valley, Western Italian Alps. *Journal of Maps*, *6*(1), 82–102. doi:10.4113/jom.2011.1121

Gasinski, A., Slaczka, A., & Winkler, W. (1997). Tectono-sedimentary evolution of the Upper Prealpine nappe (Switzerland and France): nappe formation by Late Cretaceous-Paleogene accretion. *Geodinamica Acta*, *10*(4), 137–157. doi:10.1080/09853111.1997.11105299

Gauthiez, L., Bussy, F., Ulianov, A., Gouffon, Y., & Sartori, M. (2011). Ordovician mafic magmatism in the Métailler Formation of the Mont-Fort nappe (Middle Penninic domain, western Alps) - geodynamic implications. In *9th Swiss Geoscience Meeting (Zürich), Abstract volume* (pp. 110–111).

Gebauer, D. (1999). Alpine geochronology of the Central Alps and Western Alps: new constraints for a complex geodynamic evolution. *Schweizerische Mineralogische und Petrographische Mitteilungen*, *79*, 191-208. doi:10.5169/SEALS-60205

Genier, F., Epard, J.-L., Bussy, F., & Magna, T. (2008). Lithostratigraphy and U-Pb zircon dating in the overturned limb of the Siviez-Mischabel nappe: a new key for Middle Penninic nappe geometry. *Swiss Journal of Geosciences*, *101*(2), 431–452. doi:10/cjrz78

Gerlach, H. (1861). Blatt XXII Martigny-Aoste. Carte géologique de la Suisse 1:100 000.

Gerlach, H. (1869). Die penninischen Alpen (mit Karte 1:200 000). *Neue Denkschriften der Allgemeinen Schweizerischen Gesellschaft für die Gesammten Naturwissenschaften*, (22).

Gerlach, H. (1871). Das suedwestliche Wallis mit den angrenzenden Landestheilen von Savoien und Piemont. *Beiträge zur Geologischen Karte der Schweiz*, *9*, 175.

Gerlach, H. (1883). Erläuterung zu den Arbeiten von H. Gerlach in den Blättern 17, 18, 22, 23 südlich von der Rhone. *Beiträge zur Geologischen Karte der Schweiz*, *27*(3).

Giordano, M. (1869). Notice sur la constitution géologique du Mont Cervin. *Archives des Sciences Physiques et naturelles (Genève)*, *34*, 255–267.

Girard, M. (1995). *Géologie et pétrographie de la région comprise entre Sunnegga et Täschalp (Zermatt, Suisse)* [Travail de master non publié, Université de Lausanne].

Giuntoli, F., & Engi, M. (2016). Internal geometry of the central Sesia Zone (Aosta Valley, Italy): HP tectonic assembly of continental slices. *Swiss Journal of Geosciences*, *109*(3), 445–471.

Glassey, J. (2013). *La couverture de la nappe du Mont-Fort dans la région du Sasseneire (Val d'Hérens et d'Anniviers, Valais): lithostratigraphie et structure* [Travail de master non publié, Université de Lausanne].

Gouffon, Y. (1993). Géologie de la "nappe" du Grand St-Bernard entre la Doire Baltée et la frontière suisse (Vallée d'Aoste-Italie). *Mémoires de Géologie (Lausanne)*, *12*, 150 pp.

Gouffon, Y., & Burri, M. (1997). Les nappes des Pontis, de Siviez-Mischabel et du Mont Fort dans les vallées de Bagnes, d'Entremont (Valais, Suisse) et d'Aoste (Italie). *Eclogae Geologicae Helvetiae*, *90*(1), 29-41. doi:10.5169/seals-168143

Grand, T., Dumont, T., & Pinto-Bull, F. (1987). Distensions liées au rifting téthysien et paléochamps de contrainte associés dans le bassin liasique de Bourg d'Oisans (Alpes occidentales). *Bulletin de la Société Géologique de France*, *3*(4), 699–704. doi:10.2113/gssgfbull.III.4.699

Groppo, C., Beltrando, M., & Compagnoni, R. (2009). The P-T path of the ultra-high pressure Lago Di Cignana and adjoining high-pressure meta-ophiolitic units: insights into the evolution of the subducting Tethyan slab. *Journal of Metamorphic Geology*, *27*(3), 207–231. doi:10/bsxwhs

Guillaume, M. (1986). *Révision stratigraphique des Couches Rouges de la nappe des Préalpes médianes romandes (Thèse n° 910)* [Thèse de doctorat, Université de Fribourg, Suisse].

Güller, A. (1947). Zur Geologie der südlichen Mischabel- und der Monte Rosa-Gruppe: mit Einschluss des Zmutt-Tales westlich Zermatt. *Eclogae Geologicae Helvetiae*, *40*(1), 39–164. doi:10.5169/SEALS-160900

Hable, R. (1997). *Biostratigraphie, Sedimentologie und paläogeographische Entwicklung der Préalpes Médianes des Chablais (Haute Savoie) vom Apt bis Unter-Eözan (Thesis 1166)* [Ph.D. thesis, Universität Freiburg, Schweiz].

Hagen, T. (1948). Geologie des Mont Dolin und des Nord randes der Dent Blanche-Decke zwischen Mont Blanc de Cheilon und Ferpèche (Wallis). *Beiträge zur Geologischen Karte der Schweiz*, *90*, 82.

Hagen, T. (1951). Über den geologischen Bau des Mont Pleureur (Val de Bagnes, Wallis). *Eclogae Geologicae Helvetiae*, *44*(2), 299–306. doi:10/ggbv9w

Haupert, I., Manatschal, G., Decarlis, A., & Unternehr, P. (2016). Upper-plate magma-poor rifted margins: Stratigraphic architecture and structural evolution. *Marine and Petroleum Geology*, *69*, 241–261. doi:10/f77dq6

Hermann, F.-W. (1913). *Recherches géologiques dans la partie septentrionale des Alpes Pennines (Massifs Rocs de Boudri - Bella Tola et Sasseneire - Becs de Bossons)* (A. Rey.). Lyon: A. Rey.

Hermann, F.-W. (1925). *Sur le faisceau de plis en retour de Valsavarenche et les prolongements de l'éventail de Bagnes dans les Alpes franco-italiennes*.

Hermann, F.-W. (1928). Sulla tectonica valdostana: studi geologici nelle Alpi occidentali. *Memorie degli Istituti di Geologia e Mineralogia dell'Università di Padova*, *7*, 1–19.

Herviou, C., Agard, P., Plunder, A., Mendes, K., Verlaguet, A., Deldicque, D., & Cubas, N. (2022). Subducted fragments of the Liguro-Piemont ocean, Western Alps: Spatial correlations and offscraping mechanisms during subduction. *Tectonophysics*, *827*, 229267. doi:10.1016/j.tecto.2022.229267

Homewood, P., & Lateltin, O. (1988). Classic swiss clastics (flysch and molasse) The alpine connection. *Geodinamica Acta*, *2*(1), 1–11. doi:10.1080/09853111.1988.11105150

Hunziker, J. C., Hurford, A. J., & Calmbach, L. (1997). Alpine cooling and uplift. In *O. A. Pfiffner et al. (Eds.). Deep structure of the Swiss Alps: results of NRP 20* (pp. 260–264). Basel: Birkhäuser Verlag.

Hurford, A. J., Hunziker, J. C., & Stöckhert, B. (1991). Constraints on the late thermotectonic evolution of the western Alps: Evidence for episodic rapid uplift. *Tectonics*, *10*(4), 758–769. doi:10.1029/91TC00167

Hürlimann, A., Besson-Hürlimann, A., & Masson, H. (1996). Stratigraphie et tectonique de la partie orientale de l'écaille de la Gummfluh (Domaine Briançonnais des Préalpes). *Mémoires de Géologie (Lausanne)*, *28*, 183 pp.

Institut für Geologie, Univesität Bern & Bundesamt für Wasser und Geologie (Eds.). (2005). Tektonische Karte der Schweiz 1:500 000. Bundesamt für Landestopografie, Bern.

Iten, W. B. (1948). Zur Stratigraphie und Tektonik der Zone du Combin: zwischen Mettelhorn und Turtmanntal (Wallis). *Eclogae Geologicae Helvetiae*, *41*(2), 149–244. doi:10.5169/seals-161041

Jäckli, R. (1950). Geologische Untersuchungen in der Stirnzone der Mischabeldecke zwischen Réchy, Val d'Anniviers und Visp (Wallis). *Eclogae Geologicae Helvetiae*, *43*(1), 31–96. doi:10/gfkk9n

Jaillard, E. (1988). Une image paléogéographique de la Vanoise briançonnaise (Alpes françaises). *Eclogae Geologicae Helvetiae*, *81*(3), 553–566. doi:10.5169/seals-166193

Jenkyns, H. C. (1980). Cretaceous anoxic events: from continents to oceans. *Journal of the Geological Society*, *137*(2), 171–188. doi:10.1144/gsjgs.137.2.0171

Ji, W., Malusà, M. G., Tiepolo, M., Langone, A., Zhao, L., & Wu, F. (2019). Synchronous Periadriatic magmatism in the Western and Central Alps in the absence of slab breakoff. *Terra Nova*, *31*(2), 120-128. doi:10/ggbxv7

Joukowsky, E. (1907). Communication sur une coupe du Massif d'Arzinol. *Archives des Sciences Physiques et naturelles (Genève)*, *(4) 24*, 99–100.

Kapferer, N., Mercolli, I., Berger, A., Ovtcharova, M., & Fügenschuh, B. (2012). Dating emplacement and evolution of the orogenic magmatism in the internal Western Alps: 2. The Biella Volcanic Suite. *Swiss Journal of Geosciences*, *105*(1), 67–84. doi:10/f335f6

Keller, L. M., Hess, M., Fügenschuh, B., & Schmid, S. M. (2005). Structural and metamorphic evolution of the Camughera - Moncucco, Antrona and Monte Rosa units southwest of the Simplon line, Western Alps. *Eclogae Geologicae Helvetiae*, *98*(1), 19–49. doi:10.1007/s00015-005-1149-6

Kienast, J. R. (1973). Sur l'existence de deux séries différentes au sein de l'ensemble "schistes lustrés-ophiolites" du Val d'Aoste; quelques arguments fondés sur l'étude des roches métamorphiques. *Comptes Rendus de l'Académie des sciences Paris*, *(D) 276*(3), 2621–2624.

Kienast, J.-R. (1983). *Le métamorphisme de haute pression et basse température (éclogites et schistes bleus): données nouvelles sur la pétrologie des roches de la croûte océanique subductée et des sédiments associés* [Thèse de doctorat, Université de Paris VI].

Kirilova, M., Toy, V. G., Timms, N., Halfpenny, A., Menzies, C., Craw, D., Beyssac, O., Sutherland, R., Townend, J., Boulton, C., Carpenter, B. M., Cooper, A., Grieve, J., Little, T., Morales, L., Morgan, C., Mori, H., Sauer, K. M., Schleicher, A. M., Williams, J., & Craw, L. (2018). Textural changes of graphitic carbon by tectonic and hydrothermal processes in an active plate boundary fault zone, Alpine Fault, New Zealand. *Geological Society, London, Special Publications*, *453*(1), 205–223. doi:10.1144/SP453.13

Kirschner, D. L., Cosca, M. A., Masson, H., & Hunziker, J. C. (1996). Staircase 40/Ar39Ar spectra of fine-grained white mica: Timing and duration of deformation and empirical constraints on argon diffusion. *Geology*, *24*(8), 747. doi:10.1130/0091-7613(1996)024<0747:SAASOF>2.3.CO;2

Kirst, F. (2017). Polyphase greenschist-facies reactivation of the Dent Blanche Basal Thrust (Western Alps) during progressive Alpine orogeny. *Swiss Journal of Geosciences*, *110*(2), 503–521. doi:10/gcsmnj

Kirst, F., & Leiss, B. (2017). Kinematics of syn- and post-exhumational shear zones at Lago di Cignana (Western Alps, Italy): constraints on the exhumation of Zermatt–Saas (ultra)high-pressure rocks and deformation along the Combin Fault and Dent Blanche Basal Thrust. *International Journal of Earth Sciences*, *106*(1), 215–236. doi:10.1007/s00531-016-1316-1

Kiss, D., Podladchikov, Y., Duretz, T., & Schmalholz, S. M. (2019). Spontaneous generation of ductile shear zones by thermal softening: Localization criterion, 1D to 3D modelling and application to the lithosphere. *Earth and Planetary Science Letters*, *519*, 284–296. doi:10.1016/j.epsl.2019.05.026

Klein, J. A. (1978). Post-Nappe folding southeast of the Mischabelrückfalte (Pennine Alps) and some aspects of the associated metamorphism. *Leidse Geologische Mededelingen*, *51*(2), 233–312.

Kramar, N. (1997). *La couverture mésozoïque de la région d'Artsinol (Val d'Hérens, Valais): Relations avec les nappes du Mont Fort et du Tsaté* [Travail de diplôme non publié, Université de Lausanne].

Kramer, J. (2002). *Structural Evolution of the Penninic Units in the Monte Rosa region (Swiss and Italian Alps)* [Ph.D. thesis, Universität Basel].

Krayenbuhl, T., & Steck, A. (2009). Structure and kinematics of the Jungfrau syncline, Faflertal (Valais, Alps), and its regional significance. *Swiss Journal of Geosciences*, *102*(3), 441–456. doi:10/cxbprn

Kunz, P. (1988). Ophiolites penniques et sédiments associés dans la région d'Arolla (val d'Hérens, Valais, Suisse). *Eclogae Geologicae Helvetiae*, *88*(1), 115–124. doi:10.5169/SEALS-166172

Lafosse, M., Boutoux, A., Bellahsen, N., & Le Pourhiet, L. (2016). Role of tectonic burial and temperature on the inversion of inherited extensional basins during collision. *Geological Magazine*, *153*(5–6), 811-826. doi:10.1017/S0016756816000510

Lagabrielle, Y. (1987). *Les ophiolites: marqueurs de l'histoire tectonique des domaines océaniques. Le cas des Alpes franco-italiennes (Queyras, Piémont): comparaison avec les ophiolites d'Antalya (Turquie) et du Coast Range de Californie* [Thèse de doctorat, Université de Bretagne occidentale, Brest]. https://tel.archives-ouvertes.fr/tel-00795305

Lagabrielle, Y., & Lemoine, M. (1997). Alpine, Corsican and Apennine ophiolites: the slow-spreading ridge model. *Comptes Rendus de l'Académie des Sciences - Séries IIA - Earth and Planetary Science*, *325*(12), 909–920. doi:10.1016/S1251-8050(97)82369-5

Lagabrielle, Y., & Polino, R. (1985). Origine volcano-détritique de certaines prasinites des schistes lustrés du Queyras (France); arguments texturaux et géochimiques. *Bulletin de la Société Géologique de France*, *1*(4), 461–471.

Lagabrielle, Y., Vitale Brovarone, A., & Ildefonse, B. (2015). Fossil oceanic core complexes recognized in the blueschist metaophiolites of Western Alps and Corsica. *Earth-Science Reviews*, *141*, 1–26. doi:10.1016/j.earscirev.2014.11.004

Le Breton, E., Brune, S., Ustaszewski, K., Zahirovic, S., Seton, M., & Müller, R. D. (2021). Kinematics and extent of the Piemont–Liguria Basin – implications for subduction processes in the Alps. *Solid Earth*, *12*(4), 885–913. doi:10.5194/se-12-885-2021

Le Mer, O., Lagabrielle, Y., & Polino, R. (1986). Une série sédimentaire détritique liée aux ophiolites piémontaises: analyses lithostratigraphiques, texturales et géochimiques dans le massif de la Crête Mouloun (Haut Queyras, Alpes sud-occidentales, France). *Géologie Alpine*, *62*, 63–86.

Lebit, H., Klaper, E. M., & Lüneburg, C. M. (2002). Fold-controlled quartz textures in the Pennine Mischabel backfold near Zermatt, Switzerland. *Tectonophysics*, *359*(1–2), 1–28. doi:10/bwk73v

Lefèvre, R. (1982). *Les nappes briançonnaises internes et ultrabriançonnaises dans les Alpes Cottiennes méridionales* [Thèse de doctorat, Université de Paris Sud]. https://tel.archives-ouvertes.fr/tel-00800038

Lefèvre, R., & Michard, A. (1976). Les nappes briançonnaises internes et ultra-briançonnaises de la Bande d'Acceglio (Alpes franco-italiennes): une étude structurale et pétrographique dans le faciès des Schistes bleus à jadéite. *Sciences Géologiques. Bulletin*, *29*(3), 183–222. doi:10/gfj22t

Leloup, P. H., & Kienast, J.-R. (1993). High-temperature metamorphism in a major strike-slip shear zone: the Ailao Shan—Red River, People's Republic of China. *Earth and Planetary Science Letters*, *118*(1-4), 213–234. doi:10.1016/0012-821X(93)90169-A

Leloup, P. H., Ricard, Y., Battaglia, J., & Lacassin, R. (1999). Shear heating in continental strike-slip shear zones: model and field examples. *Geophysical Journal International*, *136*(1), 19–40. doi:10.1046/j.1365-246X.1999.00683.x

Lemoine, M. (1953). Remarques sur les caractères et l'évolution de la paléogéographie de la zone briançonnaise au Secondaire et au Tertiaire. *Bulletin de la Société Géologique de France*, *S6-III*(1–3), 105–121. doi:10.2113/gssgfbull.S6-III.1-3.105

Lemoine, M. (1961). La marge externe de la fosse piémontaise dans les Alpes occidentales. *Revue de géographie physique et de géologie dynamique*, *(2) 4*(3), 163–180.

Lemoine, M. (1964). Le problème des relations des Schistes lustrés piémontais avec la zone briançonnaise dans les Alpes cottiennes. *Geologische Rundschau*, *53*(1), 113–132. doi:10/b8qwph

Lemoine, M. (1967). Brèches sédimentaires marines à la frontière entre les domaines briançonnais et piémontais dans les Alpes occidentales. *Geologische Rundschau*, *56*(1), 320–335.

Lemoine, M. (1971). Données nouvelles sur la série du Gondran près Briançon (Alpes Cottiennes). Réflexions sur les problèmes stratigraphique et paléogéographique de la zone piémontaise. *Géologie Alpine*, *47*, 181–201.

Lemoine, M., Bas, T., Arnaud-Vanneau, A., Arnaud, H., Dumont, T., Gidon, M., Bourbon, M., de Graciansky, P.-C., Rudkiewicz, J.-L., Megard-Galli, J., & Tricart, P. (1986). The continental margin of the Mesozoic Tethys in the Western Alps. *Marine and Petroleum Geology*, *3*(3), 179–199. doi:10/fkvxtk

Lemoine, M., Bourbon, M., & Tricart, P. (1978). Le Jurassique et le Crétacé prépiémontais à l'est de Briançon (Alpes occidentales) et l'évolution de la marge européenne de la Téthys : données nouvelles et conséquences. *Comptes Rendus de l'Académie des sciences Paris*, *(D) 286*(3), 1237–1240.

Lemoine, M., de Graciansky, P., & Tricart, P. (2000). *De l'océan à la chaîne de montagnes: Tectonique des plaques dans les Alpes*. Paris: Gordon and Breach Science Publishers.

Lemoine, M., Marthaler, M., Caron, M., Sartori, M., Amaudric du Chaffaut, S., Dumont, T., Escher, A., Masson, H., Polino, R., & Tricart, P. (1984). Découverte de foraminifères planctoniques du Crétacé supérieur dans les Schistes lustrés du Queyras (Alpes Occidentales). Conséquences paléogéographiques et tectoniques. *Comptes Rendus de l'Académie des sciences Paris*, *(II) 299*(11), 727–732.

Lemoine, M., Steen, D., & Vuagnat, M. (1970). Sur le problème stratigraphique des ophiolites piémontaises et des roches sédimentaires associées: observations dans le massif de Chabrière en Haute-Ubaye (Basses-Alpes, France). *C. R. Séances Soc. Phys. Hist. Nat. Genève*, *N.S., 5*, 44–59.

Lemoine, M., & Tricart, P. (1986). Les Schistes lustrés piémontais des Alpes Occidentales: approche stratigraphique, structurale et sédimentologique. *Eclogae Geologicae Helvetiae*, *79*(2), 271–294. doi:10.5169/seals-165835

Lemoine, M., & Trümpy, R. (1987). Pre-oceanic rifting in the Alps. *Tectonophysics*, *133*(3–4), 305–320. doi:10/ddmtd8

Lescoutre, R., & Manatschal, G. (2020). Role of rift-inheritance and segmentation for orogenic evolution: example from the Pyrenean-Cantabrian system. *BSGF - Earth Sciences Bulletin*, *191*, 18. doi:10.1051/bsgf/2020021

Loprieno, A., & Ellero, A. (2021). Geology of the Piemonte-Ligurian units of the Urtier area (Northwestern Alps – Italy). *Journal of Maps*, *17*(2), 778–791. doi:10.1080/17445647.2021.1986156

Lugeon, M. (1896). La région de la Brèche du Chablais (Haute Savoie). *Bulletin des Services de la carte géologique de la France et des topographies souterraines*, *49*(7), 337–642.

Lugeon, M. (1947). Hommage à August Buxtorf et digression sur la nappe de Morcles. *Verhandlungen der Naturforschenden Gesellschaft in Basel*, *58*, 108–131.

Lugeon, M., & Argand, E. (1905a). Sur les nappes de recouvrement de la zone du Piémont. *Comptes rendus hebdomadaires des séances de l'Académie des Sciences Paris*, *140*, 1364–1367.

Lugeon, M., & Argand, E. (1905b). Sur les homologies dans les nappes de recouvrement de la zone du Piémont. *Comptes rendus hebdomadaires des séances de l'Académie des Sciences Paris*, *140*, 1491–1493.

Luisier, C., Baumgartner, L. P., Bouvier, A.-S., & Putlitz, B. (2022). Interplay between fluid circulation and Alpine metamorphism in the Monte Rosa whiteschist from white mica and quartz in situ oxygen isotope analysis by SIMS. *American Mineralogist*, *107*(5), 860–872. doi:10.2138/am-2020-7523

Luque, F. J., Pasteris, J. D., Wopenka, B., Rodas, M., & Barrenechea, J. F. (1998). Natural fluid-deposited graphite: Mineralogical charcteristics and mechanism of formation. *American Journal of Science*, *298*, 471–498.

Luque, F. J., & Rodas, M. (1999). Constraints on graphite crystallinity in some Spanishfluid-deposited occurrences from different geologic settings. *Mineralium Deposita*, *34*, 215–219.

Machel, H. G., Mason, R. A., Mariano, A. N., & Mucci, A. (1991). Causes and Emission of Luminescence in Calcite and Dolomite. In C. E. Barker, R. C. Burruss, O. C. Kopp, H. G. Machel, D. J. Marshall, P. Wright, & H. Y. Colbum (Eds.), *Luminescence Microscopy and Spectroscopy: Qualitative and Quantitative Applications* (Vol. 25, p. 0). SEPM Society for Sedimentary Geology. doi:10.2110/scn.91.25.0009

Mako, C. A., & Caddick, M. J. (2018). Quantifying magnitudes of shear heating in metamorphic systems. *Tectonophysics*, *744*, 499–517. doi:10.1016/j.tecto.2018.07.003

Manatschal, G., Chenin, P., Haupert, I., Masini, E., Frasca, G., & Decarlis, A. (2022). The Importance of Rift Inheritance in Understanding the Early Collisional Evolution of the Western Alps. *Geosciences*, *12*(12), 434. doi:10.3390/geosciences12120434

Manatschal, G., & Müntener, O. (2009). A type sequence across an ancient magma-poor ocean–continent transition: the example of the western Alpine Tethys ophiolites. *Tectonophysics*, *473*(1–2), 4–19. doi:10.1016/j.tecto.2008.07.021

Manatschal, G., Müntener, O., Desmurs, L., & Bernoulli, D. (2003). An ancient-ocean-continent transition in the Alps: the Totalp, Err-Platta, and Malenco units in the eastern Central Alps (Graubünden and northern Italy). *Eclogae Geologicae Helvetiae*, *96*(1), 131–146. doi:10.5169/seals-169013

Mancktelow, N. S. (1992). Neogene lateral extension during convergence in the Central Alps: Evidence from interrelated faulting and backfolding around the Simplonpass (Switzerland). *Tectonophysics*, *215*(3–4), 295–317. doi:10.1016/0040-1951(92)90358-D

Manzotti, P., Ballèvre, M., & Dal Piaz, G. V. (2017). Continental gabbros in the Dent Blanche Tectonic System (Western Alps): from the pre-Alpine crustal structure of the Adriatic palaeo-margin to the geometry of an alleged subduction interface. *Journal of the Geological Society*, *174*(3), 541–556. doi:10/f98n78

Manzotti, P., Ballèvre, M., Pitra, P., Putlitz, B., Robyr, M., & Müntener, O. (2020). The Growth of Sodic Amphibole at the Greenschist- to Blueschist-facies Transition (Dent Blanche, Western Alps): Bulk-rock Chemical Control and Thermodynamic Modelling. *Journal of Petrology*. doi:10.1093/petrology/egaa044

Manzotti, P., Ballèvre, M., Pitra, P., & Schiavi, F. (2021). Missing lawsonite and aragonite found: P–T and fluid composition in meta-marls from the Combin Zone (Western Alps). *Contributions to Mineralogy and Petrology*, *176*(8), 60. doi:10.1007/s00410-021-01818-0

Manzotti, P., Ballèvre, M., Zucali, M., Robyr, M., & Engi, M. (2014). The tectonometamorphic evolution of the Sesia–Dent Blanche nappes (internal Western Alps): review and synthesis. *Swiss Journal of Geosciences*, *107*(2–3), 309–336.

Markley, M. J., Teyssier, C., & Cosca, M. (2002). The relation between grain size and 40Ar/39Ar date for Alpine white mica from the Siviez-Mischabel Nappe, Switzerland. *Journal of Structural Geology*, *24*(12), 1937–1955. doi:10/d37hmw

Markley, M. J., Teyssier, C., Cosca, M. A., Caby, R., Hunziker, J. C., & Sartori, M. (1998). Alpine deformation and 40Ar/39Ar geochronology of synkinematic white mica in the Siviez-Mischabel Nappe, western Pennine Alps, Switzerland. *Tectonics*, *17*(3), 407–425.

Marthaler, M. (1981). Découverte de foraminifères planctoniques dans les “schistes lustrés” de la pointe de Tourtemagne (Valais). *Bulletin de la Société Vaudoise des Sciences Naturelles*, *75*(359), 171. doi:10/gfjwv6

Marthaler, M. (1984). Géologie des unités penniques entre le Val d’Anniviers et le Val de Tourtemagne (Valais, Suisse). *Eclogae Geologicae Helvetiae*, *77*(2), 395–448. doi:10.5169/seals-165516

Marthaler, M., Fudral, S., Deville, E., & Rampnoux, J.-P. (1986). Mise en évidence du Crétacé supérieur dans la couverture septentrionale de Dora Maira, région de Suse, Italie (Alpes occidentales). Conséquences paléogéographiques et structurales. *Comptes Rendus de l’Académie des Sciences Paris*, *(II) 302*(2), 91-96.

Marthaler, M., Girard, M., & Gouffon, Y. (2020a). Feuille 1327 Evolène. - Atlas géologique de la Suisse 1:25 000, Carte 169.

Marthaler, M., Girard, M., Meisser, N., Gouffon, Y., & Savary, J. (2020b). *Feuille 1327 Evolène. - Atlas géologique de la Suisse 1:25 000, Notice explicative 169*.

Marthaler, M., Sartori, M., & Escher, A. (2008a). Feuille 1307 Vissoie. - Atlas géologique de la Suisse 1:25 000, Carte 122.

Marthaler, M., Sartori, M., Escher, A., & Meisser, N. (2008b). *Feuille 1307 Vissoie. - Atlas géologique de la Suisse 1:25 000, Notice explicative 122*.

Marthaler, M., & Stampfli, G. M. (1989). Les Schistes lustrés à ophiolites de la nappe du Tsaté: un ancien prisme d’accrétion issu de la marge active apulienne? *Schweizerische Mineralogische und Petrographische Mitteilungen*, *69*(2), 211–216. doi:10.5169/seals-52789

Martin, B. A. (1982). *Structural and metamorphic studies on the ophiolitic envelope of the Monte Rosa nappe, Pennine Alps* [Ph.D. thesis, University College of Swansea, University of Wales].

Martin, S., & Cortiana, G. (2001). Influence of the whole-rock composition on the crystallization of sodic amphiboles (Piemonte zone, Western Alps). *Ophioliti*, *26*(2b), 445–456.

Masson, H. (1972). Sur l’origine de la cornieule par fracturation hydraulique. *Eclogae Geologicae Helvetiae*, *65*(1), 27–41.

Masson, H. (2002). Ophiolites and other (ultra) basic rocks from the West-Central Alps: new data for a puzzle. *Bulletin de la Société Vaudoise des Sciences Naturelles*, *88*(2), 263–276.

Masson, H., Baud, A., Escher, A., Gabus, J., & Marthaler, M. (1980). Compte rendu de l’excursion de la Société Géologique Suisse: coupe Préalpes-Helvétique-Pennique en Suisse occidentale. *Eclogae Geologicae Helvetiae*, *73*(1), 331–349. doi:10.5169/seals-164959

Mazurek, M. (1986). Structural evolution and metamorphism of the Dent Blanche nappe and the Combin zone west of Zermatt (Switzerland). *Eclogae Geologicae Helvetiae*, *79*(1), 41. doi:10/gfxgz3

McCarthy, A., Chelle-Michou, C., Müntener, O., Arculus, R., & Blundy, J. (2018). Subduction initiation without magmatism: The case of the missing Alpine magmatic arc. *Geology*, *46*(12), 1059–1062. doi:10/gfjwsq

McCarthy, A., Tugend, J., Mohn, G., Candioti, L., Chelle-Michou, C., Arculus, R., Schmalholz, S. M., & Müntener, O. (2020). A case of Ampferer-type subduction and consequences for the Alps and the Pyrenees. *American Journal of Science*, *320*(4), 313–372. doi:10.2475/04.2020.01

Mégard-Galli, J. (1972). Données nouvelles sur le Carnien dans la zone briançonnaise entre Briançon et la vallée du Guil: conséquences tectoniques et paléogéographiques. *Géologie Alpine*, *48*, 131–142.

Mégard-Galli, J., & Baud, A. (1977). Le Trias moyen et supérieur des Alpes nord-occidentales et occidentales : données nouvelles et corrélations stratigraphiques. *Bulletin du Bureau de Recherche Géologiques et Minières (BRGM)*, *(2) 4*(3), 233–250.

Mégard-Galli, J., & Faure, J. L. (1988). Tectonique distensive et sedimentation au Ladinien superieur-Carnien dans la zone brianconnaise. *Bulletin de la Société Géologique de France*, *4*(5), 705–715. doi:10.2113/gssgfbull.IV.5.705

Meresse, F., Lagabrielle, Y., Malavieille, J., & Ildefonse, B. (2012). A fossil Ocean–Continent Transition of the Mesozoic Tethys preserved in the Schistes Lustrés nappe of northern Corsica. *Tectonophysics*, *579*, 4-16. doi:10/f4mfd6

Merle, O., & Ballèvre, M. (1992). Late Cretaceous-early Tertiary detachment fault in the Western Alps. *Comptes rendus de l'Académie des sciences Paris*, *(II) 315*(13), 1769–1776.

Michard, A., & Martinotti, G. (2002). The Eocene unconformity of the Briançonnais domain in the French–Italian Alps, revisited (Marguareis massif, Cuneo); a hint for a Late Cretaceous–Middle Eocene frontal bulge setting. *Geodinamica Acta*, 13.

Michard, A., Schmid, S. M., Ballèvre, M., Manzotti, P., Chopin, C., Iaccarino, S., & Dana, D. (2022). The Maira-Sampeyre and Val Grana Allochthons (south Western Alps): review and new data on the tectonometamorphic evolution of the Briançonnais distal margin. *Swiss Journal of Geosciences*, *115*(19), 43. doi:10.1186/s00015-022-00419-8

Michard, A., & Schumacher, F. (1973). Position des brèches et des ophiolites dans les séries piémontaises des Vals Grana et Marmora (Alpes cottiennes méridionales, Italie). *Comptes Rendus de l'Académie des sciences Paris*, *(D) 276*(3), 3009–3012.

Milnes, A. G., Greller, M., & Müller, R. (1981). Sequence and style of major post-nappe structures, Simplon - Pennine Alps. *Journal of structural Geology*, *3*(4), 411–420.

Mohn, G., Manatschal, G., Beltrando, M., & Haupert, I. (2014). The role of rift-inherited hyper-extension in Alpine-type orogens. *Terra Nova*, *26*(5), 347–353. doi:10/f6gb8m

Mohn, G., Manatschal, G., Beltrando, M., Masini, E., & Kusznir, N. (2012). Necking of continental crust in magma-poor rifted margins: Evidence from the fossil Alpine Tethys margins. *Tectonics*, *31*(1). doi:10/fzzp2v

Mohn, G., Manatschal, G., Masini, E., & Müntener, O. (2011). Rift-related inheritance in orogens: a case study from the Austroalpine nappes in Central Alps (SE-Switzerland and N-Italy). *International Journal of Earth Sciences*, *100*(5), 937–961. doi:10/dqcxhb

Mohn, G., Manatschal, G., Müntener, O., Beltrando, M., & Masini, E. (2010). Unravelling the interaction between tectonic and sedimentary processes during lithospheric thinning in the Alpine Tethys margins. *International Journal of Earth Sciences*, *99*(S1), 75–101. doi:10/dn4hf4

Moix, J.-R., & Stampfli, E. (1980). *Etude géologique et pétrographique de la région du Pic d'Artsinol* [Travail de diplôme non publié, Université de Lausanne].

Moix, J.-R., & Stampfli, E. (1981). Description géologique et pétrographique du massif du Pic d'Artsinol (Valais central). *Bulletin de la Murithienne*, (98), 24–32.

Molnar, P., & England, P. (1990). Temperatures, heat flux, and frictional stress near major thrust faults. *Journal of Geophysical Research*, *95*(B4), 4833–4856. doi:10.1029/JB095iB04p04833

Mosar, J., Stampfli, G. M., & Girod, F. (1996). Western Préalpes Médianes Romandes: Timing and structure. A review. *Eclogae Geologicae Helvetiae*, *89*(1), 389–425. doi:10.5169/seals-167907

Müller, C. (1984). *Die Geologie des Unteren Hörnligrates, Zermatt* [Unveröffentlichte Diplomarbeit, Universität Basel].

Müller, R. (1983). Die Struktur der Mischabelfalte (Penninische Alpen). *Eclogae Geologicae Helvetiae*, *76*(2), 391–416. doi:10/gfv4z3

Nabelek, P. I., Liu, M., & Sirbescu, M.-L. (2001). Thermo-rheological, shear heating model for leucogranite generation, metamorphism, and deformation during the Proterozoic Trans-Hudson orogeny, Black Hills, South Dakota. *Tectonophysics*, *342*(3–4), 371–388. doi:10.1016/S0040-1951(01)00171-8

Nakamura, Y., Yoshino, T., & Satish-Kumar, M. (2017). An experimental kinetic study on the structural evolution of natural carbonaceous material to graphite. *American Mineralogist*, *102*(1), 135–148. doi:10.2138/am-2017-5733

Negro, F., Bousquet, R., Vils, F., Pellet, C.-M., & Hänggi-Schaub, J. (2013). Thermal structure and metamorphic evolution of the Piemont-Ligurian metasediments in the northern Western Alps. *Swiss Journal of Geosciences*, *106*(1), 63–78. doi:10/f467ww

Nicolas, A., Bouchez, J. L., Blaise, J., & Poirier, J. P. (1977). Geological aspects of deformation in continental shear zones. *Tectonophysics*, *42*(1), 55–73. doi:10.1016/0040-1951(77)90017-8

Oulianoff, N. (1954). Note concernant l'origine et le métamorphisme des "schistes de Casanna" (massif du Métailler dans le Val de Nendaz, en Valais). *Bulletin de la Société Vaudoise des Sciences Naturelles*, *66*(288), 77. doi:10/gctpcb

Pantet, A., Epard, J.-L., & Masson, H. (2020). Mimicking Alpine thrusts by passive deformation of synsedimentary normal faults: a record of the Jurassic extension of the European margin (Mont Fort nappe, Pennine Alps). *Swiss Journal of Geosciences*, *113:13*, 35–59. doi:10.1186/s00015-020-00366-2

Passeri, L., Ciarapica, G., & Dal Piaz, G. V. (2018). The problematic origin of the Pancherot-Cime Bianche-Bettaforca unit (PCB) in the Piemonte zone (Western Alps). *Italian Journal of Geosciences*, *137*(3), 478–489. doi:10/gd3xvv

Pawlig, S., & Baumgartner, L. P. (2001). Geochemistry of a talc-kyanite-chloritoid shear zone within the Monte Rosa granite, Val d'Ayas, Italy. *Schweizerische Mineralogische und Petrographische Mitteilungen*, *81*(3), 329–346. doi:10.5169/SEALS-61696

Peron-Pinvidic, G., Manatschal, G., & the "IMAGinING RIFTING" Workshop Participants. (2019). Rifted Margins: State of the Art and Future Challenges. *Frontiers in Earth Science*, *7*. doi:10/ggbxxg

Peryt, D., Dubicka, Z., & Wierny, W. (2022). Planktonic Foraminiferal Biostratigraphy of the Upper Cretaceous of the Central European Basin. *Geosciences*, *12*(1), 22. doi:10.3390/geosciences12010022

Petrizzo, M. R., Falzoni, F., & Premoli Silva, I. (2011). Identification of the base of the lower-to-middle Campanian Globotruncana ventricosa Zone: Comments on reliability and global correlations. *Cretaceous Research*, *32*(3), 387–405. doi:10.1016/j.cretres.2011.01.010

Petroccia, A., Carosi, R., Montomoli, C., Iaccarino, S., & Vitale Brovarone, A. (2022). Deformation and temperature variation along thrust-sense shear zones in the hinterland-foreland transition zone of collisional settings: A case study from the Barbagia Thrust (Sardinia, Italy). *Journal of Structural Geology*, *161*, 104640. doi:10.1016/j.jsg.2022.104640

Pettke, T., Diamond, L. W., & Villa, I. M. (1999). Mesothermal gold veins and metamorphic devolatilization in the northwestern Alps: The temporal link. *Geology*, *27*(7), 641. doi:10.1130/0091-7613(1999)027<0641:MGVAMD>2.3.CO;2

Pfeifer, H., Colombi, A., Ganguin, J., Hunziker, J., Oberhänsli, R., & Santini, L. (1991). Relics of high-pressure metamorphism in different lithologies of the Central Alps, an updated inventory. *Schweizerische Mineralogische und Petrographische Mitteilungen*, *71*(3), 441–451. doi:10.5169/seals-54376

Pfeifer, H. R., Colombi, A., & Ganguin, J. (1989). Zermatt-Saas and Antrona zone: a petrographic and geochemical comparison of polyphase metamorphic ophiolites of the West-Central Alps. *Schweizerische Mineralogische und Petrographische Mitteilungen*, *69*, 217–236.

Pfeifer, H. R., & Serneels, V. (1988). La pierre ollaire en Valais. *UNI Lausanne*, *56*, 48–51.

Pfeifer, H.-R., Favre, O., Kunz, P., Lanterno, J., Anzévui, F., & Maître, G. (2011). *Répartition et utilisation de la pierre ollaire dans la région d'Evolène, Valais*. Géovisions.

Pilloud, C., & Sartori, M. (1981). *Etude géologique et pétrographique de la région des Diablons (Val de Zinal, VS)* [Travail de diplôme non publié, Université de Lausanne].

Plancherel, R., Braillard, L., & Dall'Agnolo, S. (2020). *Feuille 1245 Château-d'Oex. - Atlas géologique de la Suisse 1:25 000, Notice explicative 144*.

Plancherel, R., Caron, C., & Broquet, P. (1998). *Notice explicative de la carte géologique de la France 1:50 000. 655, Samoëns - Pas-de-Morgins.* (BRGM.). Orléans.

Pleuger, J., Froitzheim, N., Derks, J. F., Kurz, W., Albus, J., Walter, J. M., & Jansen, E. (2009). The Contribution of Neutron Texture Goniometry to the Study of Complex Tectonics in the Alps. In L. Liang, R. Rinaldi, & H. Schober (Eds.), *Neutron Applications in Earth, Energy and Environmental Sciences* (pp. 283-317). Boston, MA: Springer US. doi:10.1007/978-0-387-09416-8_10

Pleuger, J., Nagel, T. J., Walter, J. M., Jansen, E., & Froitzheim, N. (2008). On the role and importance of orogen-parallel and -perpendicular extension, transcurrent shearing, and backthrusting in the Monte Rosa nappe and the Southern Steep Belt of the Alps (Penninic zone, Switzerland and Italy). *Geological Society, London, Special Publications*, *298*(1), 251–280. doi:10.1144/SP298.13

Pleuger, J., Roller, S., Walter, J. M., Jansen, E., & Froitzheim, N. (2007). Structural evolution of the contact between two Penninic nappes (Zermatt-Saas zone and Combin zone, Western Alps) and implications for the exhumation mechanism and palaeogeography. *International Journal of Earth Sciences*, *96*(2), 229–252. doi:10/fvhwgr

Plunder, A., Agard, P., Dubacq, B., Chopin, C., & Bellanger, M. (2012). How continuous and precise is the record of P-T paths? Insights from combined thermobarometry and thermodynamic modelling into subduction dynamics (Schistes Lustrés, W. Alps): TOWARDS Continuous P-T PATHS? *Journal of Metamorphic Geology*, *30*(3), 323–346. doi:10.1111/j.1525-1314.2011.00969.x

Polino, R., & Dal Piaz, G. (1978). Geologia dell'alta Val d'Isère e del bacino del Lago Serrù (Alpi Graie). *Memorie degli Istituti di Geologia e Mineralogia dell'Università di Padova*, *32*, 1–19.

Rabowski, F. (1918). Les lames cristallines du Val Ferret et leur analogie avec les lames de la bordure NW du massif du Mont-Blanc et de l'Aar. *Archives des Sciences Physiques et naturelles (Genève)*, *45*, 226-228. doi:10.5169/SEALS-742995

Ramsay, J. G. (1967). *Folding and fracturing of rocks*. New York: McGraw-Hill.

Real, C., Froitzheim, N., & Ferrando, S. (2018). Evidence of large-scale Mesozoic detachments preserved in the basement of the Southern Alps (northern Lago di Como area). *Italian Journal of Geosciences*, *137*(2), 283–293. doi:10/gdp6ss

Reddy, S. M., Wheeler, J., Butler, R. W. H., Cliff, R. A., Freeman, S., Inger, S., Pickles, C., & Kelley, S. P. (2003). Kinematic reworking and exhumation within the convergent Alpine Orogen. *Tectonophysics*, *365*(1–4), 77–102. doi:10/bqz5tt

Regis, D., Rubatto, D., Darling, J., Cenki-Tok, B., Zucali, M., & Engi, M. (2014). Multiple metamorphic stages within an eclogite-facies terrane (Sesia Zone, Western Alps) revealed by Th–U–Pb petrochronology. *Journal of Petrology*, *55*(7), 1429–1456.

Reinecke, T. (1991). Very-high-pressure metamorphism and uplift of coesite-bearing metasediments from the Zermatt-Saas zone, Western Alps. *European Journal of Mineralogy*, *3*(1), 7–18. doi:10.1127/ejm/3/1/0007

Reinecke, T. (1998). Prograde high- to ultrahigh-pressure metamorphism and exhumation of oceanic sediments at Lago di Cignana, Zermatt-Saas Zone, western Alps. *Lithos*, *42*(3–4), 147–189. doi:10.1016/S0024-4937(97)00041-8

Rey, D. (2002). Shear2F: un logiciel de modélisation tectonique. *Mémoire de Géologie (Lausanne)*, *37*, 45 pp.

Rey, J.-M. (1992). *Socle de la Nappe du mont Fort dans la région du barrage de la Grande Dixence* [Travail de diplôme non publié, Université de Lausanne].

Ribes, C., Ghienne, J.-F., Manatschal, G., Decarlis, A., Karner, G. D., Figueredo, P. H., & Johnson, C. A. (2019). Long-lived mega fault-scarps and related breccias at distal rifted margins: insights from present-day and fossil analogues. *Journal of the Geological Society*, *176*(5), 801–816. doi:10/ggbxv4

Rolland, Y., Lardeaux, J.-M., Guillot, S., & Nicollet, C. (2000). Extension syn-convergence, poinçonnement vertical et unités métamorphiques contrastées en bordure ouest du Grand Paradis (Alpes Franco-Italiennes). *Geodinamica Acta*, *13*(2–3), 133–148. doi:10.1080/09853111.2000.11105369

Romer, R. L., Schärer, U., & Steck, A. (1996). Alpine and pre-Alpine magmatism in the root-zone of the western Central Alps. *Contributions to Mineralogy and Petrology*, *123*(2), 138–158. doi:10.1007/s004100050147

Ross, J. V., & Bustin, R. M. (1990). The role of strain energy in creep graphitization of anthracite. *Nature*, *343*(6253), 58–60. doi:10.1038/343058a0

Rubatto, D., Gebauer, D., & Fanning, M. (1998). Jurassic formation and Eocene subduction of the Zermatt–Saas-Fee ophiolites: implications for the geodynamic evolution of the Central and Western Alps. *Contributions to Mineralogy and Petrology*, *132*(3), 269–287.

Rubatto, D., Hermann, J., Berger, A., & Engi, M. (2009). Protracted fluid-induced melting during Barrovian metamorphism in the Central Alps. *Contributions to Mineralogy and Petrology*, *158*(6), 703–722. doi:10.1007/s00410-009-0406-5

Rubatto, D., Regis, D., Hermann, J., Boston, K., Engi, M., Beltrando, M., & McAlpine, S. R. B. (2011). Yo-yo subduction recorded by accessory minerals in the Italian Western Alps. *Nature Geoscience*, *4*(5), 338-342. doi:10/dtbw6m

Salamin, D. (1989). *Géologie des unités penniques du Val de Moiry (Valais, Suisse): secteur alpage de Torrent - plaine de Lona* [Travail de diplôme non publié, Université de Lausanne].

Sartori, M. (1987). Structure de la zone du Combin entre les Diablons et Zermatt (Valais). *Eclogae Geologicae Helvetiae*, *80*(3), 789-814. doi:10/gfhzz3

Sartori, M. (1990). L'unité du Barrhorn (zone pennique, Valais, Suisse). *Mémoires de Géologie (Lausanne)*, *6*, 156 pp.

Sartori, M., Bugnon, P. C., Frey, M., Ganguin, J., Masson, H., Steck, A., & Thélin, P. (1989). Compte-rendu de l'excursion commune de la SSMP et de la SGS: le profil Rawil-Zermatt 9/10/11 octobre 1988. *Schweizerische Mineralogische und Petrographische Mitteilungen*, *69*(2), 261–282. doi:10.5169/SEALS-52793

Sartori, M., Burri, M., Epard, J.-L., Masson, H., & Pasquier, J.-B. (2011). Feuille 1306 Sion. - Atlas géologique de la Suisse 1:25 000, Carte 130.

Sartori, M., & Epard, J.-L. (2011). *Feuille 1306 Sion. - Atlas géologique de la Suisse 1:25 000, Notice explicative 130*.

Sartori, M., Gouffon, Y., & Marthaler, M. (2006). Harmonisation et définition des unités lithostratigraphiques briançonnaises dans les nappes penniques du Valais. *Eclogae Geologicae Helvetiae*, *99*(3), 363–407. doi:10/b5mg2n

Sartori, M., & Marthaler, M. (1994). Exemples de relations socle-couverture dans les nappes penniques du Val d'Hérens: Compte-rendu de l'excursion de la Société Géologique Suisse et de la Société Suisse de Minéralogie et Pétrographie (25 et 26 septembre 1993). *Schweizerische Mineralogische und Petrographische Mitteilungen*, *74*, 503–509. doi:10.5169/seals-56365

Savary, J. (1982). *Etude géologique, pétrographique et géochimique de la région du Tsaté et de Bréona (Les Haudères, Val d'Hérens)* [Travail de diplôme non publié, Université de Lausanne].

Savary, J., & Schneider, B. (1983). Déformations superposées dans les Schistes lustrés et les Ophiolites du Val d'Hérens (Valais). *Eclogae Geologicae Helvetiae*, *76*(2), 381–389.

Schaer, J.-P. (1960). *Géologie de la partie septentrionale de l'éventail de Bagnes: entre le Val d'Hérémence et le Val de Bagnes, Valais, Suisse* [Thèse de doctorat, Université de Neuchâtel]. http://doc.rero.ch/record/4448

Schaltegger, U., Desmurs, L., Manatschal, G., Müntener, O., Meier, M., Frank, M., & Bernoulli, D. (2002). The transition from rifting to sea-floor spreading within a magma-poor rifted margin: field and isotopic constraints. *Terra Nova*, *14*(3), 156–162. doi:10.1046/j.1365-3121.2002.00406.x

Schärer, U., Cosca, M., Steck, A., & Hunziker, J. (1996). Termination of major ductile strike-slip shear and differential cooling along the Insubric line (Central Alps): U-Pb, Rb-Sr and 40Ar/39Ar ages of cross-cutting pegmatites. *Earth and Planetary Science Letters*, *142*(3), 331–351. doi:10.1016/0012-821X(96)00104-5

Scheiber, T., Berndt, J., Mezger, K., & Pfiffner, O. A. (2014). Precambrian to Paleozoic zircon record in the Siviez-Mischabel basement (western Swiss Alps). *Swiss Journal of Geosciences*, *107*(1), 49–64. doi:10/f6hfrc

Scheiber, T., Pfiffner, O. A., & Schreurs, G. (2013). Upper crustal deformation in continent-continent collision: A case study from the Bernard nappe complex (Valais, Switzerland). *Tectonics*, *32*(5), 1320–1342. doi:10/f5hs4c

Schlunegger, F., & Kissling, E. (2015). Slab rollback orogeny in the Alps and evolution of the Swiss Molasse basin. *Nature Communications*, *6*(1), 8605. doi:10.1038/ncomms9605

Schmalholz, S. M., & Duretz, T. (2015). Shear zone and nappe formation by thermal softening, related stress and temperature evolution, and application to the Alps. *Journal of Metamorphic Geology*, *33*(8), 887-908. doi:10/f7qmcj

Schmid, E. (1988). *Géologie des unités de Siviez-Mischabel, Mont-Fort et Tsaté dans la région de St-Martin, Val d'Hérens, Valais, Suisse* [Travail de diplôme non publié, Université de Lausanne].

Schmid, S. M., Aebli, H. R., Heller, F., & Zingg, A. (1989). The role of the Periadriatic Line in the tectonic evolution of the Alps. *Geological Society, London, Special Publications*, *45*(1), 153–171. doi:10/dp6wdq

Schmid, S. M., Fügenschuh, B., Kissling, E., & Schuster, R. (2004). Tectonic map and overall architecture of the Alpine orogen. *Eclogae Geologicae Helvetiae*, *97*(1), 93–117. doi:10/ckdqss

Schmid, S. M., Kissling, E., Diehl, T., van Hinsbergen, D. J. J., & Molli, G. (2017). Ivrea mantle wedge, arc of the Western Alps, and kinematic evolution of the Alps–Apennines orogenic system. *Swiss Journal of Geosciences*, *110*(2), 581–612. doi:10/gbj3n5

Schneider, B. (1982). *Etude géologique et pétrographique de la région Evolène-Sasseneire (Val d'Hérens)* [Travail de diplôme non publié, Université de Lausanne].

Scholz, C. H. (1980). Shear heating and the state of stress on faults. *Journal of Geophysical Research: Solid Earth*, *85*(B11), 6174–6184. doi:10.1029/JB085iB11p06174

Schroeder, J. W., & Ducloz, C. (1955). *Géologie de la Molasse du Val d'Illiez (Bas-Valais)*. Kuemmerly et Frey, Berne.

Schürmann, H. M. E. (1953). Beiträge zur Glaukophanefrage. II (Queensland, Cuba, Californien, Val de Bagnes (Schweiz)). *Neues Jahrbuch für Mineralogie - Abhandlungen*, *87*, 303–394.

Septfontaine, M. (1995). Large scale progressive unconformities in Jurassic strata of the Prealps S of Lake Geneva: interpretation as synsedimentary inversion structures; paleotectonic implications. *Eclogae Geologicae Helvetiae*, *88*(3), 553–576. doi:10.5169/seals-167687

Sinclair, H. D. (1997). Flysch to molasse transition in peripheral foreland basins: The role of the passive margin versus slab breakoff. *Geology*, *25*(12), 1123. doi:10.1130/0091-7613(1997)025<1123:FTMTIP>2.3.CO;2

Sinclair, H. D., & Allen, P. A. (1992). Vertical versus horizontal motions in the Alpine orogenic wedge: stratigraphic response in the foreland basin. *Basin Research*, *4*(3–4), 215–232. doi:10.1111/j.1365-2117.1992.tb00046.x

Skora, S., Lapen, T. J., Baumgartner, L. P., Johnson, C. M., Hellebrand, E., & Mahlen, N. J. (2009). The duration of prograde garnet crystallization in the UHP eclogites at Lago di Cignana, Italy. *Earth and Planetary Science Letters*, *287*(3–4), 402–411. doi:10/fp6hkd

Sperlich, R. (1988). The transition from crossite to actinolite in metabasites of the Combin unit in Vallée St. Barthélemy (Aosta, Italy). *Schweizerische Mineralogische und Petrographische Mitteilungen*, *68*(2), 215–224. doi:10.5169/seals-52061

Spitz, R., Bauville, A., Epard, J.-L., Kaus, B. J. P., Popov, A. A., & Schmalholz, S. M. (2020). Control of 3-D tectonic inheritance on fold-and-thrust belts: insights from 3-D numerical models and application to the Helvetic nappe system. *Solid Earth*, *11*(3), 999–1026. doi:10.5194/se-11-999-2020

Stampfli, G. M., Borel, G. D., Marchant, R., & Mosar, J. (2002). Western Alps geological constraints on western Tethyan reconstructions. *Journal of the Virtual Explorer*, *08*. doi:10/cf742q

Stampfli, G. M., & Marthaler, M. (1990). Divergent and convergent margins in the North-Western alps confrontation to actualistic models. *Geodinamica Acta*, *4*(3), 159–184. doi:10/gd3wxp

Stampfli, G. M., Mosar, J., Marquer, D., Marchant, R., Baudin, T., & Borel, G. (1998). Subduction and obduction processes in the Swiss Alps. *Tectonophysics*, *296*(1–2), 159–204. doi:10.1016/S0040-1951(98)00142-5

Staub, R. (1942a). Über die Gliederung der Bünderschiefer im Wallis. *Eclogae Geologicae Helvetiae*, *39*, 112-115.

Staub, R. (1942b). Über den Bau der Zone du Combin der Walliseralpen. *Eclogae Geologicae Helvetiae*, *35*(2), 111–112.

Staub, R. (1942c). Radiolarit im Walliser Hochpenninikum. *Eclogae Geologicae Helvetiae*, *35*(1), 101–103. doi:10.5169/SEALS-160254

Staub, R. (1942d). Gedanken zum Bau der Westalpen zwischen Bernina und Mittelmeer. *Vierteljahrsschrift der Naturforschenden Gesellschaft in Zürich, 87*(1), 1-138.

Steck, A. (1984). Structures et deformations tertiaires dans les Alpes Centrales (transversale Aar-Simplon-Ossola). *Eclogae Geologicae Helvetiae*, *77*(1), 55–100. doi:10.5169/seals-165499

Steck, A. (1989). Structures des déformations alpines dans la région de Zermatt. *Schweizerische Mineralogische und Petrographische Mitteilungen*, *69*(2). doi:10/gcwcgc

Steck, A. (1990). Une carte des zones de cisaillement ductiles des Alpes Centrales. *Eclogae Geologicae Helvetiae*, *83*(3), 603–627. doi:10.5169/seals-166604

Steck, A. (2008). Tectonics of the Simplon massif and Lepontine gneiss dome: deformation structures due to collision between the underthrusting European plate and the Adriatic indenter. *Swiss Journal of Geosciences*, *101*(2), 515–546. doi:10/cwf8jv

Steck, A., Bigioggero, B., Dal Piaz, G. V., Escher, A., Martinotti, G., & Masson, H. (1999). Carte tectonique des Alpes de Suisse occidentale, 1:100 000. Carte géologique spéciale N° 123. Service hydrologique et géologique national, Berne.

Steck, A., Della Torre, F., Keller, F., Pfeifer, H.-R., Hunziker, J., & Masson, H. (2013). Tectonics of the Lepontine Alps: ductile thrusting and folding in the deepest tectonic levels of the Central Alps. *Swiss Journal of Geosciences*, *106*(3), 427–450. doi:10/gd7gqp

Steck, A., Epard, J.-L., Escher, A., Gouffon, Y., & Masson, H. (2001). *Carte tectonique des Alpes de Suisse occidentale, 1:100 000. Carte géologique spéciale N° 123, Notice explicative*. Office fédéral des eaux et de la géologie, Berne.

Steck, A., Epard, J.-L., Escher, A., Lehner, P., Marchant, R. H., & Masson, H. (1997). Geological interpretation of the seismic profiles through Western Switzerland: Rawil (W1), Val d'Anniviers (W2), Mattertal (W3), Zmutt-Zermatt-Findelen (W4) and Val de Bagnes (W5). In *O. A. Pfiffner et al. (Eds.). Deep structure of the Swiss Alps: results of NRP 20* (pp. 123–137). Basel: Birkhäuser Verlag.

Steck, A., Epard, J.-L., Escher, A., Marchant, R., Masson, H., & Spring, L. (1989). Coupe tectonique horizontale des Alpes centrales. *Mémoires de Géologie (Lausanne)*, *5*, 9 pp.

Steck, A., Epard, J.-L., & Masson, H. (2019). The Maggia nappe: an extruding sheath fold basement nappe in the Lepontine gneiss dome of the Central Alps. *International Journal of Earth Sciences*. doi:10/ggbxzr

Steck, A., & Hunziker, J. (1994). The Tertiary structural and thermal evolution of the Central Alps - compressional and extensional structures in an orogenic belt. *Tectonophysics*, *238*(1–4), 229–254. doi:10/d773j6

Steck, A., Masson, H., & Robyr, M. (2015). Tectonics of the Monte Rosa and surrounding nappes (Switzerland and Italy): Tertiary phases of subduction, thrusting and folding in the Pennine Alps. *Swiss Journal of Geosciences*, *108*(1), 3–34. doi:10.1007/s00015-015-0188-x

Stipp, M., Stünitz, H., Heilbronner, R., & Schmid, S. M. (2002). The eastern Tonale fault zone: a 'natural laboratory' for crystal plastic deformation of quartz over a temperature range from 250 to 700°C. *Journal of Structural Geology*, *24*(12), 1861–1884. doi:10.1016/S0191-8141(02)00035-4

Studer, B. (1851). *Geologie der Schweiz. 1, Mittelzone und südliche Nebenzone der Alpen*. Stämpflische Verlagshandlung, Bern; Friedrich Schultress, Zürich. Accessed 28 May 2022

Sutra, E., & Manatschal, G. (2012). How does the continental crust thin in a hyperextended rifted margin? Insights from the Iberia margin. *Geology*, *40*(2), 139–142. doi:10.1130/G32786.1

Termier, P. (1902). Quatre coupes à travers les Alpes franco-italiennes. *Bulletin de la Société Géologique de France*, *2*, 411–433.

Thélin, P., Gouffon, Y., & Allimann, M. (1994). Caractéristiques et métamorphisme des phyllosilicates dans la partie occidentale de la super nappe du Grand St-Bernard (Val d'Aoste et Valais). *Bulletin de la Société Vaudoise des Sciences Naturelles*, *83*(2), 93–145. doi:10.5169/seals-280523

Thélin, Ph., & Ayrton, St. (1983). Cadre évolutif des événements magmatico-métamorphiques du socle anté-triasique dans le domaine pennique (Valais): données récentes, synthèse chronologique et suggestions de recherches ultérieures. *Schweizerische Mineralogische und Petrographische Mitteilungen*, *63*(2–3), 393–420. doi:10/gfj5x9

Trouw, R. A. J., Passchier, C. W., & Wiersma, D. J. (2010). *Atlas of Mylonites- and related microstructures*. Berlin, Heidelberg: Springer Berlin Heidelberg. doi:10.1007/978-3-642-03608-8

Trümpy, R. (1954). La zone de Sion-Courmayeur dans le haut Val Ferret valaisan. *Eclogae Geologicae Helvetiae*, *47*(2), 315–359. doi:10.5169/seals-161837

Trümpy, R. (1960). Paleotectonic evolution of the central and western Alps. *Geological Society of America Bulletin*, *71*(6), 843. doi:10/cm4xgk

Trümpy, R. (1966). Considérations générales sur le "Verrucano des Alpes Suisses." In M. Tongiorgio & A. Rau (Eds.), *Atti del symposium sul Verrucano. Pisa 1965* (Societa Toscana di Scienze Naturali., pp. 212-232). Pisa.

Trümpy, R. (1980). *Geology of Switzerland: a guide-book. Part A: An Outline of the Geology of Switzerland* (Schweizerische Geologische Kommission.). Basel, New York: Wepf & Co. Publishers.

Vallet, J.-M. (1950). Etude géologique et pétrographique de la partie inférieure du Val d'Hérens et du Val d'Hérémence (Valais). *Schweizerische Mineralogische und Petrographische Mitteilungen*, *30*(2), 322. doi:10.5169/seals-24449

Vannay, J.-C., & Allemann, R. (1990). La zone piémontaise dans le Haut-Valtournanche (Val d'Aoste, Italie). *Eclogae Geologicae Helvetiae*, *83*(1), 21–39. doi:10.5169/seals-166575

Vaughan-Hammon, J. D., Luisier, C., Baumgartner, L. P., & Schmalholz, S. M. (2021). Alpine peak pressure and tectono-metamorphic history of the Monte Rosa nappe: evidence from the cirque du Véraz, upper Ayas valley, Italy. *Swiss Journal of Geosciences*, *114*(1), 20. doi:10.1186/s00015-021-00397-3

Vearncombe, J. R. (1982). The tectonic significance of Triassic dolomite and cargneule in the Gran Paradiso region, Western Alps. *Geological Magazine*, *119*(3), 301–308. doi:10/d3bb7k

Viredaz, P. (1979). *Le Trias de la Motta Biantse* [Rapport annuel de thèse, non publié, EPFL]. Lausanne.

Vogel, A. (1995). *Etude géologique et minéralogique dans la région de la Fenêtre de Durand (Haut Val de Bagnes, VS)* [Travail de diplôme non publié, Université de Lausanne].

von Blackenburg, F. (1992). Combined high-precision chronometry and geochemical tracing using accessory minerals: applied to the Central-Alpine Bergell intrusion (central Europe). *Chemical Geology*, *100*(1-2), 19–40. doi:10.1016/0009-2541(92)90100-J

von Blanckenburg, F., & Davies, J. H. (1995). Slab breakoff: A model for syncollisional magmatism and tectonics in the Alps. *Tectonics*, *14*(1), 120–131. doi:10/bgnq8p

von Blanckenburg, F., & Davies, J. H. (1996). Feasibility of double slab breakoff (Cretaceous and Tertiary) during the Alpine convergence. *Eclogae Geologicae Helvetiae*, *89*(1), 111–127. doi:10.5169/seals-167896

von Raumer, J. F., Bussy, F., Schaltegger, U., Schulz, B., & Stampfli, G. M. (2013). Pre-Mesozoic Alpine basements - Their place in the European Paleozoic framework. *Geological Society of America Bulletin*, *125*(1/2), 89–108. doi:10.1130/B30654.1

Wang, Cao, Peng, Ding, & Li. (2019). Strain-Induced Graphitization Mechanism of Coal-Based Graphite from Lutang, Hunan Province, China. *Minerals*, *9*(10), 617. doi:10.3390/min9100617

Weber, S., & Bucher, K. (2015). An eclogite-bearing continental tectonic slice in the Zermatt–Saas high-pressure ophiolites at Trockener Steg (Zermatt, Swiss Western Alps). *Lithos*, *232*, 336–359. doi:10.1016/j.lithos.2015.07.010

Wegmann, E. (1922). Zur Geologie der St. Bernharddecke im Val d'Hérens (Wallis). *Bulletin de la Société Neuchâteloise des Sciences naturelles*, *47*, 3–63. doi:10/gctj9c

Weidmann, M. (1972). Le front de la Brèche du Chablais dans le secteur de Saint-Jean-d'Aulph (Haute-Savoie). *Géologie Alpine*, *48*(2), 229–246.

Weidmann, M., & Zaninetti, L. (1974). Quelques données nouvelles sur la série du Mont-Dolin (nappe de la Dent-Blanche, Valais); Description des Foraminifères triasiques. *Eclogae Geologicae Helvetiae*, *67*(3), 597–603. doi:10.5169/seals-164309

Weissert, H. (1975). Zur Geologie der Casanna bei Klosters. *Eclogae Geologicae Helvetiae*, *68*(1), 222–229.

Wiederkehr, M., Bousquet, R., Ziemann, M. A., Berger, A., & Schmid, S. M. (2011). 3-D assessment of peak-metamorphic conditions by Raman spectroscopy of carbonaceous material: an example from the margin of the Lepontine dome (Swiss Central Alps). *International Journal of Earth Sciences*, *100*(5), 1029-1063. doi:10/fvvqr5

Wilson, C. J. L. (1978). Deformation in the Theodul-Rothorn zone (Zermatt, Switzerland). *Eclogae Geologicae Helvetiae*, *71*(3), 517–549. doi:10.5169/SEALS-164744

Witzig, E. (1948). *Geologische Untersuchungen in der Zone du Combin im Val des Dix (Wallis)* [Ph.D. thesis, ETH Zürich].

Woodtli, R., Jaffé, F., von Raumer, J., & Della Valle, G. (1987). Prospection minière en Valais: le projet Uromine. *Matériaux pour la géologie de la Suisse. Série géotechnique*, *72*, 179 pp.

Wopenka, B., & Pasteris, J. D. (1993). Structural characterization of kerogens to granulite-facies graphite: Applicability of Raman microprobe spectroscopy. *American Mineralogist*, *78*(5–6), 533–557.

Wust, G. H., & Baehni, L. A. (1986). The distinctive tectonometamorphic evolution of two basement complexes belonging to the Grand-Saint-Bernard nappe (Val de Bagnes, Valais). *Schweizerische Mineralogische und Petrographische Mitteilungen*, *66*(1–2), 53–71. doi:10.5169/seals-50881

Zimmermann, M. (1955). Geologische Untersuchungen in der Zone du Combin im Val de Zinal und Val de Moiry (Les Diablons-Garde de Bordon, Wallis). *Eclogae Geologicae Helvetiae*, *48*(1), 149–246. doi:10.5169/seals-161957

Appendix

Additional file 2.1: Deformation functions parameters for the Shear2F models of Fig.2.13

Shear2F models parameters	**Model corresponding to the Roux cross-section**				
Horizontal layers input thicknesses	Brown: infinite; grey: 250 px; red: 20 px; yellow: 20 px; blue: infinite				
Modeled geological deformation events	Normal fault	Pro vergent folds	Retro vergent folds		
			1st order folds	2nd order folds	3rd order folds
Phase Id	3b	5b	free_3a	6a	3a
Shear type	Heterogen. simple shear	Heterogen. simple shear	Heterogen. simple shear	Heterogen. simple shear	Heterogen. simple shear
Function type	Step function	Sine function	Free profile*	Sine function	Sine function
Amplitude [px]	2000	1800	900	40	27
Shift [px]	200	1600	-3390	350	14
Wavelength [px]	-	4000	-	300	30
Axial plane dip direction [deg]	135	135	315	315	315
Axial plane dip [deg]	60	30	10	10	10
Trend of the flow direction ("vector a"/"shear displacement" in Ramsay 1967) [deg]	135	135	315	315	315
Plunge of the flow direction ("vector a"/"shear displacement" in Ramsay 1967) [deg]	60	30	10	10	10
Dip direction of the 2D cross-section through the 3D model [deg]	225	225	225	225	225
Dip of the 2D cross-section through the 3D model [deg]	90	90	90	90	90

Shear2F models parameters	**Model corresponding to the Arpilles cross-section**							
Horizontal layers input thicknesses	Grey: infinite; yellow: 100 px; pale blue: 20 px; dark blue: 230 px; light blue: infinite							
Modeled geological deformation events	Normal fault	Pro vergent folds					Retro vergent folds	
		1st order folds	2nd order folds (1 bis)	3rd order folds	4th order folds	5th order folds	1st order folds	2nd order folds
Phase Id	6a	8a	5a	4a	1a	2a	4b	3a
Shear type	Heterogen. simple shear	Heterogen. simple shear	Heterogen. simple shear	Heterogen. simple shear	Heterogen. simple shear	Heterogen. simple shear	Heterogen. simple shear	Heterogen. simple shear
Function type	Step function	Sine function	Sine function	Sine function	Sine function	Sine function	Sine function	Sine function
Amplitude [px]	2000	200	200	400	80	60	200	120
Shift [px]	200	450	450	50	82	34	0	15
Wavelength [px]	-	700	700	400	120	80	800	300
Axial plane dip direction [deg]	050	210	210	210	210	210	310	310
Axial plane dip [deg]	65	30	30	30	30	30	10	10
Trend of the flow direction ("vector a"/"shear displacement" in Ramsay 1967) [deg]	050	210	210	210	210	210	310	310
Plunge of the flow direction ("vector a"/"shear displacement" in Ramsay 1967) [deg]	65	30	30	30	30	30	10	10
Dip direction of the 2D cross-section through the 3D model [deg]	180	180	180	180	180	180	180	180
Dip of the 2D cross-section through the 3D model [deg]	90	90	90	90	90	90	90	90

Shear2F software version 1.1.28 F (Rey 2002)
Data of the free profile function used in the Roux model (*) are given in the Additional file 2.2

Additional file 2.2: Schear2F freely drawn profile function for the Roux model 1st order retro folds (heterogeneous simple shear)

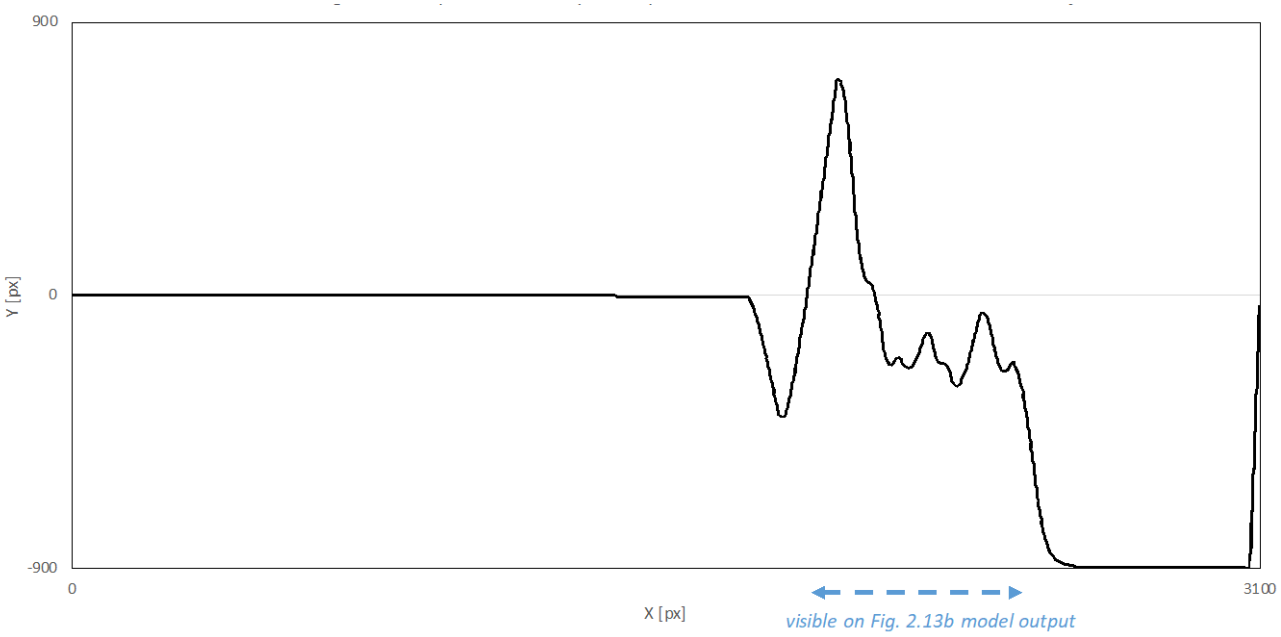

Additional file 3.1: Detailed RSCM T° calculations for Hérens valley

Series	Sample nb.	Thin section nb.	Coordinates (MN95)		Peaks positions				Overlap. mineral	Peaks fitting (Peakfit software)									Calculated Temperature (Beyssac et al. 2002)							
					D1 (1350)	D3 (1510)	G (1580)	D2 (1620)		D1 (1350)		D3 (1510)		G (1580)		D2 (1620)		Fit variance	R2 coef.		T° [°C]	uncert.	Measur. nb.	Mean T° [°C]	Standard dev. (σ)	Confid. interv. (1-α = 95%)
			X	Y						area	uncert.	area	uncert.	area	uncert.	area	uncert.	r^2	R2	uncert.						
Série Rousse	**AP16035**	S6-5	2'599'230	1'105'410	1350.5	1510.6	1581.3	1620.5	Qtz	53991	251	1754	609	59742	691	5495	388	0.997	0.453	0.005	**439**	2				
					1348.2		1580.3	1615.9	Qtz	142340	313			150700	484	7909	405	0.999	0.473	0.002	**431**	1				
					1349.4	1509.8	1581.3	1618.2	Qtz	96128	439	8687	1586	72025	1537	7476	440	0.998	0.547	0.008	**397**	4				
					1347.8	1509.6	1578.2	1615.6	Qtz	162260	693	46892	2640	137710	2861	18441	1020	0.998	0.510	0.008	**414**	3				
					1349.8	1510.7	1582.1	1619.7	Qtz	65655	235	2884	561	48060	601	4299	302	0.997	0.556	0.006	**393**	3				
					1349.4		1580.6	1617.4	Qtz	94091	195			93004	297	5792	239	0.999	0.488	0.002	**424**	1				
					1346.9		1578.4	1615.3	Qtz	160660	295			128320	471	7675	397	0.999	0.542	0.002	**400**	1				
					1349.0	1509.9	1579.8	1617.4	Qtz	103660	441	2474	1199	104480	1295	7767	615	0.998	0.480	0.006	**427**	2				
					1349.6	1509.9	1579.8	1617.4	Qtz	70332	350	5529	1134	67865	987	6149	371	0.998	0.487	0.006	**424**	3				
					1346.5		1578.4	1615.7	Qtz	172420	286			134630	455	7562	374	0.999	0.548	0.002	**397**	1				
					1350.3		1581.6	1619.4	Qtz	75649	212			88868	322	7401	264	0.998	0.440	0.002	**445**	1				
					1350.5	1508.9	1581.7	1618.2	Qtz	79285	342	4825	982	54614	829	5642	382	0.998	0.568	0.007	**388**	3				
					1350.9	1496.2	1582.4	1619.8	Qtz	42825	225	3658	694	44303	501	2927	177	0.999	0.476	0.005	**429**	2	13	**416**	19	11
Série Rousse	**AP16036**	S5-14	2'599'230	1'105'410	1349.0	1508.2	1581.3	1615.5	Qtz	46222	505	23370	1185	32237	1075	4362	418	0.995	0.558	0.015	**393**	7				
					1352.3		1583.6	1619.9	Qtz	10378	39			9417	64	855	54	0.996	0.503	0.004	**417**	2				
					1351.0	1520.4	1582.2	1618.8	Qtz	40939	687	23137	1969	36075	565	5043	535	0.995	0.499	0.014	**419**	6				
					1351.9		1585.2	1621.2	Qtz	18742	65			13081	105	1255	84	0.995	0.567	0.005	**389**	2				
					1347.1	1511.8	1580.1	1617.5	Qtz	150950	309	1411	755	85586	968	6748	473	0.999	0.620	0.005	**365**	2				
					1348.2		1580.7	1613.3	Qtz	128940	217			87981	384	6934	318	0.999	0.576	0.003	**385**	1				
					1350.5		1582.6	1619.2	Qtz	45896	108			40928	178	3514	145	0.998	0.508	0.003	**415**	1				
					1350.1		1582.5	1619.8	Qtz	91002	192			105590	325	6827	259	0.999	0.447	0.002	**442**	1				
					1349.7		1582.1	1619.0	Qtz	117790	290			124770	541	11615	448	0.998	0.463	0.003	**435**	1				
					1350.6		1582.8	1620.2	Qtz	41941	133			43120	231	3655	197	0.997	0.473	0.003	**431**	1				
					1350.5		1582.5	1619.7	Qtz	57205	139			66670	245	5146	208	0.999	0.443	0.002	**444**	1				
					1350.5		1582.5	1620.1	Qtz	62768	187			75195	348	6480	300	0.998	0.435	0.003	**448**	1				
					1348.1		1580.9	1616.6	Qtz	195320	299			128940	521	11020	427	0.999	0.583	0.002	**382**	1				
					1348.6		1581.3	1617.8	Qtz	136860	245			85136	454	7831	379	0.999	0.595	0.003	**376**	1				
					1349.1		1582.1	1618.8	Qtz	89056	184			63463	296	5413	242	0.998	0.564	0.003	**390**	1				
					1349.4		1582.9	1619.0	Qtz	87069	178			64568	294	5669	241	0.999	0.554	0.003	**395**	1	16	**408**	27	14
Série Rousse	**AP16055**	S6-18	2'599'170	1'108'585	1351.3		1582.2	1620.5	Qtz	19918	94			24131	88	2035	34	0.998	0.432	0.003	**449**	1				
					1350.2		1582.1	1619.4	Alb	22415	70			14666	111	1348	94	0.996	0.583	0.005	**381**	2				
					1348.7		1577.6	1617.0	Alb	25959	136			54577	148	1913	110	0.998	0.315	0.002	**501**	1				
					1349.9		1577.6	1616.8	Alb	18418	100			38649	107	1100	80	0.998	0.317	0.002	**500**	1				
					1350.2	1515.9	1579.2	1617.1	Alb	13266	152	1007	341	16625	300	1032	147	0.995	0.429	0.010	**450**	4				
					1349.4		1578.7	1617.0	Alb	18135	79			22920	94	1021	77	0.997	0.431	0.003	**449**	1				
					1349.8		1579.3	1617.4	Alb	20930	93			26130	111	1562	89	0.997	0.430	0.003	**449**	1				
					1348.0		1577.5	1616.8	Alb	44267	159			52473	202	1531	156	0.998	0.450	0.003	**441**	1				
					1349.0		1576.1	1615.0	Alb	22954	110			36123	133	1922	106	0.998	0.376	0.003	**474**	1				
					1349.8		1577.3	1616.0	Alb	23592	115			36196	128	1476	103	0.998	0.385	0.003	**470**	1				
					1348.2		1577.2	1616.6	Alb	37096	235			66061	172	3182	65	0.998	0.349	0.003	**486**	1				
					1350.4		1579.9	1619.3	Alb	20357	93			30251	98	1408	77	0.998	0.391	0.003	**467**	1	12	**460**	32	20

Additional file 3.1: Detailed RSCM T° calculations for Hérens valley (continued)

Series	Sample nb.	Thin section nb.	Coordinates (MN95)		Peaks positions				Overlap. mineral	Peaks fitting (Peakfit software)										Calculated Temperature (Beyssac et al. 2002)							
					D1 (1350)	D3 (1510)	G (1580)	D2 (1620)		D1 (1350)		D3 (1510)		G (1580)		D2 (1620)		Fit variance		R2 coef.		T° [°C]	uncert.	Measur. nb.	Mean T° [°C]	Standard dev. (σ)	Confid. interv. (1-α = 95%)
			X	Y						area	uncert.	area	uncert.	area	uncert.	area	uncert.	r^2		R2	uncert.						
Série Rousse	**AP17007**	S6-1	2'599'786	1'106'673	1346.7	1499.5	1577.4	1614.7	Qtz	132300	454	4071	933	134310	1171	12272	685	0.998		0.474	0.004	**430**	2				
					1350.4	1500.7	1582.1	1618.5	Qtz	102520	446	4085	1180	90204	871	12600	491	0.999		0.499	0.005	**419**	2				
					1350.4	1500.4	1582.6	1620.3	Qtz	119100	440	4070	1295	106470	833	8699	403	0.999		0.508	0.004	**415**	2				
					1349.5	1500.2	1581.2	1619.0	Qtz	96341	539	2999	1545	84564	1167	9356	558	0.998		0.506	0.007	**416**	3				
					1350.5	1499.1	1581.3	1619.3	Qtz	39272	280	4243	858	40209	663	2665	210	0.997		0.478	0.008	**428**	3				
					1349.9	1511.8	1581.2	1619.3	Qtz	51110	327	1739	905	61352	792	4480	367	0.997		0.437	0.006	**447**	3				
					1349.4	1509.3	1581.6	1618.2	Qtz	65577	314	4393	1020	42126	965	4663	408	0.998		0.584	0.009	**381**	4				
					1351.4	1498.9	1582.4	1620.4	Qtz	40297	350	6041	909	32686	689	2573	200	0.996		0.533	0.010	**404**	4				
					1350.6	1506.1	1580.6	1618.9	Qtz	45789	259	4559	785	49031	635	3963	253	0.998		0.464	0.006	**435**	3				
					1350.0		1581.2	1619.0	Qtz	55520	145			75277	209	3488	163	0.999		0.413	0.002	**457**	1	10	**423**	22	15
Série Rousse	**AP17017**	S5-17	2'605'156	1'106'891	1350.8	1506.4	1581.5	1618.8	Qtz	148130	668	14904	1588	144810	1208	21412	540	0.999		0.471	0.004	**431**	2				
					1348.6	1510.4	1581.3	1617.4	Qtz	182470	644	14425	2015	157900	1882	17430	756	0.999		0.510	0.005	**414**	2				
					1349.4	1510.5	1582.1	1616.2	Qtz	53716	530	8770	1618	43914	1337	9041	691	0.995		0.504	0.013	**417**	6				
					1349.8	1510.0	1580.5	1618.2	Qtz	121030	704	16322	1953	121070	1516	18738	633	0.998		0.464	0.006	**435**	3				
					1349.8	1509.9	1580.5	1618.2	Qtz	124990	666	11731	1843	126810	1442	14868	544	0.998		0.469	0.005	**432**	2				
					1349.8		1582.5	1618.1	Qtz	67980	255			66987	446	6563	387	0.997		0.480	0.004	**427**	2				
					1351.0		1582.9	1620.5	Qtz	60002	144			54214	225	3220	183	0.998		0.511	0.003	**414**	1				
					1351.3		1583.7	1620.5	Qtz	90629	209			83546	345	5773	281	0.998		0.504	0.003	**417**	1				
					1350.4		1583.4	1619.4	Qtz	146190	247			120130	426	7958	347	0.999		0.533	0.002	**404**	1				
					1350.5		1582.1	1619.0	Qtz	101980	251			100060	410	5803	325	0.998		0.491	0.003	**423**	1				
					1349.3		1581.8	1618.2	Qtz	104610	223			114650	352	5726	277	0.999		0.465	0.002	**434**	1				
					1349.8	1504.7	1580.7	1618.2	Qtz	73033	336	2987	919	59584	661	4013	308	0.998		0.535	0.006	**403**	3				
					1350.2		1582.1	1618.9	Qtz	130420	263			115110	444	9041	369	0.999		0.512	0.002	**413**	1				
					1350.2		1581.7	1619.3	Qtz	146870	310			113950	526	10135	448	0.999		0.542	0.003	**400**	1				
					1350.2		1581.4	1618.8	Qtz	76476	178			80075	293	5361	241	0.999		0.472	0.002	**431**	1	15	**420**	12	7
Série Rousse	**AP17040**	S5-8	2'605'156	1'106'888	1350.2	1510.1	1582.5	1619.4	Qtz	35551	161	1776	705	34095	444	4195	103	0.998		0.481	0.005	**427**	2				
					1349.8	1510.3	1580.5	1618.6	Qtz	72581	433	20456	1309	91870	1341	7771	363	0.999		0.421	0.006	**453**	3				
					1350.9	1509.1	1581.7	1619.0	Qtz	46246	463	19600	1824	38002	987	6803	391	0.995		0.508	0.011	**415**	5				
					1352.2	1509.4	1582.6	1619.6	Qtz	20681	108	755	90	21070	137	2146	94	0.997		0.471	0.004	**431**	2				
					1349.8		1582.2	1618.6	Qtz	136000	279			99689	444	8422	362	0.999		0.557	0.003	**393**	1				
					1349.2	1507.4	1580.9	1618.2	Qtz	108610	386	4334	1242	102860	1095	7972	432	0.999		0.495	0.005	**421**	2				
					1351.0	1500.6	1583.3	1620.7	Qtz	56878	227	978	441	41122	391	2354	197	0.997		0.567	0.005	**389**	2				
					1350.5		1582.7	1619.2	Qtz	92134	182			89103	284	5321	227	0.999		0.494	0.002	**421**	1				
					1351.0	1491.6	1581.9	1618.6	Qtz	70991	412	2554	1021	85052	585	4592	306	0.999		0.442	0.004	**444**	2				
					1349.7		1581.2	1618.9	Qtz	79931	183			82435	266	3695	209	0.999		0.481	0.002	**427**	1				
					1349.0		1579.8	1617.2	Qtz	130500	271			144740	398	7000	324	0.999		0.462	0.002	**435**	1				
					1350.2		1580.5	1618.3	Qtz	96582	308			143560	471	6827	378	0.999		0.391	0.002	**467**	1				
					1350.8	1512.1	1582.6	1619.4		80701	329	3984	1041	68704	1008	4914	379	0.999		0.523	0.006	**408**	3				
					1351.1		1582.4	1619.3		56361	122			70180	185	3439	152	0.999		0.434	0.002	**448**	1				
					1351.6		1582.6	1620.5		29140	128			28470	136	1274	103	0.997		0.495	0.004	**421**	2	15	**427**	21	12

Additional file 3.1: Detailed RSCM T° calculations for Hérens valley (continued)

Series	Sample nb.	Thin section nb.	Coordinates (MN95)		Peaks positions				Overlap. mineral	Peaks fitting (Peakfit software)									**Calculated Temperature** (Beyssac et al. 2002)								
					D1 (1350)	D3 (1510)	G (1580)	D2 (1620)		D1 (1350)		D3 (1510)		G (1580)		D2 (1620)		Fit variance	R2 coef.		T° [°C]	uncert.	Measur. nb.	**Mean T° [°C]**	Standard dev. (σ)	Confid. interv. (1-α = 95%)
			X	Y						area	uncert.	area	uncert.	area	uncert.	area	uncert.	r^2	R2	uncert.						
Série Rousse	**AP17C4**	S6-10	2'605'303	1'107'142	1349.0		1581.0	1617.3	Qtz	28642	88			28594	137	1892	111	0.998	0.484	0.003	**425**	1				
					1352.6		1582.2	1619.8	Qtz	26476	94			47362	136	1958	110	0.999	0.349	0.002	**486**	1				
					1352.1		1583.4	1621.2	Qtz	21223	80			23441	121	1506	99	0.997	0.460	0.003	**436**	2				
					1352.5	1509.5	1585.0	1621.7	Qtz	20960	128	1725	408	15826	373	2300	164	0.996	0.536	0.010	**402**	4				
					1352.6		1583.6	1620.7	Qtz	33000	127			26075	174	5161	140	0.995	0.514	0.004	**412**	2				
					1352.7	1510.5	1584.0	1621.3	Qtz	30675	207	4644	649	21766	553	3359	169	0.996	0.550	0.010	**396**	4				
					1351.8	1508.8	1583.6	1621.2	Qtz	28407	129	1305	304	22966	251	2754	116	0.997	0.525	0.005	**407**	2				
					1350.2		1582.5	1619.7	Qtz	83739	221			96623	381	7743	324	0.998	0.445	0.002	**443**	1				
					1349.3		1582.0	1618.5	Qtz	83739	159			73083	257	5060	209	0.999	0.517	0.002	**411**	1				
					1350.4		1583.3	1619.7	Qtz	47072	133			48881	214	2848	165	0.998	0.476	0.003	**429**	1				
					1349.8		1582.9	1619.1	Qtz	86370	163			72534	282	5940	234	0.999	0.524	0.002	**408**	1				
					1347.4	1517.7	1580.0	1616.7	Qtz	80434	237	3065	989	79817	1166	5493	359	0.999	0.485	0.005	**425**	2	12	**423**	24	15
Série Rousse	**AP1907**	S7-6	2'603'082	1'105'740	1350.4		1582.2	1619.4	Qtz	90960	178			87977	279	5865	225	0.999	0.492	0.002	**422**	1				
					1350.2		1582.2	1619.7	Qtz	60662	138			53616	210	3327	167	0.999	0.516	0.003	**411**	1				
					1350.3		1582.4	1620.3	Qtz	108390	230			104290	340	5774	267	0.999	0.496	0.002	**420**	1				
					1349.8		1581.7	1618.9	Qtz	124220	293			109990	454	8132	380	0.998	0.513	0.003	**413**	1				
					1348.6		1579.8	1617.2	Qtz	105600	203			119210	305	5527	240	0.999	0.458	0.002	**437**	1				
					1350.7		1582.4	1619.6	Qtz	65130	128			72825	188	3573	149	0.999	0.460	0.002	**436**	1				
					1351.7		1583.7	1622.0	Qtz	72267	353			108580	651	10538	568	0.996	0.378	0.004	**473**	2				
					1353.1		1584.8	1622.8	Qtz	30532	146			35331	209	2930	172	0.996	0.444	0.004	**443**	2				
					1346.7	1504.4	1575.8	1612.5	Qtz	123970	504	15217	1359	178910	1401	12363	648	0.999	0.393	0.004	**466**	2				
					1351.4		1582.5	1619.7	Qtz	91854	235			129900	337	7035	276	0.999	0.401	0.002	**462**	1				
					1352.6		1583.4	1620.9	Qtz	61489	135			81584	196	3843	158	0.999	0.419	0.002	**455**	1				
					1355.4		1586.3	1623.8	Qtz	86323	178			109570	269	5750	219	0.999	0.428	0.002	**450**	1				
					1351.5		1583.2	1620.8	Qtz	93970	186			86680	283	4391	224	0.999	0.508	0.002	**415**	1	13	**439**	21	13
Série Rousse	**AP2091**	S9-3	2'602'061	1'108'060	1350.0		1582.9	1619.8	Qtz	134990	322			107210	500	7401	404	0.998	0.541	0.003	**400**	1				
					1350.3		1582.8	1618.7	Qtz	108170	183			69424	326	7048	279	0.999	0.586	0.003	**380**	1				
					1351.4		1582.9	1620.2	Qtz	107980	256			94946	405	6340	334	0.998	0.516	0.003	**411**	1				
					1351.0		1583.7	1620.9	Qtz	67885	165			68471	302	7222	263	0.998	0.473	0.003	**431**	1				
					1350.7		1584.0	1620.5	Qtz	96571	302			83296	320	9002	131	0.999	0.511	0.003	**413**	1				
					1350.0		1582.6	1619.8	Qtz	46129	162			63117	247	2958	193	0.998	0.411	0.003	**458**	1				
					1349.6	1509.7	1581.8	1619.0		78575	253	2094	512	76116	592	7317	351	0.998	0.485	0.004	**425**	2				
					1347.8		1582.5	1618.9		87642	340			66460	555	8430	493	0.996	0.539	0.005	**401**	2				
					1349.4	1508.7	1580.2	1617.0		62046	384	4762	1204	49043	747	5970	381	0.996	0.530	0.008	**405**	3				
					1349.0		1580.9	1618.1	Qtz	104450	241			105010	374	6542	2999	0.999	0.484	0.008	**426**	4				
					1347.5		1579.7	1615.9	Qtz	88860	222			75652	365	7392	325	0.998	0.517	0.003	**411**	1				
					1347.7		1580.1	1612.2	Qtz	93568	212			85742	352	6038	287	0.999	0.505	0.003	**416**	1				
					1347.1	1507.8	1579.0	1615.5	Qtz	116260	285	3363	622	97013	809	10561	456	0.999	0.519	0.004	**410**	2	13	**414**	18	11

Additional file 3.1: Detailed RSCM T° calculations for Hérens valley (continued)

Series	Sample nb.	Thin section nb.	Coordinates (MN95)		Peaks positions				Overlap. mineral	Peaks fitting (Peakfit software)										**Calculated Temperature** (Beyssac et al. 2002)							
					D1 (1350)	D3 (1510)	G (1580)	D2 (1620)		D1 (1350)		D3 (1510)		G (1580)		D2 (1620)		Fit variance	R2 coef.		T° [°C]	uncert.	Measur. nb.	**Mean T° [°C]**	Standard dev. (σ)	Confid. interv. (1-α = 95%)
			X	Y						area	uncert.	area	uncert.	area	uncert.	area	uncert.	r^2	R2	uncert.						
Série Rousse	**AP2032**	S9-5	2'605'443	1'104'767	1350.3	1510.8	1580.6	1618.2	Qtz	46624	355	9349	971	47224	768	4785	308	0.997	0.473	0.008	**431**	3				
					1348.9	1509.2	1579.4	1618.9	Qtz	45777	423	1716	158	76416	454	7233	392	0.996	0.354	0.005	**484**	2				
					1350.9		1581.3	1620.5	Qtz	25209	153			35667	160	2587	134	0.997	0.397	0.004	**464**	2				
					1351.4	1509.5	1581.3	1619.8	Qtz	30022	126	797	171	41056	210	3709	163	0.998	0.401	0.003	**462**	1				
					1350.6		1580.5	1619.0	Qtz	36910	164			50171	225	3648	188	0.997	0.407	0.003	**460**	1				
					1351.0		1581.6	1619.7	Qtz	26448	97			28811	119	1822	98	0.998	0.463	0.003	**435**	1				
					1351.6		1581.6	1619.1	Qtz	32857	124			46055	153	1951	126	0.998	0.406	0.003	**460**	1				
					1352.1		1582.5	1620.1	Qtz	21561	96			38154	120	1986	94	0.998	0.349	0.002	**485**	1				
					1351.8		1581.3	1619.0	Qtz	33332	155			79562	190	2627	154	0.999	0.289	0.002	**513**	1				
					1350.7		1581.8	1620.2	Qtz	45890	176			77454	254	3323	199	0.998	0.362	0.002	**480**	1				
					1349.8		1580.3	1618.3	Qtz	64779	182			98175	234	4050	184	0.999	0.388	0.002	**468**	1	11	**467**	23	16
Série Grise	**AP17009**	S5-15	2'605'004	1'106'290	1349.8	1509.2	1580.5	1616.3	Qtz	66769	498	7497	1445	76845	1425	18996	1169	0.995	0.411	0.008	**458**	4				
					1351.0	1486.0	1581.4	1620.0	Qtz	52807	852	21022	2312	56172	513	6689	422	0.995	0.457	0.010	**438**	5				
					1351.3	1508.6	1582.5	1619.8	Qtz	36871	193	3430	563	39564	475	3729	212	0.998	0.460	0.006	**436**	2				
					1351.3	1505.1	1583.7	1620.7	Qtz	16794	190	1027	642	20457	360	2195	196	0.997	0.426	0.009	**452**	4				
					1350.9	1510.0	1581.7	1621.3	Qtz	30951	270	18823	770	33666	805	5357	284	0.997	0.442	0.009	**444**	4				
					1351.7	1509.7	1582.1	1619.8	Qtz	33325	195	6234	479	38192	396	3370	145	0.998	0.445	0.005	**443**	2				
					1348.7		1580.6	1618.6	Qtz	138620	281			143800	456	6963	369	0.999	0.479	0.002	**428**	1				
					1349.8	1508.1	1580.1	1618.8		51861	246	3579	829	70544	718	3784	241	0.999	0.411	0.004	**458**	2				
					1348.2	1509.7	1580.1	1617.8	Qtz	103650	428	2815	1655	95835	1760	6268	396	0.999	0.504	0.007	**417**	3				
					1349.6		1582.2	1619.1	Qtz	59689	143			76019	216	4338	176	0.999	0.426	0.002	**451**	1				
					1351.0		1582.2	1619.3	Qtz	78845	183			75143	265	3760	219	0.999	0.500	0.002	**419**	1				
					1350.2	1485.2	1581.7	1619.0	Qtz	54307	352	3216	873	40863	441	3994	247	0.998	0.548	0.007	**397**	3				
					1351.5	1491.9	1582.2	1618.9	Qtz	64741	442	2617	1059	64919	529	5162	349	0.999	0.480	0.006	**427**	3				
					1348.1		1579.6	1615.8	Qtz	137020	211			117720	350	8295	295	0.999	0.521	0.002	**409**	1				
					1350.6		1580.9	1618.1	Qtz	46887	116			58306	172	2912	152	0.999	0.434	0.002	**448**	1				
					1350.6		1580.4	1617.8	Qtz	69656	164			86887	247	4950	215	0.999	0.431	0.002	**449**	1	16	**436**	18	10
Série Grise	**AP17036**	S5-9	2'605'228	1'106'869	1353.9	1507.1	1582.1	1621.3	Qtz	19606	298	2348	724	25124	256	3371	150	0.996	0.408	0.009	**460**	4				
					1351.7	1509.4	1581.3	1619.4	Qtz	28184	191	3104	573	33930	482	2820	162	0.997	0.434	0.006	**448**	3				
					1353.2	1507.1	1581.7	1620.1	Qtz	19096	511	4504	575	24512	319	1859	106	0.996	0.420	0.014	**454**	6				
					1350.8	1494.8	1579.0	1615.9	Qtz	36383	921	11324	1480	57203	370	2977	291	0.997	0.377	0.011	**473**	5				
					1352.9	1509.7	1580.1	1618.1	Qtz	23155	264	4183	692	51653	527	2318	200	0.999	0.300	0.005	**507**	2				
					1349.6		1580.8	1618.1	Qtz	60971	174			93116	257	4883	208	0.999	0.384	0.002	**470**	1				
					1350.8		1582.2	1617.9	Qtz	65055	159			69515	238	4263	218	0.999	0.469	0.002	**432**	1				
					1351.8	1502.0	1581.7	1619.9	Qtz	33391	269	7819	832	46992	565	3516	268	0.997	0.398	0.006	**464**	3				
					1350.4		1581.0	1616.6	Qtz	25484	111			22195	170	1835	151	0.995	0.515	0.005	**412**	2				
					1352.5	1496.3	1581.4	1618.7	Qtz	26363	267	3645	715	48787	445	2378	207	0.999	0.340	0.005	**490**	2				
					1350.8		1582.1	1619.1	Qtz	60119				71157	222	3468	174	0.999	0.446	0.001	**442**	1				
					1352.5		1580.1	1618.6	Qtz	19269	118			38210	148	2636	131	0.997	0.321	0.003	**498**	1				
					1351.6	1520.6	1579.9	1617.6	Qtz	17524	201	827	365	34750	557	3854	311	0.995	0.312	0.007	**502**	3	13	**466**	29	17

Additional file 3.1: Detailed RSCM T° calculations for Hérens valley (continued)

Series	Sample nb.	Thin section nb.	Coordinates (MN95)		Peaks positions				Overlap. mineral	Peaks fitting (Peakfit software)									**Calculated Temperature** (Beyssac et al. 2002)							
					D1 (1350)	D3 (1510)	G (1580)	D2 (1620)		D1 (1350)		D3 (1510)		G (1580)		D2 (1620)		Fit variance	R2 coef.		T° [°C]	uncert.	Measur. nb.	**Mean T° [°C]**	Standard dev. (σ)	Confid. interv. (1-α = 95%)
			X	Y						area	uncert.	area	uncert.	area	uncert.	area	uncert.	r^2	R2	uncert.						
Série Grise	**AP19001**	S7-1	2'605'385	1'103'175	1351.3		1582.4	1620.2		42290	100			41095	155	2740	133	0.999	0.491	0.002	**422**	1				
					1350.2	1511.7	1581.7	1618.9	Alb	45213	171	1281	339	41642	424	4791	256	0.997	0.493	0.005	**421**	2				
					1351.3	1511.2	1579.8	1617.4	Alb	14679	241	2193	758	32085	665	1809	216	0.996	0.302	0.009	**507**	4				
					1350.0		1581.5	1617.8	Alb	39254	111			39041	179	2794	155	0.998	0.484	0.003	**426**	1				
					1349.7		1582.5	1619.6	Alb	35020	104			23770	159	2791	129	0.997	0.569	0.004	**388**	2				
					1347.2		1579.2	1616.9	Alb	104140	274			114230	398	6247	332	0.998	0.464	0.002	**435**	1				
					1347.4		1579.0	1615.5	Alb	176340	471			159390	760	10237	617	0.998	0.510	0.003	**414**	1				
					1349.6	1507.8	1580.3	1618.6	Alb	35988	147	1184	279	48808	339	3159	193	0.998	0.409	0.004	**459**	2				
					1346.8	1501.1	1575.6	1611.8	Alb	127200	1723	76152	2382	172520	1543	19047	1199	0.998	0.399	0.008	**463**	3				
					1347.6		1579.4	1616.1	Qtz	106800	205			105650	346	7696	295	0.999	0.485	0.002	**425**	1				
					1350.3		1580.6	1618.2	Qtz	52495	143			84595	212	4519	183	0.999	0.371	0.002	**476**	1				
					1352.1	1509.2	1581.3	1617.4	Qtz	35536	249	3178	709	26012	725	3410	305	0.996	0.547	0.011	**398**	5				
					1348.2	1511.8	1580.5	1617.8	Qtz	134010	1629	9827	2828	175180	3062	23190	1751	0.996	0.403	0.009	**462**	4				
					1347.8		1579.8	1617.6	Qtz	84580	228			77752	376	6648	326	0.998	0.501	0.003	**418**	1				
					1349.2	1509.5	1580.5	1616.3	Qtz	76834	438	9879	1386	62391	1459	6295	387	0.998	0.528	0.009	**406**	4	15	**435**	32	18
Série Grise	**AP19003**	S7-5	2'604'862	1'104'049	1347.3		1575.1	1613.0	Alb	76101	255			118940	374	4034	290	0.999	0.382	0.002	**471**	1				
					1349.4		1580.1	1616.6	Alb	65506	207			89774	327	4636	258	0.998	0.410	0.002	**459**	1				
					1343.8	1482.9	1574.4	1611.3	Alb	201020	925	10407	2641	214600	1636	11668	714	0.999	0.470	0.004	**432**	2				
					1348.2	1499.0	1579.0	1616.3	Alb	76814	328	967	806	80523	658	4100	313	0.998	0.476	0.004	**429**	2				
					1346.3	1499.8	1575.5	1612.2	Alb	123310	929	42044	3060	136640	2647	15377	1088	0.997	0.448	0.008	**442**	4				
					1345.9		1577.0	1613.9	Alb	181000	527			180480	957	10781	812	0.998	0.486	0.003	**425**	1				
					1347.1		1578.2	1615.4	Alb	112180	251			135400	437	7501	372	0.999	0.440	0.002	**445**	1				
					1349.2		1580.6	1617.0	Alb	73991	169			75737	274	4184	225	0.999	0.481	0.002	**427**	1				
					1347.5	1506.5	1578.2	1615.1	Alb	110410	464	14813	1278	114750	1166	10472	609	0.998	0.469	0.005	**432**	2				
					1343.9		1573.6	1610.5	Alb	128520	317			188590	487	8744	392	0.999	0.394	0.002	**465**	1				
					1350.4	1499.6	1578.2	1617.8	Alb	406	5	50	12	799	7	33	3	0.997	0.328	0.006	**495**	3				
					1350.5	1506	1580.9	1618.3	Alb	1212	5	59	12	1157	10	118	5	0.999	0.487	0.004	**424**	2				
					1345.9	1511.3	1574.7	1611.6	Alb	3099	30	2152	54	3277	44	321	20	0.997	0.463	0.008	**435**	4				
					1347.5	1509.4	1579.0	1615.9	Mica	2250	14	318	38	3740	25	184	16	0.998	0.364	0.004	**479**	2				
					1349.8	1508.5	1580.5	1617.7	Mica	979	6	102	19	964	16	85	7	0.997	0.483	0.008	**426**	3	15	**446**	23	13
Série Grise	**AP1910**	S7-3	2'602'498	1'105'612	1350.2		1581.3	1618.6	Qtz	63127	160			74426	255	5264	217	0.999	0.442	0.002	**444**	1				
					1349.0	1507.5	1580.5	1613.3	Qtz	135240	2091	40585	3641	140940	2982	27168	1388	0.998	0.446	0.012	**443**	5				
					1349.4		1581.3	1618.2	Qtz	62647	157			90489	252	4910	212	0.999	0.396	0.002	**465**	1				
					1348.6		1579.9	1616.6	Qtz	169870	589			184160	634	16865	268	0.999	0.458	0.002	**437**	1				
					1349.0	1499.6	1580.9	1618.6	Qtz	110920	456	1973	1037	156250	1131	10083	613	0.998	0.400	0.004	**463**	2				
					1350.5		1581.4	1618.7	Qtz	53164	143			68544	215	4039	188	0.999	0.423	0.002	**453**	1				
					1348.6	1512.9	1580.5	1617.5	Qtz	100990	601	17774	1308	117270	1532	20473	894	0.997	0.423	0.006	**453**	3				
					1350.6		1582.6	1619.6	Qtz	52361	123			59669	187	3626	153	0.999	0.453	0.002	**440**	1				
					1347.9	1509.5	1579.8	1615.4	Qtz	143010	576	18406	2098	138120	2198	12476	781	0.999	0.487	0.006	**424**	3				
					1348.6	1510.1	1579.5	1615.8	Qtz	127830	550	22268	2213	134600	2355	11918	637	0.999	0.466	0.006	**434**	3				
					1348.2	1511.6	1579.7	1617.0	Qtz	159620	698	3528	2428	150680	2702	11643	730	0.998	0.496	0.007	**420**	3				
					1349.8		1582.2	1619.2	Qtz	105730	213			98786	313	5726	246	0.999	0.503	0.002	**417**	1				
					1349.8		1581.2	1618.2	Qtz	58671	228			73029	224	5143	86	0.999	0.429	0.002	**450**	1	13	**442**	15	9

Additional file 3.1: Detailed RSCM T° calculations for Hérens valley (continued)

Series	Sample nb.	Thin section nb.	Coordinates (MN95)		Peaks positions				Overlap. mineral	Peaks fitting (Peakfit software)									**Calculated Temperature** (Beyssac et al. 2002)							
					D1 (1350)	D3 (1510)	G (1580)	D2 (1620)		D1 (1350)		D3 (1510)		G (1580)		D2 (1620)		Fit variance	R2 coef.		T° [°C]	uncert.	Measur. nb.	**Mean T° [°C]**	Standard dev. (σ)	Confid. interv. (1-α = 95%)
			X	Y						area	uncert.	area	uncert.	area	uncert.	area	uncert.	r^2	R2	uncert.						
Série Grise	**AP1912**	S8-14	2'603'410	1'105'465	1344.7	1509.5	1572.4	1609.5	Dol	44084	223	2858	639	60033	976	5824	518	0.998	0.401	0.007	**463**	3				
					1351.3	1510.7	1582.5	1620.5	Mica	11310	93	522	174	25395	255	1863	149	0.996	0.293	0.004	**511**	2				
					1349.9	1509.5	1581.3	1618.5	Mica	29546	176	2097	433	28154	427	2765	216	0.997	0.489	0.007	**424**	3				
					1348.6		1579.4	1618.0	Mica	75640	176			88552	255	3567	197	0.999	0.451	0.002	**440**	1				
					1350.9	1512.3	1581.0	1619.1	Qtz	66381	288	1378	615	115300	959	6638	486	0.999	0.352	0.004	**484**	2				
					1349.4	1510.5	1580.7	1618.6	Qtz	80337	309	2502	699	108200	819	7686	465	0.998	0.409	0.004	**459**	2				
					1350.1	1508.7	1581.3	1619.0	Qtz	55429	363	10217	1259	59464	1191	5445	455	0.997	0.461	0.008	**436**	4				
					1349.9	1509.1	1580.9	1618.5	Qtz	85590	305	3301	857	103130	831	5823	340	0.999	0.440	0.004	**445**	2				
					1350.2	1509.7	1582.4	1619.0	Dol	43039	328	3035	1325	38637	813	3419	345	0.997	0.506	0.010	**416**	4				
					1349.8	1510.1	1580.9	1616.6	Dol	35203	438	6279	1663	35465	852	4471	477	0.996	0.469	0.012	**433**	6				
					1349.8		1581.3	1619.4	Dol	65269	141			70797	209	3594	163	0.999	0.467	0.002	**433**	1				
					1349.5		1581.3	1618.4	Qtz	65258	147			69966	227	3955	180	0.999	0.469	0.002	**432**	1				
					1350.6		1582.1	1619.1	Qtz	38486	134			51007	158	2814	114	0.999	0.417	0.002	**455**	1				
					1350.9		1582.1	1620.3	Qtz	48137	163			77427	251	3685	193	0.998	0.372	0.002	**475**	1	14	**450**	26	15
Série Grise	**AP2080**	S9-2	2'604'400	1'103'220	1350.9	1501.7	1583.2	1621.6	Qtz	23896	111	1223	285	16459	230	2188	130	0.997	0.562	0.007	**391**	3				
					1350.4		1583.0	1620.1	Qtz	50541	144			46234	231	2893	185	0.998	0.507	0.003	**415**	1				
					1349.3		1581.8	1618.4	Qtz	36236	109			33763	187	2686	158	0.998	0.499	0.003	**419**	2				
					1347.9	1509.5	1580.5	1618.4	Qtz	129210	320	6112	753	119090	1177	15491	682	0.999	0.490	0.004	**423**	2				
					1349.5		1581.8	1619.5	Qtz	66289	183			50139	306	5469	273	0.997	0.544	0.004	**399**	2				
					1350.7		1583.3	1619.8	Qtz	16493	52			13714	83	1308	71	0.997	0.523	0.004	**408**	2				
					1348.8	1511.1	1581.0	1618.3	Qtz	151890	518	10042	1327	177720	2053	26905	1205	0.998	0.426	0.005	**451**	2				
					1350.4		1583.7	1619.8	Qtz	35740	81			26533	131	1984	107	0.998	0.556	0.003	**393**	1				
					1348.4		1580.6	1618.0	Qtz	54103	129			48507	212	3619	182	0.998	0.509	0.003	**414**	1				
					1349.7	1510.1	1582.2	1619.0	Qtz	102280	549	4328	1150	90725	1282	11788	721	0.997	0.499	0.007	**419**	3				
					1351.0		1583.7	1620.2	Qtz	25703	71			20142	108	1273	88	0.997	0.546	0.003	**398**	2				
					1350.0		1582.2	1619.8	Qtz	41695	91			32605	141	2324	114	0.998	0.544	0.003	**399**	1	12	**411**	17	11
Tracuit-AR/Cornet	**AP2083**	S9-1	2'604'255	1'100'215	1350.4	1518	1585.3	1618.6	Qtz	106540	445	7233	1937	52449	2196	9255	626	0.998	0.633	0.013	**359**	6				
					1346.9	1512.2	1584.8	1615.7	Qtz	262420	766	6572	2418	93499	3128	14355	1554	0.998	0.709	0.011	**326**	5				
					1348.8		1584.8	1614.0	Qtz	183030	650			74871	889	22764	477	0.997	0.652	0.005	**351**	2				
					1348.0		1584.5	1617.1	Qtz	240060	460			114080	1032	17645	902	0.998	0.646	0.004	**354**	2				
					1346.9	1510.6	1581.4	1612.8	Qtz	305550	858	7469	2280	170240	2831	23861	1465	0.999	0.612	0.007	**369**	3				
					1346.7	1514.2	1582.3	1613.8	Qtz	271240	579	4818	1365	145360	2818	18868	1499	0.999	0.623	0.007	**364**	3				
					1346.2	1510.4	1582.6	1615.1	Qtz	357700	1164	5051	3374	164390	4375	26904	2238	0.998	0.652	0.009	**351**	4				
					1349.7	1508.8	1586.4	1616.7	Qtz	179460	495	2214	1184	88199	1637	12959	950	0.998	0.640	0.007	**356**	3				
					1350.4	1510.9	1588.8	1620.5	Qtz	90602	375	1911	1024	34574	829	8001	211	0.997	0.680	0.008	**338**	3				
					1350.5	1511.5	1586.1	1617.1	Qtz	182740	759	4382	2414	97908	2048	22338	2048	0.998	0.603	0.010	**373**	4				
					1349.2	1511.8	1584.9	1616.7	Qtz	132630	461	5113	1712	63823	1983	10320	820	0.998	0.641	0.010	**356**	5	11	**354**	13	9

Additional file 3.1: Detailed RSCM T° calculations for Bagnes valley

Series	Sample nb.	Thin section nb.	Coordinates (CH1903)		Peaks positions				Overlap. mineral	Peaks fitting (Peakfit software)									**Calculated Temperature** (Beyssac et al. 2002)								
					D1 (1350)	D3 (1510)	G (1580)	D2 (1620)		D1 (1350)		D3 (1510)		G (1580)		D2 (1620)		Fit variance	R2 coef.		**T° [°C]**	uncert.	Measur. nb.	**Mean T° [°C]**	Standard dev. (σ)	Confid. interv. (1-α = 95%)
			X	Y						area	uncert.	area	uncert.	area	uncert.	area	uncert.	r^2	R2	uncert.						
Série Rousse	**AP1925**	S7-2	2'594'349	1'094'318	1354.4		1581.1	1621.3		21869	188			64322	224	3208	185	0.998	0.245	0.003	**532**	1				
					1350.4		1579.1	1610.5	Qtz	495	3			1551	5	65	5	0.999	0.234	0.002	**537**	1				
					1349.6		1579.9	1618.3		602	3			989	3	36	3	0.998	0.370	0.003	**476**	1				
					1351.5	1509.0	1577.8	1615.9	Mica	512	45	493	243	1047	31	148	29	0.995	0.300	0.032	**508**	14				
					1350.3		1581.2	1618.6	Qtz	46560	194			114110	267	5274	211	0.999	0.281	0.002	**516**	1				
					1349.3		1580.6	1618.2	Qtz	57832	175			86675	245	3761	197	0.999	0.390	0.002	**467**	1				
					1351.3		1582.3	1619.8	Qtz	28124	95			36853	127	1977	104	0.998	0.420	0.002	**454**	1				
					1349.8		1580.3	1617.7	Qtz	84533	248			112570	336	5542	278	0.999	0.417	0.002	**455**	1				
					1351.1		1581.1	1619.5	Qtz	38295	127			71112	168	2633	134	0.999	0.342	0.002	**489**	1				
					1348.9		1580.2	1617.2	Qtz	53230	149			59719	209	3120	181	0.999	0.459	0.002	**437**	1				
					1349.6		1580.5	1618.4	Qtz	38861	147			56828	191	2105	168	0.998	0.397	0.003	**464**	1				
					1351.3		1581.8	1618.6	Qtz	15447	87			20635	109	1108	90	0.996	0.415	0.004	**456**	2	12	**483**	33	21
Série Rousse	**AP1926**	S9-6	2'594'217	1'094'242	1353.4		1579.4	1620.1	Qtz	3712	163			12440	50	359	43	0.996	0.225	0.010	**541**	5				
					1351.1		1581.9	1619.7		53970	132			63568	181	3046	149	0.999	0.448	0.002	**442**	1				
					1351.0		1581.8	1619.9	Qtz	55747	151			63375	205	3000	169	0.998	0.456	0.002	**438**	1				
					1351.8		1581.5	1619.7	Qtz	23960	109			32436	138	2584	125	0.997	0.406	0.003	**460**	1				
					1349.7		1579.8	1619.0	Qtz	60523	326			95954	245	6041	98	0.998	0.372	0.003	**475**	1				
					1350.8		1580.3	1619.0	Qtz	42817	194			64079	158	3889	72	0.999	0.386	0.002	**469**	1				
					1351.6		1580.9	1620.4	Qtz	47031	163			65301	198	3129	152	0.998	0.407	0.002	**460**	1				
					1347.9		1578.6	1617.8		113280	331			131060	473	6313	364	0.998	0.452	0.002	**440**	1				
					1350.1		1579.7	1618.6		47350	149			53801	188	2821	153	0.998	0.455	0.003	**438**	1				
					1350.9		1580.7	1618.9		52467	166			56002	227	5186	195	0.998	0.462	0.003	**436**	1				
					1347.8		1579.0	1616.6		99961	340			124510	436	3887	318	0.998	0.438	0.003	**446**	1	11	**459**	31	21
Evolène Series	**AP15014**	S1-17	2'591'951	1'095'923	1352.4		1576.6	1618.9	Dol	10622	170			39011	136	1697	114	0.996	0.207	0.004	**549**	2				
					1350.4		1578.8	1618.2	Dol	14852	136			35252	134	1725	104	0.997	0.287	0.003	**513**	1				
					1350.2		1578.9	1618.2	Dol	11753	173			26748	110	1964	48	0.996	0.290	0.005	**512**	2				
					1350.5		1579.5	1619.8	Dol	10439	103			23839	85	1346	61	0.997	0.293	0.004	**511**	2				
					1349.3		1579.2	1618.6	Dol	15271	113			23734	82	1282	31	0.997	0.379	0.004	**472**	2				
					1349.6		1579.2	1618.6	Dol	15232	111			24035	80	1136	29	0.997	0.377	0.003	**473**	2				
					1350.0		1578.5	1618.5	Dol	16658	91			28572	92	1339	71	0.998	0.358	0.003	**482**	1				
					1348.0		1578.6	1616.2	Alb	41323	152			62329	193	1889	164	0.998	0.392	0.002	**467**	1				
					1348.6		1578.4	1616.1	Alb	36528	146			70535	192	2566	160	0.999	0.333	0.002	**493**	1				
					1350.1		1577.4	1617.4	Alb	33361	285			57873	255	1839	178	0.996	0.358	0.004	**481**	2				
					1351.4	1526.0	1579.8	1620.4	Qtz	23953	200	1625	467	22687	400	1097	118	0.995	0.502	0.009	**418**	4				
					1350.0		1579.7	1618.3	Qtz	32221	126			56609	158	1562	129	0.999	0.356	0.002	**482**	1				
					1351.1		1580.7	1619.3	Qtz	27249	121			36299	157	2093	133	0.997	0.415	0.003	**456**	1				
					1351.7		1579.2	1618.9	Qtz	39139	204			58447	206	3004	163	0.997	0.389	0.003	**468**	1	14	**484**	31	18

Additional file 3.1: Detailed RSCM T° calculations for Bagnes valley (continued)

Series	Sample nb.	Thin section nb.	Coordinates (CH1903)		Peaks positions				Overlap. mineral	Peaks fitting (Peakfit software)									**Calculated Temperature** (Beyssac et al. 2002)							
					D1 (1350)	D3 (1510)	G (1580)	D2 (1620)		D1 (1350)		D3 (1510)		G (1580)		D2 (1620)		Fit variance	R2 coef.		**T° [°C]**	uncert.	Measur. nb.	**Mean T° [°C]**	Standard dev. (σ)	Confid. interv. (1-α = 95%)
			X	Y						area	uncert.	area	uncert.	area	uncert.	area	uncert.	r^2	R2	uncert.						
Evolène Series	**AP2007**	S8-7	2'592'654	1'094'496	1351.2		1579.3	1619.9	Alb	13676	112			46098	113	790	82	0.999	0.226	0.002	**541**	1				
					1352.0		1579.0	1620.1	Alb	24801	175			51657	140	1222	98	0.997	0.319	0.003	**499**	1				
					1350.9	1509.9	1579.4	1618.5	Dol	52315	404	2216	543	74629	556	6378	367	0.996	0.392	0.005	**466**	2				
					1351.6		1580.1	1620.1	Dol	15665	207			39336	291	2100	194	0.995	0.274	0.005	**519**	2				
					1347.1		1580.9	1619.9	Qtz	27573	104			28151	140	3271	131	0.997	0.467	0.003	**433**	2				
					1350.0		1580.6	1619.3	Qtz	45553	142			58306	174	2215	128	0.998	0.429	0.002	**450**	1				
					1350.5		1579.7	1618.4	Qtz	44379	248			85477	278	5320	233	0.998	0.328	0.003	**495**	1				
					1351.6		1580.9	1620.1		34837	135			52421	153	2475	122	0.998	0.388	0.002	**468**	1				
					1350.0		1578.0	1619.0		15922	155			45312	100	1737	39	0.999	0.253	0.003	**528**	1				
					1351.3		1580.1	1620.9		36739	210			43587	187	2009	143	0.995	0.446	0.004	**442**	2				
					1350.5		1579.1	1619.6		18568	105			30625	104	1196	78	0.997	0.368	0.003	**477**	1				
					1349.0		1578.5	1617.5		45433	183			64278	199	2087	153	0.998	0.406	0.003	**460**	1				
					1351.5		1580.3	1619.9		18777	94			27691	101	1491	79	0.997	0.392	0.003	**467**	1	13	**480**	34	20

Additional file 3.2: Série Rousse and Série Grise mean RSCM°T and series attributions

Valleys	**Series/Units**	**Samples**					**RSCM Temperatures**			
		Source	Sample nb.	Thin section nb.	Coordinates (MN95) X	Y	RSCM Temp. [°C]	Errors on °T (1σ) [°C]	**Mean RSCM Temp. [°C]**	Errors on Mean RSCM°T [°C] (1σ)
Hérens	Série Rousse	Own data	AP16035	S6-5	2'599'230	1'105'410	416	19	**430**	20
			AP16036	S5-14	2'599'230	1'105'410	408	27		
			AP16055	S6-18	2'599'170	1'108'585	460	32		
			AP17007	S6-1	2'599'786	1'106'673	423	22		
			AP17017	S5-17	2'605'156	1'106'891	420	12		
			AP17040	S5-8	2'605'156	1'106'888	427	21		
			AP17C4	S6-10	2'605'303	1'107'142	423	24		
			AP1907	S7-6	2'603'082	1'105'740	439	21		
			AP2032	S9-5	2'605'443	1'104'767	467	23		
			AP2091	S9-3	2'602'061	1'108'060	414	18		
	Série Grise	Own data	AP17009	S5-15	2'605'004	1'106'290	436	18	**441**	16
			AP17036	S5-9	2'605'228	1'106'869	466	29		
			AP19001	S7-1	2'605'385	1'103'175	435	32		
			AP19003	S7-5	2'604'862	1'104'049	446	23		
			AP1910	S7-3	2'602'498	1'105'612	442	15		
			AP1912	S8-14	2'603'410	1'105'465	450	26		
			AP2080	S9-2	2'604'400	1'103'220	411	17		
		Negro et al. 2013	CO 0902		2'604'401	1'103'221	439	4		

Additional file 3.2: Série Rousse and Série Grise mean RSCM°T and series attributions (continued)

Valleys	Series/Units	Samples					RSCM Temperatures			
		Source	Sample nb.	Thin section nb.	Coordinates (MN95) X	Y	RSCM Temp. [°C]	Errors on °T (1σ) [°C]	**Mean RSCM Temp. [°C]**	Errors on Mean RSCM°T [°C] (1σ)
Bagnes	Série Rousse	Own data	AP1925	S7-2	2'594'349	1'094'318	483	33	**477**	15
			AP1926	S9-6	2'594'217	1'094'242	459	31		
		Negro et al. 2013	CO0711		2'592'929	1'093'290	492	8		
			CO0712		2'592'460	1'094'576	494	7		
		Angiboust et a. 2014	#59		2'594'464	1'091'006	478	12		
			#61a		2'593'475	1'092'251	474	20		
			#62		2'592'401	1'094'419	457	14		
	Série Grise	Negro et al. 2013	CO0708		2'595'613	1'088'050	461	4	**475**	9
			CO0709		2'595'611	1'088'037	478	5		
			CO0710		2'594'453	1'086'667	477	7		
		Angiboust et a. 2014	#57		2'595'575	1'088'363	487	23		
			#58		2'596'048	1'089'753	478	31		
		Manzotti et al. 2021	OL52		2'593'287	1'084'507	484	16		
			OL53		2'593'182	1'084'510	470	18		
			OL54		2'592'989	1'084'665	467	12		
Anniviers (incl. Moiry)	Série Rousse	Negro et al. 2013	CO0701		2'615'058	1'107'391	448	3	**447**	5
		Negro et al. 2013	CO0706		2'610'668	1'109'121	451	5		
		Angiboust et a. 2014	#44		2'610'620	1'109'022	441	12		
	Série Grise	Negro et al. 2013	CO0705		2'610'368	1'107'249	454	5	**446**	10
		Angiboust et a. 2014	#05		2'616'082	1'107'669	458	16		
		Angiboust et a. 2014	#45		2'610'625	1'108'555	440	11		
		Angiboust et a. 2014	#48		2'610'440	1'106'809	439	16		
		Angiboust et a. 2014	#49		2'610'612	1'106'597	437	14		

Additional file 3.3: Hérens valley RSCM°T and distances to the Série Grise / Série Rousse contact

Source	**Samples**					**RSCM°T**		**Distance to the SG/SR contact (orthogonal to the structures orientations)**									
	Unit	Sample nb.	Thin section nb.	Coordinates X (MN95)	Y (MN95)	**RSCM Temp. [°C]**	Errors on °T (1σ) [°C]	Mean orientations of the structures between the sample and the SG/SR contact: Azimut (***az***) [deg.] (direction used for the measur. of the horizontal distance *dh*)	Dip (***α***) [deg.]	Coordinates of the reference point on the SG/SR contact (***B***): X (MN95)	Y (MN95)	Horizontal distance between the sample and the reference point *B* following the direction *az* (***dh***) [m]	Altitude difference between the sample and the refrence pt. *B* (***Δ h***): altitude of the sample [m]	Altitude of the refernce pt. *B* [m]	***Δ h*** [m]	**Distance to SG/SR contact [m] (orthogonal with respect to S0)**	Errors on Dist. (75%) [m]
Own data	SR	AP 16035	S6-5	2'599'230	1'105'410	**416**	19	210	25	2'598'335	1'103'260	2340	2750	2800	50	**944**	708
	SR	AP16036	S5-14	2'599'230	1'105'410	**408**	27	210	25	2'598'335	1'103'260	2340	2750	2800	50	**944**	708
	SR	AP16055	S6-18	2'599'170	1'108'585	**460**	32	*Entirely eroded, approx. from the cross-section of Fig. 3.10b (following a direction parallel to the syncline)*								**50**	38
	SR	AP17007	S6-1	2'599'786	1'106'673	**423**	22	200	15	2'598'440	1'103'300	3630	2740	2800	60	**882**	661
	SR	AP17017	S5-17	2'605'156	1'106'891	**420**	12	200	10	2'605'110	1'106'735	164	1835	1690	145	**114**	86
	SR	AP17040	S5-8	2'605'156	1'106'888	**427**	21	200	10	2'605'145	1'106'775	110	1835	1780	55	**35**	26
	SR	AP17C4	S6-10	2'605'303	1'107'142	**423**	24	200	15	2'605'347	1'107'517	657	1830	2070	240	**62**	46
	SR	AP1907	S7-6	2'603'082	1'105'740	**439**	21	200	25	2'602'990	1'105'470	280	2220	2300	80	**46**	34
	SR	AP2091	S9-3	2'602'061	1'108'060	**414**	18	220	25	2'604'060	1'110'160	2900	1770	2320	550	**727**	545
	SR	AP2032	S9-5	2'605'443	1'104'767	**467**	23	170	30	2'605'435	1'104'815	43	1470	1485	15	**9**	6
	SG	AP17009	S5-15	2'605'004	1'106'290	**436**	18	200	15	2'605'050	1'106'470	190	1480	1580	100	**47**	36
	SG	AP17036	S5-9	2'605'228	1'106'869	**466**	29	200	10	2'605'230	1'106'880	10	1835	1840	5	**3**	2
	SG	AP19001	S7-1	2'605'385	1'103'175	**435**	32	190	10	2'605'460	1'103'760	590	1450	1420	30	**73**	55
	SG	AP19003	S7-5	2'604'862	1'104'049	**446**	23	230	20	2'604'960	1'104'180	160	1550	1540	10	**45**	34
	SG	AP1910	S7-3	2'602'498	1'105'612	**442**	15	210	30	2'602'550	1'105'670	80	2455	2430	25	**18**	14
	SG	AP1912	S8-14	2'603'410	1'105'465	**450**	26	*According to field observations: 6m above the base of a dolomitic slice (Frilihorn) marking the contact*								**6**	5
	SG	AP2080	S9-2	2'604'400	1'103'220	**411**	17	190	20	2'604'410	1'104'710	1500	1750	1790	40	**475**	357
	TAR/C	AP2083	S9-1	2'604'255	1'100'215	**354**	13	190	35	2'605'060	1'104'100	3980	1870	1480	390	**1963**	1473
Negro et al. 2013	SG	CO 0902		2'604'401	1'103'221	**439**	4	190	20	2'604'410	1'104'710	1500	1750	1790	40	**475**	357
Decrausaz et al. 2021	TAR/C	G1		2'601'310	1'098'650	**368**	13	170	20	2'600'450	1'103'970	5380	2900	2420	480	**1389**	1042
	TAR/C	G4		2'599'690	1'098'660	**376**	22	170	20	2'598'910	1'103'210	4620	3030	2740	290	**1308**	981
	TAR/C	G5		2'599'700	1'098'350	**373**	23	170	20	2'598'830	1'103'130	4900	3330	2770	560	**1150**	862
	TAR/C	G6		2'601'590	1'102'360	**369**	13	180	30	2'601'660	1'105'510	3160	2920	2530	390	**1242**	932
Angiboust et al. 2014	TAR/C	#17c		2'600'548	1'098'583	**364**	9	170	20	2'599'400	1'104'700	6220	3010	2840	170	**1968**	1476
	TAR/C	#127		2'604'160	1'099'880	**402**	14	190	35	2'605'025	1'104'155	3460	1810	1480	330	**1714**	1286
	MD/RZ	#65		2'601'602	1'096'885	**387**	14	170	20	2'600'450	1'103'960	7170	2600	2420	180	**2283**	1712

Additional file 3.3 (continued):

Hérens valley RSCM°T and distances to the Série Grise / Série Rousse contact